MiR-595, RPL27A And Ribosomal Dysgenesis

Alkhatabi, Heba Ahmed J

Awarding institution:
King's College London

MiR-595, RPL27A And Ribosomal Dysgenesis

Heba Ahmed Alkhatabi

A THESIS PRESENTED FOR THE DEGREE OF
DOCTOR OF PHILOSOPHY

King's College London

Department of Haematological Medicine

2014

Declaration

I hereby declare that I alone composed this thesis and that the work is my own, except where stated otherwise.

Heba Alkhatabi

September 2014

Dedication

I dedicated this work to my family (my parents, my siblings, my husband and my lovely sons).

For their endless love, support and encouraging wishes

Acknowledgements

First and foremost, I would like to thanks Allah, the Almighty, and express my deepest gratitude for having made everything possible by given me the strength and courage to do this work.

I would like to express my sincere gratitude to my supervisor Professor Ghulam Mufti for the continuous support during my PhD study and research, for his patience, motivation, enthusiasm, and insightful comments. Also, I would like to express my deepest thanks to my secondary supervisor, Dr. Joop Gaken who has been always around, guiding, advising and helping me in all times of my research and writing of this thesis. Joop you always been wonderful and I appreciate everything you did to me

In my daily work I have been blessed with friendly and cheerful group whose help, advice and friendship during the past few years have been very supportive. Many thanks to Azim "habibi", Terry, Jie Jiang, Farooq, Austin and my desk's neighbour Alex for entertaining me the last four years. Special thanks to Austin who was always willing to help, he supported me at the beginning of this project and his helpful effort continued with proof reading part of my thesis.

My special thanks also go to my friends Sneha, Nazia, Syed and Shok ping; a friends that I could not have imagined having my PhD without; all of them were busy with their work but they were willing to give their help as soon as I need. My greatest appreciation to Sneha and Nazia for sharing thoughts and stimulating discussions or working together long extended hours before deadlines. Thanks for being reliable friends for all the fun we had in the last couple of years.

To all others in the Department of Haematological medicine; Professor Shaun Thomas, such a wonderful advisor and mentor in my PhD journey; Aytug, Sahram, Thomas, David, Nigel, Rajani and Pauline, thank you all for your invaluable help and support.

A great thank you goes to Professor Alan Worn for offering me the opportunity to work in his lab. The great thanks go to Dr. Shengjiang Tan who helped me in conducting the experiments.

Beyond work, my friends in UK who have been true companions deserve an honest acknowledgment. An endless and insufficient appreciation goes to Aisha, my special friend whose willingness competes with her readiness to help. My gratitude thanks goes to my special friend Ashwag, spending the last month with her, sharing the journey and progress too as she was also submitting her own thesis, allowed me to combine joy with stress putting off a load of misery and tiredness just at the right time. I am grateful as well to my friend Raha and Safaa who were source of laughter, joy and support and all My friends in the Saudi Society of Genomic and Molecular Oncology (SSGMO) a true source of encouragement, joy and support.

Last but not the least, I would like to thank my family: my great parents in addition to my siblings: Hanadi, Shadi, Abdulrahman and Tariq; my family in-laws for and all those who are close to my heart for supporting and encouraging me with their wishes and the very important spiritual support throughout my life. My Mom and Dad thank you very much for every thing; your love and prayers were the source of my success and happiness.

My dear husband, Talal, who was always beside me, cheering me up and standing by me through the good and bad times; without you, it would not have been possible, I cannot thank you enough but simply I can say you are the love of my life.

My sons, Monther and Mutasem, sorry for being away from you, sorry for the ignorance; looking at you growing was more than enough to keep myself rewarded and motivated, so I can carry on the duties of this project. I always ask Allah to give me the chance of giving you back again.

Finally, I take this chance to acknowledge the financial and academic support of the Centre of excellence in Genomic Medicine Research, King Abdul Aziz University and the Ministry of higher Education.

Abstract

The importance of miRNAs in regulating gene expression has been addressed in several haematological cancers including myelodysplastic syndrome (MDS). In MDS, miR-145 and miR-146a have been associated with some of phenotypic features of 5q- syndrome. Monosomy 7/7q deletion is the second most common chromosomal abnormality in MDS and identifies a subgroup of patients with poor prognosis. Thus far, no studies have examined the role of miRNA dysregulation in MDS patients with monosomy 7. In this study we examined the functional consequences of deletion of miRNAs localized to 7q with particular focus on miR-595, which is localized to 7q36.3, which is commonly deleted region in 7q- and -7.

Most of the available methodologies for miRNA target identification are based on computational algorithms. Therefore, there is a relatively high incidence of false positive target identification. To enable the identification of biologically relevant microRNA targets, a novel functional assay was developed in our lab, which is based on positive/negative selection (Gaken et al, 2012). Using this assay, I identified functional targets of miR-595 and correlated this with the MDS phenotype.

Applying the functional assay to identify targets for miR-595 resulted in the identification of several targets including *RPL27A*, a large ribosomal subunit protein that was validated as a target for miR-595 by qRT-PCR and western blot analysis.

Given the recognised association of ribosomal protein (RPS14) with 5q- syndrome, subtype of MDS, I assessed the biological function of RPL27A in order to identify its contribution to the disease pathogenesis. Using Polysomes fractionation,. *RPL27A* knockdown showed a reduction in the large ribosomal subunit (60S). On day 6 of the knockdown, the depletion of *RPL27A* led to p53 activation and induced variable levels of apoptosis in all cell lines Interestingly, like *RPS14* knockdown, the effect of *RPL27A* knockdown in 48 h was *p53* dependent. The *p53* independent effect, which was observed on day 6, was attributed to a defect in ribosome biogenesis based on the disruption of nucleolar staining in HCT-116 and HCT-116 $p53^{-/-}$ with depleted *RPL27A* using fibrillarin antibody and similar effects were seen with *RPS14*.

To investigate whether the effect of *RPL27A* knockdown on erythroid differentiation is similar to the other ribosomal proteins, *RPL27A* knockdown was performed in normal CD34+ and resulted in reduce viability and apoptosis within 10 days. Post-transcriptional p53 overexpression was also observed; which led to a marked increase in the mRNA expression of p53 targets, p21 and Bax. Following 10 days in liquid culture, *RPL27A* knockdown blocked the proliferation and differentiation of erythroid cells relative to myeloid and megakaryocyte lineages. Similar observations have been made in 5q- syndrome due to *RPS14* haploinsufficiency and in Diamond Blackfan anemia patients with mutations in large or small ribosomal subunit proteins.

Lastly this study showed that *miR-595* is significantly downregulated in MDS patient samples possessing -7/-7q anomalies compared to those with a normal karyotype. In conclusion, haploinsufficency of *miR-595* in patients with -7/7q del might contributes to disease pathogenesis and these effects are mediated via *RPL27A* modulation.

Table of Contents

List of Tables

List of Figures

List of abbreviation

40S	40S ribosomal subunit
60S	60S ribosomal subunit
7-AAD	7-Aminoactinomycin D
80S	Mature ribosome
aCGH	Array comparative genomic hybridization
ADAR	Adenosine deaminase, RNA-Specific
AGO	Argonaute
ALL	Acute lymphoblastic leukaemia
AML	Acute myeloid leukaemia
ARS2	Arsenite-resistance protein 2
BAX	BCL-2-associated X protein
BCL2	B cell lymphoma 2
BM	Bone marrow
BM-MNCs	BM-mononuclear cells
BSA	Bovine serum albumin
C.elegans	Caenorhabditis elegans
C7orf33	Chromosome 7 open reading frame 33
CBL	Casitas B-lineage lymphoma proto-oncogene
CD235a	Glycophorin A
CD71	Transferrin Receptor
CDKN2B	Cyclin-dependent kinase inhibitor 2B
CDR	Commonly deleted region
CDS	Commonly deleted segment
CHH	Cartilage-hair hypoplasia
CHX	Cycloheximide
Ciproxin	Ciprofloxacin
CLL	Chronic lymphocytic leukaemia
CNV	Copy number variation
CUL1	Cullin-1
DAPI	4',6-diamidino-2-phenylindole
DBA	Diamond Blackfan anaemia
DC	Dyskeratosis
DLBCL	Diffuse large-B-cell lymphoma
DMEM	Dulbecco's Modified Eagle Medium
DNMTs	DNA methyltransferases
DNTPs	Deoxynucleotide triphosphate mix
E.Coli	Escherichia coli
EB	Ethidium Bromide
EDTA	Ethylenediaminetetraacetic acid disodium salt
EPO	Recombinant Human Erythropoietin
ESR1	Estrogen receptor 1
EZH2	Enhancer of zeste homolog 2
FAB	French-American-British

FBS	Fetal Bovine Serum
FISH	Fluorescence in situ hybridization
FITC	Fluorescein isothiocyanate
FlI-1	Friend leukaemia integration 1 transcription factor
FLT3LG	Fms-related tyrosine kinase 3 ligand
GAPDH	Glyceraldehyde 3-phosphate dehydrogenase
G-CSF	Granulocyte colony-stimulating factor
GCV	Ganciclovir
GRM5	Glutamate receptor, metabotropic 5
HIF	Hypoxia-Inducible Factor
HOXA1	Homeobox A1
HOXA9	Homeobox A9
HSC	Hematopoietic stem cell
HSPA14	Heat shock 70kDa protein 14
IB	Immunoblot
IFN	Interferon
IL-1	Interleukin-1
PI	Propidium Iodide
IP	Immunoprecipitation
IPSS	International Prognostic Scoring System
IRAK1	IL-1 receptor associated kinase 1
KSRP	KH-type splicing regulatory protein
LB	Luria Borth
LNA	Locked nucleic acid in situ hybridization
LOH	Loss of heterozygosity
MDR	Minimal deleted region
Maxiprep	Maxi preparation for plasmid DNA
MDM2	Murine double minute 2
MDS	Myelodysplastic Syndrome
MFE	Minimum free energy
Miniprep	Mini preparation for plasmid DNA
miRNAs	microRNAs
MLD	Metachromatic leukodystrophy
MPL	Myeloproliferative leukaemia virus oncogene
MTT	Tetrazoliumsalt [3-(4,5-Dimethylthiazol-2-yl) 2,5diphenyltetrazolium-bromide]
MYB	Myeloblastosis
NF-κB	Nuclear factor-κB
NK	Natural killer cells
NRG3	Neuregulin 3
PAMPs	Pathogen-associated molecular patterns
PB	Peripheral blood
PBS	Phosphate buffered saline
PCR	Polymerase chain reaction
PMSF	Phenylmethanesulfonyl fluoride

pre-miRNA	Precursor miRNA
pri-miRNA	Primary miRNA
PRODH/POX	Proline Oxidase
PS	Phosphatidylserine
qRT-PCR	Quantitative Real time PCR
RA	Refractory Anaemia
RAEB	Refractory Anaemia with Excess Blasts
RARS	Refractory Anaemia with ring sidroblast
Rba	Retinoblastoma protein RB
RCMD	Refractory Cytopenia with Multilineage Dysplasia
RIPA	RadioImmunoPrecipitation Assay
RISC	RNA induced silencing complex
RNU48	Homo sapiens small nucleolar RNA, C/D box 48 (SNORD48), small nucleolar RNA
RNU6B	Homo sapiens RNA, U6 small nuclear 2 (RNU6-2), small nuclear RNA
ROS	Reactive Oxygen Species
RPL27A	Ribosomal protein L27
RPMI-1640	Rosswell Park Memorial Institute medium
rRNAs	Ribosomal RNAs
RT	Reverse transcription
RUNX1	Runt-related transcription factor 1
SAGE	Serial analysis of gene expression
SCF	Stem cell factor
SDS	Shwachman-Diamond syndrome
SEC63	Translocation protein
SF3B1	Splicing factor 3B subunit 1
SFA	Sooty foot ataxia
shRNA	Short Hairprain RNA(shRNA)
SiLAC	Stable isotope labelling with amino acids in cell culture
SMZL	Splenic marginal zone lymphoma
snoRNA	Small nuclear RNAs
SNP array	Single nucleotide polymorphism microarray
SRSF2	Splicing factor arginine/serine-rich 2
StemSpanSFEM	Serum-Free Medium
TAE	Tris Acetate-EDTA buffer
TF	Transcription factor
THP1	Human acute monocytic leukaemia cell line
TLRs	Toll-like receptors
TP53(P53)	Tumour protein 53
TPO	Human Thrombopoietin
TRAF6	TNFR-associated factor 6
TRC	The RNAi Consortium
T-regs	Regulatory T cells
U2Af1	U2 small nuclear RNA auxiliary factor 1

UPD	Uniparental Disomy
UPL	Universal Probe Library
UTR	Un translated region
WHO	World Health Organization
X-Gal	5-bromo-4- chloro-3-indolyl-β-D-Galactopyranoside

Chapter 1: Introduction

1.1 MDS Background

Myelodysplastic Syndrome (MDS) is a group of heterogeneous clonal haematological disorders characterized by ineffective haematopoiesis, which results in hypercellular bone marrow, defective maturation of hamatopoietic stem cells, and cytopenia (Toyama *et al.* 1993b, Steensma *et al.* 2003, Van Etten *et al.* 2004).

Variability within disease severity corresponds to the diversity of the disease's pathological features. MDS patients that have progressed to a more aggressive state, are at a high risk of transforming into patients with acute myeloid leukaemia (AML) in 30% of all cases. According to clinical severity and disease progression, the survival rate of this disease ranges from a few months to ten years (Bennett *et al.* 2004). The broad heterogeneity of the clinical course, which is reflected by the diversity of its morphological features, provides the basis of classification systems and prognostic scoring systems. Classification systems, *i.e* the World Health Organization (WHO), is based on the percentage of blasts, ring sideroblasts, peripheral blood monocyte counts and cytogenetic results (Bennett *et al.* 2002). The WHO classification—which was developed from a previous classification system, the French-American British (FAB)—can be seen in Table 1.1. Prognostic scoring systems, *i.e.* International Prognostic Scoring System (IPSS), is used in the assessment of disease diagnosis and prognosis. IPSS dependent upon cytogenetic results, blast ratio and cytopenia (Greenberg *et al.* 1997, Mufti 2004, Mufti *et al.* 2008). The prognostic scoring based on IPSS shown in Table 1.2 .

Table 1.1:MDS classification based on WHO dependent FAB classification (Bennett *et al.* 2002).

French-American British (FAB)	**World Health Organization (WHO)**
Refractory Anaemia (RA)	Refractory Anaemia (RA)
	Refractory Cytopenia with Multilineage Dysplasia (RCMD)
	Myelodysplastic Syndrome (MDS) Unclassified (MDS-U)
	MDS with isolated del (5q)
Refractory Anaemia with Ringed Sideroblasts (RARS)	Refractory Anaemia with Ringed Sideroblasts (RARS)
	RCMD and Ringed Sideroblasts (RCMD-RS)
Refractory Anaemia with Excess Blasts (RAEB)	RAEB-1
	RAEB-2
RAEB in Transformation (RAEB-T)	Acute Myeloid Leukaemia (AML)

Table 1.2: MDS scoring system IPSS (Greenberg *et al.* 1997).

Score					
Prognostic Variable	**0**	**0.5**	**1.0**	**1.5**	**2.0**
Bone Marrow Blast	<5	5-10	-----	11-20	21-30
Karyotype	Good	Intermediate	Poor		
Cytopenia	0/1	2/3			
Prognosis Score	**IPSS Subgroup**		**Median AML transformation (in years)**		**Median Survival (in years)**
0	Low		9.4		5.7
0.5-1.0	Intermediate-1		3.3		3.5
1.5-2.0	Intermediate-2		1.1		1.2
>2.5	High		0.2		0.4

1.2 MDS Genetic Changes

Disease phenotypical heterogeneity such as severity of cytopenia, blast count, response to treatment and progression to AML, can all be attributed to genetic changes. These changes can be cytogenetic alterations, genetic mutations as well as, or instead of, epigenetic abnormalities. Among the different aberrations, cytogenetic abnormalities account for roughly 50% of cases and are, therefore, important for disease diagnosis and prognosis (Haase *et al.* 2007). Studies over the last 25 years on the cytogenetic examination in MDS patients, has shown an increase in the incidence rate of chromosomal abnormalities related to the disease. These rate rose from 40-50% according to the recent estimated data (Toyama *et al.* 1993b, Sole *et al.* 2005, Haase *et al.* 2007). MDS with normal karyotype considered a favourable prognostic sign (Sole *et al.* 2005). Similarly, a single chromosomal abnormality, such as t(1q), 5q-, t(7)q, 9p-, 12q, t(17q), 20q-, +21, -21, -X, -Y, is also favourable in the prognosis with a median survival rate from 32 months to more than nine years (Haase *et al.* 2007). Despite this, complex karyotypes with three or more abnormalities and chromosome 7 abnormality are poor prognostic markers with lower survival rates (Haase *et al.* 2006). The most common chromosomal abnormalities in MDS, along with their contribution to disease prognosis are shown in Table 1.3 .

Reliance purely, upon conventional cytogenetic analysis to study the changes within chromosomal aberration has become less favourable and insufficient, due to conventional technologies can only detect 50% of the genetic changes in MDS. The main limitations of this assay lie in the difficulty of obtaining metaphases with good resolution, as well as the difficulty in acquiring adequate and proper samples for analysis (Earle *et al.* 2007). Consequently, the application of other techniques—such as fluorescence *in situ* hybridization (FISH)—have overcome metaphase cytogenetic limitations and enhanced disease diagnosis (Rigolin *et al.* 2001). Rigolin *et al.* (2011) used the FISH technique to detect the common chromosomal abnormalities associated with MDS, such as -5/5q-, -7/7q, trisomy 8 and 17p- in MDS patients with normal karyotype: as identified by metaphase cytogenetic analysis (Rigolin *et al.* 2001). The FISH analysis identified chromosomal abnormalities in 17% of patients with normal karyotype. Furthermore, FISH-positive cases were not merely associated with a higher percentage of bone marrow blasts, but also with a higher tendency toward AML progression. This observation implies that utilisation of FISH

can confer changes within the IPSS categorisation, specifically in patients with normal karyotype.

Despite for the fact that cytogenetic analysis has been improved after the development of FISH, the technique has some disadvantages, for instance the fluorescent probe hybridizing to known regions only (Najfeld 2003). Despite this, other advanced techniques such as array comparative genomic hybridization (aCGH) as well as single nucleotide polymorphism microarray (SNP a) allow for the identification of novel genetic aberrations that are not predicted with the use of conventional cytogenetic analysis.

Starczynowski *et al.* applied aCGH screening on CD34+ cells that were isolated from a low–risk subtype MDS with a normal cytogenetic karyotype. This study reported cryptic changes on different chromosomes that were not previously observed by cytogenetic analysis (Starczynowski *et al.* 2008). Additionally, the prognosis of lower-risk MDS patients with minimal alteration as detected by aCGH was significantly correlated with a higher overall survival and a lower frequency of progression to AML. The differences between conventional cytogenetic analysis and aCGH in the detection of chromosomal changes can be seen in Figure 1.1.

SNPa is used to ascertain the copy number (CN) changes and detection of loss of heterozygosity (LOH) within a particular region. LOH occurs as aresult of the deletion of chromosomal material or through uniparental disomy (UPD) changes. The high-resolution of this technique allows for the prediction of UPD, which arises when a cell acquires two copies of one parental chromosome (Raghavan *et al.* 2005). Detection of UPD provides an advantage to SNPa over alternative techniques, due to the fact that UPD is a prominent defect, associated with different haematological malignancies (Fitzgibbon *et al.* 2005, Walker *et al.* 2006).

Table 1.3: Common cytogenetic abnormalities in MDS subtypes (Bejar et al 2011).

Chromosomal Abnormalities	Frequency (%)	Pathogenic Mechanism	Clinical Consequence
5q-	15	Haploinsufficiency for RPS14, miR-145/146a, CTNNA1, EGR1, APC, NPM	Good prognosis, high rate of response to lenalidomide
-7/7q-	5-10	Unknown	Intermediate and Poor prognosis. More common in therapy-related MDS
Trisomy 8	5-8	Unknown	Can help predict response to immunosuppression, some evidence as a marker of progression to AML
20q-	2-5	Unknown	Good prognosis
-Y	2-4	Age-related phenomenon that may not be disease related	Good prognosis. May be useful as a marker of clonal haematopoiesis
Complex (three or more abnormalities)	10-15	Various; often abnormal chromosome 17 (P53 locus)	Poor prognosis
-13/13q-, 11q-, 12p-, 9q-, idic(X)(q13), i(17q), t(11;16), t(3;21), t(1;3), t(2;11), inv(3), t(6;9)	Rare	Various, mostly unknown; chromosome 3q26 lesions alter expression of EVI1	Presumptive evidence of MDS in patients with otherwise unexplained refractory cytopenia and no morphologic evidence of dysplasia

One of the more significant studies on the application of SNPa upon MDS was undertaken by Mohamedali *et al.* Within this study, researchers applied SNPa analysis on low-risk MDS patients with normal karyotype, and on MDS patients with 5q deletion to detect CN and UPD. This study showed that UPD was present in 46% of low-risk MDS patients, and that most of the UPD defects were observed on the long arm of chromosome 4 within those RARS, RCMD and RAEB patients with normal cytogenetic karyotype with mean prevalence of 25%, 12% and 17%, respectively. Additionally, UPD on 4q was detected in 6% of patients with 5q-, while CN changes were detected, but with lower frequency levels, when compared to UPD. Furthermore, patients with higher IPSS score—who possessed normal cytogenetic karyotype—were identified with CN changes, specifically deletion, by SNPa. This correlation between IPSS scoring and SNP array reflects the importance of this method in disease diagnosis and prognosis (Mohamedali *et al.* 2007).

Application of SNPa and other advanced molecular techniques such as high throughput sequencing, have led to the identification of novel genetic aberrations associated with MDS. For instance, SNPa identified the TET oncogene family member 2 *(TET2)* mutation, a common mutation within myeloid malignancies, which was discovered in a micro-deletion in 4q24 (Jankowska *et al.* 2009). Other genetic mutations that are associated with myeloid malignancies have been identified by SNPa as a result of either UPD or micro-deletion such as the enhancer of zeste homolog 2 (*EZH2),* the myeloproliferative leukaemia virus oncogene *(MPL),* and Casitas B-lineage lymphoma proto-oncogene *(CBL)* (Dunbar *et al.* 2008, Szpurka *et al.* 2009, Makishima *et al.* 2010).

Some of the identified mutations, including tumour protein 53 (*P53), EZH2,* ETS variant 6 *(ETV6/TEL), AXL1* and Runt-related transcription factor 1 (*RUNX1)* have all been found in association with an overall decrease in survival rate of patients, thereby stressing the importance of detecting such mutations within disease prognosis (Bejar *et al.* 2011, Bejar 2014). Understanding the mechanism that causes these mutations as well as the effect of these mutations upon the biological function, will increase knowledge about MDS pathogenesis. A summary of the most commonly-identified mutations associated with MDS, and their consequent effect on the disease pathogenesis, can be seen in Table 1.4 .

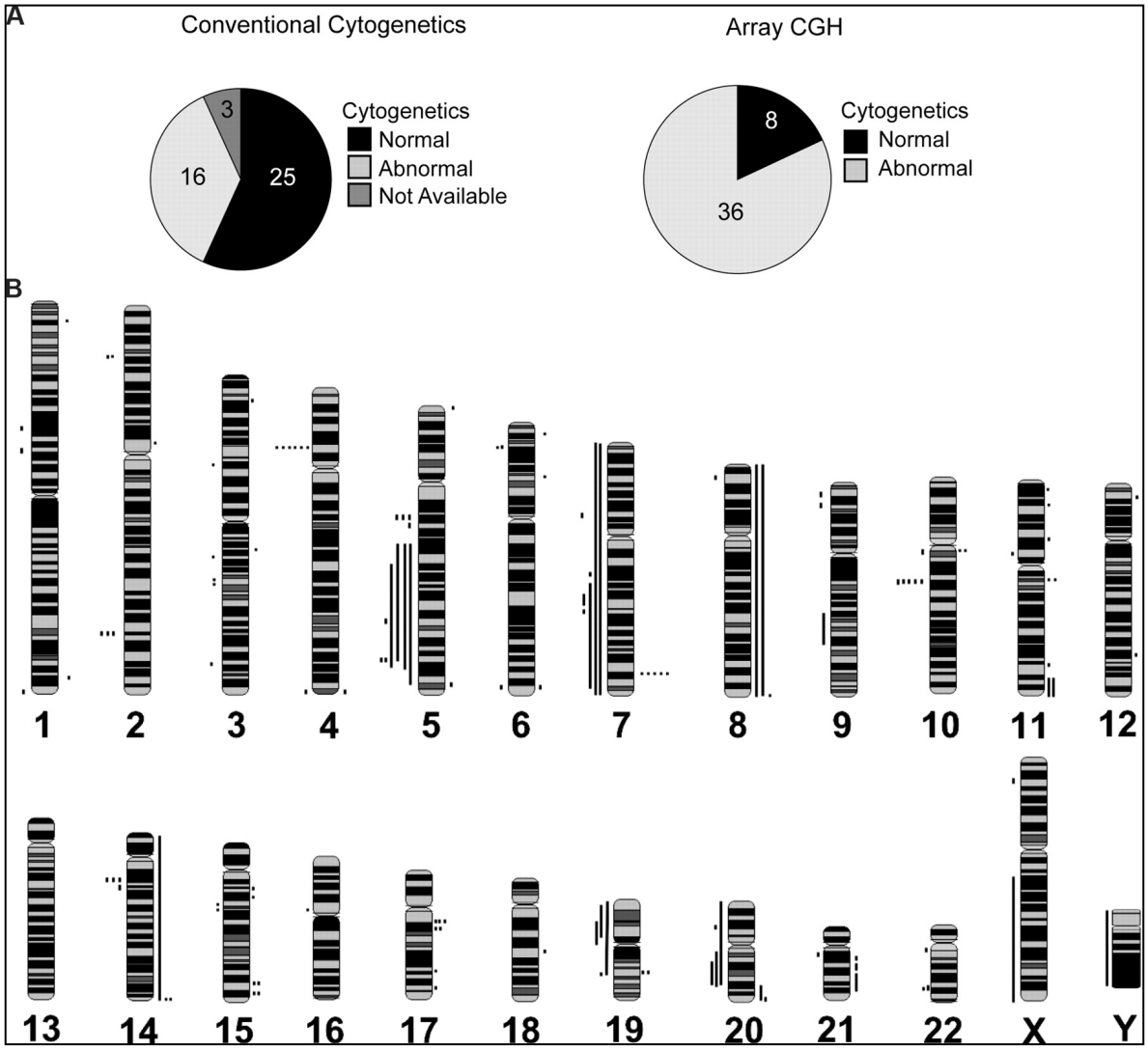

Figure 1.1: chromosomal abnormalities predicted by array CGH in MDS patients with normal cytogenetic karyotype (reproduced from Starczynowski et al. 2008).

A) Proportion of patients with chromosomal abnormalities predicted by conventional cytogenetic analysis (on the right) and by array CGH (on the left). **B)** Alterations detected by array CGH aligned to chromosomes. Lines to the right of chromosomes indicate chromosomal amplification with lines on the left indicating deletion in chromosomal material (Starczynowski et al. 2008).

Table 1.4: Common genetic changes associated with MDS (Bejar *et al* 2011)

Genetic mutations	Frequency (%)	Pathogenic Mechanism	Clinical Consequence
TET2	Approximately 20	Unknown	Unknown
RUNX1	15-20	Mutations typically alter DNA-binding domain or disrupt protein-binding domain	Increased risk of progression to AML; more common in therapy-related MDS
TP53	5-10	Loss of function of p53 tumour suppressor activity; associated with chromosomal instability	Often complex cytogenetic, relative resistance to therapy, poor prognosis
ASXL1	10-15	Unknown; most mutations are distal heterozygous frame shifts, suggesting a dominant negative function	Unknown
NRAS/KRAS	Approximately 10	Loss of GTPase activity leads to constitutive activation of serine/threonine kinase	Increased risk of progression to AML
EZH2	6	Loss of histone 3 lysine 27 methyltransferase activity	Poor prognosis
CBL/CBLB	Rare	Loss of ubiquitin ligase activity; mutants can inhibit wild-type enzymatic function	Unknown; increased risk of progression to leukaemia in MPN and in CMML where this mutation is more common
JAK2	5% of RA, 50% of RARS-T	Constitutive activation of tyrosine kinase	Unknown; does not appear to alter prognosis
MPL	5% of RARS-T	Constitutive activation of tyrosine kinase	Unknown
ATRX	Rare	Loss of function leads to decreased alpha-globin expression, likely through epigenetic dysregulation	Acquired alpha-thalassemia, often with very severe anaemia
NPM1	Rare	Terminal frame shift disrupts nucleolar localization signal leading to cytoplasmic redistribution of protein	Unknown; this mutation is very common in AML with normal cytogenetics
IDH1, IDH2	Rare	Missense mutations alter catalytic function to convert α-ketoglutarate into 2-hydroxyglutarate while consuming NADPH	Associated with more advanced disease and progression to AML
CEBPA	Rare	Loss of function known to impair granulopoiesis	Unknown; germline mutations associated with risk of AML, not MDS
WT1	Very rare	Impairment of transcription factor activity	Unknown; mutations are more common in AML and associated with poor outcomes
PTPN11	Very rare	Alters function of gene product SHP2, an adaptor protein with tyrosine phosphatase activity	More common in JMML, rare in CMML
FLT3, CSF1R, CKIT	Very rare	Constitutive activation of tyrosine kinase	Associated with more advanced disease and progression to AML

Note on Table 1.4: Rare mutations are present in 2% to 5% of patients; very rare refers to individual reports or < 2% of patients. Abbreviations: *CTNNA1*, alpha-catenin 1; *EGR1*, early growth response 1; *APC*, adenomatous polyposis coli; *NPM1*, nucleophosmin 1; GTPase, guanosine triphosphatase; MPN, myeloproliferative neoplasms; NADPH, nicotinamide adenine dinucleotide phosphate; JMML, juvenile myelomonocytic leukemia. Genes: NRAS, neuroblastoma RAS viral (V-ras)

oncogene homolog; CBL, Casitas B-lineage Lymphoma; JAK2, Janus kinase2;IDH, Isocitrate dehydrogenase (NADP+); mitochondrial PTPN11, Protein tyrosine phosphatase, non-receptor type 11;FLT3, fms-related tyrosine kinase 3; CEBPA, CCAAT/enhancer binding protein (C/EBP), alpha; wt1, Wilms tumour 1;NPM, Nucleophosmin (nucleolar phosphoprotein B23, numatrin).

Recently, high throughput sequencing discovered a new set of gene mutations affecting the RNA-splicing machinery. RNA splicing occurs after transcription in which introns are removed and exons are joined to form mRNA, a mechanism catalysed by the spliceosome (a complex of small nuclear ribonucleoproteins -snRNPs). Distinct splicesomal mutations were discovered in MDS patients; including Splicing factor 3B subunit 1 *(SF3B1*) in RARS MDS, U2 small nuclear RNA auxiliary factor 1 (*U2AF1*); and Splicing factor arginine/serine-rich 2 (*SRSF2*) in CMML MDS and other advanced forms of MDS (Papaemmanuil *et al.* 2011). In contrast to other MDS mutations predicted within other haematological malignancies, these mutations were found in 45%-85% of MDS patients, and furthermore are rarely seen in other myeloid malignancies. This phenomenon, therefore, provides an insight into the exclusive role of these mutations as part of MDS pathogenesis (Yoshida *et al.* 2011). For prognostic implications, SF3B1 is associated with a good prognosis, while *U2AF1* and *SRSF2* mutations are associated with poor prognosis, making these mutations a potential marker for both diagnosis and treatment (Makishima *et al.* 2012).

Besides all the genetic alterations that have been discovered in association with MDS subtypes, other new genetic changes have been discovered and identified as having a contributory factor to MDS. Several more studies too have demonstrated the importance of microRNAs (miRNAs) within haematological disorders as well as how these miRNAs are integrated in different myelopoiesis pathways. Expression profiling for miRNAs in MDS patients has identified dysregualtion in some miRNAs, which were subsequently associated with the pathological effects on disease development (O'Connell *et al.* 2008, O'Connell *et al.* 2011). Further details regarding miRNAs and their association with MDS subtypes, particularly MDS with monosomy 7/7q-, will be discussed in the following sections.

1.3 miRNA Background

miRNAs are single-stranded endogenous small non-coding RNAs, 18-25 nucleotides long, miRNA function as regulators of gene expression either by translation inhibition or mRNA degradation (Bartel 2004a). The first miRNAs were discovered in 1993 and 1997, were named *Lin-4* and *Let-7,* respectively. They were identified in *Caenorhabditis elegans* (*C.elgans*) and function as regulators of development (Lee *et al.* 1993, Moss *et al.* 1997). Since their discovery, knowledge about miRNAs has expanded and thousands of mature miRNAs have been identified in almost every metazoan organism, including worms, flies, plants, animals (including human), with the use of deep sequencing studies, the number of which is still increasing (Lim *et al.* 2003, Bentwich *et al.* 2005). It has now been established that many miRNAs regulate key biological processes including cell proliferation, differentiation and apoptosis of hematopoietic progenitors (Chen *et al.* 2004, Cheng *et al.* 2005, Karp *et al.* 2005, Almeida *et al.* 2011).

Several miRNAs genes are located at fragile sites and within chromosomal regions implicated in cancer (Calin *et al.* 2004). Recent studies have found that 50% of miRNA genes are identifiable within cancer-associated regions of the genome, with more than 30 miRNAs being associated with apoptosis (Calin *et al.* 2004, Yang *et al.* 2009). For instance, *miR-15* and *miR-16* contributed to apoptosis by targeting the antiapoptotic gene B cell lymphoma 2 *(BCL2*) (Cimmino *et al.* 2005). Several studies have demonstrated the involvement of miRNAs within different types of cancer through its effect on the expression of oncogene or tumour suppressor genes. For example, *miR-145 and miR-155* are differentially expressed in cancer of breast, colon, as well as lymphoma (Michael *et al.* 2003, Metzler *et al.* 2004, Iorio *et al.* 2005).

1.4 microRNA Biogenesis

miRNA genes are transcribed into long, immature primary miRNAs (pri-miRNAs). Little is known about the transcription of miRNAs, and recent analysis of the miRNAs gene location shows that the miRNAs are either transcribed either as a single transcription unit or else as a polycistronic transcription unit (a unit including regions for different, non-overlapping genes). These transcription units are located within different genetic regions; some being located within the introns of protein- coding genes or in non-coding genes, and some being present in the exon of non-coding genes (Rodriguez et al. 2004, Du et al. 2005).

The structure of six pri-miRNAs are shown in Figure 1.2. The pri-miRNAs which are generated in the nucleus through the action of RNA- polymerase II, are processed by Drosha, a type III RNAse. Consequently, a hairpin-shaped precursor miRNA (pre-miRNA) of 70-100 nucleotides is formed. This pre-miRNA is then transported to the cytoplasm and further processed by another member of the RNAse III family Dicer. This process creates in a 18-25 bp-long double strand RNA molecule: the mature miRNA/miRNA* duplex (Lee et al. 2002, Yi et al. 2003). This duplex is then separated by a helicase and one strand, the miRNA, binds to the RNA induced silencing complex (RISC) thereby becoming the active mature microRNA. The intricacies of this binding mechanism are expounded upon within the following section. The other strand, miRNA*, is degraded. Strand separation relies on thermodynamic stability; the less stable strand tends to start with uracil: the miRNA strand (Schwarz et al. 2003). When mature miRNA in the complex binds to a perfectly complementary binding region in the 3'UTR (untranslated region) of an mRNA, this results in specific degradation of the mRNA while imperfect binding results in translation inhibition (Lee et al. 1993, Bartel et al. 2004b, Eulalio et al. 2008, Garzon et al. 2008, Bartel 2009, Jadersten et al. 2009, Yang et al. 2009). The mechanisms that are involved in miRNA biogenesis are depicted in Figure 1.3.

.

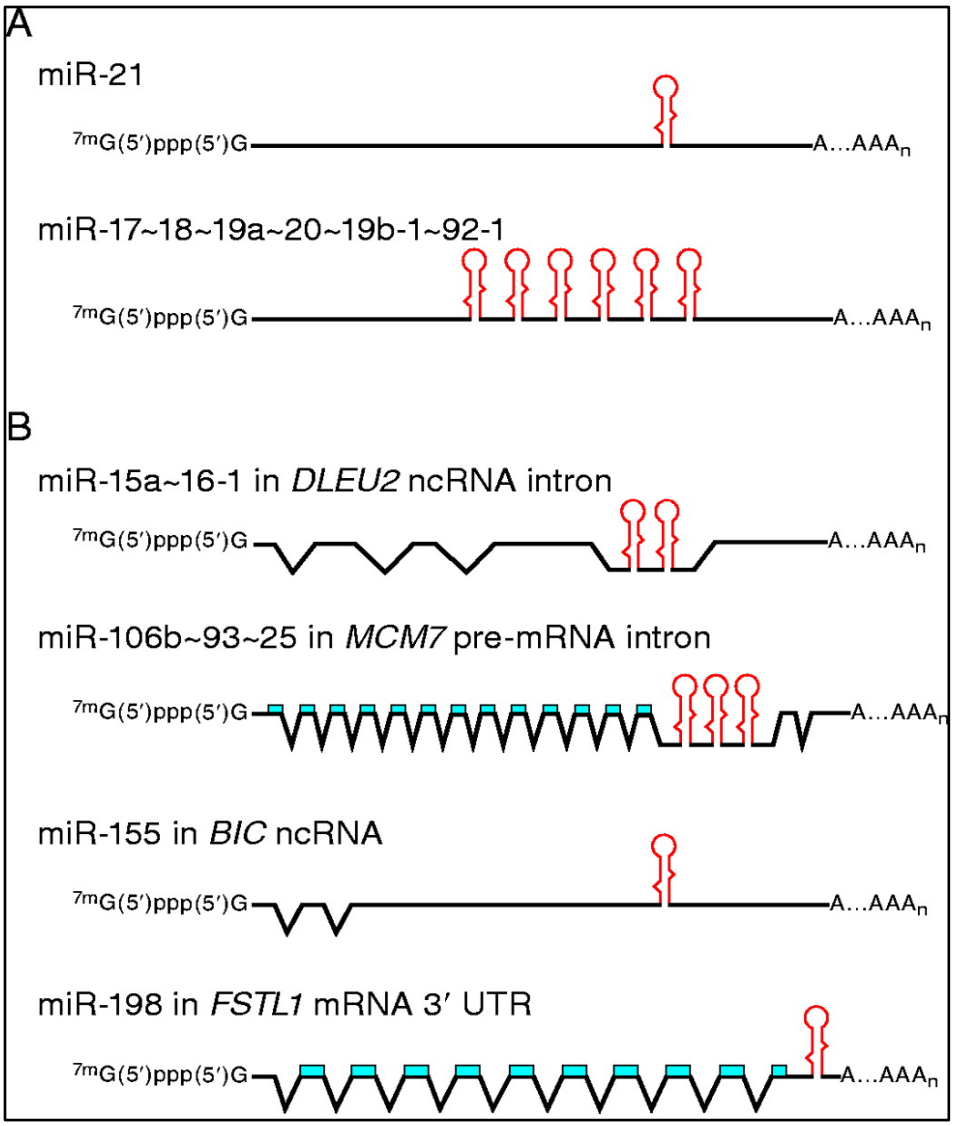

Figure 1.2: The structure of six primary miRNA transcripts that encode six different miRNAs (reproduced from Du *et al.* 2005).

The primary miRNA transcripts differ based on the following. **A)** Examples of miRNA transcription units, *miR-21* transcript is a single unit and polycistronic unit as seen in *miR-17-92-1* cluster. **B)** miRNAs that are transcribed alongside other genes (as indicated in the figure above) at different positions. *miR-15a ~16-1* in the intron of non-coding RNA. *miR-106b* in the intron of protein coding mRNA whereas *miR-155* and *miR-198* in the exon of non-coding RNA and in the exon of protein coding mRNA, respectively. *DLEU2*, deleted in lymphocytic leukaemia 2; *MCM7*, minichromosome maintenance deficient 7; *BIC*, B-cell integration cluster; *FSTL1,* follistatin-like 1(Du *et al.* 2005).

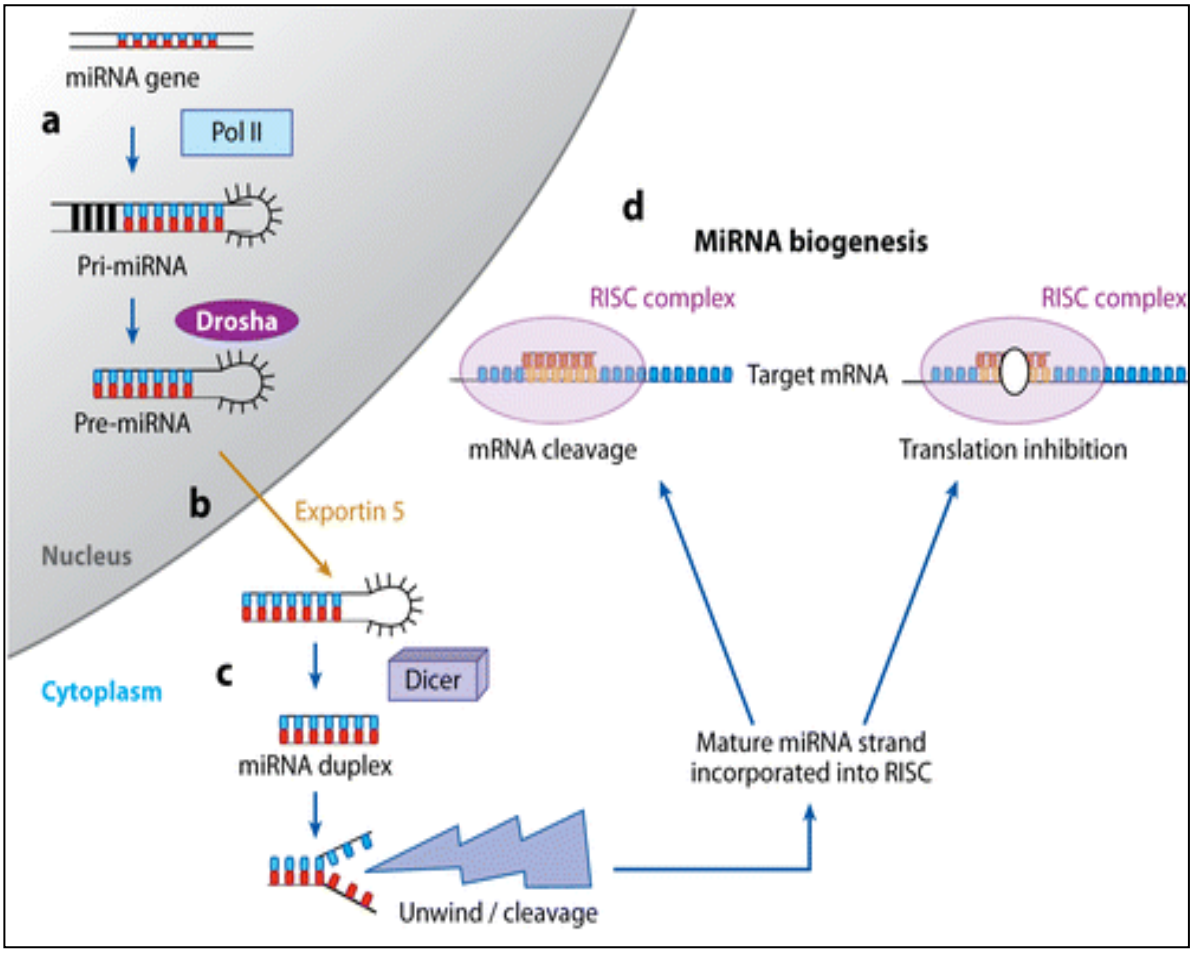

Figure 1.3: Outline of the steps involved in microRNA biogenesis (reproduced from Garzon *et al.* 2009)

MicroRNA genes are transcribed in the nucleus to produce a long nucleotide sequence (Primary microRNA). This molecule is tthen further processed by the Drosha enzyme into a precursor miRNA. The resulting molecule undergoes further processing in the cytoplasm by the Dicer enzyme and forms mature microRNA. The binding of mature miRNA with the RISC complex causes either mRNA cleavage or inhibition of translation (Garzon *et al.* 2009).

1.5 miRNA Regulation

MiRNAs regulate the expression by mRNA degradation or inhibition of translation. Although, it remains unclear how miRNAs carry out these functions, there are several potential mechanisms that may explain their role in post-transcriptional regulation.

It is a requirement that miRNAs bind to the RISC complex in order to become functional. The RISC complex is composed of the Argonaute (AGO) family of proteins, that are the effector molecules within the process of miRNA regulation. Each Argonaute protein is composed of PAZ and PIWI, domains. The PAZ domain binds to the 3'end of single stranded RNAs, whereas PIWI binds to the 5' end (Song *et al.* 2003, Yan *et al.* 2003, Parker *et al.* 2004). Furthermore, PIWI has the ability to cleave RNA strands similarly to RNase H, with which it demonstrates its structural similarities (Rhoades *et al.* 2002, Song *et al.* 2004).

The resulting miRNA/RISC complex functions as a post-transcriptional regulator based on how it binds to individual mRNA. In plants, a majority of miRNAs bind with perfect homology to their mRNA targets (Rhoades *et al.* 2002). Conversely, human and animal miRNAs usually do not bind with perfect homology. The miRNAs bind to the 3'-UTR of an mRNA *via* a 'seed' region, which it situated at positions 2-7 in the miRNA. Perfect matching of the seed region with mRNA results in cleavage of the mRNA, while mismatching and bulges in the seed region block translation (Brennecke *et al.* 2005, Lewis *et al.* 2005).

1.6 Target Identification

miRNAs influence the expression of neumerous target genes, through their interaction with mRNA and regulation of the mRNA or protein expression. Identification of miRNA targets have been achieved either through broad prediction by computational algorithms or by specific functional assays. Target identification by computational algorithms, such as Targetscan, miRanda, miRgen, and miRdb, are predominantly based on the homology of a miRNA seed region with the 3'UTR binding site in the target gene (Bartel 2009). However, the perfect matching between miRNA seeds and binding sites in their targets are neither necessary nor sufficient for all binding mechanisms. (Metzler *et al.* 2004, Didiano *et al.* 2006, Beitzinger *et al.* 2007, Easow *et al.* 2007, Alexiou *et al.* 2009). Examples for non-

seed matches were seen in the validated target for *let-7* in *C.elegans,* such as *lin-41*, which contain a bulge within the seed region (Orom *et al.* 2008). In humans, *miR-10a* targets ribosomal protein transcripts *via* non-seed sites in the 5' UTR (Orom *et al.* 2008).

Biological experimental assays play a significant role in identifying miRNAs targets with each of them possessing its own advantages and disadvantages. Some of the commonly used methodologies are specific for validating individual targets such as; western blot, qRT-PCR and Luciferase reporter assays (Kuhn *et al.* 2008). The western blot technique determines translational regulation by examining the effect of miRNA on protein expression in cells that express the protein and cells that do not express the protein, whereas qRT-PCR identifies miRNA targets on the mRNA level only, with any changes in the gene expression identifying that this target is regulated by mRNA degradation. Furthermore, these methods are unable to discriminate between direct and indirect targets, which are deregulated in response to the deregulation of a direct miRNA target (Zhang *et al.* 2007). Alternatively, luciferase assays are dependent upon cloning of the binding site of putative target downstream luciferase reporter genes in their respective vector; thereby, the binding of endogenous or introduced miRNAs to the cloned miRNA target sequence reduces luciferase expression. This assay method can predict the direct target genes of a miRNA; however it has several disadvantages such as the determination of a cloning region and transfection techniques, in addition to being a time-consuming assay method (Lytle *et al.* 2007, Kong *et al.* 2008).

Given that individual microRNAs have the ability to regulate a number of genes, several experimental assays have evolved with the intention of screening a set of genes, targeted by a specific miRNA. Most of the reported methodologies are based on identifying the differential expression within both mRNA and proteins on the basis of variations within miRNA expression (Lewis *et al.* 2003, Thomson *et al.* 2011). Differential expression of a miRNA is attained either by miRNA transfection, which promotes miRNA overexpression, or else by knocking down endogenous miRNAs with the use of miRNA inhibitors such as antagomiRS (Krutzfeldt *et al.* 2005), miRNA sponges (Ebert *et al.* 2007) or anti-miRs (Elmen *et al.* 2008, Elmen *et al.* 2008). Several techniques have been employed in the examination of the effect of miRNA overexpression or repression on target gene expression. For instance, target identification from mRNA degradation by gene expression

profiling using expression array, remains one of the most widely employed techniques. Nevertheless, this method is unable to distinguish between direct and indirect effects (Lim *et al.* 2005) and it is associated with a false positive rate, which may result from mis-hybridization (Thomson *et al.* 2004, Chiang *et al.* 2010). Although expression array studies were informative in identifying transcriptome changes in response to miRNA regulation, they were incapable of identifying the effect of miRNAs on translational repression. Thus, other methods were employed to determine the effects on translation by identifying the miRNA changes at the protein level.

Proteomic analysis has assessed in the identification of targets resulting from translation inhibition. Stable isotope labelling with amino acids in cell culture (SiLAC) is one of the proteomic methods, and is based on the quantification of the abundance of the protein. This method relies on incorporating isotope labelled amino acid into the protein in cultured cells in comparison with normal protein. Mass spectrometry measures the mass of different proteins; providing a sensitive readout and helping to confirm the fact that a single miRNA regulates the expression of several proteins (Baek *et al.* 2008). The drawback of SiLAC assay is not only that the assay is expensive; it is also very time-consuming. Similar to gene expression arrays, proteomics method are unable to distinguish between direct and indirect miRNA targets.

To identify direct miRNA targets, immunoprecipitation of the RISC components (Argonaute), which is based on using epitope–tagged Argonaute, pull down miRNA: mRNA associated pairs (Hendrickson *et al.* 2008). The immunoprecipitated target can then be identified through microarray or else by deep sequencing (Hafner *et al.* 2010). The main drawback of this assay is that it may immunoprecipitated mRNA that are not true targets when the interactions between Ago protein and mRNA occur subsequent to cell lysis. Also, this assay depends on stable binding between miRNA- mRNA and Ago protein (Mili *et al.* 2004).

Despite advancements of in our knowledge within this field, many miRNAs targets have not been identified due to the lack of highly sensitive or specific techniques. Based on miRBASE relase16, Sept 2010, there are presently 1048 identified human miRNAs, with only 206 of these having validated targets either by western blot or expression array (http://mirecords.umn.edu/miRecords/). Accordingly, novel experimental assays are

urgently required for an efficient screening and validation of miRNAs targets (Thomas *et al.* 2010).

1.7 Functional characterization of miRNA

1.7.1 miRNA Regulation of the Immune System

Inflammatory response is initiated by the activation of signalling instigated by Toll-like receptors (TLRs) that are responsive to pathogen-associated molecular patterns (PAMPs) found on different classes of pathogens (Medzhitov *et al.* 1997). In response to pathogen infection, cells of the innate immune system provide a first line of defence; these cells include granulocytes, monocytes and natural killer cells (NK). Emerging evidence has identified the contribution of miRNAs in the development and function of innate immunity cells and their regulation of the TLR responses (Kawai *et al.* 2010).

Recent studies have shown a unique expression profile of miRNAs in cells of the immune system and an important role in targeting target proteins involved in the regulation of inflammation (O'Neill *et al.* 2011). Also, miRNAs have been implicated in the regulation of the immune response, inclusive of the development and differentiation of innate and adaptive immune responses (Baltimore *et al.* 2008, Lodish *et al.* 2008).

Inflammatory responses can cause deregulation of miRNA-producing transcripts and protein regulators of the miRNA biogenesis pathways that will ultimately affect the immune responses (O'Connell *et al.* 2010). KH-type splicing regulatory protein (KSRP) is a loop-binding factor that regulates several miRNAs, including *miR-155*, and assists in the rapid increase in mature *miR-155* levels seen during inflammation (Yang *et al.* 2006). Additionally, certain inflammatory cytokines, such as interferons (IFNs), can repress dicer expression and thereby adversely affecting pre-miRNA processing (Wiesen *et al.* 2009). Figure 4 shows the effect of inflammation on regulating miRNA expression.

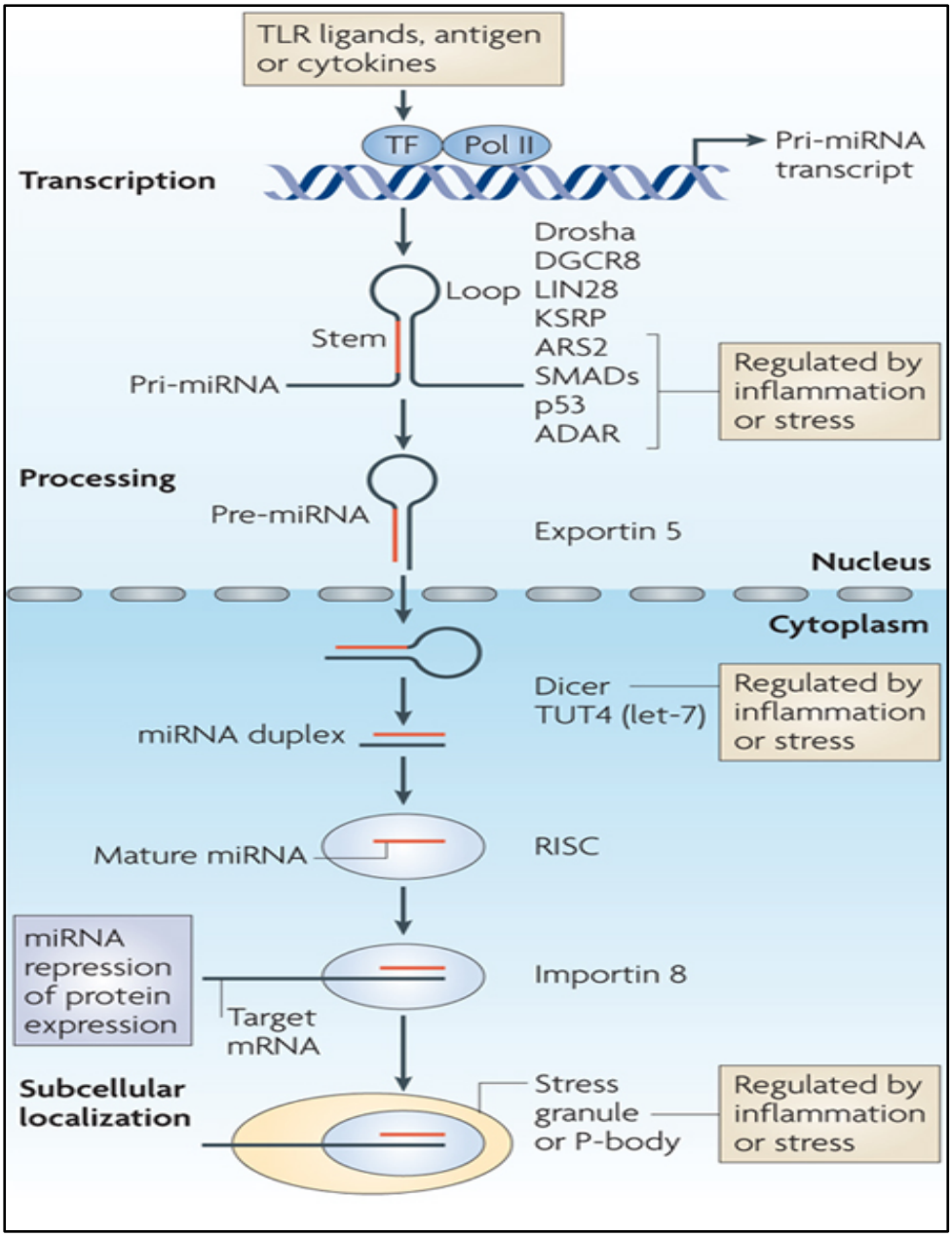

Figure 1.4: Regulation of mirRNA expression by inflammation response (reproduced from (O'Connell *et al.* 2010)

miRNA transcription is regulated by a transcription factor (TF) which is activated or repressed by Toll-Like receptors (TLRs), cytokines and antigens during immune response. Following the transcription, Pri-miRNA is processed to pre-miRNA under the regulation of multiple factors – some of these factors are influenced by inflammation. These factors include Drosha, DiGeorge syndrome critical region gene 8 (*DGCR8*), LIN28, KH-type splicing regulatory protein (KSRP), arsenate resistance protein 2 (ARS2), SMADs, *p53* and adenosine deaminase acting on RNA (ADAR). The Pre-miRNA is then transported from the nucleus to the cytoplasm by exportin 5 and processed by dicer enzyme to produce miRNA duplex. When the double strands are separated the guide strand binds with RISC, this protein is then transported by importein 8 to the complement site in mRNA leading to target repression. Finally, miRNAs can be localized to specific organelles, such as stress granules or processing (P-) bodies, some of which can be regulated by inflammation (O'Connell *et al.* 2010).

Different studies have identified the upregulation of some miRNAs such as *miR-146, miR-9, miR-147, miR-21* and *miR-155* in response to pathogen infection, following TLR activation (Taganov *et al.* 2006, O'Connell *et al.* 2007, Bazzoni *et al.* 2009, Liu *et al.* 2009, Sheedy *et al.* 2010).

Among the first miRNAs to be identified for their importance in the innate immune response to microbial infection was *miR-146*. TLR signalling leads to the upregulation of *miR-146* resulting in suppression of their targets proteins, including IL-1R associated kinase 1 (IRAK1), IRAK2 and TNFR-associated factor 6 (TRAF6) (Taganov *et al.* 2006, Hou *et al.* 2009). These proteins are an important component of the myeloid differentiation primary-response protein 88 (MYD88), which leads to nuclear factor-κB (NF-κB) activation as a result of TLR signalling – particularly of TLR2, TLR4, TLR5, TLR7, TLR8 and TLR9 that are all found to promote the expression of *miR-146* in the human acute monocytic leukaemia cell line (THP1) (Taganov *et al.* 2006). Both TRAF6 and IRAK1 molecules have been recognized for their involvement in TLR and interleukin-1 (IL-1) receptor signalling (Kawai *et al.* 2010). The association of *miR-146* with the innate immunity will be discussed later in the section on miRNAs in MDS with 5q deletion.

TLR pathways could be silenced by mRNA through the targeting of multiple TLR targets, such as signalling receptors, transcription factors, cytokines and signalling regulators, all of which are components of TLR signalling pathways (e.g. MYD88, MAL1, IRAK1, IRAK2 and TRAF6), and which bypass the excessive pro-inflammatory response toward pathogen infection by shutting down several TLR pathways. This reflects the importance of miRNAs in controlling the inflammatory response, which may result from a collaborative actions between miRNA with other well-described mechanisms (O'Neill *et al.* 2011).

Similarly, miRNAs have contributed to the regulation of the development and function of adaptive immune cells. Earlier studies on dicer deletion in T and B cells displayed the involvement of miRNAs in lymphocyte biology. In regulatory T cells (T_{regs}), the role of miRNAs in maintaining homeostasis is demonstrated by development of severe autoimmunity in mice with lineage specific deletion of dicer in T_{reg} cells that express *miR-146a*. Therefore, mice with deletion in *miR-146a* can develop a chronic inflammatory disorder (Muljo *et al.* 2005). In addition, dicer deletion in B cells caused an arrest of cell development at the pro-B cell stage (Koralov *et al.* 2008).

The importance of miRNA in the regulation of the immune responses has a potent impact in MDS, especially in low-risk MDS. Higher frequencies of natural killer cells (NK) cells and low T_{reg} number were observed in low-risk MDS as compared to high-risk MDS. Also, NK-cells mediate cytotoxicity of BM precursor cells in low-risk MDS disease (Chamuleau *et al.* 2009).

Since these initial observations, specific miRNAs have been identified in the targeting signal transduction proteins involved in TLR pathways and in intercalating immune cells development and functions, that have had a significant impact on the magnitude of the inflammatory response.

1.7.2 miRNAs in Haematological Malignancies

Given the specific role of miRNAs in the regulation of normal and leukaemic haemopoiteic proliferation and differentiation, it is of no surprise that surprise that these are a major research focus in a number of laboratories worldwide. In some haematological malignancies the reduced expression levels were obtained in association with specific genetic alterations such as chromosomal deletions (Chen *et al.* 2005). Calin *et al.* in 2002 reported the first major role of specific miRNAs in certain leukaemic subtypes. This study showed that *miR-15a* and *miR-16-1* were downregulated as a result of deletion at 13q14 in patients with chronic lymphocytic leukaemia (CLL) (Calin *et al.* 2002). Another study by Calin *et al.* was carried out to investigate the association of miRNA expression with known specific prognostic factors in CLL patients *via* miRNA microarray. Thirteen miRNAs were correlated with disease prognostic factors such as mutations in the immunoglobulin heavy-chain variable-region (IgV_H) gene or the expression of the 70-kD zeta-associated protein (*ZAP-70*) and the time between diagnosis and initial therapy (Calin *et al.* 2005).

Differential expression of miRNAs has also been recognized in other types of leukaemia. For instance, 27 miRNAs were differentially expressed between acute lymphoblastic leukaemia (ALL) and acute myeloblastic leukaemia (AML) (Mi *et al.* 2007). Moreover, differential miRNA expression in leukaemia was found in chronic myeloid leukaemia (CML), in which the *miR-17-19* cluster is induced depending on the expression of *BCR-ABL* and *c-MYC* (Venturini *et al.* 2007).

Similarly, the role of specific miRNA changes has been identified in MDS. These changes are of paramount importance in the pathogenesis of this disease and that will be discussed in more detail in the following section.

1.8 MDS and miRNA

There is growing evidence indicating that there is an association between miRNA deregulation and MDS development and progression. Some studies have provided further insight into the contribution of miRNA in MDS. For example, changes in the expression of *miR-125* and *miR-155* may induce hematopoietic stem cell (HSC) self-renewal. Furthermore, deregulation of *miR-145*, *miR-146*, *miR-150* and *miR-122* may result in anaemia, thrombocytopenia and/or neutropenia. Several studies have described apparent differential gene expression of miRNAs in MDS with the use of high throughput miRNA analysis. Other studies have also focused on studying the expression pattern of specific miRNAs in MDS. Also, further studies have provided insights into studying miRNAs residing in the commonly deleted region (CDR) in chromosome 5 in 5q- syndrome. Figure 5 shows an overview of miRNAs contribution to MDS pathogenesis (Rhyasen *et al.* 2012).

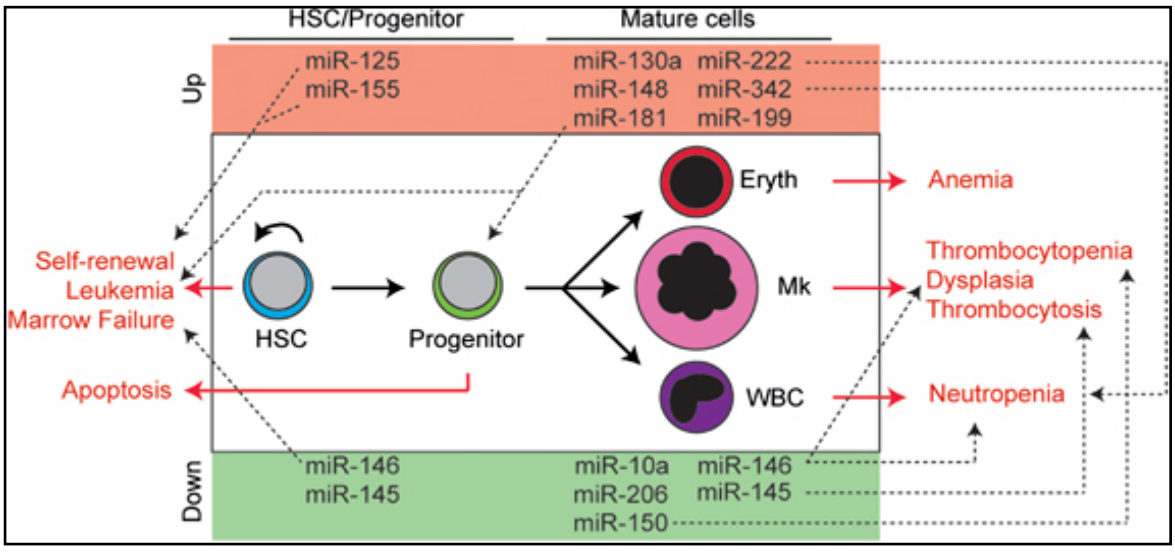

Figure 1.5: miRNAs contribution to cellular basis of MDS.

Text highlighted in red represents clinical, cellular and morphological features of MDS. The top red box includes some of the reported upregulated miRNAs in MDS and the green box includes some of the reported downregulated miRNAs. miRNAs effect in the pathogenesis of the disease is indicated by the dashed lines (Rhyasen *et al.* 2012).

1.8.1 Profiling Studies of miRNA Expression in MDS

Hussein *et al.* have published the first expression profile of miRNAs in MDS patients. (Hussein *et al.* 2010a). They examined the expression of 365 miRNAs in BM-mononuclear cells (BM-MNCs) from 24 MDS subjects with normal and abnormal karyotypes, including 5q-, -7, and +8 karyotypes in addition to three control samples. Low-density real-time PCR-based array was applied for this study. Interestingly, the authors found an association between chromosomal alteration and miRNAs regulation. The expression array used in this work included eight microRNAs located at chromosome 8, though none of these demonstrated showed any significant alteration of expression except for *miR-383 and miR-153*. In both RA/RCMB with trisomy 8 and RA/RCMB with normal karyotype, *miR-383* was upregulated. On the other hand, the overexpression of *miR-153* in association with trisomy 8 was also observed, and this finding may have previously been observed in AML cases with trisomy 8 (Garzon *et al.* 2008).

Another interesting study by Sokol *et al*. investigated miRNA expression profiles in MDS by using a high-throughput microarray platform, which analysed 290 individual miRNAs (Sokol *et al.* 2011). This study examined BM mononuclear cells from 44 MDS patients composed of 66% low/intermediate 1 and 33% high/intermediate 2 risk patient samples (based on IPSS prognostic scoring system); with 17 normal control samples were also analysed. Based on this analysis, there was an upregulation within 42 miRNAs and a downregulation in 34 miRNAs in all MDS patients and controls. Of these, 13 miRNAs (*e.g. miR-155, miR-125b* and *miR-181*) were differentially expressed between MDS and normal controls, with the majority of these have been reported previously as having a role in haematopoiesis disorders.

Further, this report showed a distinct variability in miRNA expression between low and high-risk groups, which can be used to discriminate accurately between these subtypes. Nine miRNAs were specifically upregulated (*miR-181 /b/c/d, miR-221, miR-376b, miR125b, miR-155* and *miR-130a*) and one (*miR-486-5p*) was downregulated in high risk MDS patients. Some of these miRNAs have been validated by RT-PCR and Locked nucleic acid in situ hybridization (LNA). LNAs are chemically-modified bases that confer a high melting temperature to oligonucleotides, resulting in increased affinity for its complementary sequence and thereby making it ideal for the detection of small RNA

targets). Also of interest is the fact that this study was the first investigation that showed an overexpression of *miR-155* in MDS, in accordance with the O'Connell study in murine mouse models (O'Connell *et al.* 2008).

Merkerova *et al.* also focused on using miRNA arrays (Illumina array) in studying the expression profile of miRNAs in MDS cohorts (Dostalova Merkerova *et al.* 2011). This study is one of the earliest to analyse the expression in CD34+ cells. It showed the expression of 1,145 miRNAs in CD34+ from 39 MDS and sAML in comparison with six normal control donors. Interestingly, nine out of the 22 differentially expressed miRNAs were encoded on 14q32 and these were upregulated in MDS and AML with Metachromatic leukodystrophy (MLD) patients. Moreover, this work has corroborated the suggestions and observations of other studies with regards to the discrimination between MDS subtypes based on the detected differences in the expression pattern between low and high MDS and sAML.

Finally, Erdogan *et al.* profiled 10 MDS and 10 control BM-MNCs using Agilant miRNA microarray (Erdogan *et al.* 2011). Thirteen miRNAs were differentially expressed between MDS and normal in concordance with similar studies in which some of these miRNAs *(e.g. miR-10b, miR-150* and *miR-378*) were differentially expressed between MDS and the control. These 13 miRNAs were validated by RT-PCR analysis on paraffin-embedded samples and the result has shown a high correlation of miRNA expression between the two different sample sources, *i.e.* BM-MNCs and paraffin-embedded sections.

1.8.2 Expression Analysis of Specific miRNAs in Different MDS Subtypes

One of the earliest studies was carried out in 2009 by Pons *et al.*, who examined the expression of 25 haematopoiesis-related miRNAs in the peripheral blood (PB) and bone marrow (BM) samples from 25 MDS patients and 12 controls using PCR. Twelve miRNAs were found to be overexpressed in BM in comparison with the control bone marrow sample *(miR-10a, miR-10b, miR-15a, miR-16-1, miR-17-3p, miR-17-5p, miR-18a, miR-21, miR-126, miR-155, miR-181a* and *miR-222*). Only six of the miRNAs were overexpressed in MDS-PB in comparison with the control PB, (*miR-17-3p, miR-17-5p, miR-18a, miR-15a, miR-21,* and *miR-142-3p*) (Pons *et al.* 2009). Furthermore, three of the upregulated miRNAs (*miR-17-3p, miR-17-5p* and *miR-18a*) belonged to the to the 17-19 miRNA cluster

which has been shown to be overexpressed in other cancers such as lymphomas (Mi *et al.* 2010) and are implicated in the regulation of apoptotic genes (Isken *et al.* 2008). In this study, the significant overexpression of *miR-181a* and *miR-222* was seen in 84% of patients displaying advanced stages of MDS (Pons *et al.* 2009). Differential expression of *miR-181a* has also been reported elsewhere in correlation with AML subtypes (Debernardi *et al.* 2007). In the same study, *miR-15a* and *miR-16* were differentially expressed between high and low risk patients.

There are several different studies on expression patterns of particular miRNAs in myeloid disorders by Hussein *et al.* In one of these, Hussein and his group investigated the expression of the *miR-221/miR-222* cluster, *miR-150* and *miR-155* and their targets in MDS patients (Hussein *et al.* 2010b). These miRNAs have previously reported in normal and aberrant hematopoiesis (Felli *et al.* 2005, Choong *et al.* 2007, Bruchova *et al.* 2008, O'Connell *et al.* 2008). Formalin-fixed and paraffin-embedded bone marrow samples were retrieved from 52 MDS patients at different stages, based on WHO classification, in addition to 11 secondary AML and 20 control patients. These were analysed using the Taq Man array human microRNA expression assay. Overall, *miR-155* expression was not significantly changed in MDS subjects and that contradicting the O'Connell's study (O'Connell *et al.* 2008), where upregulation of this miRNA had induced MDS development in a murine mouse model.

Furthermore, cytogenetic abnormality did not correlate with differences in the expression pattern of the *miR-221/miR-222* cluster, *miR-150* and *miR-155* in MDS, or in sAML cases with complex karyotypes. The *miR-221/miR-222* cluster showed similar expression patterns in both control and MDS, while in sAML only *miR-221* was downregulated. This observation contradicts Pons' finding with regard to the upregulation of *miR-222* in sAML (Pons *et al.* 2009). The Takada *et al.* study of AML cases also did not show a differential expression of *miR-221,* however in this study *miR-142* was overexpressed in AML cases that evolved from MDS (Takada *et al.* 2008).

In contrast to the Hussein study (Hussein *et al.* 2010b), there are other studies that indicate some correlation between cytogenetic abnormality and miRNA regulation. Bousquet *et al* examined the expression of *miR-125b* (located at chromosome 11q23) in AML and MDS patients with translocation between chromosome 2 and chromosome 11, t(2;11)(p21;q23),

when compared with MDS and AML patients without translocation and with healthy individuals (Bousquet *et al.* 2008). Only in the subjects with t(2;11)(p21;q23) *miR-125* was overexpressed. Another significant correlation of chromosomal abnormality with miRNA expression was also detected in AML patients with trisomy 8, which is one of the commonest abnormal karyotypes in MDS. It has been found that *miR-30d, miR-124a* and *miR-153*, encoded on chromosome 8 are upregulated in MDS patients with trisomy 8 (Garzon *et al.* 2008).

1.8.3 Expression Analysis of miRNAs in MDS with 5q deletion

The 5q− syndrome is a subtype of myelodysplastic syndrome (MDS), characterized by a macrocytic anaemia, a normal or elevated platelet count and hypoplastic erythropoiesis megakaryocytes. Deletion in 5q results in haploinsufficiency of genes mapping to the CDR at 5q31-5q32 (Giagounidis *et al.* 2006). Expression patterns of the miRNAs residing within the deleted region have been investigated in different studies.

Depletion of *miR-143, miR-145, miR-146a* and *miR-378* were seen in different studies of MDS patients with 5q-, thereby suggesting that the contribution of these particular miRNAs to 5q- syndrome phenotype (Oliva *et al.* 2010, Starczynowski *et al.* 2010a, Kumar *et al.* 2011, Sokol *et al.* 2011, Votavova *et al.* 2011). However, no differences in the expression of these miRNAs were seen in the studies by Hussein *et al.* and Boultwood *et al.* in MDS cases with -5q (Boultwood *et al.* 2007, Hussein *et al.* 2010a).

Additionaly, the Starczynowski *et al*. found a significant reduction in the expression of *miR-145* and *miR-146a* in MDS with 5q deletion in comparison to other MDS subtypes (Starczynowski *et al.* 2010a). As consequence of this, there was an obvious increase in the TIRAP and TRAF6 protein expression, the targets of *miR-145* and *miR-146a,* respectively. The elevated expression of these targets has been previously encountered in MDS (Hofmann *et al.* 2002, Gondek *et al.* 2008, Starczynowski *et al.* 2008). In addition, the effect of target amplification enhances innate immune signalling pathways and this leads to the development of 5q- MDS features such as a raised platelet count, megakaryocytic abnormalities and neutropenia. Thus, these observations will emphasise the significant involvement of TIRAP and TRAF6 in myelopoiesis (Starczynowski *et al.* 2010a).

Another study by Kumar *et al.* demonstrated low expression of *miR-145* in MDS with 5q- (Kumar *et al.* 2011). This study also demonstrated that the deregulation of *miR-145* alters megakaryocyte production. Furthermore, this study has shown that the overexpression of *miR-145* is associated with the reduced expression of Friend leukaemia integration 1 transcription factor (*Fli-1*) gene. *Fli-1* is known for its role in megakaryopoiesis and its overexpression can lead to myeloid malignancies.

Knockdown of *miR-145* and *miR-146a* in mouse hematopoietic stem/progenitor cells (HSPCs) leads to overexpression of TRAF 6, mediating the increase in IL-6 expression. The overexpression of interleukin 6 (IL-6) was observed in MDS patients particularly in 5q- subtype (Starczynowski *et al.* 2010d, Kumar *et al.* 2011). IL-6 is a pleotropic cytokine that induces megakaryocyte proliferation, differentiation and platelet formation (Kishimoto 2005). Therefore, IL-6 is being postulated as a target of lenalidomide in 5q- syndrome; lenalidomide suppresses the expression of IL-6 either by overexspressing *miR-145* or *miR-146a* or else by inhibiting TRAF 6 expression (Corral *et al.* 1999).

In one of Hussein studies, *miR-150* was overexpressed in MDS with 5q deletion in comparison with normal controls (Hussein *et al.* 2010b). Downregulation of this miRNA has been observed in erythroid differentiation in various studies (Choong *et al.* 2007, Guglielmelli *et al.* 2007) and the upregulation shown here might contribute to disease progression *via* the suppression of erythropoiesis. Furthermore, a significant inverse correlation between *miR-150* expression and its target *MYB* (myeloblastosis) was also observed. Moreover, the 5q- syndrome has also been correlated with the overexpression of *miR-125*. It was reported by Bousqute *et al.* that miR-125 is accumulated in RAEB and AML subjects with t(2;11)(p21;q23) in addition to 5q- (Bousquet *et al.* 2008). Table 5 and Table 6 summarises the downregulated and upregulated miRNAs in MDS patients, respectively.

Table 1.5: Downregulated miRNAs in MDS (Rhyasen and Starczynowski 2012)

miRNA	Chromosome	MDS subtype	References
miR-197	1p13.3	All MDS	Sokol et al, 2011
miR-128b	2q21.3, 3p22.3	Del(5q)	Merkerova et al,2011
miR-1284	3p14.1	All MDS	Erdogan et al, 2011
miR-95	4p16.1	Del(5q)	Votavova et al, 2010
miR-1305	4q35.1	All MDS	Erdogan et al, 2011
miR-583	5q15	All MDS	Merkerova et al,2011
miR-143	5q33.1	Del(5q), RA/RCMD(tri8)	Hussein et al, 2010
miR-145	5q33.1	Del(5q), RA/RCMD(tri8)	Hussein et al, 2010,Starczynowski et al, 2010, Oliva et al, 2010, Kumar et al,2010
miR-146a	5q33.3	Del(5q), all MDS	Sokol et al, 2011,Votavova et al, 2010, Starczynowski et al, 2010, Oliva et al,2010
miR-206	6p12.2	Del(5q), all MDS	Hussein et al, 2010, Sokol et al, 2011
miR-93	7q22.1	RA/RCMD(tri8)	Hussein et al, 2010
miR-182	7q32.2	Del(5q)	Hussein et al, 2010
miR-335	7q32.2	Del(5q), RA/RCMD(tri8)	Votavova et al, 2010
miR-124	8p23.1	All MDS	Sokol et al, 2011
miR-875-5p	8q22.2	All MDS	Sokol et al, 2011
miR-30d	8q24.22	RA/RCMD(tri8)	Hussein et al, 2010
miR-661	8q24.3	RA/RCMD(tri8), del(5q)	Hussein et al, 2010
let-7a	9q22.32, 11q24.1, 22q13.31	All MDS	Sokol et al, 2011
miR-326	11q13.4	All MDS	Sokol et al, 2011
miR-940	16p13.3	All MDS	Merkerova et al,2011
miR-423-5p	17q11.2	All MDS	Merkerova et al,2011
miR-10a	17q21.32	Del(5q), low-risk MDS, CMML	Sokol et al, 2011, Merkerova et al,2011, Votavova et al, 2010,Hussein et al, 2010
miR-196a*	17q21.32, 12q13.13	All MDS	Merkerova et al,2011
miR-150	19q13.33	Del(5q), all MDS	Sokol et al, 2011, Erdogan et al, 2011, Hussein et al, 2010
miR-520c	19q13.41	Del(5q)	Votavova et al, 2010
miR-525-5p	19q13.41	All MDS	Merkerova et al,2011
miR-507	Xq27.3	All MDS	Merkerova et al,2011

Table1.6: Upregulated miRNAs in MDS (Rhyasen and Starczynowski 2012)

miRNA	Chromosome	MDS subtype	References
miR-34a	1p36.23	Del(5q)	Votavova et al, 2010
miR-9	1q22, 5q14.3, 15q26.1	Del(5q)	Hussein,2010
miR-214	1q24.3	Del(5q)	Hussein,2010
miR-181	1q31.3	High-risk MDS, low-risk MDS	Sokol et al, 2011, Pons et al,2009
miR-29c	1q32.2	Del(5q), RA/RCMD (tri8)	Votavova et al, 2010
miR-378	5q33.1	Del(5q)	Hussein,2010
miR-133b	6p12.2	Del(5q)	Hussein,2010
miR-206	6p12.2	Del(5q), all MDS	Hussein,2010,Sokol et al, 2011
miR-148a	7p15.2	Del(5q)	Hussein,2010, Votavova et al, 2010
miR-335	7q32.2	Del(5q), RA/RCMD (tri8)	Votavova et al, 2010
miR-29a	7q32.3	Del(5q)	Hussein,2010
miR-486	8p11.21	Del(5q)	Votavova et al, 2010
miR-320	8p21.3	All MDS	Sokol et al, 2011
miR-548d	8q24.13, 17q24.2	Del(5q)	Hussein,2010
miR-151	8q24.3	Del(5q)	Votavova et al, 2010
miR-24	9q22.32, 19p13.12	Del(5q)	Votavova et al, 2010
miR-199b	9q34.11	Del(5q)	Votavova et al, 2010
miR-126	9q34.3	Del(5q)	Merkerova et al,2011
miR-130a	11q12.1	High-risk MDS, del(5q)	Sokol et al, 2011, Merkerova et al,2011
miR-100	11q24.1	All MDS	Sokol et al, 2011
miR-125b	11q24.1, 21q21.1	Del(5q), t(2;11), high-risk	Hussein,2010, Sokol et al, 2011,Merkerova et
miR-15a	13q14.3	Low-risk MDS	Pons et al,2009
miR-16	13q14.3, 3q26.1	Low-risk MDS	Pons et al,2009
miR-342	14q32.2	Low-risk MDS, del(5q)	Hussein et al,2010, Erdogan et al, 2011
miR-299-	14q32.21	All MDS	Merkerova et al,2011
miR-299-	14q32.21	All MDS	Merkerova et al,2011
miR-329	14q32.31	All MDS	Merkerova et al,2011
miR-370	14q32.31	All MDS	Merkerova et al,2011
miR-376	14q32.31	High-risk MDS	Sokol et al, 2011
miR-409-	14q32.31	All MDS	Merkerova et al,2011
miR-431	14q32.31	All MDS	Merkerova et al,2011
miR-432	14q32.31	All MDS	Merkerova et al,2011
miR-494	14q32.31	All MDS	Merkerova et al,2011
miR-654-	14q32.31	All MDS	Merkerova et al,2011
miR-665	14q32.31	All MDS	Merkerova et al,2011
miR-497	17p13.1	Del(5q)	Hussein,2010
miR-451	17q11.2	Del(5q)	Votavova et al, 2010
miR-17-92	17q13.3	Low-risk MDS	Pons,2009
miR-196a	17q21.32	All MDS	Sokol et al, 2011
miR-10a	17q21.32	Del(5q), low-risk MDS,	Sokol et al, 2011, Merkerova et al,2011, Votavova
miR-1	18q11.2, 20q13.33	Del(5q)	Hussein et al,2010
miR-133a	18q11.2, 20q13.33	Del(5q)	Hussein et al,2010
miR-199a	19p13.2, 1q24.3	Del(5q)	Hussein et al,2010, Votavova et al, 2010
miR-125a	19q13.33	Del(5q)	Hussein et al,2010,Merkerova et al,2011
miR-99b	19q13.33	Del(5q)	Votavova et al, 2010
miR-150	19q13.33	Del(5q), all MDS	Sokol et al, 2011, Erdogan et al, 2011 Metcalf et al,
miR-155	21q21.3	High-risk MDS, low-risk MDS	Sokol et al, 2011,Pons et al,2009
miR-221	Xp11.3	High-risk MDS	Sokol et al, 2011
miR-222	Xp11.3	Low-risk MDS	Sokol et al, 2011, Pons et al,2009
miR-452	Xq28	Del(5q)	Hussein et al,2010

1.9 MDS with Monosomy 7/7q-

Monosomy 7/7q- is a common feature of MDS and occurs in 10-15% of MDS patients (Toyama *et al.* 1993a). Moreover, monosomy 7 is commonly seen in children with MDS with a frequency of 50% and is clearly seen as a single chromosomal anomaly, while, it also appears regularly in adults in conjunction with other complex aberrations (Luna-Fineman *et al.* 1995, Kardos *et al.* 2003). The presences of chromosome 7 alterations are associated with poor prognosis, disease progression as well as weak response to treatment (Borgstrom *et al.* 1980, Yunis *et al.* 1986, Horiike *et al.* 1988, Schiffer *et al.* 1989).

The precise location of the deletions in the long arm of chromosome 7 with specific break points has not, as of yet, been determined and it is still unclear if the break point recognition has any prognostic significance. Earlier studies have shown that deletions are interstitial, with a maximum segment length from 7q22-7q36. Conventional cytogenetic analysis and FISH have been commonly employed to detect the precise location of the deleted segment. The commonly deleted segments (CDS) that have been predicted are: 7q22 (Kere *et al.* 1987, Kere *et al.* 1989a, Kere *et al.* 1989b, Kere 1989c, Pedersen-Bjergaard *et al.* 1990, Lewis *et al.* 1996), 7q32-34 (Horiike *et al.* 1988), 7q32-qter (Pedersen-Bjergaard *et al.* 1990), 7q22-7q36 (Johansson *et al.* 1993) and 7q35-q36 (Dohner *et al.* 1998). A number of solid tumours also show interstitial deletions in 7q at different breakpoints (7q11, 7q22 and 7q31) and this has strengthened the belief of the possible presence of tumour suppressor genes on 7q (Liang *et al.* 1998, Tosi *et al.* 1999) (Zenklusen *et al.* 1996). For instance, *CAVEOLIN-1* is one of the genes that are localized on the predicted deleted region in 7q31.1, which has been identified as a tumour suppressor gene (Hurlstone *et al.* 1999).

There was no specific genetic alteration associated with chromosome 7 abnormalities in MDS, until the discovery of acquired UPD in the q arm of chromosome 7 in MDS/MPN patients through the application of SNPa in different studies (Gondek *et al.* 2008, Heinrichs *et al.* 2009, Ernst *et al.* 2010). The Ernst *et al.* study focused on screening the region of UPD to look for other genetic alterations within the UPD region with the use of SNPa and aCGH. This study determined the minimal deleted region (MAR) in 12 patients with 7q deletion to be 7q22.3-7qter (qter: the end of the q arm). Based on SNPa and aCGH predictions, a microdeletion in 7q36.1 was detected and aCGH result showed that

microdeletion encompasses *EZH2,* chromosome 7 open reading frame 33 (*C7orf33)*, Cullin-1 (*CUL1)*. Figure 6 showes UPD in chromosome 7 based on SNPa and micro-deletion detection in 7q36.1. Furthermore, this study focused on the screening of *EZH2* that has been found in association with myeloid malignancies (Simon *et al.* 2008). *EZH2* mutation was identified in nine out of 12 individuals with acquired UPD in chromosome 7. In addition, another study by Nikoloski *et al.* has predicted *EZH2* in MDS patients and this study showed that patients with abnormal chromosome 7, who have *EZH2* mutation, have a poor prognosis and a decreased overall survival (Nikoloski *et al.* 2010).

The role of gene(s) localized on the CDS in the pathogenesis of MDS is still unclear. However, Homobox gene clusters are located in chromosome 7 and encode DNA binding transcription factors, which are themselves involved in cell differentiation and stem cellular haematopoiesis. A member of this cluster, *HOXA9* is highly expressed in CD34+ cells of MDS patients when compared with healthy controls. This gene is considered as one of the poor prognostic markers (Bei *et al.* 2005). Such genetic changes may alter the regulation of microRNAs.

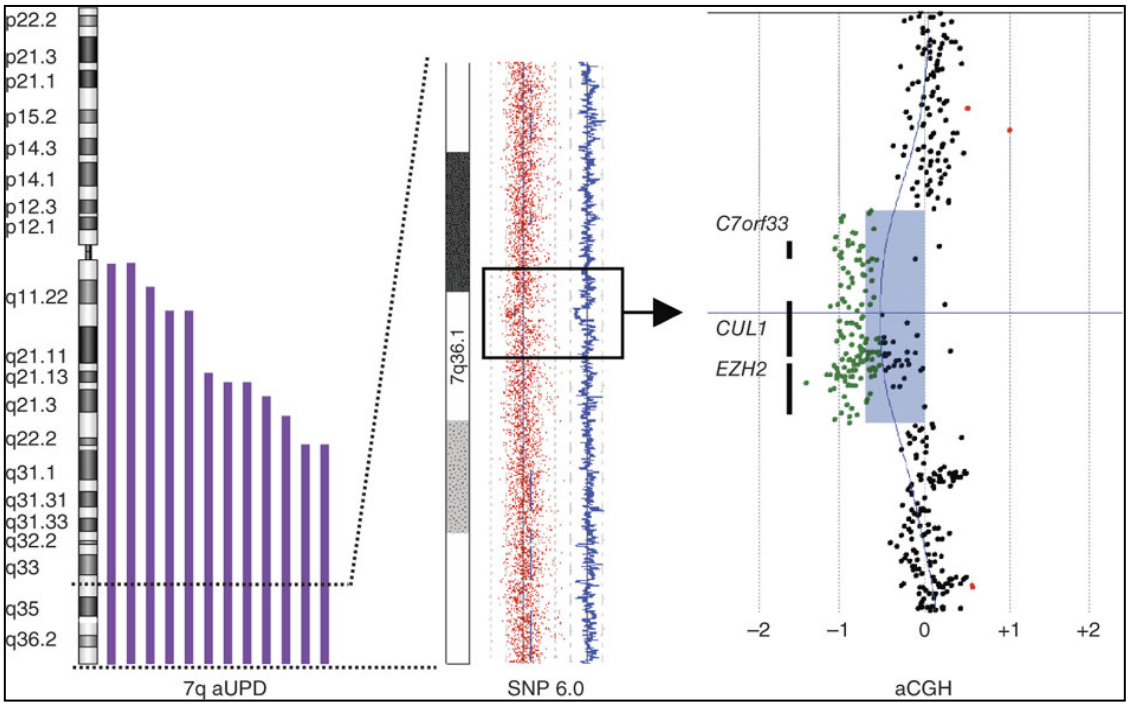

Figure 1.6: Detection of micro-deletion by SNP array and aCGH in chromosome 7 in MDS patients.

On the left side, SNP array detects UPD in the 7q in 12 individuals with MDS/MPN. The centre shows the detection of micro-deletion at 7q36.1 in one individual by SNP array. The right of the figure depicts the detection of the microdeletion by aCGH which showed that the deletion encompassing *EZH2, CLU1, C7orf33* (Ernst *et al.* 2010).

1.10 miRNA Expression in MDS with Monosomy 7/7q-

Despite the contribution of miRNAs in MDS pathogenesis, especially in their reported role with regard to 5q- syndrome, the association between microRNAs and chromosome 7 abnormalities remain ambiguous (Garzon *et al.* 2008, Takada *et al.* 2008, Pons *et al.* 2009, Hussein *et al.* 2010b). On the basis of the most contemporary release of the miRbase resource, as of November 2011, there are 67 validated miRNAs on human chromosome 7, 44 being situated on the q arm, and 29 being located within the predicted deleted segment by SNP array (q22-qter). (These data were obtained from: http://miRecords.umn.edu/miRecords/).

From all the studies of the expression patterns of miRNAs in MDS and AML, there was no clear evidence of a correlation between miRNA expression in MDS and the occurrence of monosomy 7/7q- in patients with MDS. However, there is only one study that examined the expression of some of chromosome 7 miRNAs in relation to other disorders. Chigrinova *et al,* 2010 profiled DNA, RNA and miRNA from patients with diffuse large-B-cell lymphoma (DLBCL) who also possessed 7q+ (19%) though without 7q+ abnormality (Chigrinova *et al.* 2011). As expected overexpression of chromosome 7 miRNAs, *miR-96, miR-182, miR-589, miR-25, miR-339, miR-489, miR106B* and *miR-29a,* were present in DLBCL.

Other studies too have detected a deregulation in some of chromosome 7 miRNAs utilizing expression profiling of hundreds of miRNAs in different diseases. For instance, *miR-25,* localized to 7q22.1*,* was upregulated in mantle cell lymphomas in comparison with normal B-cells (Di Lisio *et al.* 2010). Furthermore, *miR-96*, localized to 7q32.2, is upregulated and has been associated with carcinogenesis (Myatt *et al.* 2010). Also, *miR-489* and *miR-653*, localized to 7q21.3, were deregulated in diffuse large B-cell lymphoma (Li *et al.* 2009).

Some miRNAs within chromosome 7, particularly *miR-29*, were found to be significantly deregulated in different disorders in several independent studies. A study by Ruiz-Ballesteros *et al.* has shown a downregulation of *miR-29a/, miR-29b-1*, 7q32.3, in patients with splenic marginal zone lymphoma (SMZL) that was considered as a B-cell malignancy lymphoma with deletion 7q32 (Mateo *et al.* 1999, Ruiz-Ballesteros *et al.* 2007). This study also reported the potential role of losing *miR-29a/ miR-29b* on the upregulation of *TCL1A,*

T-cell leukemia/lymphoma protein 1A. Interestingly, *miR-29a / miR-29b* were both downregulated in SMZL subjects with 7q deletions. This result implies the contribution of this deletion in haematological neoplasm and emphasises the biological importance of this region, which including *miR-29a/ miR-29b,* and *TCL1A* in MDS with -7/7q-.

In 2009, Garzon *et al*, presented another significant observation on the impact of *miR-29b* expression on AML *via* DNA methyl transferases (DNMTs). Expression of *miR-29b* induces DNA hypomethylation resulting in a decrease in the expression of *DNMT3A* and *3B* along with re-expression of cyclin-dependent kinase inhibitor 2B *(CDKN2B)* and estrogen receptor 1 (*ESR1)*. Similarly, it was reported that *miR-29b* decreased the expression of *DNMT1* indirectly through the reduction of Sp1 expression, a known transactivating factor of the *DNMT1* gene that is involved in the cell cycle, proliferation, apoptosis, and malignant transformation (Garzon *et al.* 2009).

Furthermore, the formally discussed Hussein *et al.* (2010a) study, found 13 miRNAs encoded by chromosome **7** detected by miRNAs array (Hussein *et al.* 2010a). These miRNAs are : *miR-96, miR-339, miR-182, miR-93, miR-25, miR-106b, miR-196b, miR-550, miR-148a, miR-153, miR-29a, miR-183* and *miR-335*. They were downregulated in RAEB-2 with monosomy 7 as well as with the normal karyotype. Table 7 shows some studies that have identified an association between some of chromosome 7 miRNA and haematological malignancies.

Hence, the identification of the deregulated miRNAs and their target genes might help with regards to developing an understanding of the dysregulation of haematopoiesis in patients with monosomy 7/7q-.

Table 1.7: Studies on miRNAs localized to chromosome 7q.

MIRNAs	Function	References
miR-29a/miR-29b1	Down regulation in patients with splenic marginal zone lymphoma (SMZL) which is considered to be a B-cell malignancy lymphoma	Ruiz-Ballesteros, 2007
miR-106b	Overexpression in multiple myeloma	Pichiorri *et al,* 2008
miR-29b	Decrease the expression of *DNMT1* indirectly by the reduction of *Sp1* expression, a known transactivating factor of the *DNMT1* gene that is involved in the cell cycle, proliferation, apoptosis, and malignant transformation	Garzon, 2009
miR-489	Deregulated in diffuse large B-cell lymphoma (DLBCL)	Cheng Li et al , 2009
	Changes in Zinc finger protein growth factor lead to loss of function and changes in myeloid development	Chinavenmeni et al,2009
miR-653	Deregulated in diffuse large B-cell lymphoma (DLBCL)	Cheng Li et al ,2009
miR-25	Upregulated in mantle cell lymphomas	Di Lisio, Gomez-Lopez et al. 2010
miR-96	Upregulation was contributed in carcinogenesis	Myatt, Wang et al. 2010
miR-595	Upregulation in relation to POX in renal cancer cell	W Liu et al, 2010
	Upregulated in $CD4^+$ in comparison to $CD8^+$ in single positive thymocyte.	Ghisi et al, 2011
miR-93, miR-106b, miR-25, miR-96, miR-29b	Downregualted in AML	Garzon et al. 2008
miR-96, miR-182 miR589, miR-25, miR-339, miR-489, miR106B and *miR-29a*	Overexpression in patients with diffuse large-B-cell lymphoma (DLBCL) with +7q	Chigrinova *et al,* 2010
miR-96, miR-339, miR-182, miR-93, miR-25, miR-106b, miR-196b, miR-550, miR-148a, miR-153 miR-29a, miR-183 and *miR-335*	Down regulated with different fold in RAEB-2 with monosomy as well as with normal karyotype	Hussein et al,2010

1.11 Project Aim

It has been established that miRNAs expression plays an important role in the pathogenesis of MDS. However, there remain several limitations within published studies of the role of miRNA's in patients with monosomy 7/7q-, which itself is a poor prognostic subgroup of MDS. Accordingly, this project studied the expression of some of chromosome 7 encoded miRNAs and identified their functional targets. However, due to the low sensitivity of the available target identification assays, a novel functional assay was developed in house by Dr. Joop Gäken will be applied within this study (Gaken *et al.* 2012). This assay has the potential for the rapid and specific detection of targets for a given miRNA, that might be of pathogenic importance in monosomy 7 disease. Therefore the aims of my thesis are:

- To use the novel function assay to identify targets for miR-595 that is localized to the terminal of chromosome 7.
- To elucidate the biological function of the identified target by deregulating the expression level of the target gene and examine the consequent effects on cellular function.
- To compare the expression level of the selected miRNA and its validated targets in MDS patients with monosomy 7/7q- along with other MDS subtypes

Chapter 2: Materials and Methods

2.1 Materials

2.1.1 PCR, Gel Electrophoresis and Sequencing Materials

Reagents	Brand
Agarose, molecular biology grade/electrophoresis grade	Melford/Sigma
BigDye® Terminator v3.1 Cycle Sequencing Kit	Applied biosystems
BigDye® XTerminator purification Kit	Applied biosystems
deoxynucleotide triphosphate mix (dNTP) (10mM)	Promega
Ethanol	Sigma
Ethidium Bromide (EB)	Sigma
Gel cleaning kit QiAEX II, gel extraction kit	Qiagen
GoTaq® Colorless Master Mix	Promega
GoTaq® Flexi DNA Polymerase (5u/µl)	Promega
Nuclease-free water	Sigma
O'Gene Ruler ladder mix (0.1µg/µl)	Fermentas
6x Orange DNA loading Dye	Fermentas
Tris Acetate-EDTA buffer (TAE buffer)	Sigma

2.1.2 DNA and RNA Extraction Materials

Reagent	Brand
Chloroform	Sigma
DNeasy blood and tissue kit	Qiagen
Dimethyl sulfoxide (DMSO)	Sigma
2-Propanol (Isopropanol)	Sigma
Ethanol	Sigma
RNeasy Micro Kit	Qiagen
Phase lock Gel Heavy 2 ml	5 PRIME
RNase free water	Qiagen
TRIzol®	Invitrogen

2.1.3 Cloning Materials

Reagent	Brand
Bacto™ agar	BD
5-bromo-4- chloro-3-indolyl-β-D-Galactoside (X-Gal)	Melford
Carbenicillin solution 100mg/ml in 50% Ethanol (10ml)	Bioline
Ligation buffer 10x buffer for T4 DNA ligase with 10 mMATP (10mM)	New England Biolab
Ligation enzyme T4 DNA ligase (400U/ml)	New England Biolab
Luria Borth (LB)	Sigma
Maxi prep kit Gen Elute plasmid maxi Prep kit	Sigma
MegaX DH10B Electrocomp™ Cells	Invitrogen
One Shot® Mach1™-T1^{R} Chemically Competent E.coli	Invitrogen

Pure Yield™ plasmid Mini prep system	Promega
Restriction endonuclease and buffer	New England Biolabs
Topo TA cloning kit dual PROMOTER pcri-Topovector	Invetrogen
Wizard® Plus SV Minipreps DNA Purification System	Promega

2.1.4 Cell Culture Materials

Reagent	Brand
Ciprofloxacin (Ciproxin)	Sigma
Coomassi brilliant stain	Sigma
Dulbecco's Modified Eagle Medium (DMEM) High glucose with (4.5 g/l) l-Glutamin, sodium pyruvate	PPA/ Life Technologies
Ethylenediaminate tetra acetic acid disodium salt 0.02% (EDTA)	Sigma
Fetal Bovine Serum (FBS)	PAA/Sigma
L-Glutamine-Penicillin – Streptomycin solution	Sigma
Phosphate buffered saline (PBS)	PPA
Rosswell Park Memorial Institute medium (RPMI 1640)	Sigma
Sodium Pyruvate solution	Sigma
Trypan Blue 0.4% , 0.85% NaCl	Lonza
TrypLE™ Express Enzyme (1x), phenol red	Gibco
Trypsin Solution (10x)	Sigma

2.1.5 Transfection Materials

Reagent	Brand
Amaxa cell line neuclofector kit V	Lonza
Amaxa cell line neuclofector Kit R	Lonza
Ganciclovir (GCV) (250 mg)	Invivo gene
Geneticin (G418) disulfite salt	Sigma
Lipofectamine® RNAiMAX Reagent	Invitrogen
Lipofectamine® LTX with Plus ™ Reagent	Invitrogen
miRIDIAN Hairpin Inhibitor, Human hsa-miR-595 (5nmol)	Thermo Scientific
Opti-MEM®I Reduced Serum Medium (Minimal Essential Medium(MEM))	Life Technologies
Polybrene	Sigma
Puromycin	Sigma
Ribosomal protein L27a siRNA (h) 10µM	Santa Cruz biotechnology
Stealth RNAi™ siRNA Negative control	Invitrogen
The RNAi Consortium (TRC) human RPL27A shRNA (4)	Open Biosystem-Thermo scientific

TRC human RPL5 shRNA(5)	Open Biosystem-Thermo scientific
TRC human RPS14 shRNA (4)	Open Biosystem-Thermo scientific
Tube Ultraclear	VWR
Zeocin (100mg/ml)	Invivo gene

2.1.6 qRT-PCR Materials

Reagent	**Brand**
FastStart Universal Probe Master 12.5 ml	Roche Diagnostic Limite
MicroAmp™ Fast Optical 96 well reactions Plate with Barcode (0.1ml)	Life technologies
SuperScript® VILO™ cDNA Synthesis Kit	Life Technologies
Primers	Integrated DNA Technologies, Sigma
TaqMan® MicroRNA Reverse Transcription kit	Life technologies
TaqMan® Universal PCR Master Mix	Life technologies
TaqMan® MicroRNA Assay (has-miR-595)	Life technologies
TaqMan® MicroRNA Assay (RNU6B: Homo sapiens RNA, U6 small nuclear 2 (RNU6-2), small nuclear RNA)	Life technologies
TaqMan® MicroRNA Assay (RNU48: Homo sapiens small nucleolar RNA, C/D box 48 (SNORD48), small nucleolar RNA)	Life technologies
Universal Probe library Probes	Roche Diagnostic Limited

2.1.7 Western Blot and IP Materials

Reagent	**Brand**
Bovine serum albumin (BSA)	Fisher Scientific
4',6-diamidino-2-phenyllindole (DAPI)	Sigma
ECL Prime Western Blotting Detection Reagent	GE Healthcare
Formaldehyde	Sigma
Hyper film ECL	GE Healthcare
2-Mercaptoethanol	Sigma
Methanol	Sigma
Mounting medium	Merk
Nitrocellulose Membrane	Invitrogen, GE Healthcare
Non fat dried milk (Marvel)	Sainsbury's
Novex sharp protein standards	Invitrogen
NuPAGE® Bis-Tris Mini Gel	Invitrogen

Nupage® LDS Sample buffer (4x)	Invitrogen
Nupage® Tris –Acetate SDS Running buffer (20x)	Invitrogen
Nupage® Transfer buffer (20x)	Invitrogen
cOmplete Protease Inhibitor Cocktail Tablets	Roche Diagnostic Limited
PBS tablet	Severn Biotech
Protein A/G Plus-Agarose Immunopreceipitation Reagent	Santa Cruz
RadioImmunoPrecipitation Assay (RIPA) Buffer	Thermo Scientific
Sample Buffer, Laemmli 2x Concentrate	Sigma
Sheep serum	Sigma
Sodium chloride (NaCl)	Sigma
Tris Base	Fisher Scientific
TWEEN®20	Sigma

2.1.8 Polyribosome Profiling Materials

Reagent	**Brand**
Cycloheximide (CHX) (20mg/ml)	Sigma
cOmplete Protease Inhibitor Cocktail Tablets	Roche Diagnostic Limited
Polymer centriguge tubes, 14x 95 mmm	Beckmen Coulter
RNAsin® Plus RNase Inhibitor (40U/ul)	Promega
Sucrose	Fisher scientific

2.1.9 Cell cycle, Apoptosis and Viability Assays Materials

Reagent	**Brand**
7-Aminoactinomycin D (7-AAD) Viability Staining Solution	BioLegand
Cell- based Assay Annexin V Binding buffer	Cayman
75% Ethanol	Sigma
Fluorescein isothiocyanate (FITC)	Sigma
Pacific Blue™ Annexin V	BioLegand
Propodium Iodide (PI)	Sigma
RNase A	Sigma
Tetrazoliumsalt[3-(4,5-Dimethylthiazol-2-yl) 2,5diphenyltetrazolium- bromide] (MTT)	Sigma

2.1.10 CD34+ Isolation, Culturing and Flow Cytometer Analysis Materials

Reagent	**Brand**
Anti-Human CD235a (Glycophorin A) APC	eBioscience
Anti-Human CD71 (Transferrin Receptor) PE	eBioscience
CD34 MicroBead Kit, human	Miltenyi Biotec
Recombinant Human Erythropoietin-α (EPO-α)	BioVision

Fixable Viability Dye eFluor® 780	eBioscience
FITC anti-human CD41	BioLegend
Histopaque 1077	Sigma
Human Interleukin-3 (IL-3) premium grade (10 μg)	Miltenyi Biotec
Human Interleukin-6 (IL-6) premium grade (10 μg)	Miltenyi Biotec
Human Thrombopoietin (TPO) Research grade (10 μg)	Miltenyi Biotec
Leukocyte cones	National Blood Transfusion Service
MACS BSA Stock Solution	Miltenyi Biotec
MACS Rinsing Solution	Miltenyi Biotec
MethoCult® H4034 Optimum (Methylcellulose Medium with Recombinant Cytokines for Human Cells)	StemCell
PerCP/Cy5.5 ant-human CD11b	BioLegend
Recombinant Human Granulocyte Colony-Stimulating Factor (G-CSF) (10 μg)	Millipore
Recombinant Human Fms-related tyrosine kinase 3 ligand (FLT3LG) (10 μg)	PeproTech
Stem cell factor (SCF), human recombinant, expressed in Escherichia coli cell culture tasted (10 μg)	Sigma
StemSpan™SFEM (Serum-Free Medium for expansion and culture of Hematopoeitic cells	StemCell

2.1.11 Plasmids

Plasmid	**Provider**
pBabePuro	Dr.Joop Gaken
p3'Tkzeo	Dr.Joop Gaken
P3xFLAG-myc-CMV-26	Dr.Joop Gaken
pSUPER.retro.neo	Dr.Joop Gaken
PLKO.1 lentiviral vector	Dr. Jie Jiang

2.1.12 Cell lines

Cell line	**Provider**	**Cell Source**
MCF7	Dr. Joop Gaken	Human breast adenocarcinoma
HeLa	Dr. Joop Gaken	Cervical cancer adenocarcinoma
HepG2	Dr. Joop Gaken	Hepatocellular carcinoma
HCT-116	Professor. Mahvash Tavassoli	Colorectal carcinoma
HCT-116 $p53^{-/-}$		Colorectal carcinoma with P53 knockout
K562	Dr.David Darling	Chronic myelogenous leukaemia
HEL	Dr.Nick Lee	Erythroleukaemia

U937	Dr. Terry Gaymes	Histiocytic lymphoma
Jurkat	Dr. Terry Gaymes	T lymphocyte
KG-1	Dr. Terry Gaymes	Acute myelogenous leukaemia

2.1.13 Antibodies

Antibody	Description	Source	Working Dilution
*Anti-RPL27A antibody *RPL27A Antibody (C-term)	*Rabbit polyclonal	*Abcam(ab74731) *Abgent (AP10937b)	1:1000
Anti-HSPA14 antibody	Rabbit monoclonal	Abcam (ab108612)	1:1000
P53 Antibody(DO-1)	Mouse monoclonal antibody	Santa cruz biotechnology (sc-126)	1:500
γTubulin (C-20)	Goat polyclonal antibody	Santa cruz biotechnology (sc-7396)	1:1000
Anti-MDM2 antibody [2A10]	Mouse monoclonal antibody	Abcam(ab16895)	1:500
Anti-RPL5 antibody	Rabbit polyoclonal	Abcam	1:500
Anti-Fibrillarin antibody	Rabbit polyclonal	Abcam (ab5821)	1:200
Phosph-Rb (Ser807/811)	Rabbit clonal	Cell signalling	1:1000
Rabbit	Anti Rabbit IgG	ECL	1:2000
Goat	Anti goat IgG	Alpha Diagnostic	1:2000
Mouse	Anti mouse IgG	ECL	1:2000

2.1.14 shRNA Sequences

shRNA Target	Sequence
Mature hsa-miR-595 Inhibitor	GAAGUGUGCCGUGGUGUGUCU
RPL27A shRNA1	GATCCCCCCACCGGATCAACTTCGACAAATCAAGAG TTTGTCGAAGTTGATCCGGTGGTTTTT
RPL27A shRNA2	GATCCCCCCTTGACAAATTGTGGACTTTGGTCAAGA GCCAAAGTCCACAATTTGTCAAGGTTTTT
RPL27A shRNA3	GATCCCCGTGAAGGCCAAATTCTTCAGCAGTCAAGA GCTGCTGAAGAATTTGGCCTTCACTTTTT
RPL27 lenti shRNA (**sh1**) TRCN0000117396	ATCGCACCACATCAATGATGG
RPL27 lenti shRNA (**sh2**) TRCN0000117392	TATTTGTCGAAGTTGATCCGG
RPL27 lenti shRNA (**sh3**)TRCN0000117395	TTCCCAGAACTTTGTAGTAGC

RPL27 lenti shRNA (**sh4**) TRCN0000117393	AACTTTCCCAAAGTAGCCTGG
RPL5 lenti shRNA (**sh1**) TRCN0000074993	TTTGTCACACGAACTATCATC
RPL5 lenti shRNA (**sh2**) TRCN0000074997	AATCGTTTGGTACTGTGAGGG
RPL5 lenti shRNA (**sh3**) TRCN0000074994	ATCTCTGTTTGTCACACGAAC
RPL5 lenti shRNA (**sh4**)TRCN0000074996	TTGGTATCTCTTAAAGTAGGC
RPL5 lenti shRNA (**sh5**)TRCN0000074995	ATCTTCTTCCATTAAGTAGCG

2.1.15 qRT-PCR Primer Sequences

Description	Sequence	Probe	Supplier
RPL27A-F	5' - ACGGGTGAATGCTGCTAAAA - 3'	32	Sigma
RPL27A-R	5' - GAAGAATTTGGCCTTCACGA - 3'		Sigma
RPS14-F	5'-GGTCCAGGGGTCTTGGTC-3'	17	Sigma
RPS14-R	5'-GGTCCAGGGGTCTTGGTC-3'		Sigma
RPL5-F	5'-CACTGGCAATAAAGTTTTTTGGTG-3'	24	Sigma
RPL5-R	5'-AACCAGGGAATCGTTTG-3'		Sigma
P53-F	5'-AGGCCTTGGAACTCAAGGAT-3'	12	Sigma
P53-R	5'-CCCTTTTTGGACTTCAGGTG-3'		Sigma
MDM2-F	5' - GACTCCAAGCGCGAAAAC - 3'	68	IDT
MDM2-R	5' - CAGACATGTTGGTATTGCACATT - 3'		IDT
CDKN1A (p21)-F	5' - TCACTGTCTTGTACCCTTGTGC - 3'	32	IDT
CDKN1A(p21)-R	5' - GGCGTTTGGAGTGGTAGAAA - 3'		IDT
Bax-F	5' - AGCAAACTGGTGCTCAAGG - 3'	69	IDT
Bax-R	5' - TCTTGGATCCAGCCCAAC - 3'		IDT
GAPDH-F	5' - AGCCACATCGCTCAGACAC - 3'	60	IDT
GAPDH-R	5' - GCCCAATACGACCAAATCC - 3'		IDT
RNU6B	CGCAAGGATGACACGCAAATTCGTGA AGCGTTCCATATTTTT	NA	Life Technologies
RNU48	GATGACCCCAGGTAACTCTGAGTGTGT CGCTGATGCCATCACCGCAGCGCTCTG ACC	NA	Life Technologies

2.1.16 Oligonucleotide Sequences

Oligo's name	Sequence	Restriction enzyme	Supplier
miR-489F	TTGGATCCTTGGTTGCATCAGTTTGTGG	EcoR1	Sigma
miR-489R	AAGAATTCAATCATGGAATTACTACTGCTTAAAA	BamH1	Sigma
miR-653F	TTGGATCCTTGAACCAATCTTGGATAGAA	Sal	Sigma
miR-653R	TTGTCGACTGGACCATTTTCTCACCATCT	BamH1	Sigma
miR-595F	AAGGATCCAGGGTGCACTGAGGAAGATG	EcoR1	Sigma
miR-595R	AAGAATTCGCCTCTGTCCATTCTCAAGC	BamH1	Sigma
miR-671F	AAGGATCCGGAGCTCCAGACCCATTTCT	EcoR1	Sigma
miR-671R	AAGAATTCGTGTGGTCATTGGAAACTG	BamH1	Sigma
miR-595F2	AGCCATCAAGATGGTCTGC	EcoR1	Sigma
miR-595R2	CCGGGACATGATGTGATTAG	BamH1	Sigma
miR-671F2	ATTTGACCGGCAGGCTTCT	EcoR1	Sigma
miR-671R2	CCTAGCCCCTCCAGGTTG	BamH1	Sigma
RPL27A-F	AGCTAGCAGGCCTTCCTTTTTCGTCTG	NheI	IDT
RPL27A-R	AGAATTCAATGAAACTCCCTCCATGTG	EcoR1	IDT

2.2 Buffer, Solutions and Media

Solution	Preparation
Blocking buffer for western blot	5%(w/v) Marvel milk powder was dissolved in 1xTBST buffer
BSA wash buffer	5g BSA was dissolved in 1L PBS
Cell cycle staining solution	400 µl of propidium iodide, 50 µl FITC, 500 µl RNase A (10mg/ml) and completed to 10 ml with PBS. Stored in dark at 4°C for up to two weeks.
Coomassie brilliant blue stain	0.25% Coomassie brilliant blue, 45% methanol, 10% acetic acid. Made up in dH_2O and stored at room temperature.
Destain solution	40%(v/v) methanol and 10% (v/v) acetic acid. Made up in dH_2O and stored at room temperature.
DMEM, complete culture medium	10% FBS, 1% sodium pyruvate and 1% L-Glutamine-Penicillin- Streptomycin Solution and stored at 4°C
EPO	500U was made up in 1 ml dH_2O and stored at -20°C
FLT3L (1000ng/ml)	Stock solution was prepared in 1ml dH_2O to a final concentration of 10µg/ml and further dilution was made for

	small working aliquots in 0.1%BSA in PBS at 1µg/ml final concentration and stored at -20°C
TPO	Stock solution was prepared in 1ml dH_2O to a final concentration of 10µg/ml and further dilution was made for small working aliquots in 0.1%BSA in PBS at 1µg/ml final concentration and stored at -20°C
G-CSF	Stock solution was prepared in 1ml dH_2O to a final concentration of 10µg/ml and further dilution was made for small working aliquots in 0.1%BSA in PBS at 1µg/ml final concentration and stored at -20°C
Freezing medium for cell culture	10% (v/v) DMSO was added to 90%(v/v) FBS and stored in -20°C
FITC	1µg/ml PBS. Stored at 4°C in the dark
GCV	10 mM stock solution was made in dH_2O and stored in the fridge
RNase A	10mg/ml dH_2O stored at -20°C
lL-3	Stock solution was prepared in 1ml dH_2O to a final concentration of 10µg/ml and further dilution was made for small working aliquots in 0.1%BSA in PBS at 1µg/ml final concentration and stored at -20°C
SCF	Stock solution was prepared in 1ml dH_2O to a final concentration of 10µg/ml and further dilution was made for small working aliquots in 0.1%BSA in PBS at 1µg/ml final concentration and stored at -20°C
lL-6	Stock solution was prepared in 1ml dH_2O to a final concentration of 10µg/ml and further dilution was made for small working aliquots in 0.1%BSA in PBS at 1µg/ml final concentration and stored at -20°C
LB medium	Prepared by suspending of 10 g of LB in 500 ml of dH_2O. The solution was autoclaved and stored at room temperature.
Ampicillin LB agar plates	LB Agar plate was prepared by dissolving 10g of LB and 7.5 g Agar in 500ml dH_2O. After autoclaving, the solution was allowed to cool to 50°C; 500 µl of carbenicillin (1µg/ml) was added. Then poured into sterile 100mm dishes at room temperature and stored at 4°C.
MTT	5 mg/ml was made by dissolving MTT powder in PBS. The solution was filtered under sterile and small aliquot was frozen and stored at -20°C in dark.
4% paraformaldehyde	40 g of paraformaldehyde powder was mixed with 40 ml PBS, heated at 60°C. To dissolve completely, the pH was adjusted with 1 N NaOH until the solution clears. Then, the volume was completed to 50ml with PBS and the solution was stored at 4°C.
PBS	10 PBS tablet (phosphate buffer, potassium chloride0.02%(w/v), sodium chloride 0.8%(w/v)) dissolved in 1L dH_2O. Stored at room temperature.
DNA Loading dye	The solution was made up in dH_2O and composed of

	30%(v/v) glycerol and 0.25% (w/v) Orange R. Stored at room temperature.
Puromycin	1mg/ml working solution was made in dH_2O from10 mg/ml stock solution.
Primary antibody (for western blot)	Primary antibodies were diluted in the blocking buffer with milk or in PBS with1% BSA and stored at 4°C. Sodium Azid (10µl/ml) was added for longer storage.
Secondary antibody (for western blot)	Secondary antibody was diluted in the blocking buffer with milk or in PBS with1% BSA. Antibody freshly made prior to use.
RPMI 1640, complete culture medium	10% (v/v) FBS, 1% (v/v) sodium pyruvate and 1% L-Glutamine-Penicillin- Streptomycin Solution. Stored at 4°C.
1x MES SDS Running buffer	Buffer made by 1: 20 dilution of 20x Running buffer in dH_2O. The 1x Solution composed of 50mM MES, 50mM Tris Base, 0.1% SDS and 1mM EDTA with pH7.3. The solution was stored at room temperature and used several times within a period of 3 weeks to 1 Month.
1 x Transfer buffer	For 1L of 1x transfer buffer 50 ml of 20x transfer buffer was mixed with 20%(v/v) methanol and completed to 1L with dH_2O. The 1x solution composed of Bicine, 25mMBis-Tris and 1mM EDTA, pH7.2. Solution was prepared freshly.
2 x Sample buffer for western blot	20% (v/v) NuPAGE LDS Samples Buffer (4 x), 10% (v/v) β- mercaptoethanol were made up in dH_2O and stored at -20°C.
10 xTBS (Trsi -buffered saline) buffer	12.11 g of 100 mM Tris-base was mixed with 87.66g of 1.5M NaCl and made up in 1L of dH_2O. The solution stored at room temperature.
1xTBST(1xTBS/0.1% Tween-20) western blot washing buffer	The solution was prepared by mixing 100 ml of 10 x TBS with 1 ml of Tween-20 and completed the volume to 1L with dH_2O. Solution was stored at 4°C to avoid bacterial contamination.
Solubilisation buffer for MTT assay	The solution was prepared by mixing 10% (v/v) Triton X-100 with 90% (v/v) Isopropanol and 2 drops of HCl 37% (12M). Stored at room temperature.
1xTAE (Tris Acetate-EDTA)	Concentrated buffer powder (10x) was dissolved in 1L of dH_2O to produce 1x TAE with 40mM Tris-acetate and 1 mM EDTA. The solution was stored at room temperature.
X-Gal	20 mg of X-Gal was dissolved in 1 ml of dimethylformamide (DMF) to make a final concentration of 20 mg/ml. The solution was stored at -20°C.
RIPA buffer	50 mM Tris pH7.4, 150 mM NaCl, 1% (v/v) Triton X-100, 0.1% (w/v) SDS, 0.1%(v/v) Deoxycholate and made up in dH_2O.
Immunoprecipitation (IP) buffer	50mM Tris-HCl pH8.0, 0.5% (v/v) NP-40, 1mMEDTA,150 mM NaCl, 1mM phenylmethanesulfonyl fluoride (PMSF) and made up in dH2O. Prior to use protease inhibitor tablet was dissolved in 50 ml of the buffer.
10-50% (w/v) Sucrose	0.5 ml of 1M Tris-HCl pH7.4 was mixed with 2.5 ml of 1.5

Solution (50 ml)	M KCl, 75µl of 1M $MgCl_2$ and 5g (10%) or 25g (50%) of sucrose. The solution was made up to 40 ml with dH_2O, mixed well and was boiled in the water bath for 10 minutes to dissolve the sucrose. After cooling to room temperature, the solution was completed to 50 ml with dH2O and filtered through 0.45micron filter cup.
55% (w/v) sucrose	27.5 g was dissolved in 50 ml dH_2O.
2xRSB (150 ml)	3 ml of 1M Tris-HCl pH7.4 was mixed with 3 ml of 1M NaCl and 450 µl of 1M $MgCl_2$, solution was made up to 150ml with dH_2O.
Protease Inhibitors (100x)	1 tablet was dissolved in 500 µl.
Polysome lysis buffer	Solution was made by mixing 375 µl of 2 x RSB, 300 µl of 10% (v/v)Triton X, 300 µl of 5% Deoxycholate, 37.5 µl of 4mg/ml CHX,15 µl of Protease Inhibitors (100x), 18.75 µl of RNAsin and made up to 1.5ml with dH2O

2.3 Method

2.3.1 Polymerase chain reaction (PCR)

2.3.1.1 Oligonucleotide primers

The microRNA primers were designed based on the primary sequence of the miRNA (80-100bp) which was obtained from miRbase web resource (http://www.miRbase.org/). This sequence was blast analysed *via* NCBI nucleotide Blast (http://www.ncbi.nlm.nih.gov/) to find the complementary genomic region to the miRNA sequence, and ~4Kb size was selected. Primer3 software (http://frodo.wi.mit.edu/) was used to design primers for the amplification of ~1Kb fragment containing the miRNA. Restriction sites were incorporated into the primers sequences to facilitate cloning; enzymes were selected based on NEB cutter from New England Bio Lab database (http://tools.neb.com/NEBcutter2/index.php). miRNA Primers are listed in (2.1.16).

Other oligonucleotide primers were designed to anneal to template genomic DNA using Primer3 software. DNA sequences were obtained from NCBI-gene (http://www.ncbi.nlm.nih.gov/gene). Also, for the cloning of the generated PCR products, the endonuclease restriction sites were incorporated in the primers sequences and they were selected based on the NEB cutter as explained previously for the miRNA. Oligonucleotide primers were dissolved in Nuclease free water at a final concentration of 100µM.

2.3.1.2 DNA amplification *via* PCR

For PCR amplification, genomic DNA from human cell lines was used to obtain genomic fragments. The PCR reaction mixtures were setup as illustrated in Table 2.1. Primer concentrations were adjusted to 100µM based on the oligodeoxynucleotide quality assurance document provided with the freezdried oligo's.

PCR reactions were carried out using a Thermocycler (Applied biosystem), with appropriate cycling conditions for each primer, as shown in Table 2.2. Subsequently, PCR products were checked on an 0.8-1 % (w/v) agarose gel which is described in the following section.

Table 2.1: PCR reaction mixture

Component	**Amount**
Template DNA (10-100 ng/µl)	≈2 µl
5x PCR buffer	10 µl
$MgCl_2$	5 µl
0.25 mM dNTP-mix	1 µl
Forward primer (0.2µM)	0.2 µl
Reverse primer (0.2µM)	0.2 µl
Go Taq DNA polymerase	0.25 µl
H_2O	(to 50 µl)
Total	50 µl

Table 2.2: PCR cycle conditions

Stage	**Temperature**	**Duration**	**Cycles**
1	95°C	5 min	1
2	95°C As appropriate for the primers used 72°C	1 min 45 sec 2.30 min	X40
3	72°C	5 min	1
4	4°C	Infinity	-

2.3.2 Gel Electrophoresis and DNA Purification

2.3.2.1 Agarose gel electrophoresis

PCR products were run on an 0.8-1% (w/v) agarose gel prepared in 100 ml of 1 x TAE. The agarose was dissolved by heating the mixture to boiling point until it dissolved completely. After the agarose solution had cooled down to hot at the touch, ethidium bromide (0.08mg/ml) was added to allow visualization of DNA fragments under UV light. The edges of the electrophoresis tray were sealed with tape and wells' combs were placed in the tray. The agarose solution was poured into the tray and allowed to solidify at room temperature. Following that, combs and seals were removed and the gel was transferred to the electrophoresis tank, which was filled with 1 x TAE buffer. Subsequently, the DNA samples were mixed with (1/6-1/10(v/v) 10 x gel loading dye and loaded into the wells. 5µl of the DNA ladder (10kb) was run in parallel with DNA samples as a marker for DNA fragment sizes. The gel was run at 120-145V for 20 to 45 minutes and visualised on a UV transilluminator. Pictures were taken by GeneFlash photo imager.

2.3.2.2 Purification of DNA fragments from agarose gel

The desired DNA fragments from the agarose gel were carefully excised under UV light using a clean scalpel. DNA was extracted from the gel and purified using QIAEX II Agarose Gel Extraction Kit (Qiagen), following manufacture's protocol. The agarose gel was solubilized in 2 volumes of Buffer QX 1 and 10 µl of QIAEX II beads. The suspension was incubated for 10 minutes at 50°C and mixed every 2 minutes to enhance gel melting and mixing of the DNA binding beads. Once the gel had completely dissolved, the suspension was centrifuged for 30 seconds at 13,000 x g. Supernatant was discarded and the pellet was washed again with 500 µl QX1 buffer followed by another two washes with 500 µl PE buffer to eliminate any agarose residue. Pellet was air-dried for approximately 15-30 minutes. Subsequently, the bead pellet was resuspended in 20 µl dH_2O and incubated for 5 minutes at 50 °C. Finally, the suspension was centrifuged for 30 seconds at 13,000 x g and the supernatant transferred into a new sterile tube and stored at -20°C.

2.3.3 Plasmid DNA Construction and Enzymatic Manipulation

2.3.3.1 Cloning of PCR product into pCRII-TOPO

The isolated DNA was cloned into the pCR2.1-TOPO vector using pCRII-TOPO TA cloning kit. Topo cloning was performed by mixing 1-2 µl of DNA with 0.5 µl PCR II-TOPO vector (10ng/ µl), 0.5 µl salt (200 mM NaCl, 10 mM $MgCl_2$), and the volume was adjusted to 3 µl with dH_2O and the mixture was incubated for 10 minutes at room temperature. Subsequently, the plasmid was introduced into bacterial cells by transformation of plasmid DNA into chemically competent cells.

2.3.3.2 Transformation of plasmid DNA into bacterial cells

MACH1 chemically competent *E.coli* Top 10 cells were used. A tube containing 50µl MACHI cells was thawed on ice and mixed with 1µl of plasmid construct and the mixture was then flicked and incubated on ice for a further 30 minutes. Then, the tube was heated for 30 seconds at 42°C and immediately transferred to an ice bucket for an extra two minutes. The heating enables the permeabilisation of the bacterial membrane, this allow the penetration of DNA molecules, then membrane integrity is restored by incubation on ice (Panja *et al.* 2008). The plasmid mixture was then mixed with 350 µl LB medium and incubated for 30-45 minutes at 37°C and 100-150 µl of the bacterial suspension was plated on LB-agar plates with Carbenicillin (50µg/ml). Prior to plating the transformed bacteria, 50µl of X-Gal (20mg/ml) substrate was spread on the agar plate to distinguish between colonies with an insert (which have a creamy white colour) and colonies without an insert (which are blue). X-gal is used to indicate the activity of β-galactosidase, an enzyme encoded by the *LacZ* gene that hydrolyses X-gal and produces blue colonies. The successful ligation of the interested gene into the plasmid with the *LacZ* gene, which has a multiple cloning sites, results in the disruption of *LacZ* gene and no activation of β-galactosidase, which results in the formation of white colonies.

After overnight incubation at 37°C, three to six white colonies were picked and each of them was grown in 2ml LB medium with (50µg/ml) Carbenicillin for a minimum of 4 hours and to a maximum of overnight in a shaking incubator (lab companion shaker-IS-971) at 37°C at 250 rpm. Plasmid DNA was purified according to the miniprep purification

method described in (2.3.4.1).

2.3.3.3 Restriction digestion of DNA

Restriction enzyme digestion was carried out to create the desired DNA fragment for cloning. Also, it was used to confirm the plasmid insertion and orientation of the inserted DNA during the generation of recombinant plasmid. A reaction mixture for digestions was made of 5-10 U of selected restriction enzyme, 1/10 volume of the accompanying 10x restriction enzyme buffer, 1-2µg DNA, 0.1µg/ml BSA if required and volume completed to 20µl with dH_2O. The reaction mixture was incubated for 1 hour at the recommended temperature for the enzyme. For double digest, which requires the use of two different enzymes, the buffer was selected based on the highest activity by both enzymes. The digested DNA was analysed on an 0.8-1 % agarose gel (2.3.2.1). Plasmids with the desired inserts were then processed for sequencing to confirm the presence of the correct sequence (2.3.5).

2.3.3.4 Ligation

After confirming the correct DNA sequence was present in the TOPO vector this DNA was digested to remove the insert for ligation into expression vector. The desired fragments were cut and the gel was purified as explained (2.3.2.2). Then, a small amount of the extracted DNA was run on the gel to determine the DNA concentration required for the ligation.

Based on the gel result, ligations were performed in a 1:3 vector to insert ratio. The reaction was performed with vector DNA, inserts DNA (3 times vector concentration), 1µl of 400U T4 DNA ligase, 1µl of 1x ligase buffer and was made up to 10 µl with dH_2O. As control, a vector only ligation was also setup. The ligation mixtures were incubated at 4°C overnight. Then MACH1 cells were transformed with ligated DNA as described in section (2.3.3.2). Single colonies were expanded and plasmid DNA was prepared and verified for the correct insertion by restriction digestion. Bacteria with a correct plasmid were streaked on ampicillin plates for plasmid maxiprep (2.3.4.2).

2.3.4 Plasmid DNA isolation and purification

2.3.4.1 Minipreparation for plasmid DNA (Miniprep)

Miniprep purification was done for all small-scale plasmid preparation using Wizard® *Plus* SV Miniprep DNA purification System as specified in the kit's protocol. Briefly, 2 ml of bacterial culture was centrifuged for 5 minutes at 10,000 x g. Supernatant was discarded and pellet was resuspended in 250 µl of the Cell Resuspention Solution. Subsequently, cells were lysed in 250 µl of the Cell Lysis Solution and mixed by inverting the tube 4-5 times followed by the addition of 10 µl of Alkaline Protease Solution and again mixed by inverting the tube 4-5 times. After 5 minutes incubation at room temperature, reaction was neutralized by adding 350 µl of Neutralization Solution and mixed immediately by inverting 4-5 times then centrifuged for 10 minutes at 13,000 x g. After centrifugation, the cleared supernatant was transferred to the Spin Column and centrifuged at 13,000x g for 1 minute. The flow through was discarded and the column was washed with 750 µl Column Wash Solution, and centrifuged at 13,000 x g for 1 minute. The washing step was repeated with 250 µl Column wash Solution and was centrifuged for 2 minutes at 13,000 x g. After transferring the column into a new 1.5ml micocentrifuge tube, 100µl dH_2O was loaded on the column and centrifuged at 13,000 x g for 1 minute to elute the plasmid DNA.

2.3.4.2 Maxipreparation for plasmid DNA (Maxiprep)

A single colony from the plate streaked with the bacteria containing the correct plasmid was picked and grown in 150 ml LB medium with 150µl Carbenicillin (50 µg/ml) and incubated overnight shaking at 250 rpm at 37°C in shaking incubator. Cells were harvested and plasmid was extracted using a GenElute™ High Performance (HP) Plasmid Maxiprep Kit, from Sigma following the manufacturer's protocol. Bacterial cells were centrifuged for 15 minutes at 6000xg at 4°C. The bacterial pellet was resuspended in 12 ml of Resuspention/ RNase A Solution and mixed well until pellet completely dissolved. Then cell suspension was lysed with 12 ml Lysis Solution; mixed gently by inverting 4-6 times, and followed by incubation at room temperature for 5 minutes until the solution becomes clear and viscous. Lysed cell were neutralized by mixing with 12 ml of chilled Neutralization Solution; mixed by inverting 4 to 6 times. 9 ml of Binding Solution was mixed with the solution by inverting 1-2 times then suspension was immediately poured

into the barrel of a filter syringe and incubated for 5 minutes. During the 5 minutes incubation, the GenElute HP Maxiprep Binding Column was placed into 50 ml collection tube and washed with 12 ml of the Column Preparation Solution and centrifuged for 2 minutes at 3000 x g. The cell lysate was expelled into the column by passing through the syringe filter using the plunger. Half of the lysate filled the column and was centrifuged for 2 minutes at 3000x g then the rest of the lysate was processed similarly. After passing all sample suspension through the column, the column was washed with 12 ml Wash Solution 1 and centrifuged for 2 minutes at 3000 x g, the eluted solution was discarded. Then column was washed with 12 ml Wash Solution 2 and centrifuged for 5 minutes at 3000 x g. Transfer the column to a new 50 ml collection tube and plasmid DNA was then eluted with 3 ml Elution Solution and was centrifuged at 3000 x g for 5 minutes.

The eluted DNA was sterile filtered and aliquoted under sterile conditions. A small amount of DNA was checked and digested with the same enzyme that had been used for digesting the ligated plasmid. The recovered DNAs were stored in -20°C.

2.3.5 DNA Sequencing

Sequencing started with a PCR amplification reaction. It was performed in a total volume of 20µl in a 96 well plate from ABI. The reaction mixture was composed of the following:

Template DNA (100-300ng/µl	Xµl
5x sequencing buffer	4 µl
*Big Dye terminator v3.1	1 µl
Primer (5 µM)	2 µl
H_2O	to 20 µl

* Big dye is a pre-mix of Dye, dNTPs, chain terminators and enzymes that are required for sequencing.

The prepared plate was placed on the PCR machine and the cycle conditions illustrated in Table 2.3 were applied.

The X-terminator purification reaction was subsequently performed to remove unincorporated dye by shaking for 30 minutes at 2000 rpm in Mix Mate shaker from eppendorf after which the plate was loaded into the ABI 3130/3130xl genetic analyser.

The resulting sequences were blast analysed *via* NCBI nucleotide Blast (http://www.ncbi.nlm.nih.gov/).

Table 2.3: Sequencing cycle condition

Stage	**Temperature °C**	**Duration**	**Cycle**
1	96	1 min	1
2	96 55 60	10 sec 5 sec 1.15 min	X 5
3	96 55 60	10 sec 5 sec 1.30 min	X5
4	96 55 60	10 sec 5 sec 2 min	X5
5	4	Hold	-

2.3.6 Cell Culture

2.3.6.1 Culturing of cell lines

Adherent cells (MCF7, HeLa, HepG2, HCT-116 and HCT-116p53$^{-/-}$) were cultured in DMEM media supplemented with 10% (v/v) FBS, 1% (v/v) L- Glutamine, penicillin-streptomycin, and 1% (v/v) sodium pyruvate. Cells were cultured under humidified condition at 37°C in 5% CO_2. Cells were harvested by removing the DMEM medium and washing the culturing surface with EDTA solution. Then, cells were trypsined by using 1x Trypsin and incubated for 5 minutes at 37°C to allow the cells to detach from the culture surface. To neutralise the trypsin, DMEM was added in greater volume; then cells pelleted at 300 x g for 5 minutes. Supernatant was removed and cell pellet resuspended in a suitable volume of culturing medium at a specific densities for seeding, determined after counting the cells.

Trypsinisation of cells was also done using TrypLE™ Express (1X), Phenol Red. It reduces the damage to the cells due to the specific action of a single enzyme that cleaves the peptide bonds on the c-terminal sides of lysine and Arginine. Its exceptional purity increases specificity and reduces damage to cells that can be caused by other enzymes present in some trypsin extracts (Lori Nestler *et al.* 2004). This trypsin solution was used with very sticky and clumpy cells such as HCT-116.

Using TrypLE™ Express did not require a wash with EDTA, it was added directly to the cells after removing the culture medium and incubated for 5-10 minutes. Then, the cell suspension was collected and pelleted by centrifugation at 300 x g for 5 minutes.

Suspension cells (K562, KG-1, HEL and U937) were cultured in RPMI medium supplemented with 10% FBS, 1% L-Glutamine, penicillin-streptomycin, and 1% sodium pyruvate. Cells were harvested by centrifugation of the entire culture medium for 5 minutes at 300 x g. Then, cell pellet was resuspended in the culture medium similarly as for the adherent cells. HEL cell line is suspension cells but it has a tendency to stick to the culture surface, therefore a cell-scraper was used to detach the cells from the surface.

2.3.6.2 Cell Counting

Cell suspension was mixed with Trypan Blue dye in 1:1 ration to distinguish live and dead cells. Then, 10 µl from the stained cells was load into Haemocytometer (Neubauer cell counting champer, depth 0.1µl) to count the cells. When counting, only the healthy unstained cells, which represent the live cells, were counted. Cells from 4 corner squares were counted the cell number per ml was determined following this calculation:

Cells/ml= average cell count from 4 squares $x10^{-3}$ x dilution factor

2.3.6.3 Cryo-preservation of Cell lines

Adherent cells trypsinised as described earlier (2.3.6.1) then centrifuged at 300 x g for 5 minutes and suspension cells were centrifuged directly. Cell pellet was resuspended in suitable freezing media i.e. DMEM freezing medium for adherent and RPMI freezing medium for suspension cells, at a density of $1\text{-}2x10^{6}$/ml. The freezing vials were frozen at -80°C in a Cryo Freezing Container (Nalgene Mr Frosty) overnight, then vials were transferred to liquid nitrogen for longer storage.

2.3.6.4 Coomassie Blue staining

To assess cell viability and drug resistance or sensitivity, adherent cells were stained with Coomassie Blue. First, when cells in the culture reached the desired stage, the culture medium was removed. Cells were washed twice with PBS and fixed by adding adequate amount of 4% paraformaldehyde, and incubated for 10 minutes at room temperature. After removing the fixation solution, cells were washed twice with PBS and stained for 10 minutes with Coomassie Brilliant stain. Finally, staining solution was removed and the culture surface was rinsed with dH_2O and dried at room temperature.

2.3.6.5 Isolation of CD34+ from human buffy coat

All CD34+ cells were isolated from peripheral blood mononuclear cells (PBMCs), which were isolated from buffy coats using Ficoll density-gradient centrifugation. Buffy coat was extracted from leukocyte cones, obtained from the National Blood Service. Leukocytes were diluted 4x with PBS in 50 ml Ficoll tube to facilitate cells separation. Cell suspension

was layered on top of 20 ml of Histopaque (1077 density) and was separated by centrifugation at 560 x g for 30 minutes without braking. PBMCs that were concentrated at the interphase were carefully removed to a new tubed using a Pasteur pipette, resuspended in 50 ml PBS and centrifuged at 400 x g for 10 minutes. Supernatant was discarded and cell pellet was washed twice in 50 ml PBS with 2% (v/v) FBS and spun at 200 x g for 10 minutes. Then, to proceed to $CD34^+$ isolation, cells were counted as explained in (2.3.6.2) and centrifuged for 10 minutes at 300 x g.

CD34+ isolation was performed using CD34 MicroBead Kit following the manufacture's protocol. Briefly, for up to 10^8 total cells, cell pellet was resuspended in 300 µl MACS Rinsing Solution, 100µl of FcR Blocking Reagent (Human IgG) and 100µl of CD34 MicroBeads (conjugated to monoclonal mouse anti-human CD34 antibodies). Cell mixture was incubated for 30 minutes at 4 °C. Subsequently, 5 ml of MACS buffer was added to the cell suspension and centrifuged for 10 minutes at 300 x g. Cell pellets were resuspended in 500 µl MACS buffer and magnetic separation was performed using MACS columns. Columns were selected depending on the total number of cells, (MS for $2x10^8$ total cells or LS $2x10^9$ column). Columns were placed in the suitable MACS Separator. The columns were rinsed with the recommended amount of MACS buffer based on the used column size according to the manufacture's protocol. Following that, the cell suspension was loaded onto the column; the unlabeled cells were run through. The columns were washed with the appropriate volume of MACS buffer. Subsequently, column was removed from the magnetic field; the labeled CD34+ cells were eluted to a new clean tube with the recommend volume of MACS buffer. Then the cell suspension was centrifuged for 10 minutes at 300 x g followed by washing the cell pellet with the StemSpan™ Hematopoietic Cell Expansion Media and centrifuged at 300 x g for 10 minutes. Subsequently, cells were grown according to the hematopoietic progenitor cells culture system.

2.3.6.6 Hematopoietic progenitor cell culture

CD34+ cells were cultured under certain condition to induce erythroid differentiation using specific cytokines. Cells were cultured in Serum-Free Medium supplemented with 100U/ml penicillin/streptomycin, 2mM glutamine, 100 ng/ml SCF, 10 ng/ml IL-3, 10 ng/ml IL-6 and 0.5U/ml EPO. Cells were seeded into 24 wells plate in 1 ml medium per well and kept at a density of $5x10^5$ to $1x10^6$ cells/well. Cells were counted every 48 hours and they were

expanded and grown in a larger well based on the cell number. On day 6, two different liquid culture differentiation systems were applied. Cells were counted and aliquots for RNA and protein extraction were collected, the remaining cells were split into two cultures and centrifuged at 300 x g for 5 minutes. In one culture, cells were induced to differentiate to both erythroid and megakaryocytic lineage by addition of EPO (3 U/ml) and 50ng/ml TPO. To induce erythroid and myeloid differentiation, 3 U/ml EPO, 15 ng/ml G-CSF and 40 ng/ml FLT3 was added. Cells were harvested on day 10 or 11 (day 4 of the differentiation cycle) and stained for flow cytometrey analysis.

For flow cytometrey the cells were washed with PBS and centrifuged at 300 x g for 5 minutes. Cell pellets were resuspended in 1ml PBS and mixed with 1µl of live dead stain (eFluor® 780) and incubated in the dark for 30 minutes. Following that, cells were washed twice with FACS buffer and centrifuged for 10 minutes at 300 x g. Supernatant was removed and cell pellet was resuspended in 200 µl FACS buffer and stained with the marker antibodies and incubated for 30 minutes in the dark. Cells were washed twice with FACS buffer and centrifuged at 300x g for 10 minutes. Supernatant was removed and cell pellet was resuspended in 500 µl FACS buffer and analyzed by FACS scan.

2.3.7 Transfections of cells

2.3.7.1 Transfection by lipofectamine

Adherent cells were seeded into 24 well plates at a density of $2x10^5$ per well in 500 µl of DMEM complete medium 24 hours prior to transfection. Suspension cells were seeded in 1ml RPMI complete medium at the same density on the same date. Transfection was carried out using RNAiMAX or Lipofectamine LTX according to the manufacture's protocol. For siRNA, RNAiMAX was used and different concentrations of siRNA were used (100nmol-250nmol), siRNA was diluted with OPTIMEM medium to bring the final volume to 50µl. 5µl of RNAiMAX was diluted with 45µl OPTIMEM. Both solutions were mixed and incubated at room temperature for 10 minutes then 50µl from the mixture was mixed with the cells. At relevant time points, cells were harvested as described in (2.3.6.1) and RNA and protein samples were collected.

For plasmid DNA and shRNA transfections Lipofectamine LTX reagent was used. Cells were seeded similarly as above. The plasmid or shRNA concentration was adjusted to 10

µg and diluted with 50 µl OPTIMEM. The transfection reagent was prepared by mixing 5µl plus reagent with 10µl lipofectamin solution then diluted with OPTIMEM. The two diluents were mixed and incubated at room temperature for 10 minutes then 50µl was mixed with cells. After 24 hour, adherent cells were transferred to a T75 flask containing 20ml culture medium. Puromycin selection was performed 48 hours post transfection and samples collected for analysis on day 6 or 7 post transfection.

2.3.7.2 Transfection by Nucleofection

Cells were harvested as explained earlier in (2.3.6.1). After harvesting and counting the cells, $2x10^6$ cells were prepared per transfection. Cells were washed once with PBS, centrifuged at 300 x g for 5 minutes; supernatant was discarded and cell pellets were resuspended in 100 µl of the appropriate Nucleofection solution. 5µl (2µg) of plasmid DNA/shRNA or siRNA 100nmol-250nmol was added to the mixture. The cell suspension was transferred to a Nucleofector cuvette, which was then placed in the Nucleofector II device. Transfection programme was selected based on the cell type. The transfected cells were immediately transferred to tissue culture flasks based on the cell number and experiment type *i.e* adherent cells were cultured in T175 flask, suspension cells were cultured in 6 well plates and siRNA experiments were carried out in 24 well plates.

2.3.8 Lentivirus ShRNA Virus Particle Production

2.3.8.1 Lentiviral packaging

The human embryonic kidney cell line (293T) was used to package lentiviral particles for transduction of target cells. Cells were seeded at a density of $3x10^6$ per 100mm culture dishes and cultured in 10ml complete DMEM and incubated overnight in humidified incubator at 37°C, 5%CO2. Plasmid constructs expressing the components for lentiviral packaging (pLKO.1-shRNA) were then transfected using $CaPO_4$ co-precipitation method. The transfection complex was made up of three plasmids: 3µg pMD2.G (encoding VSV-G), 7µg pCMV8.9 (gag/pol) (These were kindly provided by Dr. David Darling) and 10µg of vector plasmid [pLKO.1 empty, pLKO.1 RPS14 shRNA (kindly provided by Dr. Jie jiang) pLKO.1 RPL27A shRNA and pLKO.1 RPL5 shRNA], shRNA sequences are listed in (2.1.14). The plasmids were diluted to a total volume of 500µl with dH_2O and mixed

with 500µl 0.5 M $CaCl_2$. Subsequently, 1ml of 2x HEBS buffer was added drop wise whilst the tube was vortexed. The mixture was incubated for 30 minutes at room temperature to allow DNA precipitation. The mixture was added drop wise to the 293 cells. Two transfections were carried out per shRNA plasmid. After overnight culture, medium was changed and fresh 10 ml DMEM medium was used. Cells were then cultured for further 24hrs, and the lentivirus containing culture medium was collected and filtered through a 0.45µm filter. Lentiviral particles were aliquoted in smaller volume and stored at -80°C.

2.3.8.2 Lentiviral concentration

Lentiviral particles (vector supernatants) were concentrated by centrifugation using an SW 41Ti rotor at 100,000 x g for 2 hours at 4°C. To make 100x concentrated lentiviral pellets were resuspended in 100µl of suitable culture medium and incubated for 30 minutes at 4°C. The suspension was aliquoted in smaller volume and stored at -80°C.

2.3.8.3 Lentiviral transduction

Adherent cells were seeded in 24 well plates at density of $4\text{-}5x10^5$ cells per well in 1ml of DMEM 24 hours prior to transduction. Suspension cells were seeded at the same density in 1ml RPMI and transduced on the same day. Viral particles (100µl) were added to the cells and 4µg/ml polybrene was added. After 24 hours, cells were transferred into a T75 flask containing 20 ml of DMEM. Culture medium was supplemented with puromycin (2 µg /ml) and maintained for 6-10 days.

2.3.9 DNA and RNA Extraction and Concentration Determination

2.3.9.1 Genomic DNA extraction

Genomic DNA was extracted using the QIAamp DNA Mini Kit according to the kit's instruction. Cells for DNA extraction were pelleted and preserved in 200µl PBS. 20µl Qiagen Protease (or Proteinase K) was mixed with the cell suspension. 200µl of Buffer AL (lysis buffer) was mixed with the suspension and incubated at 56°C in a heat block for 1 hour. The tube was centrifuged briefly to bring everything down. 200µl of 100% ethanol was added to the mixture and the mixture was applied to a QIAamp Mini spin column in 2ml collection tube. Column was centrifuged at 6000xg for 1 minute and the supernatant

was discarded. Subsequently, 500 µl Buffer AW1 was applied to the column and centrifuged at 6000 x g for 1 minute. Then, the column was washed with 500µl of Buffer AW2 and centrifuged at full speed (13,000 x g) for 3 minutes. Column was transferred into a new collection tube and centrifuged again at full speed for 1 minute to eliminate any possible carryover from AW2. After transferring the column into a new 1.5ml microcentrifuge tube, DNA elution was carried out with 50µl water or elution buffer which was applied to the column and incubated for 5 minutes then centrifuged for 1 minute at 6000 x g. Isolated DNA was stored at -20°C and DNA concentration was determined using NanoDrop (2.3.9.4).

2.3.9.2 RNA Extraction using TRIZOL

$5x10^{5}$ to $2x10^{6}$ cells from culture were centrifuged at 300 x g for 5 minutes and the supernatant was discarded. The cell pellet was resuspended in 500 µl of Trizol for less than $1x10^{6}$ cells to 1 ml Trizol for $2x10^{6}$ cells; mixed well by pipetting and stored at -80 °C. For extraction, manufacture's protocol was applied. Briefly, samples were thawed at room temperature for 5 minutes till the sample was completely defrosted. Per 1ml Trizol, 200µl of chloroform was added to the sample; the mixture was mixed vigorously for 15 seconds and incubated at room temperature for 2-3 minutes. Then the mixture was transferred to a gel phase lock tubes to facilitate sample separation followed by centrifugation at 12,000 x g for 15 minutes at 4°C. The sample mixture was separated into three layers, a lower (red, phenol-chloroform, phase), an interphase and the upper (colourless aqueous phase). The upper aqueous phase was transferred to a clean centrifuge tube and mixed with 500µl isopropanol to precipitate RNA. Samples were incubated for 10 minutes at room temperature then they were centrifuged at 12,000 x g for 10 minutes at 4°C. Supernatant was removed from all samples and the invisible RNA precipitate was washed with 1ml 75% (v/v) ethanol and vortexed. Samples were centrifuged at 7,600 x g for 5 minutes at 4°C. Supernatant was discarded and the remaining ethanol was removed carefully and RNA pellet was air dried at room temperature for 10-20 minutes. The dried pellet was dissolved in 30-45µl RNase-free dH_2O. The RNA concentration was determined by Nanodrop, as described in 2.3.9.4 and RNA was stored at -80°C.

2.3.9.3 RNA extraction using RNeasy Micro kit

RNA from patient's CD34+ or CD34+ cultured cells were isolated using RNeasy Micro kit from Qiagen following the kit's protocol. First, cells were processed similarly as explained in (2.3.9.2) until the chlorophorm separation step. Once the aqueous layer was collected, it was mixed with 70% (v/v) ethanol then the suspension was transferred into RNeasy column and centrifuged for 15 second at 7,000 x g at 4°C. The flow through was discarded and the washing with ethanol was repeated. Subsequently, column was washed with 800µl RW1 washing buffer and centrifuged at 8000 x g for 15 seconds. The column was placed into a new collection tube and washed twice with 500 µl of RPE buffer and centrifuged at 8000 x g for 30 seconds. Finely, column was transferred to a clean 1.5 ml microcentrifuge tube and the RNA was eluted with RNase free water by adding 20-30µl of the water on top of the column membrane and column was centrifuged for 2 minutes at 8000 x g. RNA samples were stored at -80°C and the concentration was determined by NanoDrop (2.3.9.4).

2.3.9.4 Determination of nucleic acid concentration by NanoDrop

RNA and DNA concentration was determined by NanoDrop spectrophotometry (Thermo Scientific). Nanodrop optical surfaces were first cleaned with 70% (v/v) ethanol then 1µl of nucleic acid free water was placed on the lower optical surface to initialize the instrument, following the instrument's instructions. Following that, both optical surfaces were wiped with tissue and blanking was performed by loading1µl of the sample elution solution i.e. dH_2O or elution buffer on the NanoDrop and blank the instrument. After cleaning the surfaces, nucleic acid type was selected, either DNA or RNA, and 1µl of each sample was loaded onto the optical surface and the concentration measurement was performed. Sample quality was determined based on the 260nm/280nm ratio and the accepted purity had to be above 1.6. RNA samples were kept on ice during the concentration measurement to avoid RNA degradation.

2.3.10 Quantitative Real time PCR (qRT-PCR)

2.3.10.1 miRNA reverse transcription (RT)

miRNA Reverse Transcription kit was used and the manufacture's protocol was followed. RT master mix of 15µl volume was made up of 7µl master mix, 3µl 5x RT primer of individual miRNA and 5µl RNA sample.

Master mix was prepared on ice and it was composed of:

Component	Volume
100mM dNTPs	0.15 µl
MultiScribe Reverse Transcriptase, 50 U/µl.	1µl
10x Reverse Transcription Buffer	1.5 µl
RNase Inhibitor, 20U/ µl	0.19µl
Nucease-free water	4.16µl

Master mix was mixed in microcentrifuge tube and centrifuged for 15 seconds at 300 x g to bring the solution down. Subsequently, the master mix was combined with 5µl total RNA of 5-10 ng/ml concentration. The 12µl reaction mix was loaded into a 96 well palate. For every miRNA, master mix of each RNA sample was doubled; one volume was mixed with the miRNA primer and the other was mixed with the non \coding RNA control primer. 5xRT primer was thawed on ice and tube was vortexed and centrifuged for few seconds to bring the primer solution to the bottom of the tube. 3µl of 5xRT primer from each assay (i.e. each miRNA and control non coding RNA primers) was mixed with the 12µl RT master mix containing the RNA. Plate was sealed and centrifuged for two minutes at 300 x g to bring the solution to the bottom of the well. Following that, plate was placed on the thermal cycler and incubation was carried out according to the following conditions:

Hold 30 minutes at 16 °C

Hold 30 minutes at 42 °C

Hold 5 minutes at 85 °C

Hold ∞ at 4 °C

Reaction was stored at -20°C if not processed immediately to PCR amplification.

2.3.10.2 miRNA quantitative PCR amplification

qPCR reaction was performed according to the manufacture's recommendations. 20µl reaction was made for each sample in triplicate. The qPCR reaction mix was made according to the following:

Component	Volume
TaqMan® Small RNA Assay (20X)	1µl
Product from RT reaction	1.33 µl
TaqMan® Universal PCR Mix II (2X)	10 µl
Nuclease free water	7.67µl
Total volume	20 µl

qPCR Reaction mix (20µl) was loaded in triplicate for each miRNA or control non coding RNA into MicroAmp™ Fast Optical 96 well reactions Plate with Barcode and sealed with the appropriate plate caps and was centrifuged for 2 minutes at 300 x g. The plate was loaded into an ABI PRISM 7700 instrument (Applied biosystem) and the following cycling condition was applied:

qPCR cycling condition

Stage	Temperature	Duration	Cycle
1	50°C	2 minutes	1
2	95 °C	10 minutes	1
3	95 °C 60 °C	15 sec 60 sec	x 40

2.3.10.3 cDNA synthesis

The first strand cDNA was generated from 1 µg of total RNA using SuperScript® VILO™ cDNA Synthesis Kit following manufacture's protocol. The RT reaction was made on ice and it was composed of 2µl 10x Super Script ®III Enzyme Blend, which contains: SuperScript® III RT, RNase OUT Recombinant Ribonuclease Inhibitor, and a proprietary helper protein. Enzyme was mixed with 4µl 5x VILO™ Reaction Mix, which composed of random primers, $MgCl_2$, and dNTPs. The mixture was mixed with 1µg RNA (100-500ng of total RNA was used when RNA concentration was very low), and the volume was made up to 20 µl with RNAse free water.

All reaction mixtures were centrifuged, to bring down the suspension mixture, and several incubations were carried out on thermal cycler according to the following condition:

RT samples were incubated at 25°C for 2 minutes. Followed by 60 minutes incubation at 42°C. Then reaction was terminated by 5 minutes incubation at 85°C. cDNA samples were stored at -20°C if was not used immediately for qPCR.

2.3.10.4 Determination of mRNA relative expression by qRT-PCR

Quantitative Real time PCR was performed using Universal Probe Library (UPL) from Roche, which is based on analyses of any gene in the genome by using a specific probe (short fluorescently-labelled hydrolysis probe) from the library in addition to a pair of gene specific PCR primers.

The PCR primers were designed using a LightCycler® Probe Design Software 2.0 which is available at the Roche website. This software provides the primer sequences and the compatible UPL probe, which are optimal for amplifying the target DNA by RT-PCR using the light cycler instrument.

Reaction mixtures of 20 µl were made for each cDNA in triplicate. cDNA was diluted according to the initial RNA concentration i.e. for 1µg RNA, cDNA diluted as 1:100. The reaction master mix was prepared according to the following:

Component	**Volume**
Diluted cDNA	5 µl
Forward primer (100µM)	1 µl
Reverse primer (100µM)	1 µl
UPL probe	0.25 µl
Fast start master mix	10 µl
dH_2O	3.75 µl
Total	20 µl

Real time PCR reaction mixtures were loaded into MicroAmp™ Fast Optical 96 well reactions Plate with Barcode and sealed with optical tube cabs. Then plate was centrifuged at 2000 x g for 2 minutes. Then PCR plate was placed on an ABI PRISM 7700 instrument (Applied biosystem) and the same cycling condition described in (2.3.10.4) was applied.

The comparative cycle threshold (CT) method was used also called 2(- ΔΔCT) to determine the mRNA relative expression. First, the ΔCT value for each sample was calculated by determining the difference between the CT mean of the target gene and the CT mean of the endogenous control gene such as GAPDH. Then, ΔΔCT was determined by calculating the differences of the ΔCT value of the calibrator samples and the test samples. The fold change or the mRNA expression level was calculated according to this formula: $2^{-\Delta\Delta CT}$

2.3.11 Western Blotting

2.3.11.1Protein extraction

Total cell protein was extracted from cells growing in the culture. The cell culture medium was removed and cells were harvested as explained in (2.3.6.1). The cell pellet was washed once with PBS and then resuspended in protein lysis buffer. The volume of the lysis buffer was based on the cell number, 50 µl lysis buffer was used for 2x 10^5 cells. Lysates was incubated at 95°C for 5 minutes then stored at -20°C.

2.3.11.2 SDS- Polyacrylamide gel electrophoresis (Nu-PAGE)

Nu-polyacrylamide gel (4-12% Bis -Tris Gel) was placed in the electrophoresis tank and the comb was removed. Subsequently, the tank was filled with 1x running buffer and protein samples were loaded. Novex sharp pre-stained protein standard (Novex) was run simultaneously with samples to determine protein size. Electrophoresis was carried out at a constant voltage (200V) until the dye reached the bottom of the gel.

2.3.11.3 Protein transfer to nitrocellulose membrane

Separated proteins were transferred onto a 0.45µm pore nitrocellulose membrane (Amersham) using Xcell™ blot module. Before transferring, Blotting pads, filter papers and nitrocellulose membrane were pre –soaked in 1x transfer buffer. On the cathode (-) core of the transfer module, three soaked fibre pad were placed followed by filter paper, the gel, the nitrocellulose membrane, again filter paper and a fibre pads. The nitrocellulose paper was cut to the size of the gel. Once the anode core was placed on top of the pad, the module was placed in the transfer tank and filled with 1x transfer buffer. The outer tank was filled with dH_2O and transfer was performed on ice for 2 hours at 25 volts.

2.3.11.4 Probing of western blot and detection by Enhanced Chemi-Luminescence

The transferred nitrocellulose membrane was blocked in blocking solution for 1 hour at room temperature or overnight at 4 °C. Subsequently, the membrane was incubated with primary antibody overnight at 4 °C. The membrane was rinsed with TBST and washed three times for 10 minutes each. Then, the membrane was incubated with secondary

antibody for 1 hour at room temperature. Following that, another three washes with TBST were performed. Protein bands were detected using the ECL™ western blot analysis system following manufacture's protocol. The blot was incubated for 4-5 minutes in the reaction solution, then drained and sealed in Saran wrap. The nitrocellulose membrane was then exposed to Hyper film™ECL™ for the preferable time and subsequently developed.

2.3.11.5 Co- immunoprecipitation (Co-IP)

5-7 x 10^6 Cells were centrifuged at 3000x g for 5 minutes. Cell pellets were lysed in 1 ml cold IP buffer with fresh protease inhibitor. Cell suspension was incubated on ice for 10 minutes then centrifuged for 10 minutes at 10,000 x g at 4°C. The supernatant was collected from each cell lysate tube and an aliquot of 20µl was stored as IN PUT at -20°C and the rest of the supernatant was divided over two tubes. In one tube 10 µl of primary antibody was added and in the other tube, which is the control tube, 5µl secondary antibody was added. Subsequently, tubes were incubated overnight, rotating at 4°C. For the pull down protein A/G beads were used, 35µl of beads used per tube which means 70µl used for sample and control tubes. Beads were washed twice with IP buffer and briefly spun for 15 second at 10,000 x g. The third wash of the beads was performed with RIPA buffer and beads resuspended in 70µl RIPA buffer. 35 µl of bead suspension was added to each of the cell lysate samples and the samples were incubated for 1 hour rotating in the cold room. Then lysate was washed three times with RIPA buffer, and spun for 15 seconds each time. Laemmli buffer was thawed in a water bath and was diluted with RIPA buffer to reach a 1 x concentration by mixing 30 µl of 2 x laemmli buffer with 30 µl of RIPA buffer. Then, 30 µl of the mixture was used to resuspend the lysate pellet after the third wash. Subsequently, tubes were heated on the heat block at 100 °C for 5 minutes and stored at -20 °C. To analysis the samples, samples were loaded directly on polyacrylamide gel and regular western blot protocol (2.3.11) was followed. For the In Put sample, which is run as a control, the sample was mixed with the 2 x laemmli buffer in a volume equal to the sample volume to reach a 1x concentration, sample was processed similarly as the other samples regarding heating and storing condition.

2.3.11.6 Immunofluorescence Assay

$5x10^4$ cells were re-suspended in 200µl PBS and cells were spun onto slides using a Cytospin at 300 rpm for 5 minutes. The slides were marked and left to dry at room temperature. Subsequently, cells were fixed with 100µl 4% PFA in PBS for 15 minutes at room temperature. Slides were washed three times with PBS for 5 minutes each with continuous shaking on the shaker. The cells were permeabilised in 100µl 0.1% Triton x-100 in PBS. Then, slide was washed three times with PBS for 5 minutes each. Followed by blocking for 1 hour with 100µl (1% BSA, 5% (v/v) sheep serum in PBS), cells were washed briefly in PBS. Subsequently, cells were incubated for 1hour at room temperature with primary antibody at 1:200 dilutions in TPBS. Cells were washed twice in TPBS for 10 minutes and incubated in the secondary antibody conjugated with fluorescent dye at a dilution of 1:200 in TPBS for 1hour at room temperature. Cells were washed twice for 10 minute each and stained with 100µl DAPI for 5 minutes at room temperature. Slides were washed with TBS for 10 minutes and air dried for 4 minutes at room temperature. 10µl mounting media was applied on the slide and covered with 22 x22 mm coverslip. Slides were analysed with confocal microscopy to visualize signals on the nucleolus. Confocal microscopic analysis has been performed in Cambridge university-MRC-Lab with the help of Dr. Shengjiang Tan.

2.3.12 Polyribosome Fractionation

Polyribosome experiment was performed in Cambridge University in the lab of prof. Alan Warren. All the reagents and the assay materials were kindly provided by them and all the work was done with the help of Dr. Shengjiang Tan.

Cyclohexamide was added to the cells in the culture to a final concentration of 100 µg/ml and incubated for 15 minutes in a tissue culture incubator. Cyclohexamide is an inhibitor of protein synthesis; it blocks the translation elongation and holds ribosomes on the mRNA. After incubations, $1\text{-}10x10^6$ cells were harvested as explained (2.3.6.1) and centrifuged for 5 minutes at 300 x g, medium was aspirated completely and cell pellet was washed with PBS containing 50 µg/ml cyclohexamide. Supernatant was completely discarded and cell pellet was frozen at -80°C. All these steps were carried out on ice; both cells and solution were kept on ice, to avoid translation elongation. Samples were transferred to MRC lab-Cambridge University in dry ice and processed immediately upon arrival.

Cell pellet was partially defrosted on ice and transferred to a 1.5 ml microcentrifuge tube, for consistency approximate similar pellet sizes were collected from all samples. Cells were lysed in polysome lysis buffer according to the pellet size. Cells were resuspended in 200-250µl of lysis buffer and were incubated on ice for 15 minutes and mixed several times by vortexing. Subsequently, lysed cells were centrifuged at 10,000 x g for 10 minutes at 4 °C. After centrifugation, cytoplasmic extract was transferred to a new collection tube from which 10µl was used to measure the concentration using a spectrophotometer. The concentration of the nucleic acid in the lysate was determined by mixing 10µl of the lysate with 490µl of dH_2O and blank was made by mixing 10µl of lysis buffer with 490µl dH_2O and reading the OD_{260} with a spectrophotometer. Equal lysate should be loaded on the sucrose gradient, thus all lysates were adjusted corresponding to the lowest OD and the volume of each sample was made up to 200 µl with lysis buffer. Then, the 200 µl of the cytoplasmic extract was layered on top of 10-50 % (w/v) sucrose gradient, which was prepared by Dr. Shengjiang Tan. The sucrose gradient was placed in SW41Ti rotor bucket and kept in the refrigerator, to reduce possible RNAse activity, until the lysate fractions were collected. The cytoplasmic extract was separated by centrifugation for 1 hour and 57 minutes at 40,000 x g at 4°C in a SW41Ti rotor (Beckman). The sucrose gradient tubes were carefully removed from the centrifuge and placed on the ice. To avoid disturbing gradient, tube wells in the ice were premade with an empty tube. The gradients were fractionated using the polysome profile fractionator, which is composed of syringe pump, UV monitor, amplifier (amplifying the signals to enhance the resolution), fractionator and data acquisition module. Figure 2.1 shows the polysome fractionator in prof. Warren's laboratory. Gradient was placed in the fractionator (tube holder), the top of the tube was connected to the outlet and the bottom of the tube was placed on a stage in which needle penetrate the bottom of the tube. Then, the gradient underwent an upward movement with 55% (w/v) sucrose, which was placed in the syringe pump. Polysome profiles signals were detected using UV monitor at A_{254} and these signals were translated into a digital format, which can be viewed and saved on a PC using the data acquisition software. The monitor was recording signals starting with free materials followed by 40S ribosomal subunit, 60S ribosomal subunit and polyribosome complexes. Fractions from each subunit were collected through the outlet in 1.5 ml tube as 1ml/ tube. Fraction tubes were stored in -20°C.

2.3.13 Cell cycle

Cells were counted and 2-5 x10^5 cells were pelleted by centrifugation at 300 x g for 5 minutes. Supernatant was aspirated and cells were fixed in 1ml 70% (v/v) ice cold ethanol which was added drop wise while vortexing then stored at -20°C. For cell cycle analysis, ethanol-suspended cells were centrifuged for 5 minutes at 300 x g. Ethanol was decanted and cell pellet was washed in PBS twice and centrifuged in FACS tubes at 300 x g for 10 minutes. Pellets were resuspended in 500 µl of cell cycle staining buffer and incubated in the dark for 15-30 minutes at 37°C. Cell cycle analysis was performed by flow cytometric analysis using Canto 2. The data was analysed using FlowJo. To exclude artefact and double cells, doublet discrimination gate was performed with forward scatter Area(FSC-A) against width (FSC-W) and another doublet discrimination gate was performed similarly with side scatter (SSC). Then PI (A) Histogram was generated.

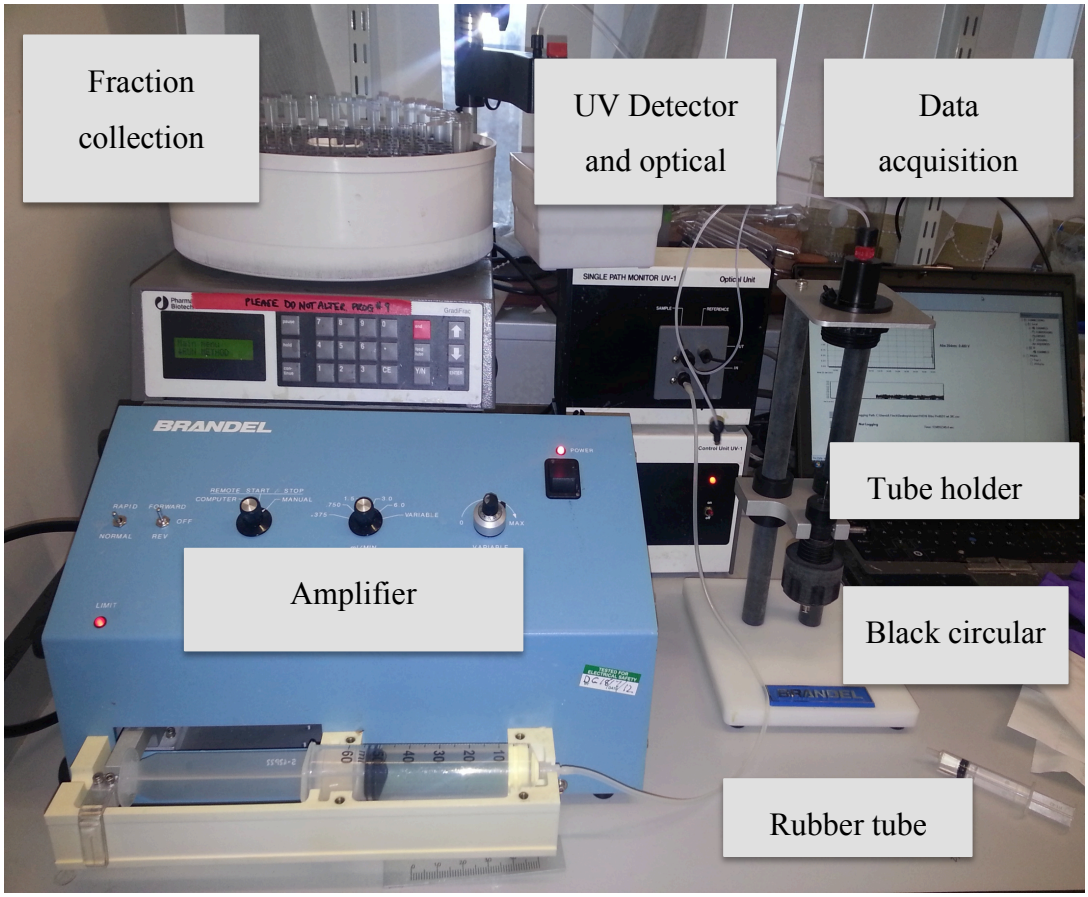

Figure 2.1: polysome fractinationationa and profiling.

Syring was filed with 50 ml 55% (w/v) sucrose and placed on the pump holder. Ruber tube was attached to the syring and to the metal needle attched to the underside of the black circular knob. Pump motor was turned on using the Reverese flow rapid setting to accommodate the syring. Then, Forword flow was done to get the air puple out of the rubber tubing, once the scrouse comse throgh the needel, power was turned off. Sucrose tube was assembeled on the tube holder attched to the optical unit and the needle on the knob was adjusted to be centered beneath the tube. Then, screw on the top of the hloder was tighten around the tube to hold it and the stage was adjusted to allow the needle to come throgh the botom of the tube.Forward option was turnd up with high sensitivy adjustment on the UV detector. A rubber tube was connected from the optical unit to the fractinator and 1.5ml tubes were placed on the fractinator for samples collection with setting which was adjusted as 1ml/ tube.

2.3.14 Annexin V staining

Annexin V is a cellular protein that binds with phosphatidylserine (PS), which is normally located in the inner plasma membrane. During apoptosis, PS translocates to the extracellular membrane which makes it target for phagocytosis and can be detected by fluorescently labelled Annexin V (Koopman *et al.* 1994). To stain the cells, cell pellets of 2-5 $x10^5$ cells were washed in ice cold PBS and centrifuged at 300 x g for 5 minutes. Then, cells were washed with 1x Binding buffer, and spun in FACS tube at 300 x g. The pellet was resuspended in 250µl of 1x Binding buffer and stained with 3-5 µl of Annexin V, based on the cell number, and incubated in the dark at room temperature for 10 minutes. The stained cells were then washed twice with the binding buffer and spun at 300 x g for 10 minutes and cells were resuspended in 250-500µl binding buffer. Before analysing the cells on the flow cytometer, the cell suspension was stained with 3µl of fluorescently labelled 7-ADD. 7-ADD can penetrate the membrane of dying cells and stain them to discriminate between dead and live cells and in apoptotic assay it is used to distinguish necrotic cells from apoptotic cells. FACS analysis was performed in FACS Canto 2. And the data was analysed using FlowJo.

2.3.15 MTT assay

MTT assay was used to assess cell viability, which is based on determining the metabolic activity of the cells. The yellow MTT is reduced by NAD(P)H dependent oxidoreductase enzyme in metabolically active cells to generate a purple insoluble formazan products. This assay was performed by seeding the cells in 96 well plates (Flat bottom) at density of 1000-5000 cells/ 100µl of medium. Cells from each sample were plated in triplicate and three wells were filled with medium alone and were used as a control. 20µl of 5mg/ml MTT was mixed with each well, then the plate was incubated for 2-4 hours, until purple particle were visible, in a humidified incubator 5% CO_2 at 37°C. After this incubation 150 µl of solubilisation solution was added to each well including control wells and the plate was incubated in the incubator in the dark for a further 2-4 hours or overnight. The absorbance of each well was measured at 610 nm in a microtiter plate reader. If the readings were very low the plates were incubated for longer. Data was analysed by calculating the average value from the triplicate readings, then it was normalized with the blank by subtracting the average value of the blank.

2.3.16 Colony forming cell assay using methylcellulose

This assay was used to study the potential of haematopoietic progenitor cells to proliferate and differentiate into colonies in semi-solid media under the stimulation of cytokines. The media bottle was thawed at 2°C to 8 °C overnight. After the media completely thawed, it was liquated as 3ml in 15ml falcon tube, which is the amount required for a single experiments and stored at -20C.until use. Aliquots were thawed again at 2°C to 8 °C overnight and mixed with cell suspension. Cells were counted and the required number which was (3-5x103, was spun at 300 x g for 5 minutes. The cell pellet was resuspended in 100 µl STSFM and mixed with the methylcellulose media. Subsequently, cell suspension was vortexed vigorously and incubated for 30 minutes at room temperature to allow air bubbles escaped. The 3ml suspension was layered on 6 well tissue culture plate using a 5ml syringe fitted with 16 gauge needle. One well was filled with 3-4 ml sterile water to avoid drying. The plate was placed in larger dish filled with sterile water and covered to preserve humidity. Plate was incubated for 14-16 days in a humidified incubator 5% CO_2 at 37°C to allow colony formation and the analyses was performed according to the cell morphology.

2.3.17 Statistical analysis

The significance of the experimental results was calculated using Student's *t-test.* If other statistical analysis were used they are explained and indicated within the text.

Chapter 3: Application of a novel functional assay to identify targets regulated by *miR-595*

3.1 Introduction

MicroRNAs play a vital role in regulating a large number of normal biological processes including cell proliferation, differentiation, development and apoptosis (Ambros 2004). Therefore, dysregulation of miRNAs expression contributes to a variety of cancers (Lujambio *et al.* 2012, Mendell *et al.* 2012). There has been a lot of progress regarding the understanding of the mechanism of action of miRNA and the identification of miRNAs targets, which is a key step in understanding miRNA cellular function. Despite the progress in miRNA target prediction methods, including bioinformatics approaches and biological experiments; these methods which have been explained in the Introductory Chapter, have a major drawback. The most common feature in the available target prediction methods is based on the base pairing between the miRNA and the complementary sequence(s), which are often in the 3' UTR of mRNA (Didiano *et al.* 2006, Brodersen *et al.* 2009). Computational algorithms are based on seed pairing, the seed region being the interaction region of the miRNA, which is a 6-8 nucleotides-long stretch at the 5' end of the miRNA. However, this seed matching principle is not applicable to all miRNA-target interactions and therefore algorithms based on this, result in the prediction of thousands of false positive targets (John *et al.* 2004, Witkos *et al.* 2011). There were many examples showing that perfectly matched seed pairing is not necessary and the interaction between miRNA and mRNA can be located at any other region. For example, *miR-24* and *miR-146a* regulate their target genes by binding outside the seed region (Lal *et al.* 2009, Lu *et al.* 2010).

However, due to the low sensitivity of the available target identification assays, most miRNAs targets have not been identified. At the time of the research the last miRBase Release 16 in Sept 2010, showed 1,048 identified human miRNAs and only 206 of them have validated targets, either by western blot or expression array, based on the last update in miRecords at that time (http://mirecords.umn.edu/miRecords/). These findings had not much changed in the last miRBase release (Release 20, June 2013), there are 1872 precursors and 2578 mature human miRNAs; only 286 of them have validated targets based on the last update from miRecords (April 27, 2013). Accordingly, novel experimental assays are urgently required for an efficient screening and the identification of miRNAs targets (Thomas *et al.* 2010).

Therefore, Dr. Joop Gäken has developed a novel functional assay, which has the potential for rapid and specific detection of targets for a given miRNA in a single assay (Gaken *et al.*

2012). This methodology relies on the functional activity of a miRNA *via* positive/negative selection, which will overcome the limitations in the other methodologies, which use miRNAs target predictions that are mostly based on the perfect complementary of the seed sequence with target binding sites. Another advantage of this methodology is the ability to identify targets that are either downregulated by mRNA cleavage or translation inhibition.

This assay is based on the directional cloning of a cDNA library (Sigma) derived from 10 different human tissues and 10 human cell lines, representing 16,923 unique genes, downstream of a TKzeo fusion gene in plasmid p3'TKzeo conferring zeocin resistance and Ganciclovir sensitivity. The assay is illustrated in Figure 3.1. The library was introduced into a cell line selected based on the miRNA expression profile data of 470 miRNAs in several adherent cell lines (293T, HeLa, CHO, MCF7, COS7, NIH/3T3, TE671, HepG2 and Saos2) using Illumina bead assay.This work was performed by the company Geneservice. Normalised expression levels were between 1 (no expression) and 60,000 and therefore Dr. Gäken decided to take a 500-fold change as the cut-off point for expression of the miRNA of interest. This was based on the qRT-PCR results of the miRNA expression, which had shown a strong correlation between the qRT-PCR and the array profiling data. For example, *miR-10a* expression was tested in several of the above cell lines and was found to be very low in MCF7 cells in both assays. These results were obtained by Dr.Gäken before the start of this project and the data obtained were used for selecting miRNAs for this project.

However, to better understand the genomic complexity of MDS with abnormal chromosome 7, I chose to focus on miRNAs localised to this chromosome. Previous studies have shown differences in disease progression between patients with monosomy 7 and those with del 7q (Cordoba *et al.* 2012, Jerez *et al.* 2012). Loss of genetic material from this region, suggests its importance in disease progression and transformation. In order to identify the miRNA relevant to MDS pathogenesis in MDS with chromosome 7 abnormalities, I selected miRNAs from the long arm of chromosome 7 that are either not expressed on the MCF7 cell line, the functional assay cell line, or are expressed below 500 as explained above. Therefore I selected 4 miRNA's that are expressed at very low levels in MCF7 cells *i.e*; *miR-489* and *miR-653* which are localized on 7q21, *miR-671* at 7q36.1 and *miR-595* at 7q36.3.

Figure 3.2 shows some of the miRNAs that are located on 7q and the miRNAs with low expression in all cell lines have been highlighted

Furthermore, I was interested in the miRNAs located on the terminal of chromosome 7(q36.1-q36.3). This region is part of the commonly deleted region of 7q- as determined by SNP array karyotyping, as identified by Wang et al (7q22–7q36.3) (Wang *et al.* 2008) and by Ernst et al (7q22.3-7qter) (Ernst *et al.* 2010). This part of chromosome 7 contains the *EZH2* gene; *EZH2* mutations recurrently occur in MDS patients with -7/7q- as explained in the introduction (Ernst *et al.* 2010, Makishima *et al.* 2010). Also, haploinsufficiency of *EZH2* and other genes located at 7q have been identified in MDS patients that had a cytogenetically normal chromosome 7, which implies that other genetic or epigenetic changes may down-regulate the expression of these genes (Jerez *et al.* 2012). Therefore, all the selected miRNAs were cloned into pBabePuro vector and the most terminal (7q36.3) miRNA (miR-595) was the first miRNA used in the functional assay.

3.2 Aim

- Application of novel functional assay to identify putative targets for the selected miRNAs located on the long arm of chromosome 7.
- Validation of the identified targets at both mRNA and protein level.

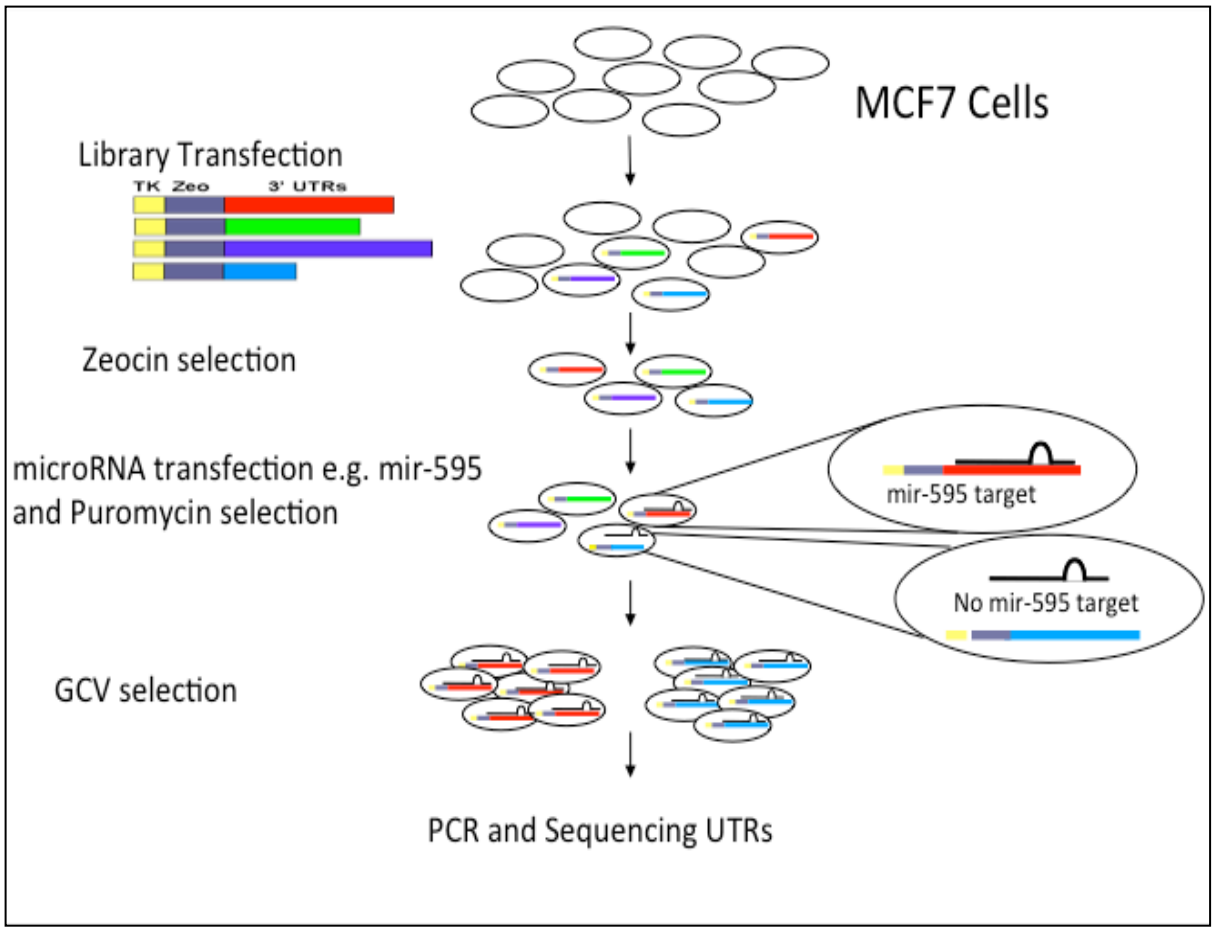

Figure 3.1: Principal of functional assay.

Transfect MCF7 cells with plasmid library with thymidine kinase-zeocin fusion protein (TKzeo). Transfected cells are selected with zeocin for 10 days. Zeocin resistance cells are transfected with pBabePuro expressing the miRNA and after 48 hrs cells are selected in puromycin. After 96 hrs, cells are treated with GCV and only cells in which the miRNA has downregulated the Tkzeo expression should survive. Genomic DNA isolated from the GCV resistant cells are PCR-amplified, and PCR products sequenced to identify the possible miRNA targets (Gaken *et al.* 2012).

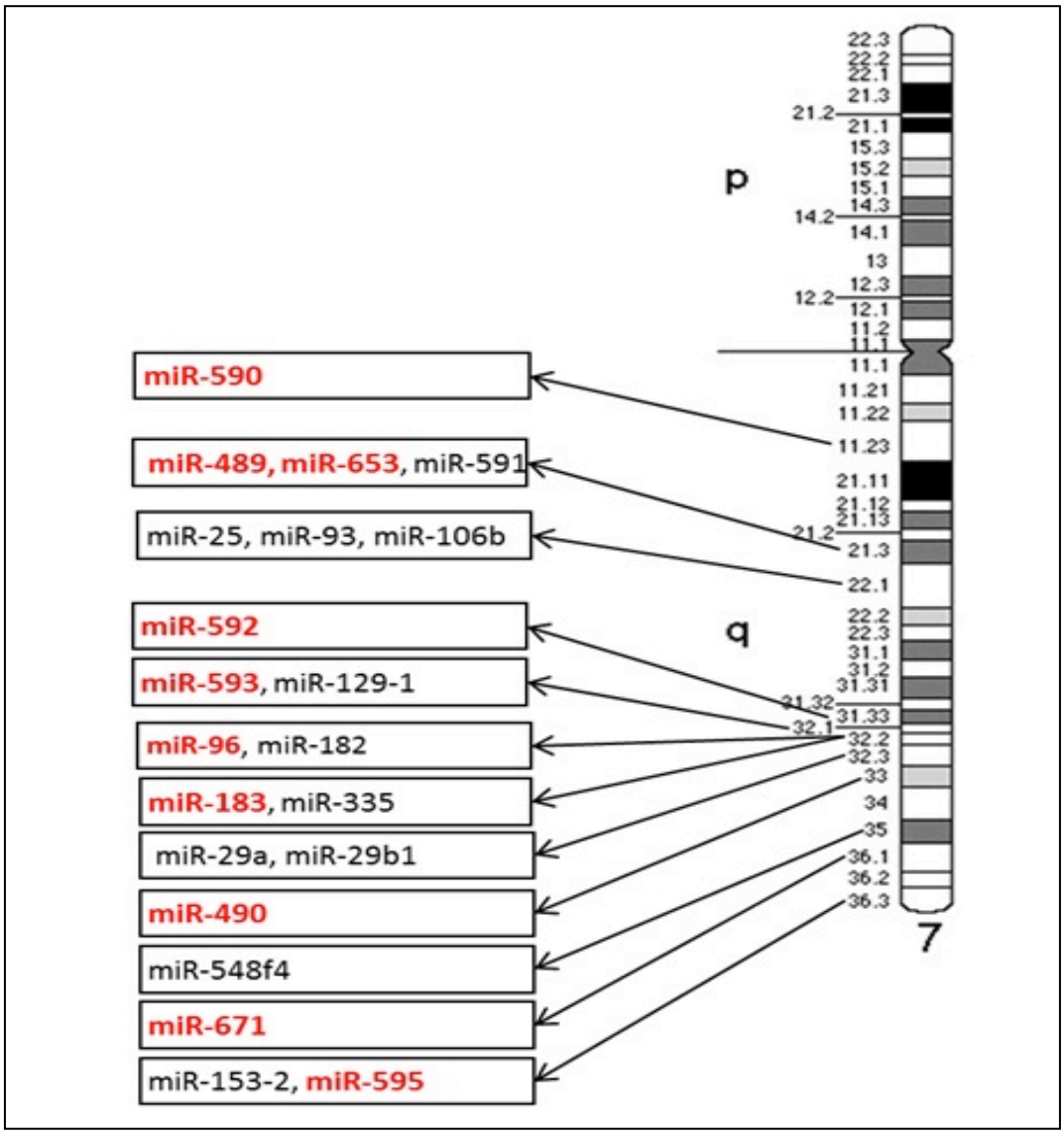

Figure 3.2: Common microRNAs located on the q arm of chromosome 7.

miRNAs highlighted in red are not expressed or are very low expressed in the adherent cell lines profiled for expression of 470 miRNAs, including 293T, HeLa, CHO, MCF7, COS7, NIH/3T3, TE671, HepG2, MCF7 and Saos2.

3.3 Method

3.3.1 Plasmid construction

The primary sequences of selected miRNAs (80-100bp) were obtained from the miRBase web resource (http://www.miRbase.org/). This sequence was BLAST analysed *via* the NCBI nucleotide BLAST (http://www.ncbi.nlm.nih.gov/) to find the complementary genomic region to the miRNA sequence, and the ~4Kb size was selected. Primer3 software (http://frodo.wi.mit.edu/) was used to design primers for amplification of a ~1Kb fragment containing the pre-miRNA hairpin sequence, miR-595 primer sequence is available in the Appendix A1.1. Restriction sites were incorporated into the primer sequences to facilitate cloning and enzymes were selected based on the NEB cutter from the New England Biolab database (http://tools.neb.com/NEBcutter2/index.php). The primers sequence and restriction enzymes are given in Section 2.1.16.

For PCR amplification, MCF7 genomic DNA was used to obtain genomic fragments containing the miRNA of interest. PCR products were checked on an 0.8% (w/v) agarose gel and the correct fragment was purified and cloned into the PCR II-TOPO vector (PCR set up, DNA extraction from agarose gel and TOPO cloning were described in Sections 2.3.1, 2.3.2 and 2.3.3).

All plasmid colonies were screened by restriction endonuclease digestion to search for the presence of a correctly sized insert (the amounts of the enzyme, DNA, type of buffer and reaction temperature followed the manufacture's recommendations). Plasmids with the desired inserts were then processed for sequencing as described in Section 2.3.5. After confirming the desired DNA sequence, this DNA was digested to cut the insert for subcloning and was cloned into the pBabePuro retroviral vector plasmid (Morgenstern *et al.* 1990). This plasmid acts as a mammalian retroviral vector conferring puromycin resistance, which is useful for mammalian selection. Figure 3.3 shows the plasmid clone map and indicates the insert cloning site. pBabePuro was digested with the same restriction enzyme to leave compatible ends to the insert. The desired fragments were cut and the gel was purified, as previously explained. Then, a small amount of the extracted DNA was run on the gel to determine the DNA concentration required for ligation.

Then MACH1 cells were transformed with ligated DNA as described in Section 2.3.3. A single colony was expanded by plasmid miniprep and plasmid DNA was prepared. The correct insertion was verified by restriction digestion. The bacteria with a correct insert were streaked on an ampicillin plate to obtain single colony to start a maxiprep of plasmid DNA. Plasmid amplification by mini prep and maxi prep are explained in Section 2.3.4.

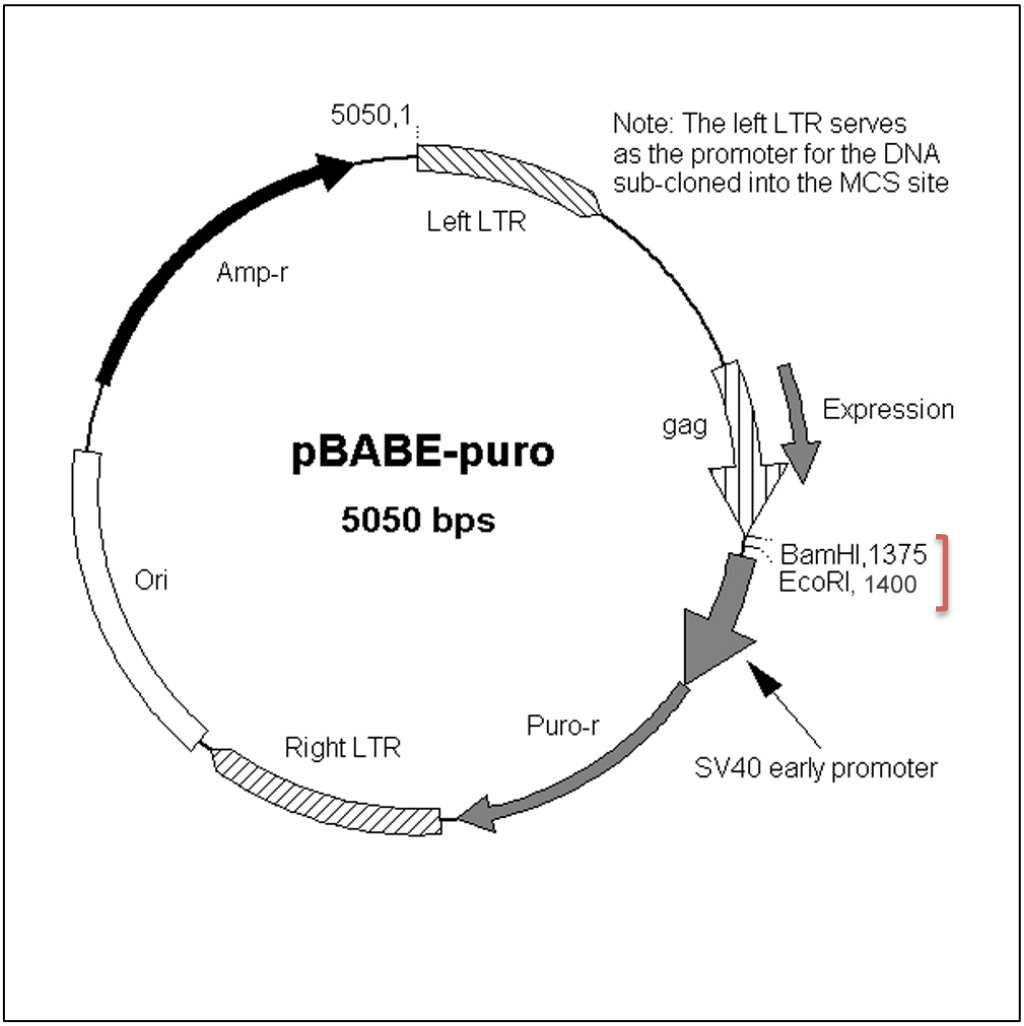

Figure 3.3: pBabePuro vector map

The genomic DNA containing mir-595 inserted into pBabePuro vector *via* its restriction sites *BamHI* and *EcoRI.*

3.3.2 Library construction

3'UTR cDNA library (Sigma, MREH01) derived from 10 different human tissues and 10 human cell lines and representing 16,923 unique genes was cloned downstream of the *TKzeo* fusion gene into *Sfi1* sites in p3'TKzeo vector. p3'TKzeo contains two different *Sfi1*

sites (bold) that are different in their interpalindromic sequence (underlined) to allow directional cloning (TCGA**GGCC**<u>**ATTAA**</u>**GGCCGGCC**<u>**GCCTC**</u>**GGCC**CCACTTC)

The cloned library was electroporated into MegaX DH10B^{TM} T1^{R} Electrocomp^{TM} Cells by electroporation following the manufacturer's protocol. Approximately one million individual colonies were isolated from 25 square 20x20 cm^2 plates; they were scraped off, pooled and expanded by maxi prep. The isolated plasmid library DNA was used for transfection into MCF7 cell line.

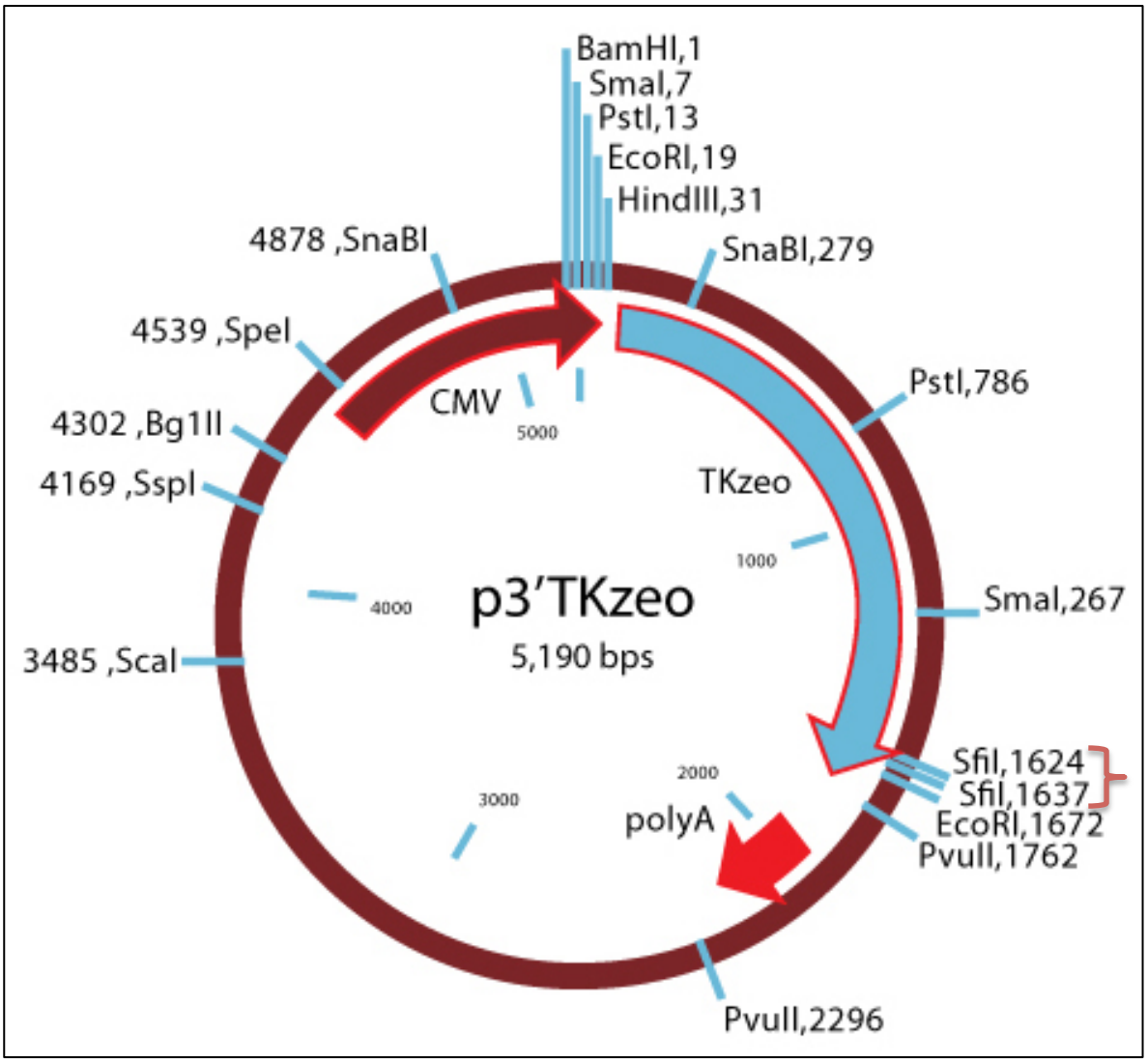

Figure 3.4: P3' Tkzeo vector map.

A human cDNA library was inserted directionally downstream of a *TKzeo* fusion gene *via* 2 *SfiI* sites that are different in their interpalindromic sequence. (http://www.sigmaaldrich.com)

3.3.3 Transfection and selection

For library transfection, a Lonza nucleofector kit was used and the kit's protocol was followed (Amaxa Cell Line Nucleofector Kit V for MCF7, VCA-1003). 25 transfections were required for each miRNA with $2x10^6$ cells/ transfection. To approach this number of cells, MCF7 cells were grown and expanded in five T-175 flasks to give a sufficient number of cells for transfection. Cells were trypsinized at 80-90% confluence and counted, and $2x10^6$ cells were centrifuged at 300xg for 5 minutes. The pellet was resuspended in 100µl Nucleofector solution per transfection and mixed with 5µl Library DNA. The transfection was carried out using Neuclofector according to the method described in Section 2.3.7.2. Electroporated cells were grown in large flasks filled with 40 ml medium. After 48 hours, cells were selected with zeocin (500 µg/ml) for 10 days. Transfected cells should express the TKzeo fusion protein, and confer zeocin resistance. After zeocin selection, ~100,000 colonies were obtained, expanded and stored in liquid nitrogen.

3.3.4 miRNA transfection

For miRNA transfection, MCF7 cells containing the library were transfected, using Nucleofector (as explained in Section 2.3.7.2), with a pBabePuro plasmid expressing *miR-595* (24 transfections). Furthermore, empty vector pBabePuro was transfected into another aliquot of the library-transduced cells to act as a control (1 transfection). After 48 hours, cells were treated with puromycin (2 µg/ml) to enable the selection of the transduced cells. 96 hours after the start of puromycin selection, cells were selected with GCV (8µM). The control cells transfected with pBabePuro, were divided into two and either selected with puromycin only to determine the transfection efficiency or selected with puromycin and GCV to determine the false positive rate. Dr.Gäken has determined the concentration for all drugs previously in a 'lethal dose' screening that was applied to the same cell line. After 10 days under GCV selection, DNA from the remaining GCV resistant cells were extracted separately from each of the 24 flasks for PCR amplification and sequencing for target identification.

3.3.5 PCR amplification of DNA from GCV resistant colonies and sequencing

DNA was extracted according to the manufacturer's instruction and amplified by PCR as explained in 2.3.1.2.

To optimize the PCR amplification several primer pairs flanking the *SfiI* sites were tested. The differences between these primers (Table 3.1) are only a few base pairs; primer alignment in *TKzeo* sequence is illustrated in the Appendix (A1.4). Also, annealing temperature was selected after examining 6 gradients with each primer pair. After the last optimization, PCR amplification for all isolated DNAs was performed with the preferred pair of primers (3 forward and 10 reverse) using the cycling conditions given in Table 3.2.

To obtain sufficient DNA for sequencing, the PCR volume was increased to 50 µl instead of 20µl. PCR products were run on 2% (w/v) agarose gel and bands of different fragment sizes were cut and purified as explained previously. The sequencing process with PCR primers was done and processed as mentioned earlier in Section 2.3.5.

Table 3.1: p3'TKzeo primers used for PCR optimization.

miRNA	Primer Sequence	Restriction Enzyme site introduced in the primers	Tm° of full-length primer
9 F	ATGGATCCGATGCGCCCTCGATCTTC	79°C	56°C
11 F	CCTTAGGCCATTAAGGCC	61°C	56°C
13F	CCTCGAATCCTTAGGCCA	54°C	56°C
14F	TCGACCTCGAATCCTTAG	52°C	54°C
15F	GGGTCGACCTCGAATCC	55°C	56°C
3F	GGGTCGACCTCGAATCCTTA	56°C	62°C
10R	CGAGGCGGCCGACATGTTT	61°C	62°C

Table 3.2: PCR cycle conditions for DNA extracted from transfected cells.

Stage	Temperature	Duration	Cycles
1	95	5 min	1
2	95 65 72	1 min 45 sec 2.30 min	x40
3	72	5 min	1
4	4	Infinity	-

3.3.6 Western blot

Western blot experiments were performed as described in Section 2.3.11, and immuneblotting was done with the following primary antibodies: RPL27A and HSPA14 in addition to the loading control antibody which was γ tubulin.

3.3.7 qRT-PCR

Total RNA was isolated from 0.5-1x10^6 cells using Tri-reagent following the protocol described in Section 2.3.9.2 and RNA concentration was measured by Nanodrop (see Section 2.3.9.4). cDNA for miRNA amplification was generated from 5ng of RNA using specific primers for the miRNA of interest and primers for two endogenous controls RNU6B and RNU48 following the TaqMan Universal Mastermix-NoUNG manufacturer's protocol, as described in Section 2.3.10.1. The relative expression of the miRNA was calculated using ΔΔ CT method after normalization with endogenous control.

cDNA for gene expression was synthesized according to the protocol described in section 2.3.10.3. For qRT-PCR specific gene primers and probes were used (The primer sequences and probe details are listed in 2.1.16). Relative expression was determined using ΔΔ CT method after normalization to *GAPDH*.

3.3.8 miRNA knockdown

HeLa cells transfected with miR-595-pBabePuro using Nucleofection as described earlier, were transfected with MIRIDIAN hairpin miR-595 inhibitors (25nM final concentration) and control inhibitor (Dharmacon) following Nucleofection protocol as well. Also, as a control, wild type HeLa cells were transfected similarly with miR-595 inhibitors and control inhibitors. Cells were cultured for 48hrs after which RNA and protein extracts were prepared for qRT-PCR and western blot analysis.

3.4 Results

The first miRNA used in the functional assay was mir-595 and all the data presented in this chapter is related to this miRNA.

3.4.1 TOPO cloning of PCR amplified miRNA

The isolated DNA fragment was cloned into the TOPO vector and transformed into chemically competent cells. The isolated plasmid DNA was examined in order to confirm the presence of the miR-595 insert by restriction digestion. *EcoRI* was used because it cuts the PCR II-TOPO vector flanking the insert, releasing a 4000 bp and a 976bp fragments, which represent the PCR II-TOPO vector and the inserted DNA encoding miR-595 respectively. Figure 3.5 shows the *EcoRI* digestion for three plasmids containing miR-595.

3.4.2 Sequencing of plasmid DNA

The three plasmids were sequenced using the Sanger chain termination method. Data were analysed with an ABI 3130/3130xl genetic analyser. The analysed sequences were aligned to the human genome with NCBI BLAST (http://blast.ncbi.nlm.nih.gov/).

The sequence reads did not cover the complete amplified DNA fragment; therefore, new internal primers were designed and used in sequencing. The new oligonucleotides are listed in Table 3.3

Table 3.3: New primers for miR-595

miRNA	Primer Sequence	Annealing Temp
595F2	AGCCATCAAGATGGTCTGC	62 °C
595R2	CCGGGACATGATGTGATTAG	63 °C

There was a single base change detected in the pre- miRNA sequence in all three plasmids. This base change turned out to be a known SNP after analysis with the UCSC genome browser (http://genome.ucsc.edu/). The sequencing results are available in the Appendix Section A1.2. Whilst the influence of this SNP on miR-595 expression and function is not clear, we decided to re-amplify this miRNA from a different source of genomic DNA, namely HeLa cells. The new mir-595 PCR product that came from HeLa cells was Topo cloned as described previously. The sequencing of two plasmids confirmed the presence of the correct insert without the SNP present in genomic DNA that is derived from MCF7

cells, sequencing results are available in the Appendix Section A1.3. Figure 3.6 shows the digestion products of TOPO cloned miR-595 amplified from HeLa cells.

3.4.3 Subcloning and amplification

The miR-595 sequence was released from the PCR II-TOPO vector by *EcoRI* and *BamHI* digestion, gel purified and ligated into pBabePuro, which was digested with the same restriction enzymes *EcoRI/BamHI,* at 4^{o}C overnight. The ligated mixture was used to transform MACHI bacteria. Plasmid DNA was isolated and verified by restriction digestion (*SmaI*); this enzyme should cut the pBabePuro-miR-595 construct in three positions resulting in bands of 2514, 1867 and 1554 bp. The digestion products were assessed by gel electrophoreses and gave the predicted restriction pattern, confirming the correct insertion of miR-595 into pBabePuro. The digestion result is shown in Figure 3.6. Bacteria containing the correct plasmid were streaked for single colony and maxi prepped, and the resulting plasmid was then once again verified by the same restriction digests.

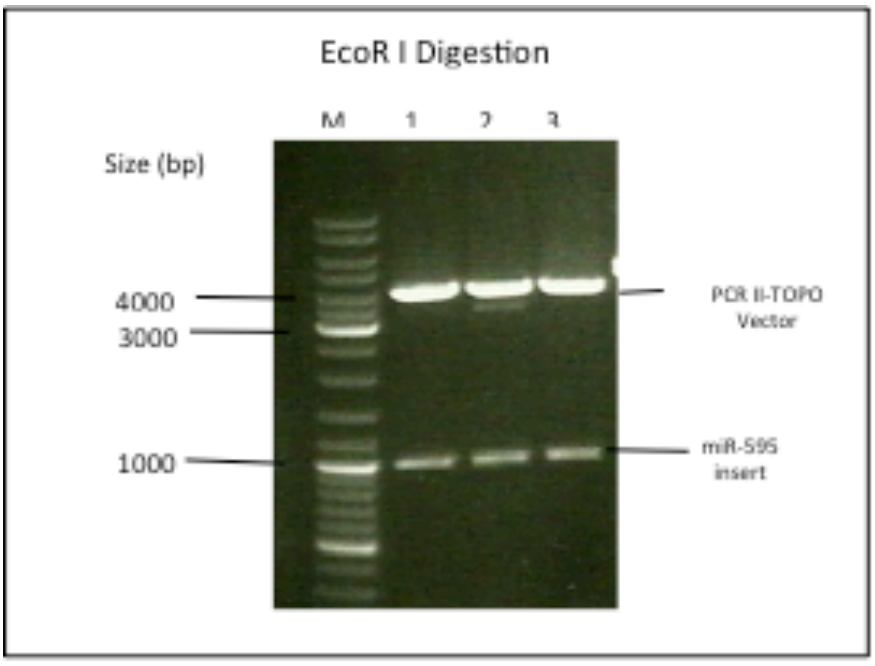

Figure 3.5: Digestion result of plasmid containing miR-595 DNA from MCF7 cells.

PCR amplification of a 976bp product from genomic DNA from MCF7 cells containing the miR-595 sequence was cloned into the PCR II-TOPO vector. Following bacterial transformation, isolated DNA was digested by *EcoRI*. The three lanes represent a digestion of plasmid derived from three different colonies. *EcoRI* digestion cut the plasmid to two fragments, vector at 4000 bp and the inserted miR-595 at 976bp.

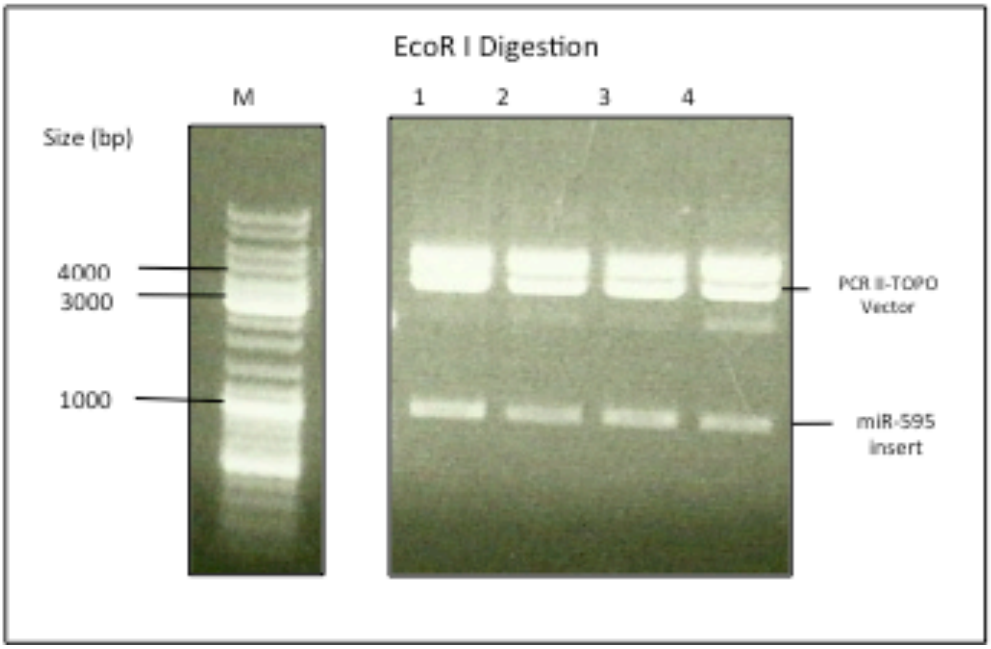

Figure 3.6: Digestion result of plasmid containing miR-595 DNA from HeLa cells

The PCR amplification of a 976bp product from genomic DNA from HeLa cells containing the miR-595 sequence was cloned into the PCR II-TOPO vector. Following bacterial transformation, isolated DNA was digested by *EcoRI*. The four lanes represent a digestion of plasmid derived from four different colonies. *EcoRI* digestion cut the plasmid to two fragments, vector at 4000 bp and the inserted miR-595 at 976bp.

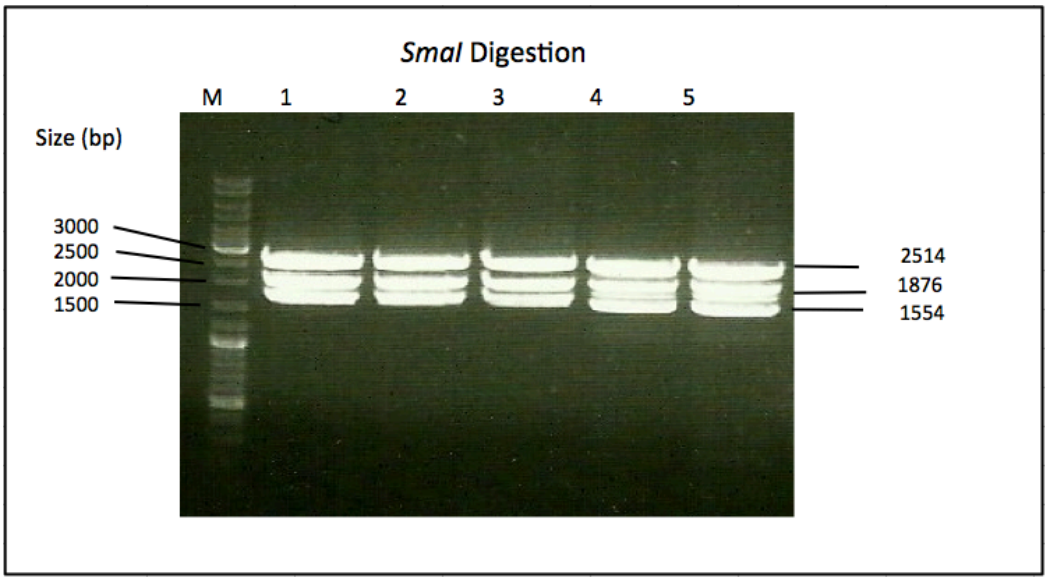

Figure 3.7: Digestion of DNA encoding miR-595 ligated into pBabePuro

This image shows *SmaI* digestion of isolated plasmids derived from ligation of pBabePuro and miR-595. *SmaI* cuts once within the miR-595 sequence and twice in the vector resulting in three fragments: 2514, 1867 and 1554bp respectively (arrowed in the figure).

3.4.4 Library cloning and transfection

The cDNA library inserted downstream of *TKzeo* fusion gene in the p3'TKzeo vector was electroporated into electrocompetent DH10α bacteria and plated on 25 (20 x 20 cm) square plates. Around $1x10^6$ colonies were recovered and they were scrapped off the plates and maxi prepped. The MCF7 cell line that does not express *miR-595*, was transfected with library DNA. 24 independent transfections were performed using nucleofection which require $2 x10^6$ cells/transfection. Subsequently, the transfected cells were put under zeocin selection. After expansion of the zeocin resistant cells, pBabePuro expressing *miR-595* and empty pBabePuro were introduced into the library transfected MCF7 cells and after 48 hours the cells were placed under puromycin selection. GCV was added after 96 hours of puromycin selection. After 10 days of GCV selection, genomic DNA was extracted from the surviving cells in individual flasks; there were about ~600 surviving colonies after GCV selection in 21 out of the original 24 transfections with a range of 4 to 58 colonies per flask.

3.4.5 Targets amplification and detection

The colonies in individual flasks were expanded and genomic DNA was isolated and PCR amplified. DNA extraction was performed separately for colonies isolated from each flask. Several primer pairs were tested for their ability to generate optimal amplification of target sites, and primer 3 forward combined with primer 10 reverse were subsequently used for PCR amplification of all DNAs. During PCR optimization all other primers failed to amplify the isolated DNA and with some of them the amplification resulted in amplifying region from the TKzeo vector. Therefore, the last designed pairs, which were very closed to *Sfi1* sites overcome this problem. The gel image in Figure 3.8 shows a typical result of PCR amplification and the presence of many bands at different lengths, with the majority being between 500-1000bp. 20 bands of different sizes were isolated and sequenced. Sequencing of 8 bands failed. The remaining sequences (12 sequenced bands) were aligned to the human gene bank sequences using the program BLAST. The alignment identified matches with the human genome sequences in 12 blasted sequences. Two of them were identified with high homology to two different transcripts; *RPL27A* (ribosomal protein L27A) and *HSPA14* (heat shock protein 14). Apart from *RPL27A* and *HSPA14,* a number of other sequences were analysed that mapped to chromosomes 3, 6 and 7 in positions without known genes or in positions close to some genes such as: Neuregulin 3 (*NRG3*), 10q23.1,

glutamate receptor metabotropic 5 (*GRM5*), 11q14.3, and translocation protein (*SEC63*), 6q21.

Furthermore, a DNA mixture derived from DNA from all flasks was prepared by mixing the same amount of template DNA and then amplifying it with primer 3 forward and 10 reverse; the PCR result of this DNA showed an amplification of the common bands presents in the other DNA and some distinct bands which were seen in some of the DNA were not observed in the DNA mix.

3.4.6 Computationally predicted targets

The miRecords website allows to predict miRNA targets with 7 different prediction programs. This website was used to search for *miR-595* targets; there are no validated targets for *miR-595* as yet, whereas there are more than 3,000 targets predicted by at least one program (http://miRecords.biolead.org/). This website provides a filtering option to compare target prediction by multiple programs. Using the 5 programs targetscan, rnahybrid, pita, miRtarget 2 and Miranda a shorter list of 133 predicted targets was generated. Table 3.4 shows the 133 predicted targets. *RPL27A* and *HSPA14* are not present in this list, they were not predicted by any program. However, another software program RNAhybrid (http://bibiserv.techfak.uni-bielefeld.de/rnahybrid/), which relies on finding the minimum free energy (MFE) of hybridization between a mature miRNA sequence and the predicted target sequence, was used to identify the binding energy between *miR-595* and the identified targets (*RPL27A* and *HSPA14)* as shown in Figure 3.9. The lower the energy (<-20kcal/mol) is the more likely that a miRNA binds to the putative target site. The binding between the mature *miR-595* sequence and its putative target gene sequences was good because the MFE value for binding with *RPL27A* was -29.3 kcal/mol and -30.1 kcal/mol for binding with *HSPA14*. These values are comparable to those obtained for the binding of other miRNAs to their known validated targets.

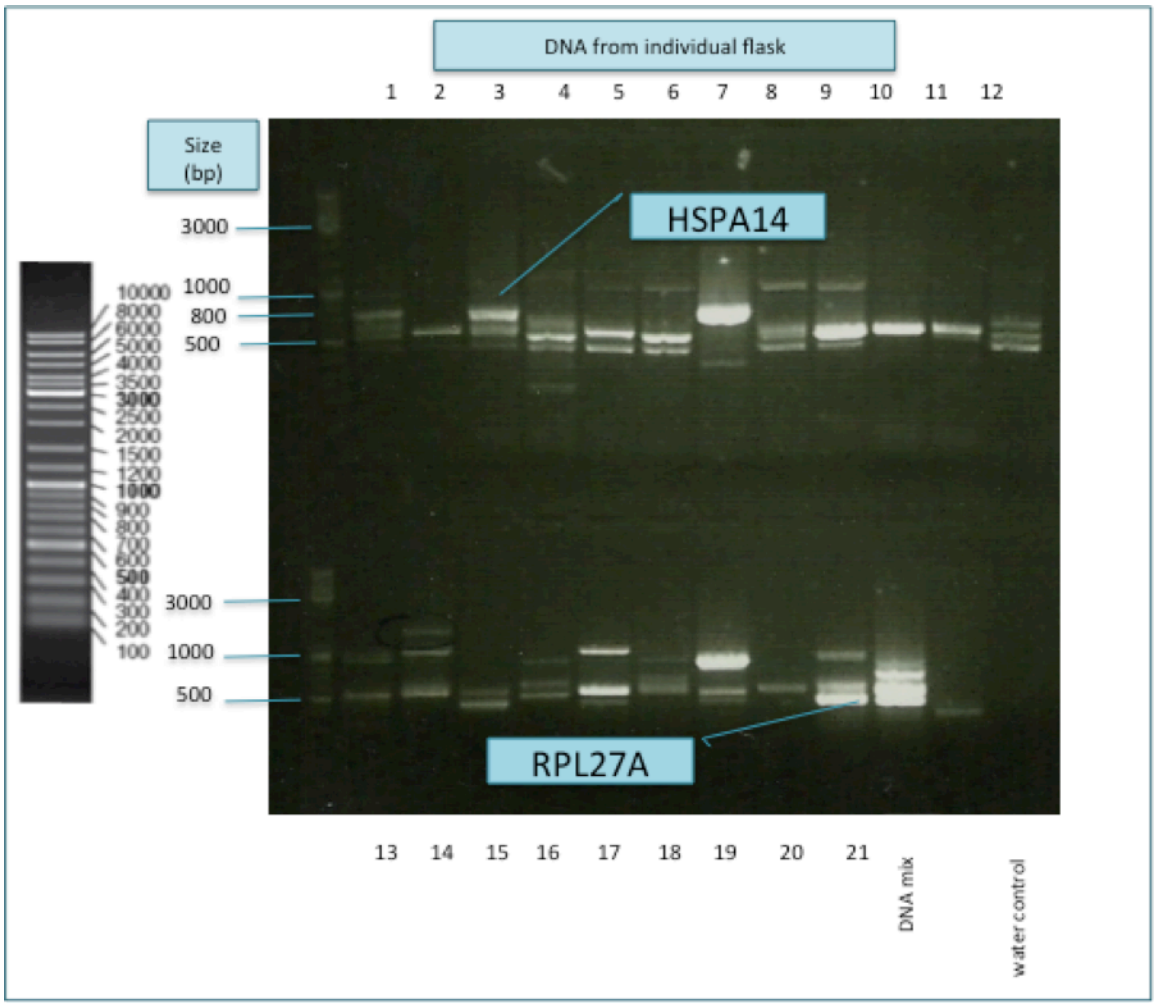

Figure 3.8: A typical result of PCR amplification of genomic DNA extracted from GCV resistant cells.

After transfecting pBabePuro expressing miR-595 into MCF7 cells containing the TKzeo library, puromycin and GCV selection was applied. Genomic DNAs were isolated from GCV resistant cells from 21 flasks and PCR amplified using vector specific primers. PCR products were visualized on a 2% (w/v) agarose gel and the gel image shows the PCR products of individual flasks. Each lane represents a DNA from one flask. Some of the bands are present in multiple samples and might represent identical targets in different transfections. Bands of different sizes were purified and sequenced. A BLAST search of the sequences obtained identified two transcripts; *RPL27A* (≈500bp) and *HSPA14* (≈800bp) as indicated. DNA mix (a combination of isolated DNAs from all flasks) gives amplification for some bands.

Table 3.4: list of miR-595 predicted target by 5 programs: targetscan, rnahybrid, pita, mirtarget2 and miranda

Gene Symbol	Description	Gene Symbol	Description
SH3YL1	SH3 domain containing, Ysc84-like 1 (S. cerevisiae)	C18orf19	chromosome 18 open reading frame 19
TCL6	T-cell leukemia/lymphoma 6	SLC16A12	solute carrier family 16, member 12 (monocarboxylic acid transporter 12)
DECR2	2,4-dienoyl CoA reductase 2, peroxisomal	TIPARP	TCDD-inducible poly(ADP-ribose) polymerase
SLC24A3	solute carrier family 24 (sodium/potassium/calcium exchanger), member 3	GNRHR	gonadotropin-releasing hormone receptor
RNF150	ring finger protein 150	DARS	aspartyl-tRNA synthetase
KIAA1377	KIAA1377	FMO2	flavin containing monooxygenase 2 (non-functional)
ZNF273	zinc finger protein 273	CAPN2	calpain 2, (m/II) large subunit
ZNF708	zinc finger protein 708	CTNNA1	catenin (cadherin-associated protein), alpha 1, 102kDa
GREM2	gremlin 2, cysteine knot superfamily, homolog (Xenopus laevis)	DPT	dermatopontin
CCDC21	coiled-coil domain containing 21	AFF2	AF4/FMR2 family, member 2
USP46	ubiquitin specific peptidase 46	PRELP	proline/arginine-rich end leucine-rich repeat protein
MLF1IP	MLF1 interacting protein	RASA1	RAS p21 protein activator (GTPase activating protein) 1
NAT11	N-acetyltransferase 11	SNRPB2	small nuclear ribonucleoprotein polypeptide B""
PPP1R14C	protein phosphatase 1, regulatory (inhibitor) subunit 14C	UBE2G2	ubiquitin-conjugating enzyme E2G 2 (UBC7 homolog, yeast)
TMEM133	transmembrane protein 133	USP4	ubiquitin specific peptidase 4 (proto-oncogene)
LYRM2	LYR motif containing 2	CUL5	cullin 5
CHST7	carbohydrate (N-acetylglucosamine 6-O) sulfotransferase 7	RGS5	regulator of G-protein signaling 5
WDR45L	WDR45-like	CREG1	cellular repressor of E1A-stimulated genes 1
NSFL1C	NSFL1 (p97) cofactor (p47)	BCL2L1	BCL2-like 1
HSD17B11	hydroxysteroid (17-beta) dehydrogenase 11	ADCY9	adenylate cyclase 9
GDE1	glycerophosphodiester phosphodiesterase 1	REPS2	RALBP1 associated Eps domain containing 2
ZC3H7B	zinc finger CCCH-type containing 7B	FGA	fibrinogen alpha chain
KIF21A	kinesin family member 21A	NCAM1	neural cell adhesion molecule 1
MTMR10	myotubularin related protein 10	DCK	deoxycytidine kinase
SLC35A5	solute carrier family 35, member A5	GABRA1	gamma-aminobutyric acid (GABA) A receptor, alpha 1
TMEM106B	transmembrane protein 106B	PRRG1	proline rich Gla (G-carboxyglutamic acid) 1
LSG1	large subunit GTPase 1 homolog (S. cerevisiae)	CLEC6A	C-type lectin domain family 6, member A
ANLN	anillin, actin binding protein	FLJ46838	FLJ46838 protein
CTTNBP2NL	CTTNBP2 N-terminal like	ARHGAP28	Rho GTPase activating protein 28
AJAP1	adherens junctions associated protein 1	DUXA	double homeobox A
TBC1D16	TBC1 domain family, member 16	LRRC66	leucine rich repeat containing 66
RBM47	RNA binding motif protein 47	GLUL	glutamate-ammonia ligase (glutamine synthetase)
FAM172A	family with sequence similarity 172, member A	MDH1B	malate dehydrogenase 1B, NAD (soluble)
B3GNT5	UDP-GlcNAc:betaGal beta-1,3-N-acetylglucosaminyltransferase 5	CLDND1	claudin domain containing 1
SPRED1	sprouty-related, EVH1 domain containing 1	C6orf91	chromosome 6 open reading frame 91
LCORL	ligand dependent nuclear receptor corepressor-like	CDKL2	cyclin-dependent kinase-like 2 (CDC2-related kinase)
REXO1L1	REX1, RNA exonuclease 1 homolog (S. cerevisiae)-like 1	FGF12	fibroblast growth factor 12
CACNA2D4	calcium channel, voltage-dependent, alpha 2/delta subunit 4	LYVE1	lymphatic vessel endothelial hyaluronan receptor 1
C11orf47	chromosome 11 open reading frame 47	DDX52	DEAD (Asp-Glu-Ala-Asp) box polypeptide 52
SLC30A8	solute carrier family 30 (zinc transporter), member 8	KIF3A	kinesin family member 3A
KRT28	keratin 28	MACF1	microtubule-actin crosslinking factor 1
C2orf50	chromosome 2 open reading frame 50	TLK1	tousled-like kinase 1
FAM33A	family with sequence similarity 33, member A	C11orf58	chromosome 11 open reading frame 58
RNF212	ring finger protein 212	C1orf107	chromosome 1 open reading frame 107
C6orf167	chromosome 6 open reading frame 167	AFF4	AF4/FMR2 family, member 4
TPRG1	tumor protein p63 regulated 1	TOR1B	torsin family 1, member B (torsin B)
GJB7	gap junction protein, beta 7, 25kDa	VASH1	vasohibin 1
TMEM215	transmembrane protein 215	CPEB3	cytoplasmic polyadenylation element binding protein 3
ZNF417	zinc finger protein 417	SORCS3	sortilin-related VPS10 domain containing receptor 3
WDR21C	WD repeat domain 21C	GLT25D2	glycosyltransferase 25 domain containing 2
C2orf63	chromosome 2 open reading frame 63	TRIM2	tripartite motif-containing 2
DSEL	dermatan sulfate epimerase-like	NTS	neurotensin
C15orf41	chromosome 15 open reading frame 41	AFF1	AF4/FMR2 family, member 1
UBASH3B	ubiquitin associated and SH3 domain containing, B	ABI2	abl interactor 2
PCDH11X	protocadherin 11 X-linked	ARHGAP1	Rho GTPase activating protein 1
PCDH11Y	protocadherin 11 Y-linked	CYP8B1	cytochrome P450, family 8, subfamily B, polypeptide 1
ZFP91	zinc finger protein 91 homolog (mouse)	GPC5	glypican 5
GRIN3A	glutamate receptor, ionotropic, N-methyl-D-aspartate 3A	USP6	ubiquitin specific peptidase 6 (Tre-2 oncogene)
ZNF431	zinc finger protein 431	FOXK2	forkhead box K2
NUS1	nuclear undecaprenyl pyrophosphate synthase 1 homolog (S. cerevisiae)	LRP2	low density lipoprotein-related protein 2
ADAMTS16	ADAM metallopeptidase with thrombospondin type 1 motif, 16	USP9Y	ubiquitin specific peptidase 9, Y-linked (fat facets-like, Drosophila)
MAPK1IP1L	mitogen-activated protein kinase 1 interacting protein 1-like	EIF2AK3	eukaryotic translation initiation factor 2-alpha kinase 3
TTC30A	tetratricopeptide repeat domain 30A	SEL1L	sel-1 suppressor of lin-12-like (C. elegans)
SCYL1BP1	SCY1-like 1 binding protein 1	H3F3B	H3 histone, family 3B (H3.3B)
ABCA1	ATP-binding cassette, sub-family A (ABC1), member 1	HINT1	histidine triad nucleotide binding protein 1
LEPROTL1	leptin receptor overlapping transcript-like 1	MCF2	MCF.2 cell line derived transforming sequence
YES1	v-yes-1 Yamaguchi sarcoma viral oncogene homolog 1		

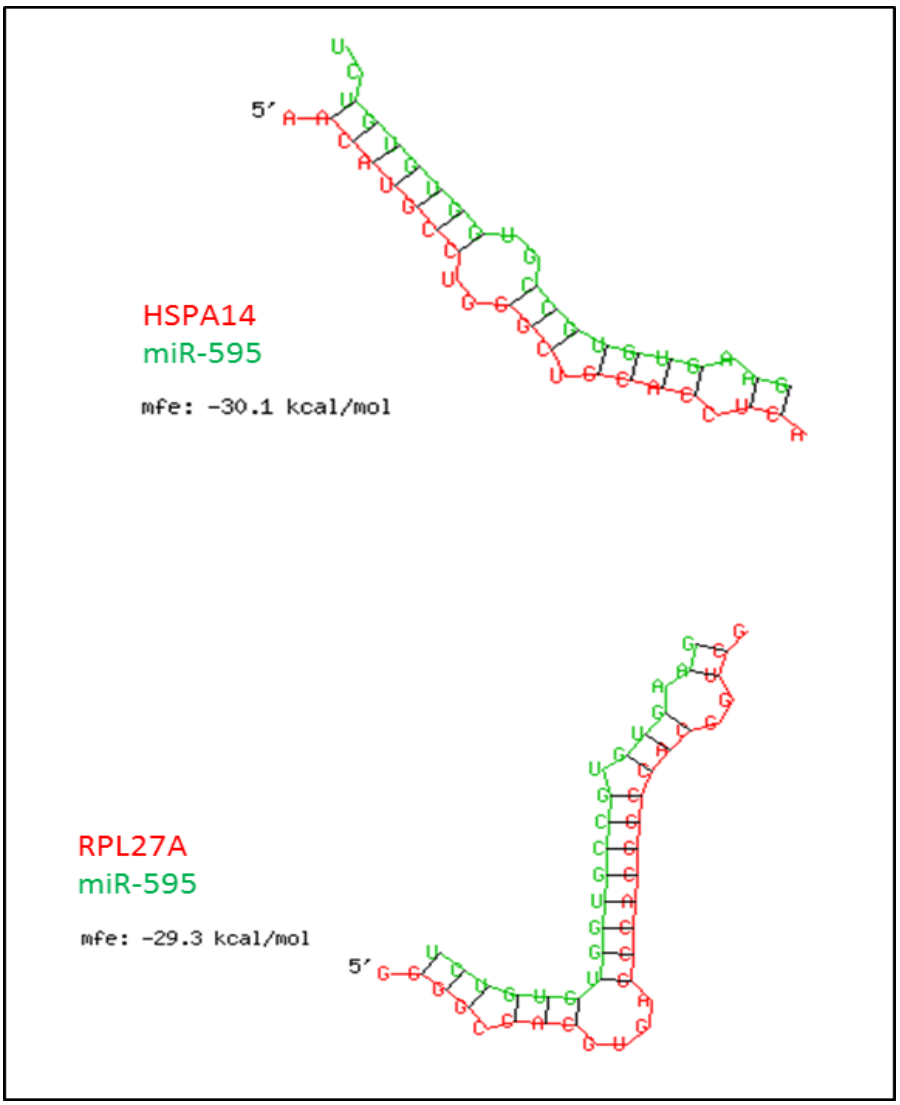

Figure 3.9: Binding between *miR-595* and its identified targets based on the hybridization energy.

RNAhybrid software was used to determine the minimum free energy (MFE) of hybridization of the mature *miR-595* sequence with *RPL27A* and *HSPA14* sequences. The values obtained as shown in the image indicate favourable binding.

3.4.7 Target validation

Several experiments have been done to validate the putative targets for miR-595 (*RPL27A* and *HSPA14*). First, the expression level of *miR-595* was examined in different cell lines including HeLa, HepG2 (human liver carcinoma cell line), KG-1 (acute myelogenous leukemia) and K562 (human erythroleukemic cell line) to decide which validation method will be applied, that is either knocking down *miR-595* in the cells that express the miRNA, or introducing the miRNA into cells that do not express or express the miRNA at very low level and then examining the effect of the miRNA knockdown/overexpression on the putative targets.

RNA was isolated from all selected cell lines (from $1x10^6$ cells) using the Trizol extraction method and the concentration was measured by Nanodrop as described in Section 2.3.10.4. To make cDNA for *miR-595*, 10 ng/ml from the RNA was used and miRNA Taq man assay was applied as explained in Section 2.3.10.2. Two endogenous controls were used (RNU6b and RNU48) and miRNA expression level in each cell line was calculated using ΔCT; results are presented in Figure 3.10-A. The Taq man assay showed that the expression level of *miR-595* is absent or very low in these four cell lines. Therefore, the selected method for target validation was the ectopic expression of *miR-595* in these cell lines. Also, before introducing the miRNA in the cell lines, the expression level of *RPL27A* and *HSPA14* was also examined in the same cell lines to ensure that these genes are expressed in all of them. For qRT-PCR, 1μg RNA was used to make cDNA, which was then diluted to 1:100 for qRT-PCR, and then the data was normalized with *GAPDH*. The mRNA expression showed that *RPL27A* and *HSPA14* are expressed in all selected cell lines at variable levels based on ΔCT fold change calculation; results are shown in Figure 3.10-B and C.

Hence, based on the expression result of *miR-595* and its putative target, cell lines were transfected with pBabepuro-miR-595 and empty vector pBabePuro (control) using the Nucleofection method as explained previously. Cells were selected with 2μg/ml puromycin at 48hrs post transfection, except KG-1 which had shown high sensitivity to puromycin and it was therefore selected with 1μg/ml puromycin. After introducing the miRNA into the cell lines, the miR-595 expression was examined by qRT-PCR in all of them to confirm that they express the miRNA. The screening confirmed the increases in miR-595 expression level as shown in Figure 3.11-A. The expression level was increased on average of 60-80% in all cell lines in comparison with wild type cells.

Samples for qRT-PCR and the western blot were isolated on day 6 post-transfection. RNA was extracted from all cells from three independent experiments and analysed by qRT-PCR. The *RPL27A* expression in all cell lines was downregulated as a result of *miR-595* overexpression in comparison with untransfected cells or cells transfected with an empty vector. The *RPL27A* expression level was decreased by 83% in KG-1, 73% in K562, 88% in HeLa and 55% in HepG2, see Figure 3.11-B. The percentages were determined by comparing the RNA expression levels from cells expressing *miR-595* to cells transfected with the empty pBabePuro plasmid.

Protein extracts from HeLa and HepG2 cells were isolated from $2.5x10^5$ cells lysed in 40 µl lysis buffer; they were probed with antibodies to RPL27A (ABCAM), HSPA14 (ABCAM) and γ-tubulin as loading control (Santa Cruz). The protein levels in cells expressing the miRNA were down-regulated in comparison with proteins from wild type cells and cells transfected with empty pBabePuro, see Figure 3.11-C.

These results confirmed that RPL27A is a real target for *miR-595* as the overexpression of *miR-595* resulted in a clear down regulation of RPL27A at both mRNA and translational level. Also, HSPA14 was validated as a real target for *miR-595* on the protein level by western blot.

To further investigate *RPL27A* as a target for *miR-595*, HeLa cells (wild type cells), and HeLa cells transfected with *miR-595*, were transfected with hairpin inhibitor directed against *miR-595* (MIRIDIAN) and a control hairpin inhibitor (Dharmacon). Cells were transfected using Nucleofection and analysed after 48hrs for mRNA and protein expression (Figure 3.12). Wild type HeLa cells (the control) showed no or minor changes on RPL27A expression level as a result of inhibitor transfection which showed the specificity of the inhibitors because the expression of *miR-595* is absent or very low in normal HeLa cells as shown earlier in Figure 3.11-A, whereas HeLa cells transfected with *miR-595* showed reduced expression of RPL27A which could be restored to normal levels by treatment with *miR-595* inhibitor and resulted in a 4 to 5 fold upregulation of RPL27A on both mRNA and protein level. (Figure 3.12).

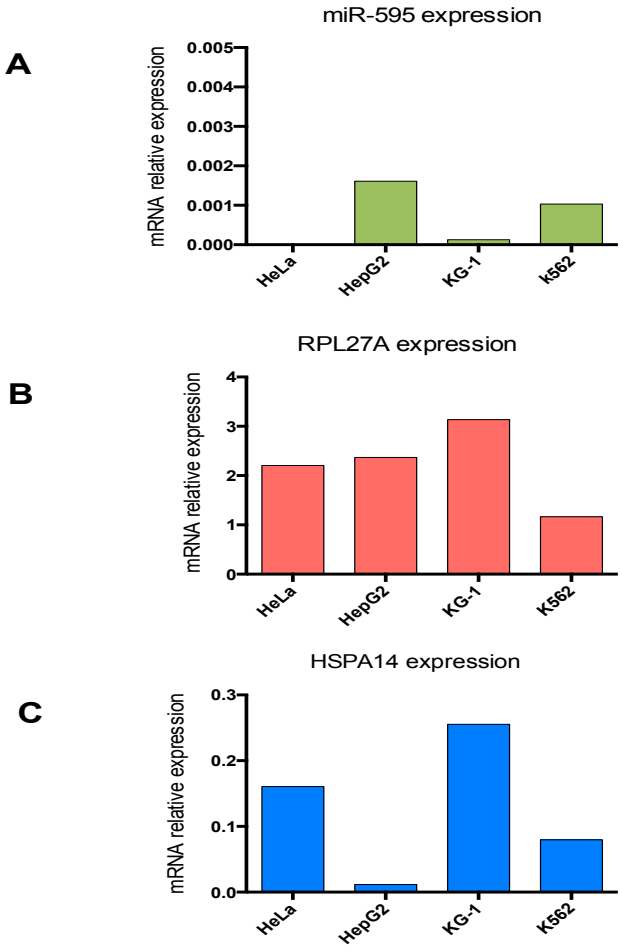

Figure 3.10 Expression levels of endogenous *miR-595* and *RPL27A* in different cell lines

Endogenous levels of *miR-595*, *RPL27A* and *HSPA14* mRNA were determined by qRT-PCR in HeLa, HepG2, KG-1 and K562. **A)** Total RNA isolated from each cell line and *miR-595* expression level was quantified by qRT-PCR. The expression level, which was normalized to the endogenous control (RNU6B) showed no expression in HeLa cell line and very low expression level in the other cell lines. **B &C)** Total RNA isolated from each cell line; *RPL27A* & *HSPA14* mRNA expressions were determined by qRT-PCR. After normalizing to *GAPDH*, expression level was determined by $2^{-\Delta CT}$ in which *RPL27A* and *HSPA14* were expressed in all cell lines at variable levels.

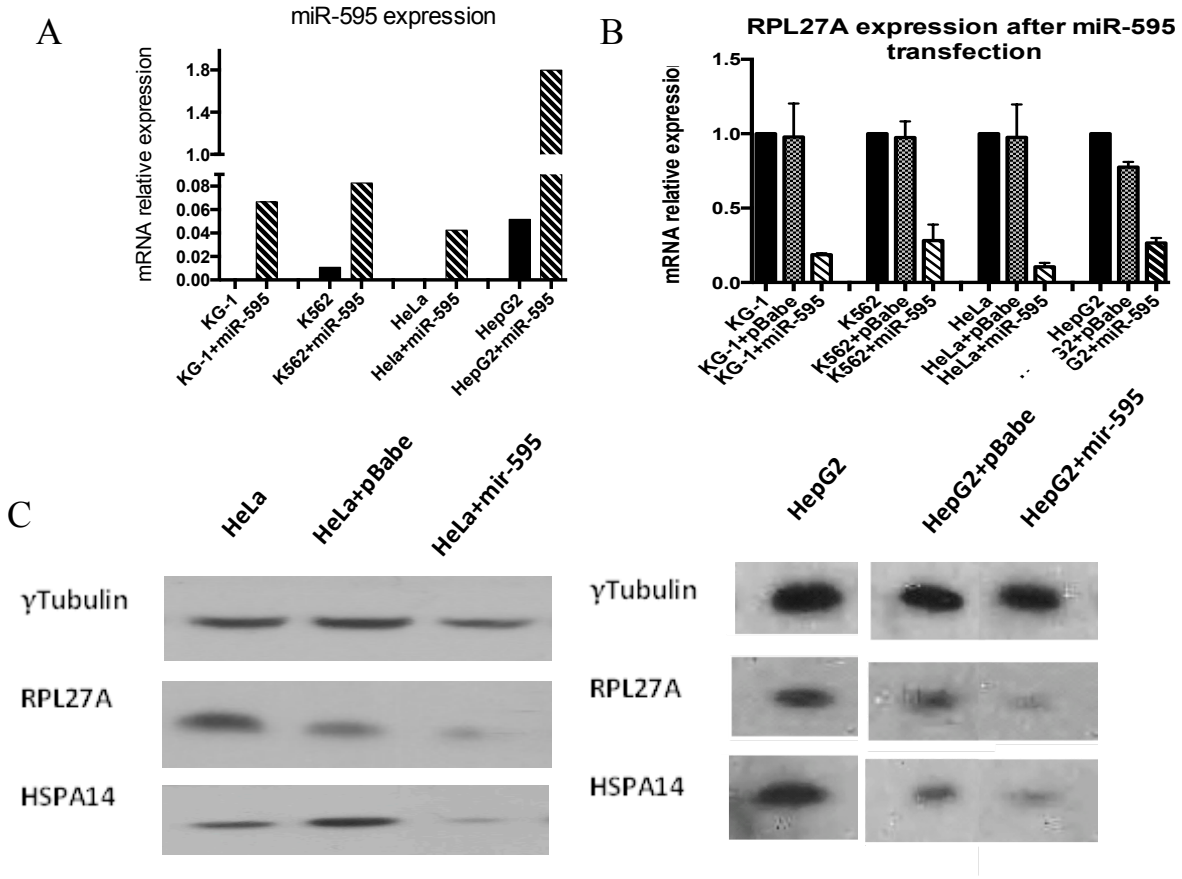

Figure 3.11: Validation of RPL27A and HSPA14 as a target for *miR-595* by qRT-PCR and western blot analysis.

Endogenous mRNA and protein level for RPL27A in addition to the protein level for HSPA14, were all determined in untransfected, pBabe (pBabePuro empty vector), and *miR-595* (pBabePuro-miR-595) transfected cells. Transfection was done by Nucleofection and samples were collected after 4 days from puromycin selection. **A)** *miR-595* expression level was determined in four different cell lines 48hrs after miRNA transfection. The result confirmed that all the cell lines were expressing *miR-595* after the transfection. **B)** To investigate if *miR-595* overexpression will down regulate *RPL27A*, mRNA was quantified by qRT-PCR on untransfected cells, cells transfected with empty vector and cells transfected with *miR-595* from three independent experiments. The result was determined after normalization to *GAPDH* and relative expression was calculated by $2^{-\Delta\Delta CT}$. *RPL27A* was down regulated in all cell lines that are expressing *miR-595* in comparison with cells transfected with pBabe or untransfected cells. **C)** Proteins Isolated from HeLa and HepG2 that were transfected with empty vector and *miR-595*, were probed with RPL27A, HSPA14 antibodies and loading control tubulin antibody. The results showed that RPL27A and HSPA14 were downregulated in cells expressing *miR-595*.

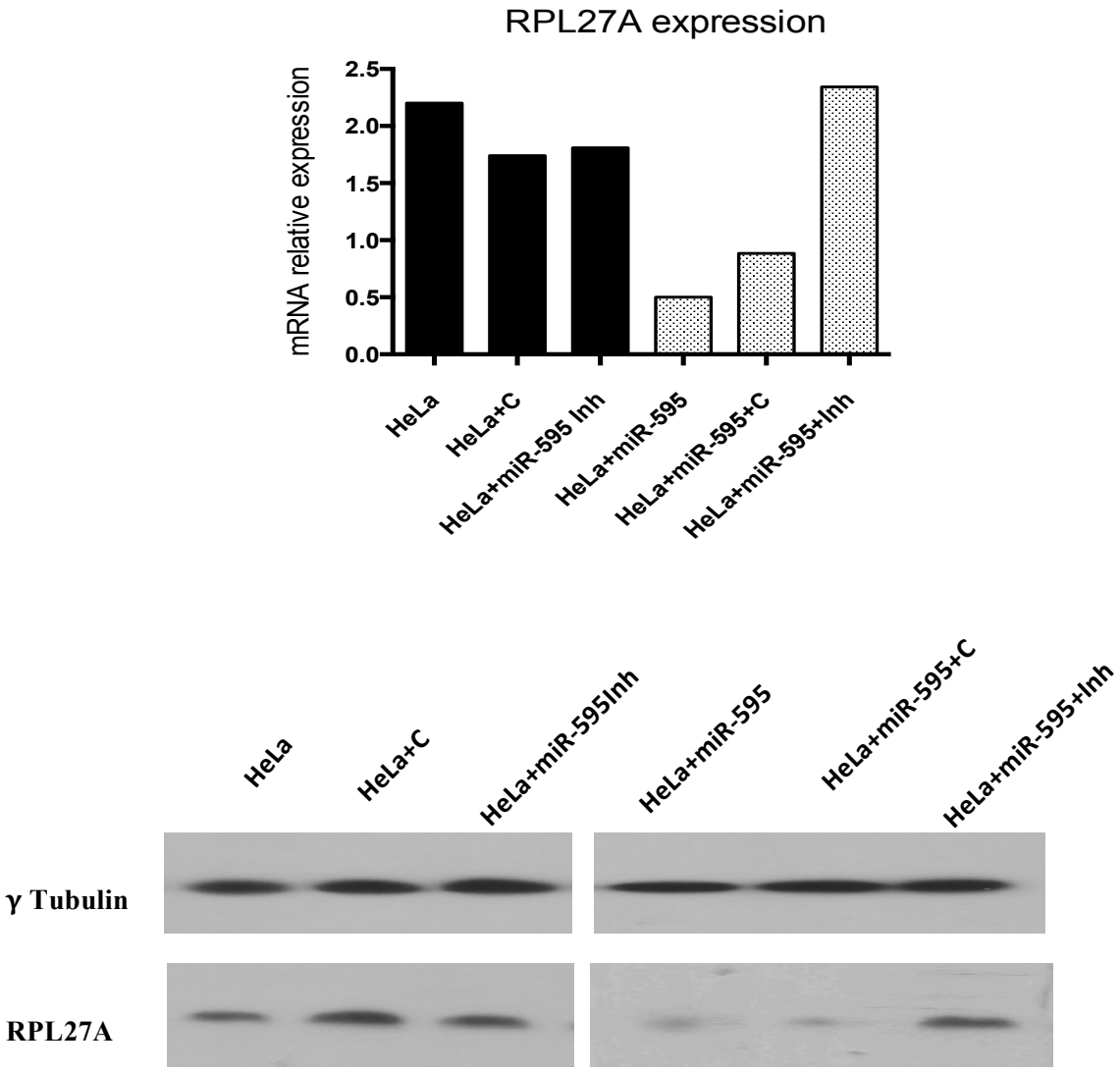

Figure 3.12: Inhibition of *miR-595* expression by MIRIDIAN hairpin inhibitor.

HeLa cells which do not express miR-595 were transfected with control inhibitors (HeLa+C) and *miR-595* inhibitor (HeLa+ miR-595Inh). Also, HeLa cells were transfected with miR-595 to examine the effect of the inhibitors in the cells expressing the miRNA. HeLa cells that are expressing miR-595 were also transfected with hairpin control and inhibitor against *miR-595*. **A)** *RPL27A* mRNA expression level quantified by qRT-PCR showed up-regulation for *RPL27A* in HeLa cells expressing *miR-595* which was transfected with *miR-595* inhibitor. **B)** RPL27A protein expression was determined by western blot using RPL27A antibody and tubulin control antibody. RPL27A overexpression was observed in HeLa cells with *miR-595* and *miR-595* inhibitor, indicating that the down-regulation of *miR-595* resulted in up-regulation of RPL27A.

3.5 Discussion

Several studies have shown an association between microRNA expression and MDS pathogenesis as illustrated in the introduction. MDS patients with chromosome 7 abnormalities, specifically monosomy 7, are considered as a poor prognostic class and a high-risk group. To the best of my knowledge, no single study has examined the contribution of miRNAs in MDS with chromosome 7 abnormalities. Studying the expression of miRNAs encoded by chromosome 7 and their targets might clarify the pathogenesis of MDS with -7/7q-.

Since the discovery of the miRNA in 1993 (Lee *et al.* 1993) rapid developments in miRNA target prediction assays, mainly bioinformatics, have led to the identification of many new miRNAs and a very large number of predicted possible targets. However, only a very small proportion of these predicted targets have been experimentally validated. Based on the last miRBase release (Release 20, June 2013), there are 1872 precursors and 2578 mature human miRNAs; only 286 of them have validated targets based on the last update from miRecords (April 27, 2013). The main obstacle in miRNAs research is the accurate detection of target genes at the post-transcriptional level without relying on the homology to a putative target. Therefore, the application of our novel functional assay allows an efficient identification of miRNA targets that interact with or without a seed sequence with their targets. This assay has the potential to identify down-regulated targets at both mRNA and protein levels. However, the identified number of putative targets by this assay is smaller than the number of target predicted by computational algorithms and expression arrays. The assay isolates only the targets that are significantly down-regulated which therefore can be considered as the most crucial targets (Gäken *et al*, 2012).

The novel functional assay relies on using a large cDNA library, representing approximately 77% of the human transcriptome, inserted downstream of a fusion gene (*TKzeo*). The presence of this large library will increase the possibility of identifying many targets for many miRNAs.

As mentioned earlier in this chapter, several miRNAs were initially selected because they were located in the 7q region. The four selected miRNAs were: miR-489 and miR-653, which are located on 7q21, miR-671 at 7q36.1 and the most terminal miR-595 at 7q36.3.

These miRNAs were cloned into pBabePuro and the functional assay was started with miR-595.

Literature searches on *miR-595* revealed no studies that specifically discuss the differential expression of this particular miRNA in certain diseases. However, a few studies have shown the differential expression of *miR-595* by microRNA profiling. Using microarray analysis, Liu *et al.* showed that overexpression of *miR-595* was accompanied by a reduction of *PRODH/POX* (Proline Oxidase) in a renal cancer cell line as compared to a normal renal cell line, (Liu *et al.* 2010). *POX* is a mitochondrial inner membrane enzyme that has been identified as a mitochondrial tumour suppressor that is functionally involved in promoting apoptosis by secreting ROS (Reactive Oxygen Species) and minimizing the signalling of HIF (Hypoxia-Inducible Factor) (Liu *et al.* 2009). This target might be of interest in our study, as it was reported that *POX* upregulation is possibly driven by *p53* mutation (Donald *et al.* 2001), and *p53* mutations are noted for their contribution to MDS pathogenesis (Kitagawa *et al.* 1994). POX was not predicted as a target for miR-595 neither by any of the prediction algorithms nor by the applied functional assay and this is probably due to the low frequency of POX in the used library (only 126 reads) as deduced from the next generation sequencing results of the Mission Target ID library (see attached CD).

Another interesting study has shown that *miR-595* was up-regulated in $CD4^+$ cells as compared with $CD8^+$ cells in thymocytes at the single positive maturation stage (Ghisi *et al.* 2011). This observation implies an interesting correlation between this miRNA and the immune system. miRNAs dysregulation has been associated with their effect on innate immune signalling, which plays an important role in MDS prognosis and treatment. Recent studies on MDS with 5q- showed that the reduction of *miR-145* and *miR-146a* in $CD34^+$ bone marrow cells from individuals with del 5q MDS relative to normal controls, was inversely associated with the increased expression of TIRAP and TRAF6, which are involved in the innate immunity pathway, and activated the innate immunity which caused abnormalities in the megakaryocyte (Baltimore *et al.* 2008, Starczynowski *et al.* 2010, Olnes *et al.* 2011). A more detailed description of miRNAs contribution and involvement in regulation of the immune system has been provided in the introduction.

The application of the novel functional assay has identified several putative targets for *miR-595* including *RPL27A* and *HSPA14*. These targets were present in the DNA isolated from

multiple individual flasks. Also, during the optimization of PCR primers, these putative targets were also isolated with most of the other primer pairs tested. This is a further indication of the sensitivity of the assay**.** The functional details of *RPL27A* and *HSPA14* are described in Table 3.6.

Interestingly the PCR amplification of the DNA mixture consisting of genomic DNAs from all 21 extractions did not show similar results to that from individual DNA. It only showed the common bands whilst the other isolated bands from individual DNA were absent. This is probably due to the higher abundance of these bands resulting in preferential PCR of these fragments.

To find out if there is any correlation between the *miR-595* identified targets *RPL27A* and *HSPA14*, and the computational algorithm predicted targets, gene clustering was performed based on gene function or pathways. David Bioinformatics Resources database was used for that purpose (http://david.abcc.ncifcrf.gov/). The 133 genes, identified by 5 different computational algorithms, in addition to the two targets identified by our functional assay (RPL27A and HSPA14), clustered into 10 different functional groups. Interestingly *RPL27A* clustered under phosphoprotein function, the group in which most (58 of the 133 predicted targets) of the *miR-595* predicted targets cluster. *HSPA14* clustered to ATP-binding function together with 15 other predicted target genes. However, pathway analysis did not show any possible involvement of these genes in known pathways.

Interestingly, analysis of possible binding between *miR-595* and its identified targets *(RPL27A* and *HSPA14)* using RNAhybrid, shows favourable binding between them with low MFE comparable to other miRNAs and their validated targets. For example, Garzon *et al*., identified the mRNA encoding Homeobox A1 **(***HOXA1)* as a target for *miR-10*a (Garzon *et al.* 2006). The binding energy of hybridization of this miRNA with *HOXA1*mRNA is -19.8 Kcal/mol, which is higher than the calculated energy for *miR-595* with its targets, *RPL27A* (-29.8 Kcal/mol) and *HSPA14* (-30.1 Kcal/mol). This further indicated that the identified targets by the functional assay are valid targets for *miR-595*. In order to confirm this finding, target validation using functional assays was carried out.

As mentioned earlier in the introduction, ribosomal protein *RPS14* has been identified as an important gene involved in the pathogenesis of MDS with 5q-, mainly through its

involvement in controlling erythroid differentiation. Therefore, it was of interest to validate the ribosomal protein *RPL27A,* which can be then further investigated in terms of its biological function and possible contribution to MDS.

The validation was carried out in several cell lines, which were chosen based on the several reasons. To insure high efficiency for the transfection, two adherent cell lines were used (HeLa and HepG2), which are in general easier to transfect than suspension cell lines. Also, suspension cell lines were selected due to our interest in studying the miRNA implication in myeloid disease. Therefore, two myeloid cell lines were chosen (K562 and KG-1). The main reason for using more than one cell line is to rule out the differences in the genetic background of each cell line which might affect the miRNA regulation of its target, especially if that target is mutated, or regulated by other genetic variants. Although MCF7 cell line was the assay model, it was excluded from the selected cell lines for the validation due to the earlier identification of SNP in *miR-595* sequence as mentioned in Section 3.5.2. Even though this SNP was not identified with any biological effect it was preferred to exclude these cells from the validation experiments.

Ribosomal protein *RPL27A* which was isolated from different clones from different flasks was validated as a real target for *miR-595* regulated at both mRNA and protein level. Interestingly, Mendiburu et al have shown that *RPL27A* is highly overexpressed in MDS patients with refractory anaemia with excess blasts (RAEB). This observation relies on analysing bone marrow samples by serial analysis of gene expression (SAGE) (Mendiburu *et al.* 2008). Furthermore, it has been found that *RPL27A* knockdown resulted in the induction of p53 in sooty foot ataxia mice (Terzian *et al*, 2011). This study used mutated *RPL27A* transgenic sooty foot ataxia mice and they showed that the mice developed p53 phenotype including pancytopenia, epidermal hyperpigmentation and cerebellar ataxia. This ribosomal stress, which occurs through changes in the ribosomal proteins level, interferes with *p53* expression level. The relation between ribosomal protein and p53 was first discovered in 1994, when Levine and his group discovered the binding complex between RPL5, p53 and its regulator MDM2 (Levine *et al*, 1994). Since then, several other ribosomal proteins have been identified with their effect on the p53-MDM2 pathway and their implication in disease pathogenesis. For instance, haploinsufficiency of ribosomal gene *RPS14*, which is localized to the critical deleted region (CDR) in 5q- patients, was

associated with *p53* overexpression which inhibited erythroid differentiation and contributed to the development of 5q- syndrome phenotype, a subtype of MDS (Ebert *et al.* 2008, Dutt *et al.* 2011, McGowan *et al.* 2011). Therefore, it was of interest to investigate the biological function of this ribosomal protein in human cell lines and human hematopoietic progenitor stem cells CD34+ to identify the effect on ribosome biogenesis, p53 pathway and the biological effect on hematopoietic stem cells, mainly erythroid cells differentiation.

Conclusion

Deregulation of specific miRNAs correspondingly results in biological changes, which might contribute to MDS. Therefore, identification of miRNA targets is essential for understanding the function of the miRNA. The application of the functional assay described here led to the identification of a biologically relevant target, *RPL27A*, which has been experimentally validated.

Thus, studying the biological function of this validated target might provide insight into the function of *miR-595* and its contribution to MDS mainly via its functional effect on p53 pathway and erythroid differentiation.

Table 3.5: Predicted genes by sequencing and their biological function and involved pathways. Data adapted from www.genecards.org.

Gene	Gene Map	Gene Function	Pathways
RPL27A (Ribosomal protein L27)	11p15	• RNA binding • Protein binding • Structural constituent of ribosome	• Translation • Translational elongation • Translational termination • Gene expression • Viral reproduction • Viral infectious cycle • Viral transcription • Endocrine pancreas development • Cellular protein metabolic process
HSPA14 (Heat shock protein)	10p13	• Nucleotide binding • Protein binding • ATP binding	'de novo' cotranslational protein folding

Chapter 4: Identification the biological function of RPL27A

4.1 Introduction

Ribosomal proteins are a major component of ribosomes; which were first identified in *Escherichia coli (E.coli)* more than 40 years ago (Waller *et al.* 1961). Ribosomes are ribonucleoprotein complex that are responsible for protein synthesis in all living cells and consist of two subunits. The primary structure of the ribosome in *E.coli* identifies three ribosomal RNAs (rRNAs) and 54 ribosomal proteins. The rRNA is composed of 5S and 23S in a large 50S subunit, and 16S in a small 40S subunit. The 54 ribosomal proteins are divided into 33 proteins in the large subunit and 21 in the small subunit, reviewed in (Stelzl *et al.* 2001).

Subsequently, a variety of ribosomal proteins (from 50 to 80 proteins) were identified in other organisms; some of which are conserved among pro and eukaryotes, and others are organism specific. Initially, separated by two-dimensional polyacrylamide gel electrophoresis, which allowed researchers to distinguish ribosomal proteins in all organisms (Dzionara *et al.* 1970, Kaltschmidt *et al.* 1970). The ribosomal proteins were numbered according to their protein sizes on the gel, with the larger proteins having a small number, and the smaller proteins with higher number. Approximately 50-60 different polypeptides were found in bacteria and archaea ribosomes, and approximately 70 different polypeptides have been identified in eukaryotic ribosomes(Strom *et al.* 1973, Tsurugi *et al.* 1977). However, with the advancement that occurred in whole-genome sequencing, a large-scale study on ribosomal protein genes from 66 genomes from different organism was performed. 102 families of ribosomal proteins were identified and only 34 proteins were conserved in all organisms (Lecompte *et al.* 2002).

4.1.1 Ribosome biogenesis

The eukaryotic mature ribosome (80S) consists of two subunits, large (60S) and small (40S), which together contain four rRNAs, 18S in the small subunit and 5S, 5.8S and 28S in the large subunit, along with 80 different ribosomal proteins. Ribosome biogenesis starts in the nucleolus by the production of ribosome and synthesis of pre ribosomal particles, which are then exported to the cytoplasm for the formation of functional ribosome. This process involves the synthesis of four rRNAs, 80 ribosomal proteins, more than 150 other supportive proteins and 70 small nuclear RNAs (snoRNAs). The 47S pre-RNA molecules transcribed with the action of RNA polymerase I to generate 18S RNA, which is

incorporated in the synthesis of the small ribosomal subunit (40S). RNA polymerase II transcribed the 47S to release 5.8S and 28S RNAs, where RNA polymerase III transcribed 5S RNA; all of which are involved in the making of the large ribosomal subunit 60S. These subunits are then exported to the cytoplasm and undergo several maturation steps to form the 80S ribosome (Warner 1999, Rudra *et al.* 2004, Rodnina *et al.* 2009, Panse *et al.* 2010). The 80 ribosomal proteins are transcribed by RNA polymerase II and exported to the cytoplasm for translation, then imported into the nucleolus for the assembly of the ribosome (Lempiainen *et al.* 2009). All the reported information about ribosome biogenesis was based on the genetic studies of prokaryotic biogenesis. Although, there is a high level of conservation on ribosome biogenesis elements between mammalian cells and yeast, knowledge acquired about mammalian ribosomes is still somewhat limited.

4.1.2 Ribosomal proteins functions

The role of ribosomal proteins in the assembly of eukaryotic ribosomes has been studied for several years and shows similarities with prokaryotic ribosome assembly (Ferreira-Cerca *et al.* 2007, Budkevich *et al.* 2008). However, some distinct features in translation initiation, termination and recycling were different among different kingdoms. Consistent with that, the ribosome from different kingdoms composed of different ribosomal proteins, which can modulate specific functions related to the organism. Of the 80 eukaryotic ribosomal proteins, some of them are homologous between two or more kingdoms and some are eukaryotic specific. The identification of the role of individual ribosomal proteins is difficult due to the cooperative role between ribosome components. However, the major change in the understanding of ribosomal protein function came in 2003 when Steitz and Moore, identified that ribosomal proteins are responsible for ribosome assembly and for the accurate folding of rRNA, which is required for the cleavage and processing (Steitz *et al.* 2003). Analyses of eukaryotic ribosomal proteins identified that ribosomal proteins have a distinct function in ribosome assembly and are required for different steps of ribosome biogenesis; for example: some ribosomal proteins are responsible for translational accuracy, peptide bond formation and interaction with translation initiation factor (Caldarola *et al.* 2009).

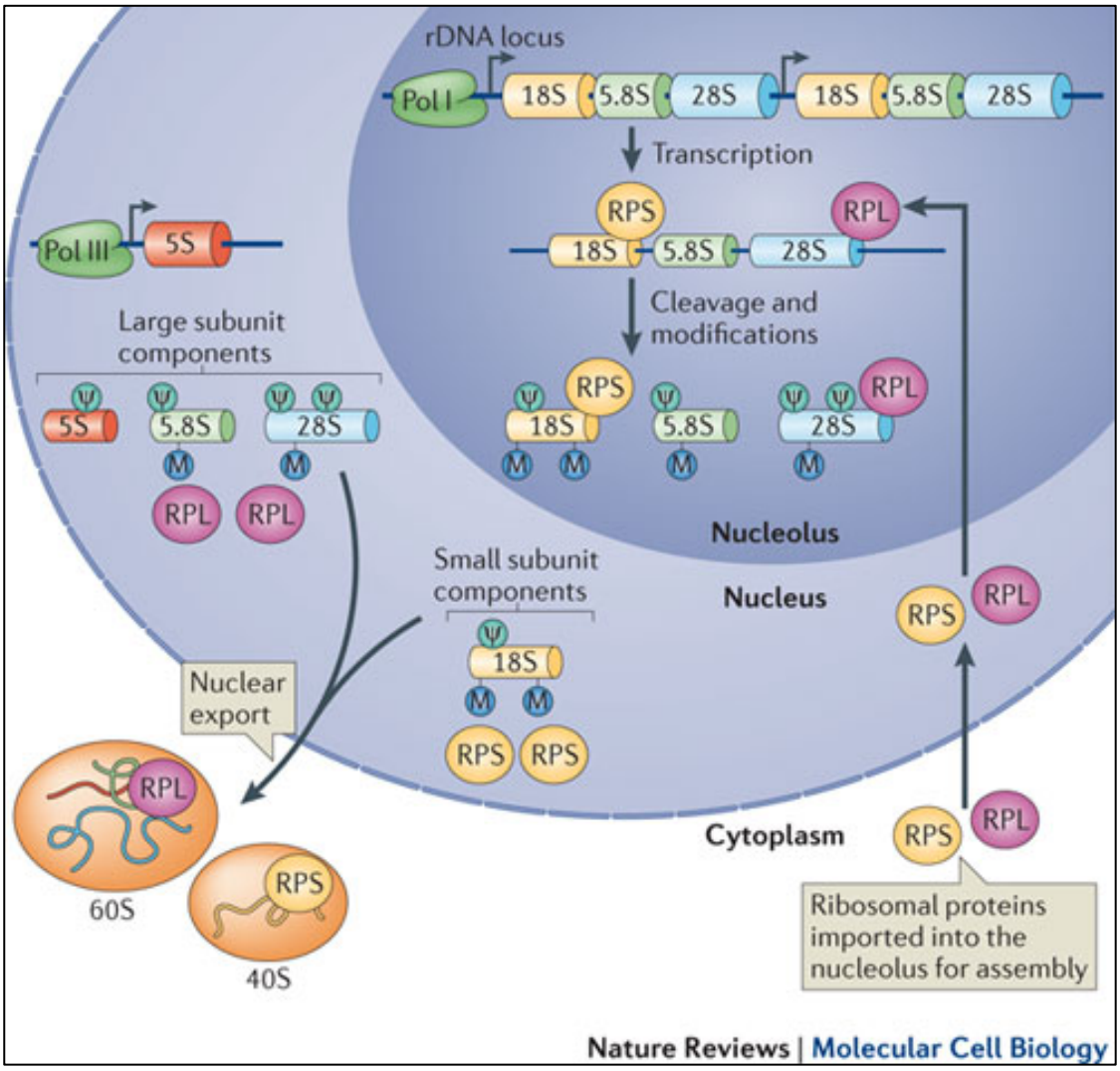

Figure 4.1: Ribosome biogenesis (reproduced from (Xue *et al.* 2012)

Ribosome biogenesis is a highly coordinated process that is responsible for protein synthesis through a series of steps, which mostly take place in the nucleolus. The pre-RNA 47S is transcribed by Pol I and generates 3 of the 4 rRNAs (18S, 5.8S and 28S) this step occurs in the nucleolus. The fourth rRNA, 5S, is transcribed in the nucleus by Pol II. Ribosomal proteins are transcribed by Pol II in the cytoplasm then exported into the nucleus and involved in the ribosome assembly. 18S with 32 ribosomal proteins are assembled into the 40S small subunit. The other rRNAs (18S, 5.8S and 28S) along with 47 ribosomal proteins are assembled into the large subunit, 60S. Both subunits are exported into the cytoplasm to generate the mature ribosomal subunit. RPL: large subunit ribosomal proteins, RPS small subunit ribosomal proteins.

4.1.3 Ribosomal protein and extra-ribosomal functions

In addition to their contribution in ribosome biogenesis, ribosomal proteins have been identified with extra-ribosomal functions (Wool 1996, Lindstrom 2009). These functions, recognized through the damaging defect that occurs in ribosome synthesis and leads to apoptosis and cell cycle arrest through ribosomal protein accumulations or haploinsufficiency and this is one of the mechanism in carcinogenesis (Montanaro *et al.* 2008, Narla *et al.* 2010).

Impaired ribosome biogenesis as a result of ribosomal stress causes accumulation of ribosomal proteins. Therefore, cell growth and proliferation are affected with changes in ribosome activity and production. This accumulation could be due to defective ribosome assembly resulting from imbalanced expression of ribosomal proteins and the other components of the ribosome machinery and downregulated ribosome activity and protein synthesis (Lempiainen *et al.* 2009). Disruption of ribosomal protein production causes defects in ribosome biogenesis and disrupts the survival of the cells, which suggests p53 involvement, as p53 being the major guardian of the cells (Deisenroth *et al.* 2010). The tumour suppressor protein p53 is known for its ability to induce apoptosis, cell-cycle arrest and senescence in response to ribosomal stress, DNA damage and oncogene activation (Kruse *et al.* 2009).

The p53 pathway plays a major role in preserving the integrity of ribosomes. Disruption of ribosomal integrity results in the release of several ribosomal proteins from the nucleolus, which interact with murine double-minute 2 (MDM2) called HDM2 in humans, the main negative regulator of p53. MDM2 negatively regulates p53 activity by acting as an E3 ubiquitin ligase, leading to p53 ubiquitination and degradation. Nucleolar stress causes a disruption of rRNA synthesis which inhibits the assembly of the ribosome and that results in an excess of free ribosomal proteins, which become available to interact with MDM2 (Zhang *et al.* 2009). The binding of the ribosomal proteins with MDM2 interferes with its transactivation activity, resulting in the stabilization and activation of p53 either by protecting *p53* from degradation by MDM2 or inducing *p53* translation and therefore arresting cell cycle progression in a *p53* dependent manner (Dai *et al.* 2004).

Several ribosomal proteins have extra-ribosomal functions such as binding to MDM2 and protecting p53 from degradation. In 1994, it was found that RPL5 and 5S RNA can bind to

MDM2 and MDM2-p53 complexes in murine cells (Marechal *et al.* 1994). Overexpression of *RPL5* and *RPL11* causes an accumulation of *p53*, which leads to apoptosis and consequent G1 arrest through their interaction with MDM2 (Lohrum *et al.* 2003, Zhang *et al.* 2003, Bhat *et al.* 2004, Dai *et al.* 2004). RPL23 can also associate with MDM2 and it's overexpression or suppression leads to cell-cycle arrest and apoptosis (Dai *et al.* 2004, Jin *et al.* 2004). RPS7 also binds with MDM2-p53 complex, protecting p53 from degradation (Chen *et al.* 2007). Additional MDM2 binding partners were identified such as RPL26 (Ofir-Rosenfeld *et al.* 2008), RPS14 (Zhou *et al.* 2013) and RPS3 (Yadavilli *et al.* 2009). These studies led to unravelling of the RP-MDM2-p53 pathway, which is active in responses to ribosomal or nucleolar stress, see Figure 4.2.

Inhibition of certain ribosomal proteins by small interfering RNA (siRNA) has also been shown to induce p53 accumulation. Work on a mouse model has shed light on the induction of the RP-MDM2-P53 pathway in response to ribosome imbalance. In mice, mutations in ribosomal protein genes or heterozygous deletion have shown a diverse effect on the mice phenotype and developmental defects and have been associated with a high p53 phenotype. Also, most homozygous mutant ribosomal proteins are embryonic lethal. The differences in the identified phenotypes are mainly due to the differences in the basal level of some ribosomal proteins, tissue specificity and development stage. Table 4.1 summarizes the ribosomal proteins studies on mice, indicating the mutations and the corresponding phenotypic defects.

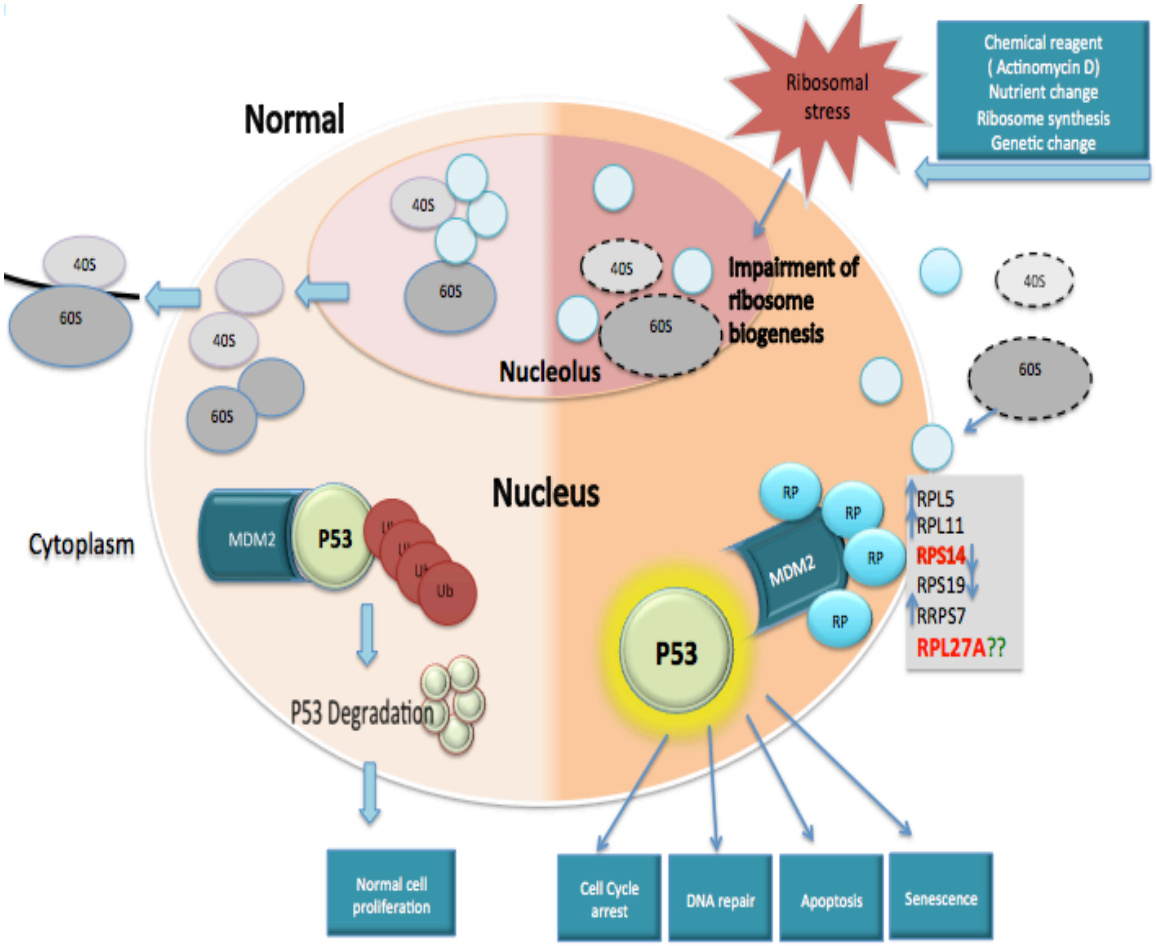

Figure 4.2:The RP-MDM2-p53 pathways

In steady state conditions (left side) ribosome biogenesis takes place in the nucleolus and ribosome subunits are exported to the cytoplasm for the formation of mature ribosomes and initiation of mRNA translation. During this normal phase, MDM2 mediates the attachment of ubiquitin (Ub) molecules to p53 and induces p53 degradation, which leads to normal cell proliferation. Under stress condition (right side), ribosomal stress impairs ribosome biogenesis and disrupts the ribosome assembly. This causes a release of free ribosomal proteins (RP), which interact with MDM2 and block its interaction with p53, resulting in p53 accumulation. Subsequently, an activated p53 may cause cell cycle arrest, apoptosis, DNA repair or senescence

Table 4.1: Ribosomal protein knockouts and phenotypes in mice (reproduced from(Terzian *et al.* 2013))

Ribosomal protein gene	Mouse phenotype	P53 defect
RPL22	+/-: No phenotype -/-: Viable, defect in alpha-beta T-cells	 Yes
RPL24	*Bst/+:* small body size, bell spot and abnormal skeletal and eye morphology *Bst/Bst*: Embryonic lethal	Yes No
RPL27A	*SFA/+:* Small body size, Pancytopenia, epidermal hypermelanosis, cerebellar ataxia *SFA/SFA*: Embryonic lethal	Yes No
RPL29	+/-: No phenotype -/-: Viable, mild growth retardation	Yes
RPL38	*Ts/+:* Skeletal patterning abnormalities *Ts/Ts:* Embryonic lethal	No N/A
RPS6	+/-: Embryonic lethal	Partial
RPS7	*Zma/+:* Small body size, belly spot, skeletal, eye and neuro-anatomical defect. *Zma/Zma:* Embryonic lethal *Mtu/+:* Small body size, belly spot, skeletal and neuro-anatomical defect *Mtu/Mtu:* Embryonic lethal	Yes N/A N/A N/A
RPS14	*CD74-Nid67$^{+/-}$:* Macrocytic anemia *CD74-Nid67$^{-/-}$:* N/A	Yes
RPS19	*Dsk3/+:* Small body size, belly spot, anemia and epidermal hypermelanosis *Dsk3/Dsk3:* Embryonic lethal +/-: No Phenotype -/-: Embryonic lethal	Yes N/A N/A N/A
RPS20	*Dsk4/+:* Small body size, belly spot, anemia and epidermal hypermelanosis *Dsk4/Dsk4:* Embryonic lethal	Yes No

+/_: heterozygous gene deletion, -/-: homozygous gene deletion, Bst: Belly spot, Dsk: Dark skin, SFA: Sooty Foot Ataxia,Ts:Tail short, Mtu: Montu: Zma: Zuma

4.1.4 Ribosomal protein RPL27A

The human *RPL27A* gene is a ribosomal protein belongs to the 60S subunit and is localized on chromosome 11p15.5 → p15.1. It composed of 32,349 bases and the mRNA encodes a protein of 148 amino acids.

The importance of *RPL27A* in haematopoiesis become clear from sooty foot ataxia (SFA) mouse models (Terzian *et al.* 2011). In that report the authors emphasized the importance of this gene and the potential need for further investigation of its biological function in the human haematopoiesis. Therefore this project focused on the functional importance of *RPL27A* on the ribosome biogenesis and its relation to the MDM2-P53 pathway.

4.2 Aim

The identification of individual ribosomal protein function is challenging due to the cooperative role between rRNA and ribosomal proteins and between the ribosomal proteins themselves. The role of several ribosomal proteins which was mentioned earlier was determined by causing changes in the gene/protein expression level either by inserting a mutation that silences the gene or knocking down the gene and examining the effect of haploinsufficiency on cell survival. Therefore, I proceeded to study the biological effects consequent to *RPL27A* knockdown.

In order to examine the effects in detail, I examined the following:

- Effects of *RPL27A* knockdown in different human cell lines expressing p53 and p53 null cells and specifically focused on the effects on p53 pathway.
- The effects of knockdown on apoptosis, cell cycle and cell viability.
- The effects of *RPL27A* knockdown on the ribosome assembly, particularly large ribosome subunit.
- The possible interaction between MDM2 and RPL27A.
- Overexpression of *RPL27A* and its effect on cellular function.

4.3 Experimental design

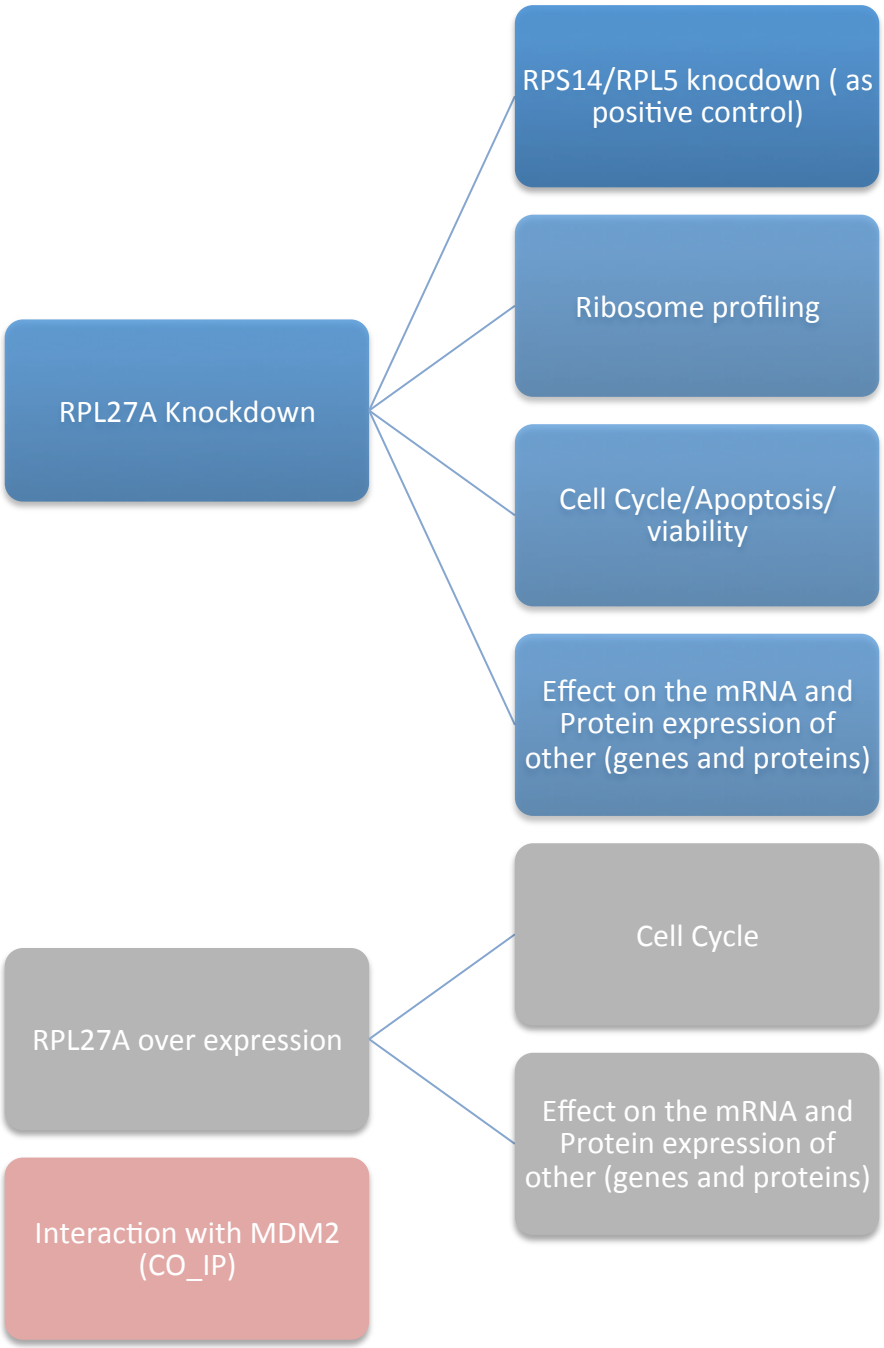

4.4 Results

4.4.1 Production of pSUPER retroviral plasmid expressing *RPL27A* shRNA and cell transduction

4.4.1.1 *RPL27A* shRNA cloning in pSUPER retroviral plasmid

I created a stable knockdown of *RPL27A* by designing shRNA that could be cloned into pSUPER plasmid, which is the standard vector used for delivering small interfering RNA (Tuschl 2002).The shRNA sequences were generated from the online shRNA design tool (http://www.genelink.com/sirna/shrnai.asp.) The *RPL27A* mRNA sequence was uploaded and several shRNA sequences were generated at different positions in the coding DNA sequence (CDS). Three shRNA sequences at 485 (sh-1), 588 (sh-2) and 735 (sh-3) CDS were selected, see Section 2.1.14. Restriction sites were incorporated at each end of the oligonucleotide to facilitate the subsequent cloning into pSUPER. The manufacture's recommended restriction enzymes are *HindIII* and *BglII* but because these sites are close to each other (*BglII*:1447 and *HindIII*:1441) *XhoI* (1420) was used instead of *HindIII* .An *XhoI* site was incorporated into the reverse primer and a *BglII* site was inserted into the forward sequence.

Each shRNA primer was diluted to 1μg/ml and annealed to create a synthetic DNA molecule with *XhoI* (5') and *BglII* (3') overhangs. The annealing was performed by combining 5 μl of each primer (forward and reverse) with 10μl NEB 2 and 80μl dH_2O. The mixture was placed in a beaker containing hot water (95°C); and left until the water temperature cooled to room temperature. This was subsequently ligated into *XhoI/BglII* linearized pSUPER-retro-puro overnight at 4°C. Then, an aliquot from the ligation was transformed into MACHI competent cell, as explained in Section 2.3.3.2. Six colonies were selected grown overnight and mini prepped (as explained in Section 2.3.4.1). Plasmid DNA was verified by restriction digest and sequencing (see, Sections 2.3.3.3 and 2.3.5). The result of restriction digest and sequencing of all selected colonies confirmed the successful cloning of *RPL27A* sh-1 and sh2 into pSUPER but not for *RPL27A* sh-3 which was not ligated properly and was excluded.

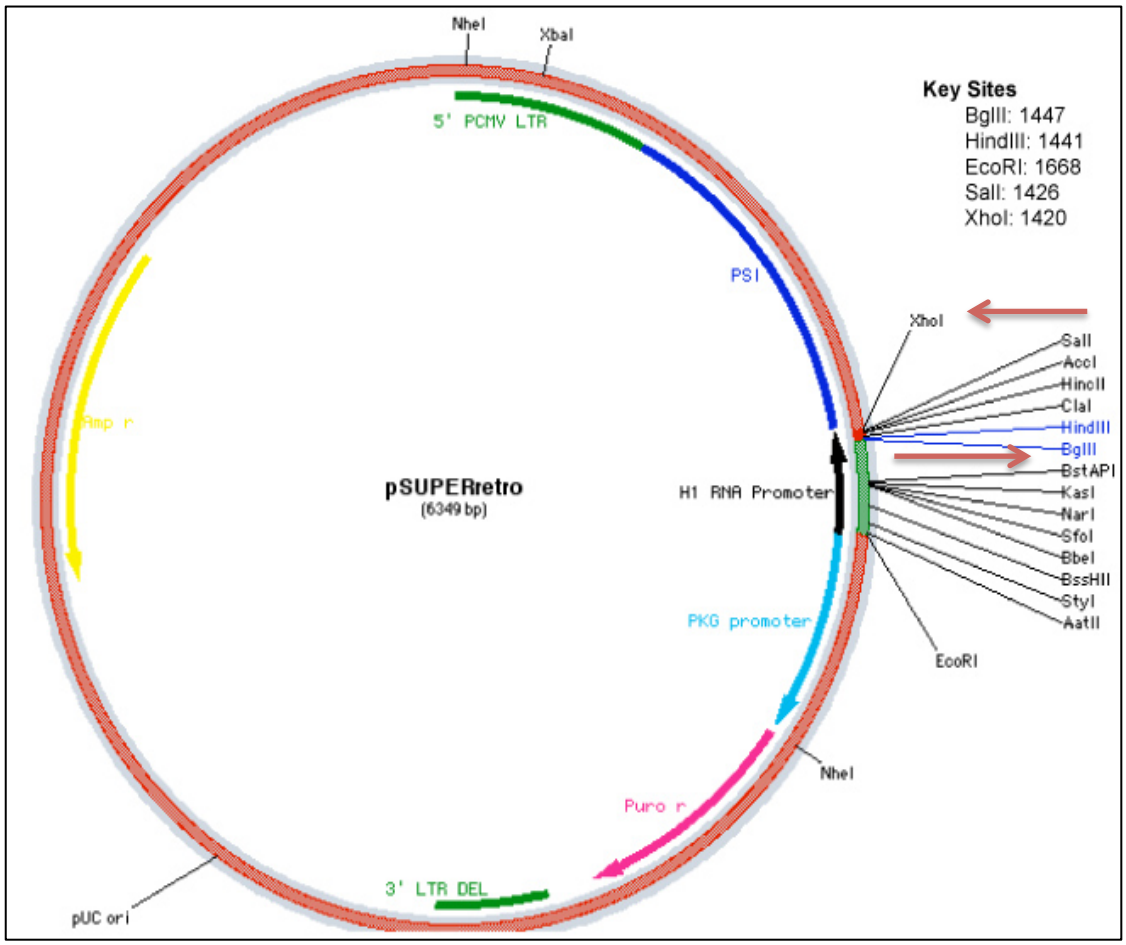

Figure 4.3: Schematic representation of pSUPER-retro-puro vector (reproduced from:www.oligoengine.com)

The *RPL27A* shRNA oligo's inserted into the vector *via* its restriction sites *XhoI* and *BaglII.*

4.4.1.2 Efficiency of *RPL27A* depletion using pSUPER cloned shRNA

RPL27A knockdown was performed on the MCF7 cell line, which is known for its high transfection efficiency, as mentioned in Chapter 3. MCF7 cells were transfected with empty pSUPER, *RPL27A* shRNA-1 and *RPL27A* shRNA-2 using nucleofection, (see Section 2.3.7.2) and cells were selected with 2μg/ml puromycin 48 hours post-transfection. RNA and protein samples were isolated at two different time points from the three independent replicates. Unselected cells were collected on day 2 post-transfection and selected cells were harvested on day 10 post-transfection. RNA was extracted, cDNA was synthesized and *RPL27A* mRNA expression was measured by qRT-PCR. The relative expression was calculated relative to the untransfected control after normalizing all tested samples with *GAPDH*. The results from three independent experiments showed ineffective silencing of *RPL27A*, with a very small (less than 20%) reduction on the cells transfected with shRNA-2 and no changes in the cells that were transfected with shRNA-1 compared with the cells with empty pSUPER. Also, the analysis of the protein samples by western blotting resulted in the same finding of small changes on the protein expression level, which was inconsistent within the replicates, see Figure 4.4. To rule out the possibility of inefficient transfection, the assay was performed in other cell lines including KG-1, K562 and Jurkat. The qRT-PCR and western bolt results confirmed the ineffective silencing of *RPL27A* using these shRNAs. However, the experiment which was performed on KG-1 showed less than 30% reduction with RPL27A-sh-1 at both mRNA and protein levels, which was not seen in any other cell lines. Therefore, to save time, the plan was modified to try other knockdown methods rather than optimizing or cloning more shRNAs into pSUPER.

4.4.2 *RPL27A* transient knockdown (*RPL27A* siRNA)

RPL27A siRNA was obtained from Santa Cruz and transfection was performed using the lipofectamine RNAiMAX method, see Section 2.3.7.1. In a 24 well plate, 2-5x10^5 cells were seeded in 1ml of complete medium. Then the siRNA concentration was optimized for a maximal silencing effect, by diluting the stock siRNA (10μM) and testing several concentrations (10, 50, 100, and 200 nM) on MCF7 and KG-1 cell lines. Results showed variability in the knockdown efficiency at different concentrations and at different time points between the two cell lines, Figure 4.5 shows an example of the data obtained from two different concentrations which has shown small variations not seen by the other tested

concentrations. Also, there was a contradiction seen between qRT-PCR and western blot results in the MCF7 cell line, in which the knockdown with 100nM at 48hrs gives 40% reduction at mRNA level, which was not detected at the protein level, as shown in Figure 4.5. Efficient silencing was not achieved with multiple repeats. Therefore, for practical reasons, with regard to cell numbers required for multiple assays, stable knockdown was required, and I used lentiviral strategy for knockdown, which leads to highly efficient delivery of expression constructs into cells and stable expression.

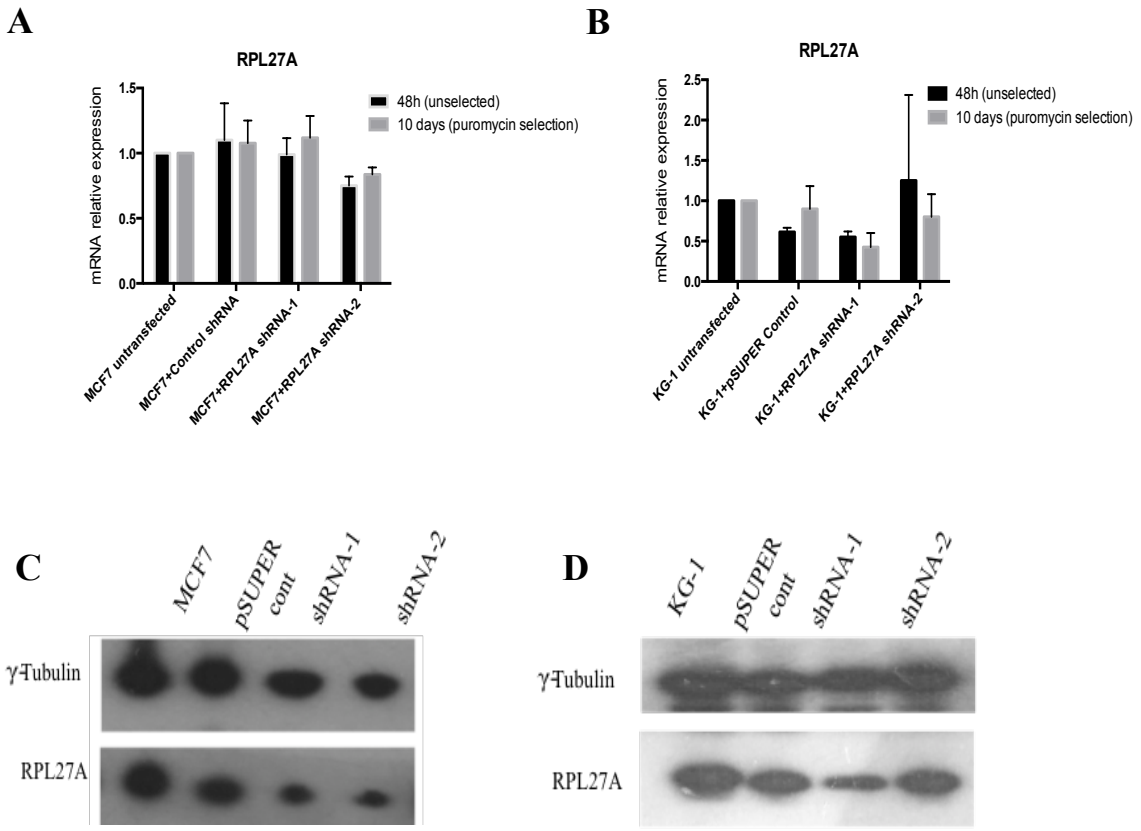

Figure 4.4: *RPL27A* depletion using shRNAs cloned into pSUPER.

MCF7 and KG-1 cell line were transfected with two different shRNAs against *RPL27A* in addition to an empty vector. **A-B)** The mRNA expression of *RPL27A* in MCF7 and KG-1 cells was determined at 48hrs and 10 days post transfection, the data were normalized to *GAPDH* mRNA, and were compared with a control empty vector as measured by qRT-PCR. Results are representative of the mean ±S.D of three independent experiments. **C-D)** Cellular proteins were isolated from MCF7 and KG-1 cells (wild-type and transfected cells) at day 10 post-transfection, then studied by western blots analysis for the expression of RPL27A and γ-tubulin antibody was used as loading control**.**

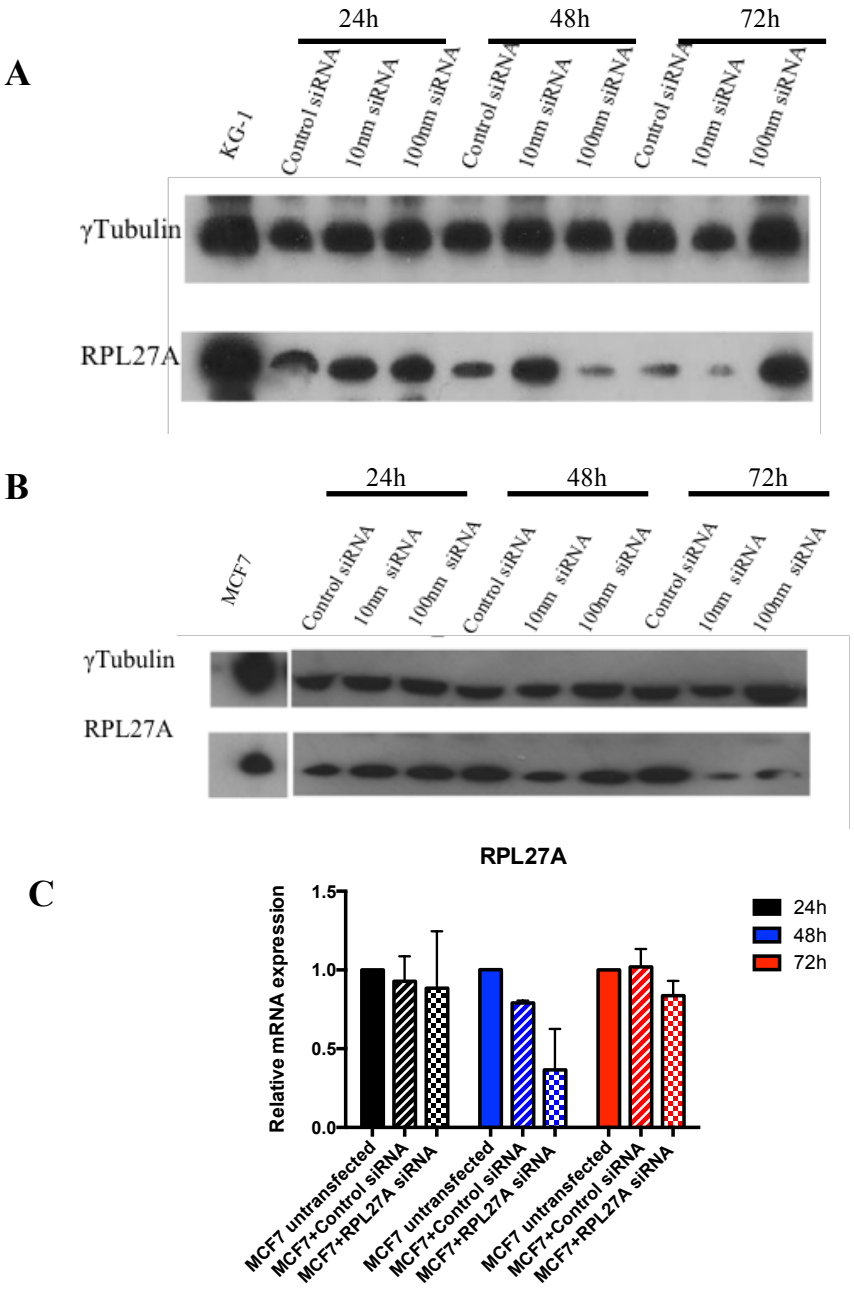

Figure 4.5: Analysis of *RPL27A* expression in cells transfected with siRNA

A-B) western blot analysis of RPL27A expression in MCF7 and KG-1 transfected with control siRNA and *RPL27A* siRNA, which was used at two different concentrations: 10nM and 100nM. Cells (1-2x10^5) were lysed 24, 48 and 72 h after transfection and analysed by western blot. RPL27A expression was measured by probing with antibodies against RPL27A and γ tubulin, the loading control. **C)** mRNA levels of cells transfected with 100nM *RPL27A* siRNA were normalized to the expression of *GAPDH* mRNA and the data were calibrated to non transfected cells (normalized to 1), The result was based on the comparison with cells transfected with an empty vector and are representative of triplicate independent experiments. Bars represent the mean ±S.D

4.4.3 RPL27A Lentivirus production and knockdown efficiency

4.4.3.1 *RPL27A* lentivirus shRNA production

Lentiviral infection has the capability of efficient delivery of expression construct with high stability in the transduced cells. The pre-designed *RPL27A* shRNAs (4) expression constructs, which were cloned into the lentiviral vector (pLKO.1), (obtained from Open Biosystem). As a control, the pLKO.1 empty lentiviral vector was used; this vector was kindly gifted by Dr. Jie Jiang. The shRNA sequences are listed in Section 2.1.14 and the pLKO.1 vector map is shown in Figure 4.6.

Before starting any experiment, the cells infectability with lentiviral vectors was examined and lentiviral titre was determined. The cell lines used in this experiment were HCT-116 and HCT-116 $p53^{-/-}$, which have been used extensively to examine the relationship between ribosomal protein depletion and MDM2-p53 pathway. Two other myeloid cell lines were selected, HEL and K562, former expresses p53 whereas the later dose not. Lentivirus production and titre estimation was performed with the help of Dr. David Darling. Based on his experience, the K562 cell line is infectable and therefore infectability was examined in the other 3 cell lines. Cells were infected with GFP- lentivirus (Gifted by Dr. David Darling). The infection efficiency in HCT-116 and HEL cell lines was more than 80% at 48hrs post-infection which is similar to K562 and that indicated the feasibility of delivering lentivirus into these cell lines. To determine the required volume of the viral supernatant to cause sufficient knockdown, $5x10^5$ HCT-116 cells were seeded into a 24 -well plate in 1ml complete medium (DMEM) and transduced by recombinant lentivirus, empty pLKO.1, at four different virus dilutions (0.1µl, 1µl, 10µl and 100µl.); virus production and transduction were performed as explained in Section 2.3.8, and infections were carried out in the presence of 8 µg/ml polybrene. After 24hrs the medium was changes and cells were selected with 2µg/ml puromycin. After 10 days of puromycin selection, cells, which were transduced with 0.1 µl and 1 µl had all died. The cells transduced with 10 µl viral supernatant showed some live cells and the cells transduced with 100µl supernatant showed more than 80% transduced cells after 10 days puromycin selection. Therefore, cell lines were infected with 100 µl of each shRNA and selected with puromycin. After 6 days, RNA and protein samples were isolated from all infected cells to examine the knockdown level. The results shown in Figure 4.7-A showed that *RPL27A*-sh2 caused an 80% reduction in

RPL27A expression at both mRNA and protein levels, *RPL27A*-sh4 caused a reduction of 50% at mRNA and approximately 30-40% at protein level (Figure 4.7-B). The other two shRNAs did not show any significant changes at mRNA by qRT-PCR, so these shRNAs were not used any further. Therefore, *RPL27A*-sh2 and *RPL27*-sh4 were re-examined in K562 and HEL cell lines and the knockdown level was very close to what was seen in HCT-116 cell lines, (Figure 4.7-C). Therefore, the rest of the experiments were carried out using *RPL27A*-sh2 and *RPL27A*-sh4. As a control, knockdown of *RPS14* was carried out in parallel, *RPS14* shRNA was kindly provided by Dr. Jie Jiang. In some experiments, the knockdown of RPL5 was also studied. The *RPL5* shRNA was obtained from Open Biosystem; lentivirus production and transduction were performed as explained in Section 2.8.3. *RPS14* and *RPL5* knockdown levels were measured by qRT-PCR and the result (Figure 4.8) showed a reduction in *RPS14* expression by more than 80% in both HEL and K562 cell lines and *RPL5* expression was reduced by 80% in HEL cell line and approximately 50% reduction in K562 cells. Data was obtained from three independent experiments and results were compared with empty vector.

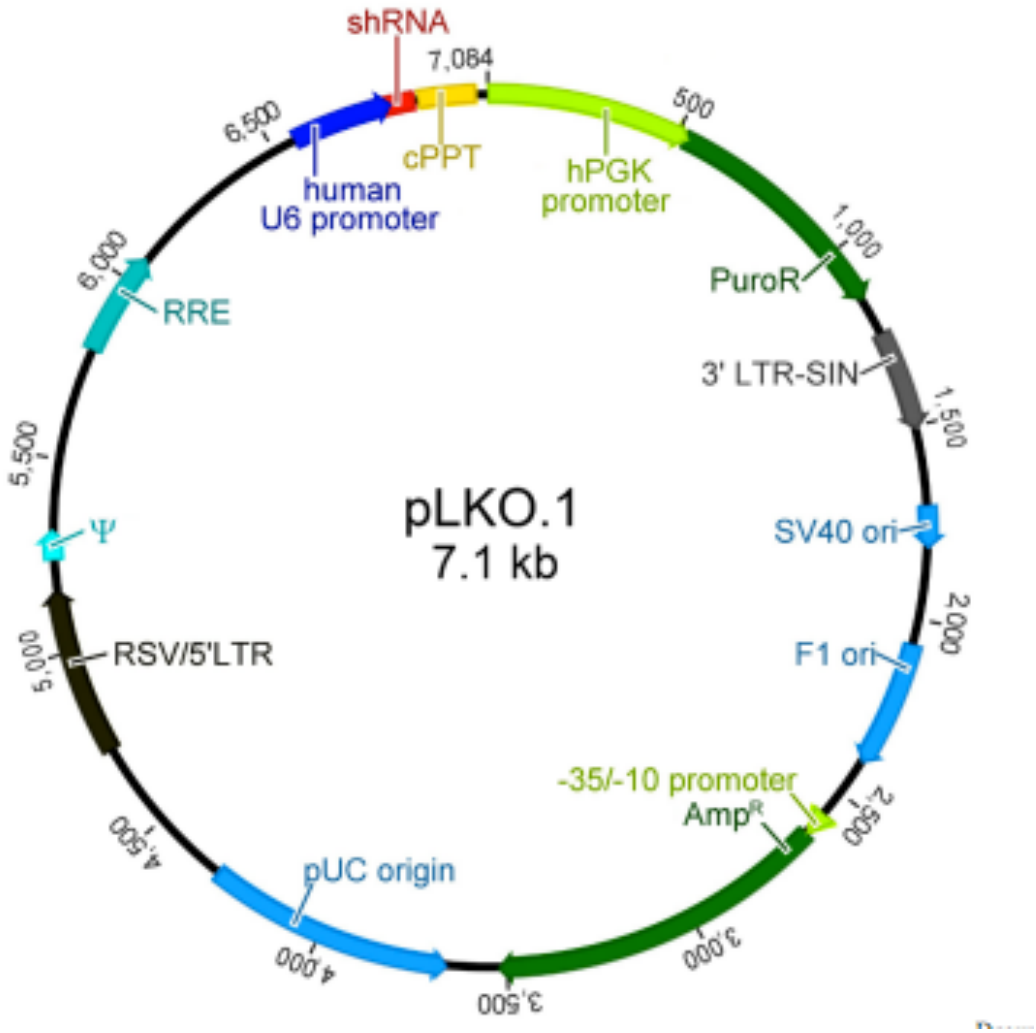

Figure 4.6: pLKO.1 vector map (reproduced from www.dharmacon.gelifesciences.com).

The pLKO.1 vector is the backbone of the RNAi Consortium (TRC) for expressing different shRNAs. pLKO.1 encodes puromycin selectable marker which allow for convenient stable selection.

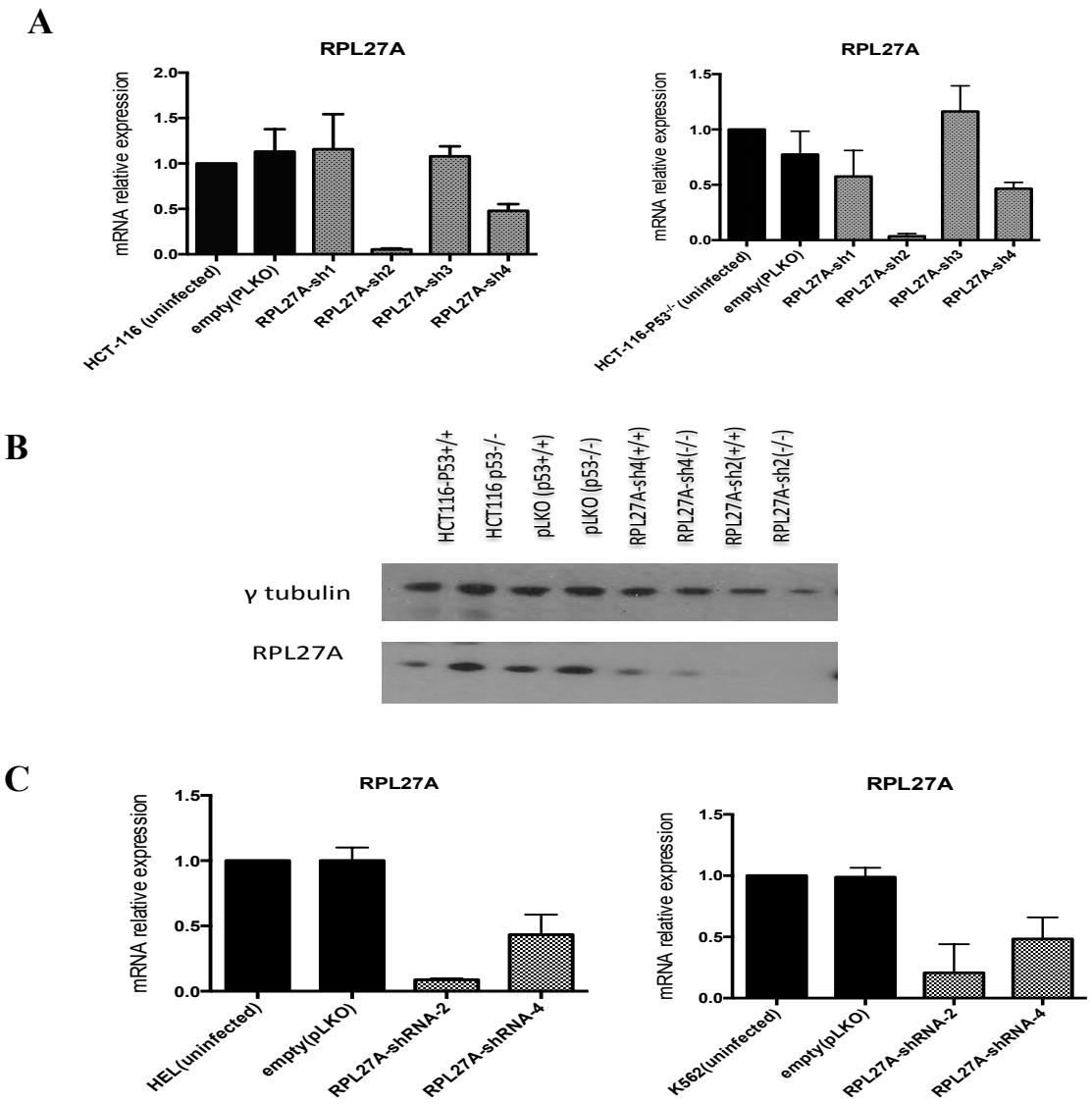

Figure 4.7: *RPL27A* depletion using lentivirus shRNA.

A) *RPL27A* mRNA expression was examined in HCT-116 and HCT-116 $p53^{-/-}$ infected with four different shRNAs, showed a reduction in *RPL27A* with sh2 and sh4 **B)** Western blot analysis of proteins collected from HCT-116 and HCT-116 $p53^{-/-}$ cells, infected with *RPL27A*-sh2 and *RPL27A*- sh4. Antibodies against RPL27A and the loading control γ tubulin were used to detected proteins expressions; the results confirmed the qRT-PCR result and showed a reduction in protein expression by both shRNAs **C)**. *RPL27A* mRNA expression in HEL and K562 cell lines infected with *RPL27A*-sh2 and *RPL27A* sh4 also showed a reductions in the gene expression by both shRNAs at different levels. mRNA expression was normalized with *GAPDH* mRNA, calibrated to the non infected cells and compared with empty vector. Bars represent the mean ±S.D. from three independent experiments.

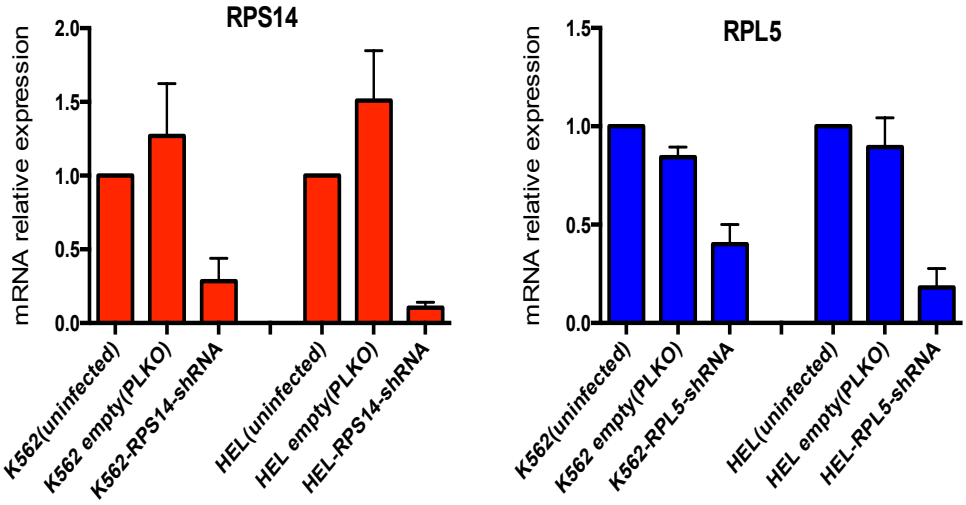

Figure 4.8: *RPS14 and RPL5* depletion using lentivirus shRNA.

RPS14 and *RPL5* mRNA expression in HEL and K562 cell lines which were infected with *RPS14* shRNA and *RPL5* shRNA showed a reduction in the gene expression in both cell lines. mRNA expression was normalized with *GAPDH* mRNA, calibrated to the uninfected cells and compared with empty vector. Bars represent the mean ±S.D from three independent experiments.

4.4.4 *RPL27A* depletion causes p53 activation

Given the evidence for *p53* overexpression in a mouse model with reduced *RPL27A* expression (Terzian *et al.* 2011), this project examined the effects of reduced *RPL27A in vitro* in a variety of human cell lines including HCT-116, HCT-116-p53$^{-/-}$, K562 and HEL cell lines. HEL and K562 are myeloid cell lines of erythroleukemia type; both have different *p53* mutations. The K562, human chronic myelogenous leukaemia cell line, is known to contain a p53 mutation in exon 5 leading to a frame-shift mutation resulting in an inactive truncated p53 (Law *et al.* 1993). The identified mutation in p53 in the erythroleukemic HEL cell line is a homozygous mutation in exon 5 which does not affect the p53 expression (Zhao *et al.* 2012). I examined p53 expression in all selected cell lines at both mRNA and protein levels. RNA and protein samples were isolated from the wild type cells and qRT-PCR and western blot analyses were performed. p53 expression was confirmed in HCT-116 and HEL cell lines and the absence of p53 expression in the other cell lines as shown in Figure 4.9. Cells that do not express p53 either due to p53 mutations or double knockout termed "null p53 cells" and p53$^{-/-}$ only referred to HCT-116 with p53 double knockout.

To investigate the cellular consequences of *RPL27A* knockdown on the p53 pathway, the selected cell lines were infected with control empty lentivirus, two shRNAs targeting *RPL27A* (sh2 and sh4), which were shown earlier to decrease RPL27A expression by 80% and 40%-50% respectively at mRNA and protein levels. In addition, *RPS14* and *RPL5* were also knocked down in all cell lines. The reason for choosing *RPS14* is because of its recognised importance in the pathogenesis of 5q- syndrome, subtype of MDS. *RPL5* is a ribosomal protein that belongs to the large ribosomal subunit and its depletion does not lead to p53 induction (Dai *et al.* 2004, Teng *et al.* 2013). Therefore, re- examining the knock down effects of these ribosomal proteins alongside with *RPL27A* will address any functional similarities or discrepancies between the different knockdowns.

Cell lines were infected as explained in Section 2.3.8.3. After 24hrs, infected cells (HCT-116 and HCT-116-p53$^{-/-}$) were transferred to 75-mm flasks and selected with 2μg/ml puromycin where as K562 and HEL infected cells were transferred to 6 well plate and selected with 2μg/ml puromycin as these cells grew better in smaller culture volumes at low cell density (density should not exceed $1x10^6$ / ml in any culture vessel). Independent experiments were performed in triplicate for each infection of each cell line, two

independent biological replicates were performed as single infection for each shRNA. After 6 days, samples were isolated to investigate the knockdown effect on *p53* and its target gene *p21* (also know as cyclin-dependent kinase inhibitor 1-CDKN1A), *Bax* (pro apoptotic Bcl-2-associated X protein) and *MDM2*, at mRNA level by qRT-PCR. 1-2 x10^5 cells were preserved in trizol and RNA extraction was performed as explained (see Section 2.3.9.2) cDNA synthesis was done on 100-500ng/ml of RNA and the cDNA was diluted 1:10-1:50 respectively. The qRT-PCR was carried out as explained in Section 2.3.10.4 using primer specific probe combinations as listed in 2.1.15. *GAPDH* mRNA was also quantified and was used as endogenous control to normalise signals obtained for each mRNA. Each cDNA sample was amplified in triplicate for a total of 40 cycles, and the relative quantification analysis was performed by normalizing with *GAPDH* mRNA and using ΔΔCT method. The ΔCT value was calculated as explained in 2.3.10.4. The ΔΔCT value was generated by subtracting the ΔCT value of the calibrator sample (the non infected wild type cells) from the ΔCT value of the shRNA-infected cells. p53, MDM2 and RPL27A were examined at protein level and γtubulin was used as loading control (antibody details are listed in 2.1.13). In HCT-116 which express p53, the depletion of *RPL27A* using sh2 and *RPS14* were resulted in a significant increase in *p53* mRNA level of 2-2.5 fold (*RPL27A*-sh2 $p < 0.005$ and *RPS14* shRNA $p < 0.01$). *RPL27A*-sh4 increased *p53* by 1.5 fold, relative to control empty vector ($p < 0.05$) as assessed by qRT-PCR, result shown in Figure 4.10-A. On the other hand, *RPL5* depletion did not cause any changes in *p53* level. In the HEL cell line, which express p53, no significant changes were detected in *p53* expression by any of the shRNAs that target ribosomal protein genes (Figure 4.10-A).

To investigate weather the induction of *p53* resulted in transcriptional activation, the expression of p53 downstream targets *p21* and *Bax* were examined in HCT-116 and HEL cell lines by qRT-PCR. The result in Figure 4.10-B showed that *p21* mRNA was significantly increased ± 5 fold in HCT-116 by all shRNAs except *RPL5* shRNA ($p < 0.05$). In the same cell line *Bax* expression was significantly increased ($p < 0.05$) by 2-3 fold with *RPL27A*-sh2 and *RPS14* shRNA. Increased expression with *RPL27A*-sh4 did not reach significance. In the HEL cell line, *RPL27A*-sh2, *RPS14* shRNA and *RPL5* shRNA caused a significant increase in *p21* ($p < 0.05$) by ± 4 fold, whereas *RPL27A*-sh4 did not increase the *p21* expression ($p = 0.2057$). A two folds increase in *Bax* mRNA level occurred in cells infected with *RPL27A*-sh2, *RPS14* shRNA and *RPL5* shRNA, the difference were

statistically significant. *RPL27A*-sh4 did not show any significant increase in *Bax* mRNA level.

As expected, for the null p53 cell lines (HCT-116 $p53^{-/-}$ and K562) no changes in *p21* and *Bax* levels,with all targeted shRNAs Figure 4.10-D. This indicated that *p21* and *Bax* inductions were p53 dependent in the p53 expressing cell lines.

To verify the p53 induction, p53 expression was examined at the protein level. 1-2 $x10^5$ cells were lysed in 30-50 µl lysis buffer; western blotting analyses was carried out as explained in Section 2.3.11. The result in Figure (4.11-A and C) showed that *RPL27A*-sh2 and *RPS14* shRNA increased the p53 expression compared to control empty vector in both HCT-116 and HEL cell lines in three independent experiments. In HEL cell lines, the inductions of *p21* with *RPL27A* and *RPS14* depletion, did not show significant increase in *p53* mRNA level, confirming that *p53* gene was transcriptionally active. The increase in p53 expression with *RPL27A*-sh4 was not distinguishable when compared with the empty vector.

Interestingly, knockdown of *RPS14* also resulted in a decreased expression of RPL27A, the reasons for this are unknown as shown by western blot (Figure 4.11).

Depletion of *RPL27A, RPS14* and *RPL5* resulted in reduced MDM2 expression at both transcriptional and post-transcriptional level in all cell lines tested except K562, which did not show a clear reduction at the post-transcriptional level. However, a significant reduction of MDM2 was observed in cells infected with *RPL27A*-sh2 at mRNA

To determine whether RPL27A interacts directly with MDM2 and the reduction in RPL27A inhibited the MDM2- mediated p53 ubiquitination and degradation resulting in the induction of p53, co-immunoprecipitation assays with anti-RPL27A and anti-MDM2 were performed (See 4.4.11).

In order to determine the effect of *RPL27A* depletion on the p53 surveillance mechanism, proliferation assays, apoptosis and cell cycle analysis were carried out to investigate if there were any cellular changes in both $p53^{+/+}$ and $p53^{-/-}$ cell lines.

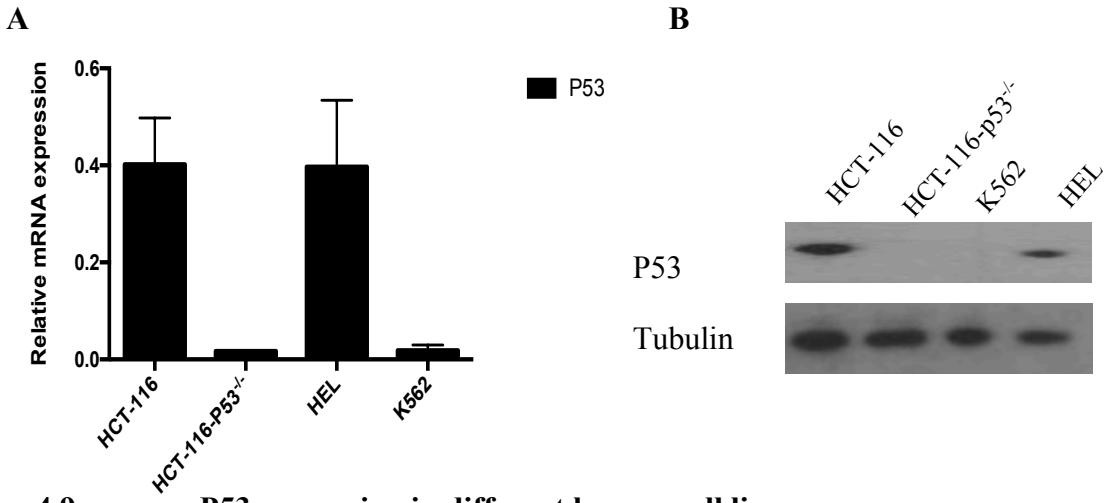

Figure 4.9: P53 expression in different human cell lines.

A) The mRNA expression of *p53* in four different cells lines (HCT-116, HCT-116 p53-/-, K562 and HEL) relative to *GAPDH*, as assessed by quantitative real time-PCR. Results showed that *p53* is expressed in HCT-116 and HEL cell lines only; the result is representative of 2 independent experiments and bars represent the mean± S.D. **B)** Western blot analysis of p53 expression in four different cell lines using antibody against p53 and the loading control γ tubulin. The results confirmed the p53 expression in HCT-116 and HEL cell lines.

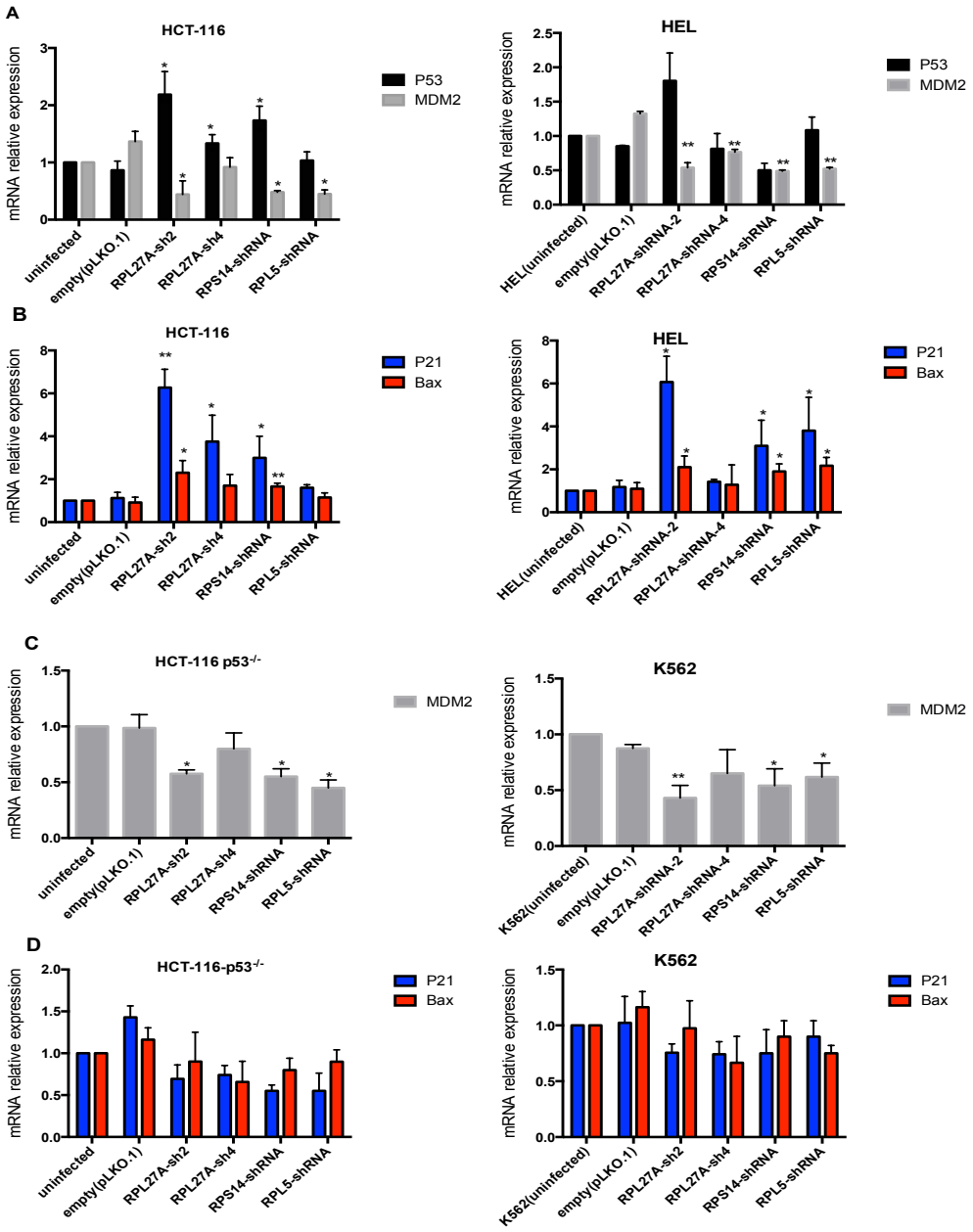

Figure 4.10: Decreased expression of *RPL27A* activates the p53 pathway.

A) The mRNA expression of *p53* and *MDM2* in HCT116 and HEL cell lines relative to *GAPDH*, was measured by qRT- PCR. *p53* induction with *RPL27A* and *RPS14* depletion was seen in HCT-116 cells compared with the control empty vector. Depletion of *RPL27A, RPS14* and *RPL5* reduced *MDM2* expression in both cell lines. **B)** The mRNA expression of p53 target genes *p21* and *Bax* in HCT116 and HEL cell line relative to *GAPDH*, was measured by qRT- PCR, showed increased expression of *p21* and *Bax* with *RPL27A* and *RPS14* depletion in both cell lines **C-D)** The mRNA expression of p53 target genes *p21*, *Bax* and *MDM2* in HCT116 $p53^{-/-}$ and k562 cell line relative to *GAPDH*, as assessed by qRT-PCR, showed a significant reduction in *MDM2* only with all knockdowns and no changes of the other genes. Results are representative of 3 independent experiments and bars represent the mean± S.D. *p* values were determined using tow tail student *t-test** $P<0.05$. **$P<0.005$.

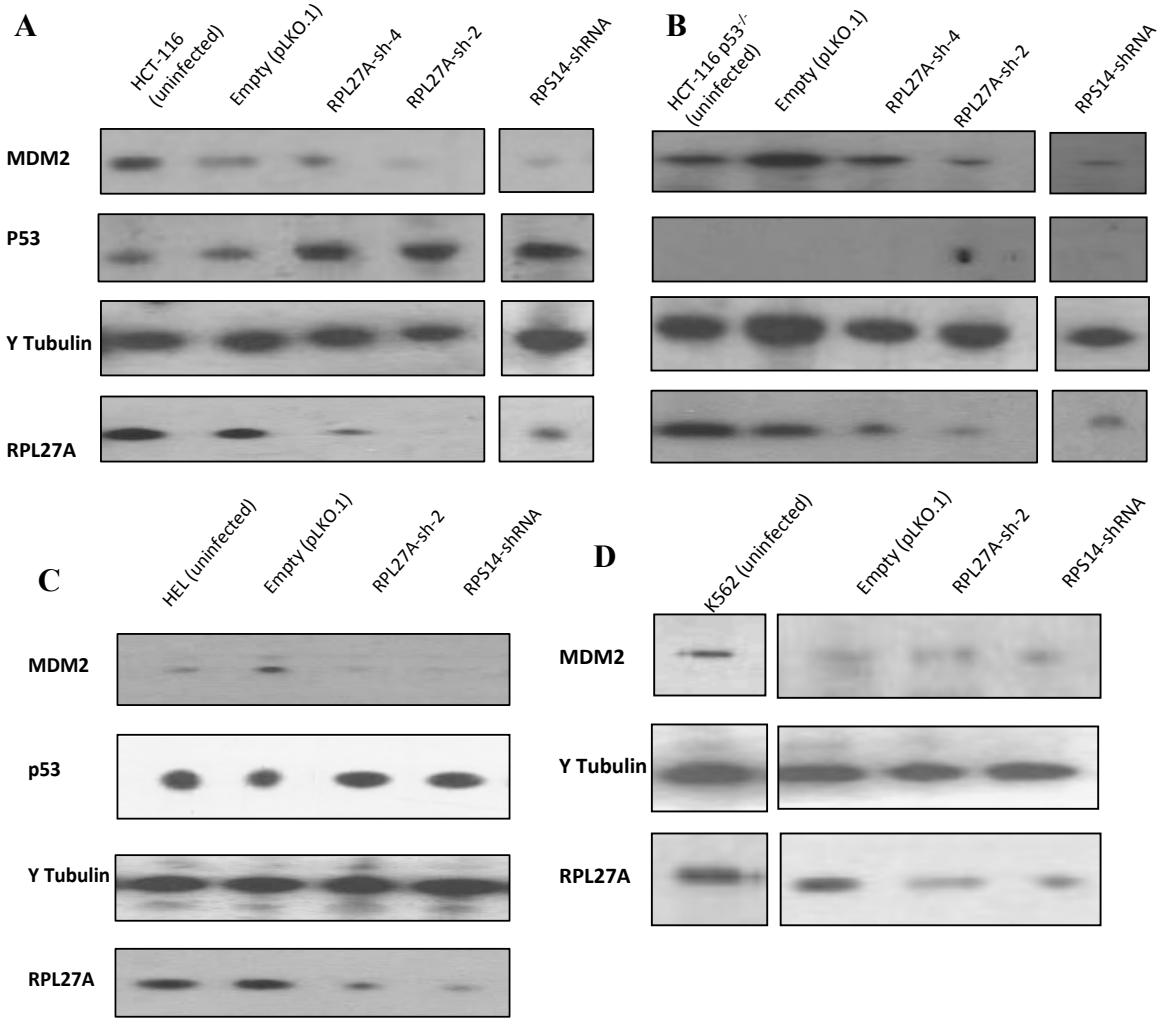

Figure 4.11: *RPL27A* depletion increased p53 expression and reduced MDM2 level at the post-transcriptional level.

Protein extracts were collected form wild type cell lines and cells infected with empty vector and shRNAs against *RPL27A* and *RPS14* and analysed on 4-12% polyacrylamide gels with antibodies to detect RPL27A, p53 and MDM2. Equal protein loading per well was determined by γ tubulin loading control. **A)** HCT-116 cell line, the depletion of *RPL27A* and *RPS14* induced p53 expression and reduced MDM2. **B)** The reduction of *RPL27A* and *RPS14* in HCT-116 $p53^{-/-}$ reduced MDM2 and p53 were not detected. **C)** In HEL cells the depletion of *RPL27A* and *RPS14* induced p53 and reduced MDM2. **D)** The reduction of MDM2 in K562 infected with *RPL27A* shRNA and *RPS14* shRNA was not very distinguishable at the post-transcriptional level. In all cell lines, infection with *RPS14* shRNA, caused a reduction in RPL27A expression.

4.4.5 Depletion of *RPL27A* inhibits cell proliferation and reduces cell viability

To further study the effect of *RPL27A* inhibition on cell proliferation and viability، HCT-116 and HCT-116 $p53^{-/-}$ cells were transduced with the shRNA constructs and counted every 48hrs as explained in Section 2.3.6.2. Both cell lines were very clumpy and after trypsinization it was very difficult to get an accurate cell count to monitor the knockdown effect on the cell proliferation at different time points. Therefore, MTT assay was performed to determine the metabolic activity of the shRNA transduced cells compared to cells infected with empty vector. On day 6 post infection, 2000 cells in 100µl medium were seeded on a 96 well plate (flat bottom) and incubated with 20 µl MTT reagent at 37°C and 5% CO_2. After 2h, formazan crystals were observed under the microscope and 150µl solubilisation buffer was added to each well. Each sample was seeded in triplicate and three wells were filled with complete medium only, which was used as a blank. The plate was analysed after 24hrs with a plate reader set at 630nm. The data was analysed by calculating the average of each triplicate and normalizing with the blank average. Fold change was determined by dividing the normalized average of the samples by the normalized average of the calibrator sample, which is the empty control. The results in Figure 4.12-A and B, showed a clear reduction in the metabolic activity relative to the control empty vector in both HCT-116 and HCT-116 $p53^{-/-}$ cells infected with *RPL27A*-sh2 and *RPS14* shRNA; *RPL27A*-sh4 caused a small but significant change in HCT116 only. In order to show the knock down effect on cell surveillance, HCT-116 cells were stained on day 6 post infection (see Section 2.3.6.4). The results in Figure 4.12-C, showed severe cell death in cells treated with *RPL27A* -sh2 and *RPS14* shRNA where as *RPL27A*-sh4 and *RPL5*-shRNA showed a relatively less cell death.

Although the reduction in the metabolic activity in HCT-116 $p53^{-/-}$ was significant, it was less than what was seen in the cell with normal p53. This might be due to the fact that HCT-116 $p53^{-/-}$ cells clearly proliferate more slowly than the wild type cells. For example after seeding the same cell number in culture flasks, HCT-116 with normal p53 required passaging after 72hrs while cells with null p53 needed passaging after 6 days. Also, null p53 cells showed an increased sensitivity to trypsinization. The staining result in Figure 4.12 –D, clearly showed that many p53-/- cells were lost both with the empty control as well as with *RPL27A*-sh2, though more cells were lost with the cells with reduced *RPL27A*.

In K562 and HEL cells the proliferation was determined by counting the cells every 48hrs and a reduction in cell number was detected by day 4 which increased over time in cells treated with *RPL27A*-sh-2, *RPS14* shRNA and *RPL5* shRNA (see Figure 4.13-A and B). Cells infected with *RPL27A*-sh4 showed a reduction in cell number but this was less marked. The unexpected observation was that there was no difference in cell death was noted between the p53 expressing (HEL) cells and the p53 null (K562) cells. In order to investigate this p53 independent effect, which was not clear in the HCT-116 cell lines, I chose U937 cells which also do not express p53, due to a large deletion in p53 gene (Sugimoto *et al.* 1992). These cells were infected with *RPL27A*-sh2 only and compared to empty vector, cell numbers were decreased in *RPL27A*-sh2 infected cells but this was not lethal during the assay period as compared to cell lines, which do express p53 (see Figure 4.13-C). These results suggested that the observed cell death in the null p53 cell line is may be due to the defects in the ribosome biogenesis. To further investigate these p53 independent effects, apoptosis screening was performed on all selected cell lines.

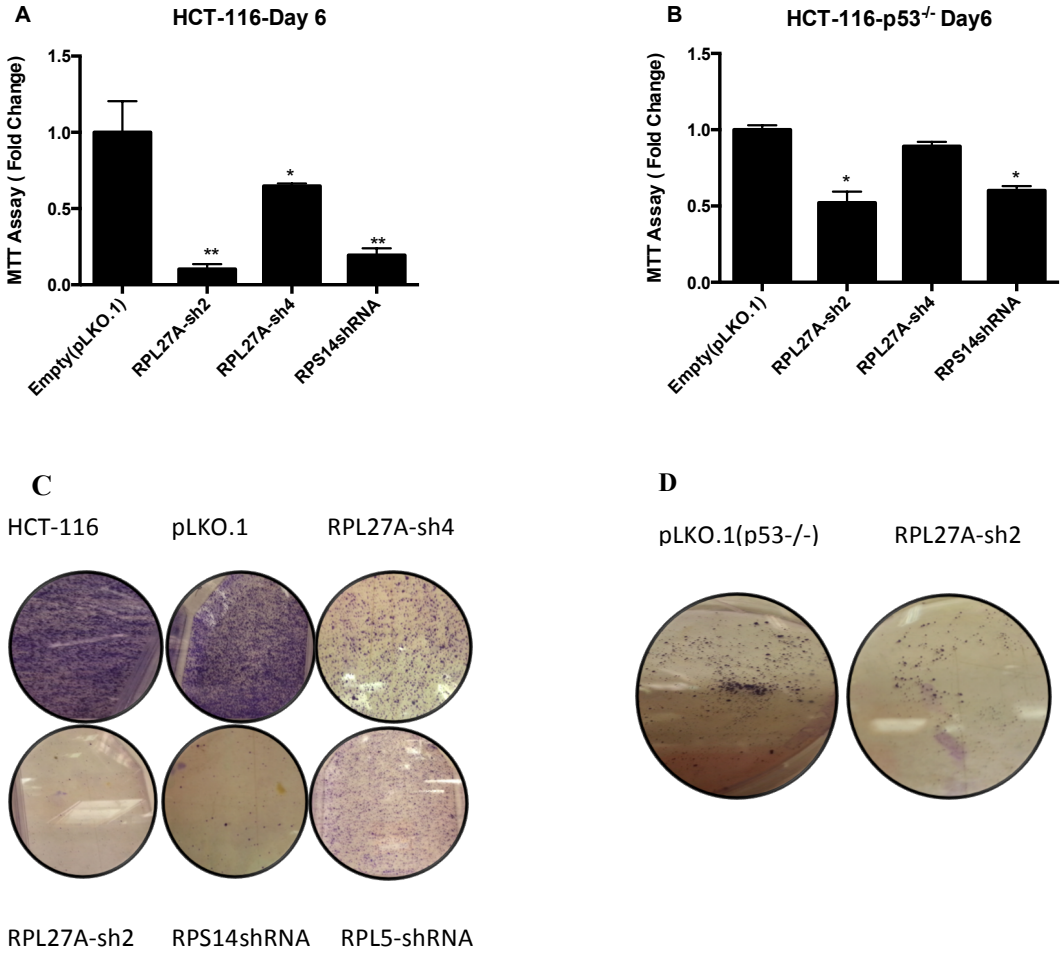

Figure 4.12: *RPL27A* depletion reduces cell viability.

MTT assay of cells **A)** HCT-116 and **B)** HCT-116 $p53^{-/-}$, which were infected with *RPL27A*-sh2, sh4 and *RPS14* shRNA on day 6 post infection, under puromycin selection. The result showed significant reduction in cell viability with *RPL27A*-sh2 and *RPS14* shRNA in both cells at variable level. *RPL27A*-sh4 caused a significant reduction in HCT-116 cells while the reduction in HCT-116 $p53^{-/-}$, was not significant. Results are expressed as fold change mean ±S.D. relative to the control empty vector and are representative of three independent experiments each performed in triplicate **P*<0.05,**P*<0.005**. C)** HCT-116 cells, infected with empty pLKO.1, *RPL27A* shRNAs, *RPS14* shRNA and *RPL5* shRNA stained with coomassie stain on day 6 post infection, results showed a marked cell death in cells infected with *RPL27A*-sh2 and *RPS14* shRNA with moderate reduction in cell viability in cells infected with *RPL27A*-sh4 and *RPL5* shRNA. **D)** HCT-116 $p53^{-/-}$ infected with empty pLKO.1 and *RPL27A*-sh2 stained with coomassie stain on day 6 post infection showed small differences between the control empty vector and *RPL27A*-sh2 expressing cells.

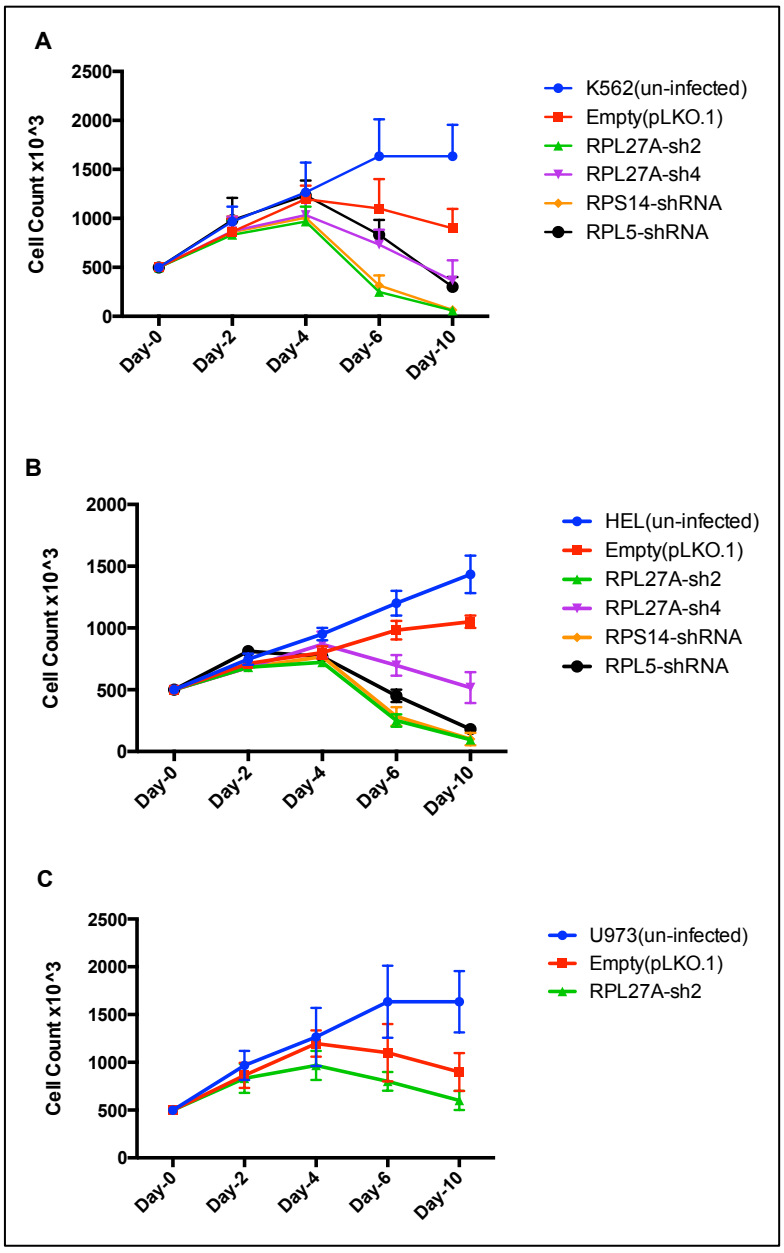

Figure 4.13: *RPL27A* reduction decreases cell proliferation

Cells were counted every 48hrs. A reduction in cell number was noted by day 4 which almost resulted in complete cell death by day 10 in cells infected with *RPL27A*-sh2, *RPS14* shRNA and *RPL5*-shRNA in **A)** K562, **B)** HEL cell lines. *RPL27A*–sh4 also decreased the cell count but less than the other shRNAs. **C)** U937 cells, which were infected with control empty vector and *RPL27A*-sh2 showed a reduction in cell number but less than the other cell lines. Error bars represent the mean ±S.D from three independent experiments.

4.4.6 *RPL27A* depletion induces apoptosis independent of p53

To investigate whether the observed cell death in the cells with depleted *RPL27A* was due to apoptosis and if that was dependent on the p53 induction or not, cells treated with the shRNAs used above stained with Annexin-V/7-AAD. On day 6 post infection, approximately 1-2x 10^5 cells from all studied cell lines were stained with Annexin V/7-AAD to distinguish apoptotic from necrotic cells, staining was performed as explained in Section 2.3.14 and cells were analysed by flow cytometry. Annexin-V verses 7-AAD analysis revealed four populations: negative for both fluorescence which represent the living cells; Annexin V^+/7-AAD^- which identify early apoptotic cells; Annexin V^+/7-AAD^+ which characterize late stage apoptosis and Annexin V^-/7-AAD^+ which represent dead cells with permeabilized membrane only. To adjust the analysis grids, control staining with single dye was performed in cells infected with empty vector and the adjusted alignment was applied to all samples from each experiment. This adjustment step was performed with every cell line in all replicates. The analysed data showed significant increase in apoptosis in all cell lines. HCT-116 cells treated *RPL27A*-sh2 showed an increased number of cells at the early stage of apoptosis as compared to *RPS14* shRNA and *RPL5* shRNA as assessed by the quantification of Annexin V^+/7-ADD^- staining with an average increase of 55% with sh2 and 40%- 35% with *RPS14* and *RPL5* shRNAs, respectively. The substantial increase in apoptotic cells as compared to control vector were significant with the following *p*-values *RPL27A*-sh2 P =0.00052, *RPS14* shRNA P =0.00157 and *RPL5* shRNA P =0.01804 as estimated by two tail student *t-test*. *RPL27A*-sh4, which caused less than 50% knockdown also showed a 25% increase in apoptotic cells compared to the control vector (P =0.03126). The number of cells at late stage apoptosis had also increased by an average of 10-15% compared to control vector (*RPL27A*-sh2 P =0.00141, *RPL27A*-sh4 P =0.0056, *RPS14* shRNA P=0.001924 and *RPL5* shRNA P =0.00238). Interestingly, the p53 null cells HCT-116-$p53^{-/-}$ also showed an average increase in apoptotic cells of 15-20% in all knockdowns as compared to control at early stage apoptosis and 8-10% increases at late stage apoptosis. Even though the increase in apoptotic cells was far less than what was observed in cell lines that express p53, these increases were also significant (Early Apoptosis: *RPL27A*-sh2 P =0.00278, *RPL27A*-sh4 P=0.0516, *RPS14* shRNA P =0.00359 and *RPL5* shRNA P =0.00202; Late Apoptosis: *RPL27A*-sh2 P =0.01707, *RPS14* shRNA P =0.02747 and *RPL5* shRNA P =0.017855). *RPL27A*-sh4 caused a slight increase of late

stage apoptosis but this was not significant, see Figure 4.14. In HEL and K562 cells the observed cell death was confirmed to be a result of apoptosis. In the HEL cells there were a 40-50% increase in apoptotic cells with all the shRNAs infected cells at late stage of apoptosis with no differences at early apoptosis as compared to the control vector. The increase in apoptotic cells at late stage was significant (*RPL27A*-sh2: *P*=0.001024, *RPL27A*-sh4 *P*=0.000606, *RPS14* shRNA *P*=0.00087 and *RPL5* shRNA *P* =0.000179). However, in null p53 K562 cells the depletion of *RPL27A*, and *RPS14* led to an increase in apoptotic cells by an average of 15-20 % at both early and late stagse. Therefore, to address the p53 independent induction of apoptosis, U937 cells were investigated. The result showed a significant increase in apoptosis in cells infected with *RPL27A*-sh2 but that increase was less than what was detected with other cell lines, see Figure 4.15.

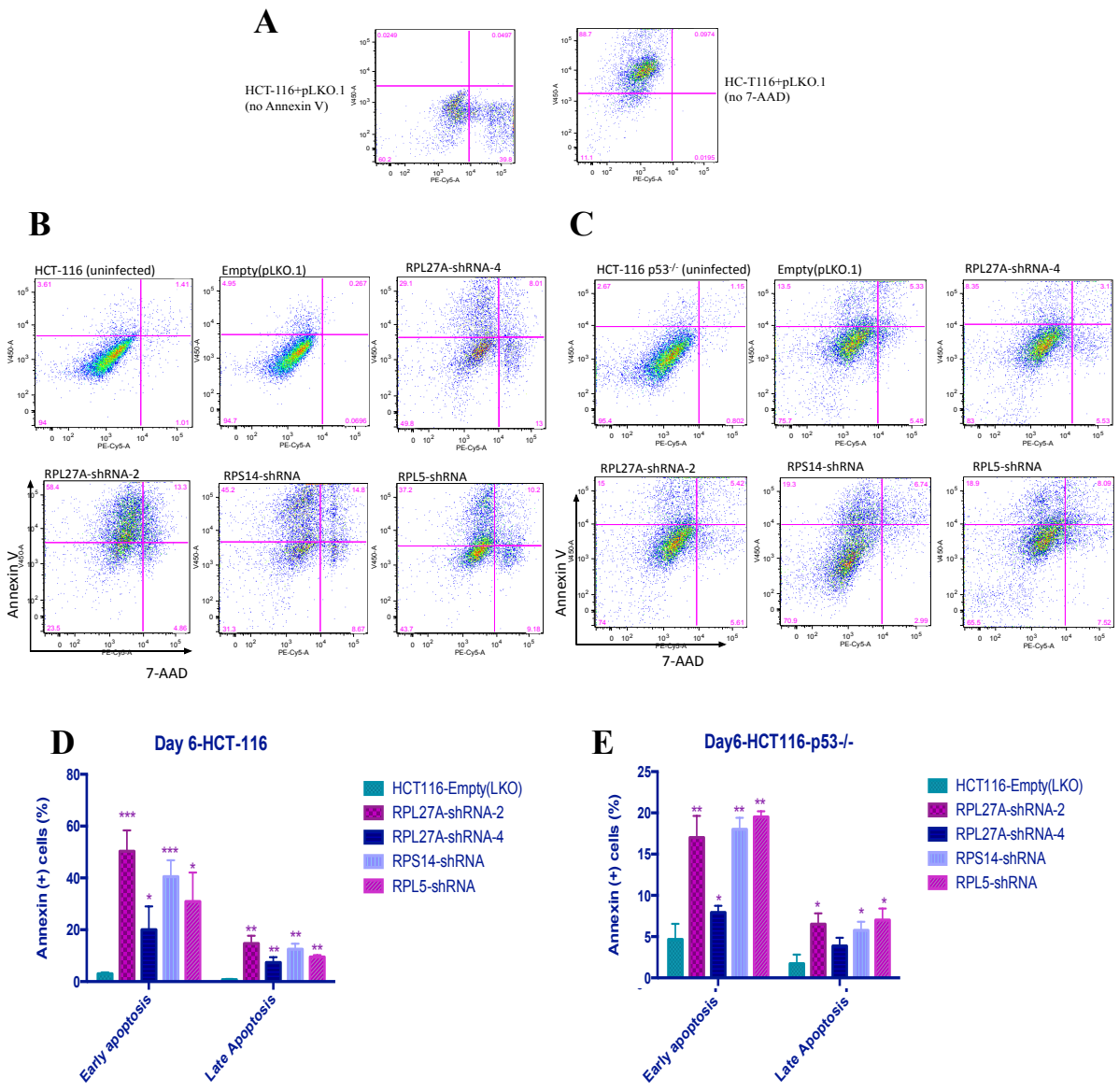

Figure 4.14: *RPL27A* reduction induces apoptosis in HCT-116 and HCT-116 p53$^{-/-}$

(**A**) Grid alignment in HCT-116 cells infected with empty pLKO.1 using single stain. **B and C)** HCT116.and HCT-116 p53$^{-/-}$cells were infected with empty vector, *RPL27A* shRNAs, *RPS14* shRNA and *RPL5* shRNA and selected with puromycin. 6 days after infection, cells were stained with Annexin and 7-AAD followed by flow cytometer analysis. Cells on the upper left quadrant indicate Annexin positive, early apoptotic cells. The cells in the upper right quadrant indicate Annexin-positive/ 7-AAD-positive, late apoptosis. In comparison with empty vector, *RPL27A* sh-2 significantly induced apoptosis in both cell lines with effects been more marked in HCT-116. Also, *RPS14* and *RPL5* reductions significantly induced apoptosis in both cell lines with a greater degree in HCT-116. *RPL27A*-sh4 induced significant apoptosis in HCT-116 cells only. **D and E)** Column diagram represents the mean of apoptotic cells from three independent experiments ±S.D. **P*(<0.05), ***P*(<0.005).

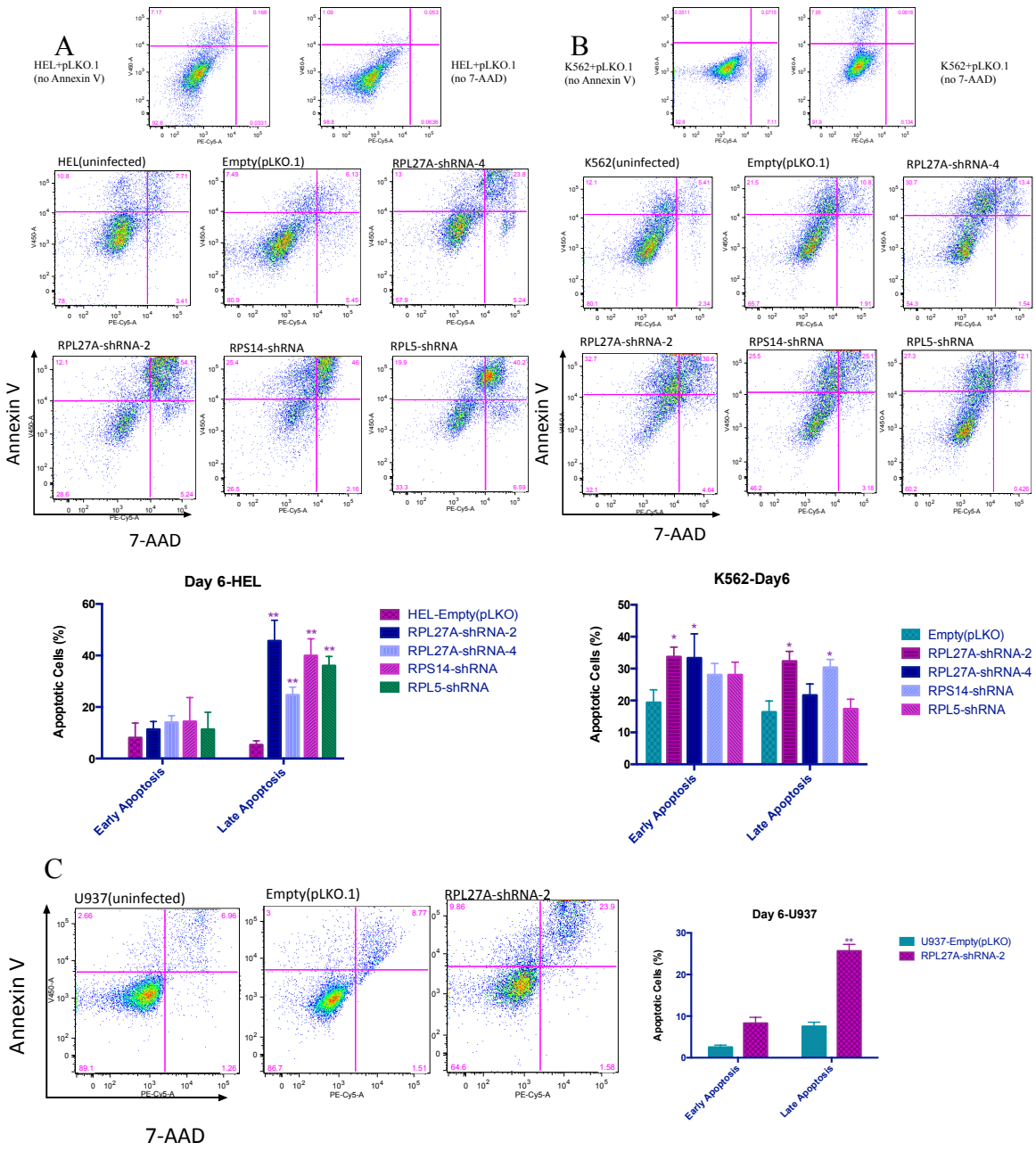

Figure 4.15: *RPL27A* induces apoptosis in K562, HEL and U937

HEL(**A**) and K562(**B**) cells were infected with empty vector, *RPL27A* shRNAs, *RPS14* and *RPL5* shRNAs and selected with puromycin. 6 days after infections, cells were stained with Annexin V and 7-AAD followed by flow cytometer analysis. Cells in the upper left quadrant indicate Annexin positive, early apoptotic cells. The cells in the upper right quadrant indicate Annexin-positive/ 7-AAD-positive, late apoptosis. In K562, *RPL27A* sh-2 and RPL27A-sh4 significantly induced apoptosis at early stage and *RPL27A*-sh2 and *RPS14* shRNA induced apoptosis at late stage, relative to the control empty vector. In HEL cells, all targeted shRNAs significantly increased late stage apoptosis. Column diagram represents the mean of apoptotic cells from three independent experiments ±S.D. **P*(<0.05), ***P*(<0.005).**C)** U937 cells infected with empty vector and *RPL27A*-sh2 only, the flow cytometric analysis revealed that *RPL27A*-sh2 significantly increased the percentage of apoptotic cells but less than other cell lines.

4.4.7 *RPL27A* reduction induces cell cycle arrest

The results described in the previous sections showed that *RPL27A* depletion induces apoptosis and reduces cell viability, which suggesting a possible defect in the cell cycle. Therefore, at the same time point, day 6, 1-2x 10^5 cells were isolated from the uninfected cells, control infected with empty vector and cells infected with shRNAs targeting *RPL27A*, *RPS14* and *RPL5*. Subsequently, cells were fixed with 75% ethanol, stained with PI (DNA content) and processed as explained in Section 2.3.13. Flow cytometric analysis was performed to determine the percentages of cells in each phase of the cell cycle by analysing the DNA content. Cell cycle analysis was performed on all cell lines but the data obtained for the HEL cell line was unusable probably because the cell population was not very homogeneous. Repeated experiments on HEL cell line also failed. In HCT-116, there was a considerable reduction in cells in G0/G1 in cells infected with *RPL27A*-sh2 and *RPS14* shRNA (43.4%± 10% and 47% ± 8% respectively), compared to the control (84.5%± 3%), and a smaller reduction 61.7% ± 13%, and 55.9% ± 7%, was observed in cells infected with *RPL27A*-sh4 and *RPL5*-shRNA, respectively. No changes were observed in either the S or G2/M phases in all conditions. However, a high percentage of cells accumulated in the sub-G1 phase in cells infected with shRNA targeting *RPL27A* (sh2: 45.2% ± 10%, sh4: 23.1%± 7%), *RPS14* (38%± 10%) and *RPL5* (25%± 7%) compared to control empty vector (1.84% ± 2%), and non-infected cells (2.84% ± 3%) (n=3, mean±S.D.), as shown in Figure 4.16-A.The increases in sub-G1 is consistent with the induction of apoptosis, which had been shown earlier (Section 4.4.6).

In K562 cells, similar result were observed with a reduction in cell content in G0/G1 phase and no changes in S or G2/M with all shRNAs apart from RPL5 shRNA. An increased in sub-G1 was observed (Figure 4.16-C). For other p53 null cell lines, (HCT-116 $p53^{-/-}$ and U937), there was a reduction in G0/G1 phase as well as an increase in cells in G2/M consistent with an increase in the sub-G1 phase. In HCT-116 $p53^{-/-}$, 26.3% of cells were in G0/G1 in *RPL27A*-sh2 transduced cells, 40.3% in *RPS14* shRNA and 39.5% in *RPL5* shRNA infected cells, as compared with control 75.8%. The observed increases in G2/M were seen in cells infected with *RPL27A*-sh2 (23.3% ± 5%) *RPS14* shRNA (9.5% ± 15%) and *RPL5* shRNA (14.9% ± 7%) compared to the control (5.9% ± 3%). The observed increase in G2/M for cells infected with *RPL27A*-sh2 and *RPL5* shRNA was significant ($p \leq 0.005$) compared to control; the observed increase with *RPS14* did not reach

significance (*P*=0.07) (see Figure 4.16-B). In U937, 43.5% ± 3% of cells infected with *RPL27A*–sh2 were in G0/G1, 10%± 4% in S and 19.6% ± 5% in G2/M, compared with 64.5%± 5%, 13.5%± 3% and 10.7% ± 1% respectively for cells infected with the control empty vector (n=3, mean ±S.D.), see Figure 4.16-D. The observed increase in cells in G2/M, which was significant (*P*=0.0046), suggested that these cells were arrested *via* different pathways independent of p53. However, the observed increase in cell numbers in sub-G1 (*RPL27A*-sh-2 infected cells: 26.5 %± 7% compared with control 10.7%± 2), in the null p53 cell lines was less than what was seen in the other cell lines and that is consistent with the obtained results from apoptosis analyses (see Section 4.4.6).

From these results, it was clear that at day 6, the cells undergo apoptosis and it was unclear at which phase the cells were arrested. In order to determine whether the cell cycle defect occurred at an early time points, I performed the analysis at 24hrs, 48hrs and 72hrs. In HCT-116 and HCT-116 $p53^{-/-}$, the results were not clear and it was difficult to interpreted due to clumping of cells resulting in histograms with several spikes making the gating for each phase of cell cycle unclear, data not shown (Cell Cycle data was kindly reviewed by prof. Shaun Thomas, KCL). These results suggested increase in apoptosis occurs at sub-G1 phase, which increases with time in the cells that express p53. The null p53 cells did not show any significant differences from control cells in sub-G1 at early time points suggesting that depletion of *RPL27A* and *RPS14* are p53 dependant at an early time point while this effect become independent at a later time points, this was confirmed by experiments presented in the Section 4.4.10. The p53 independent effect can be attributed to the defect in the ribosome biogenesis. In order to investigate that ribosome profiling and nucleolar staining were performed as explained in the following sections.

A

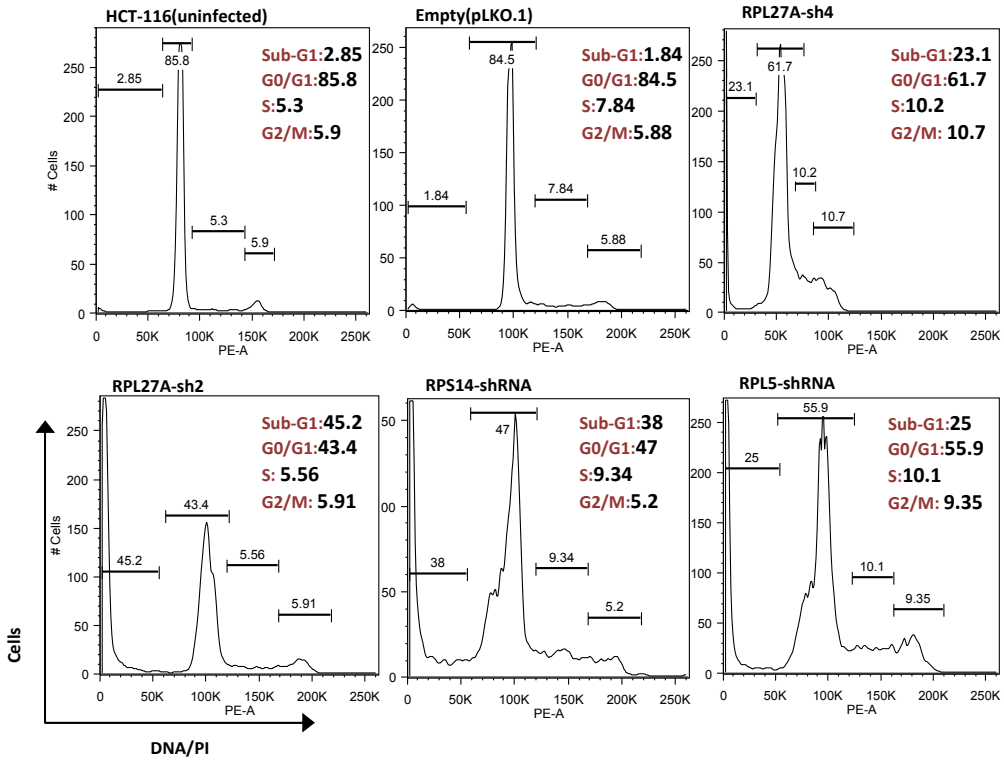
HCT-116(uninfected)
Sub-G1:2.85
G0/G1:85.8
S:5.3
G2/M:5.9
Empty(pLKO.1)
Sub-G1:1.84
G0/G1:84.5
S:7.84
G2/M:5.88
RPL27A-sh4
Sub-G1:23.1
G0/G1:61.7
S:10.2
G2/M: 10.7
RPL27A-sh2
Sub-G1:45.2
G0/G1:43.4
S: 5.56
G2/M: 5.91
RPS14-shRNA
Sub-G1:38
G0/G1:47
S:9.34
G2/M:5.2
RPL5-shRNA
Sub-G1:25
G0/G1:55.9
S:10.1
G2/M: 9.35
Cells
PE-A
Cells
DNA/PI

B

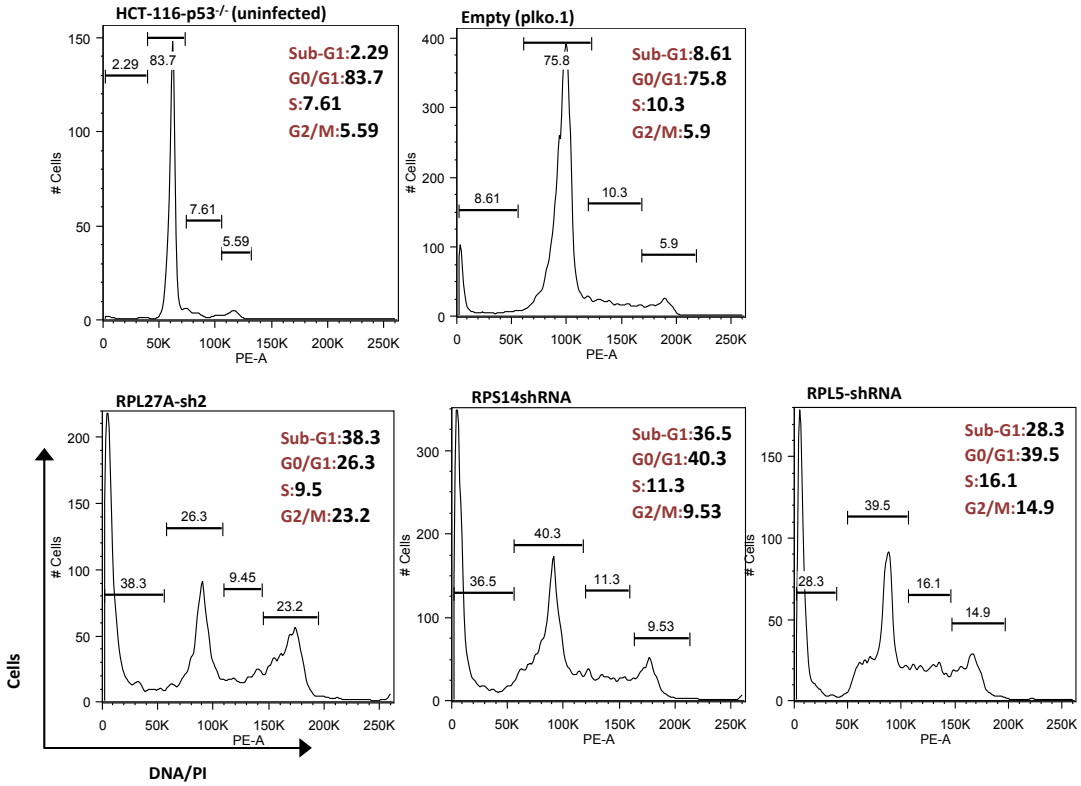
HCT-116-p53-/- (uninfected)
Sub-G1:2.29
G0/G1:83.7
S:7.61
G2/M:5.59
Empty (plko.1)
Sub-G1:8.61
G0/G1:75.8
S:10.3
G2/M:5.9
RPL27A-sh2
Sub-G1:38.3
G0/G1:26.3
S:9.5
G2/M:23.2
RPS14shRNA
Sub-G1:36.5
G0/G1:40.3
S:11.3
G2/M:9.53
RPL5-shRNA
Sub-G1:28.3
G0/G1:39.5
S:16.1
G2/M:14.9
Cells
PE-A
Cells
DNA/PI

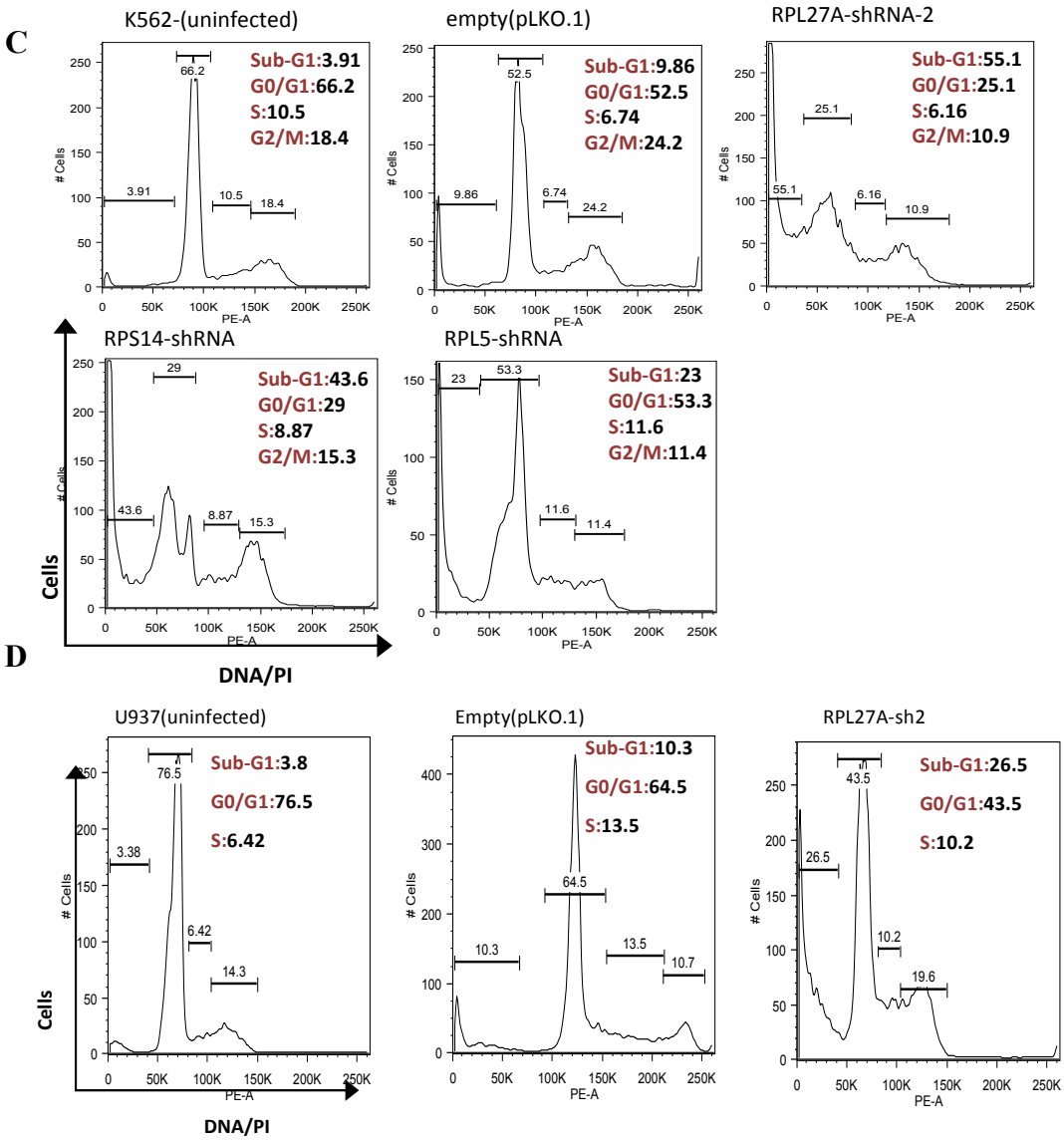

Figure 4.16: Cell cycle analysis in different cell lines infected with shRNAs against *RPL27A*, *RPS14* and *RPL5*.

Cell cycle analyses of uninfected, control and shRNAs infected cells on day 6 post-infection. The cells were fixed with ethanol and stained with PI. Graphs of the percentage of cells in sub-G1, G0/G1, S and G2/M phases were determined by flow cytometry. **A)** Cell cycle results of HCT-116 cells which were infected with control, *RPL27A*-sh2 and *RPL27A*-sh4, *RPS14* shRNA and *RPL5* shRNA; this showed increased in subG1 cells in all shRNAs infected cells compared with the relevant control. **B)** Cell cycle result on HCT-116 $p53^{-/-}$ cells which were infected with control, *RPL27A*-sh2 and, *RPS14* shRNA and *RPL5* shRNA; and showed increased percentage of cells in subG1 and G2/M in all shRNAs infected cells compared with the relevant control. **C)** K562 cells were infected with control, *RPL27A*-sh2 and, *RPS14* shRNA and *RPL5* shRNA; and showed increases of cells in subG1 in all shRNAs infected cells compared to the relevant control. **D)** U937 cells were infected with control and *RPL27A*-sh2; also showed a high percentage of cells in subG1 and in G2/M in the infected cells compared to the relevant control. The results represent three independent experiments

4.4.8. Effect of *RPL27A* deficiency on ribosome assembly

We postulated that a striking abnormality in *RPL27A* deficient cells may be a consequence of a primary defect in the ribosome formation and function and maturation of 60S subunit. Therefore, I performed polysome profiling of cells infected with *RPL27A* shRNA-2 by sucrose gradients fractionation. This experiment required a large numbers of cells to generate an analysable profiles; approximately 1 μg cell pellet was required. However, due to the knockdown effect on cell viability, this experiment was carried out several times to find the minimum analysable cells. Therefore, HCT-116, HCT-116-p53$^{-/-}$, K562 and HEL cell lines were infected with empty vector pLKO.1, *RPL27A* shRNA2 and *RPS14* shRNA (see Section 2.3.8.3). It has previously been shown that *RPS14* depletion results in the reduction of the 40S subunit (Ebert *et al.* 2008), therefore I used this as my control only in HCT-116 and HCT-116-p53$^{-/-}$ cells. In each experiment, three infections with the individual shRNAs were performed to recover sufficient numbers of cells for the analysis. On day 6 post-infection, pellets were collected from triplicates and mixed together; the minimum collected pellet contained approximately $8x10^5$ cells. Cells were treated with cyclohexamide for 15 minutes before collection and stored at -80 °C until analysed. The Polysome profiles were performed at the University of Cambridge in Prof. Alan Warren's lab with the help of Dr. Shengjiang Tan. Samples were transferred on Dry Ice and processed immediately upon arrival. Samples were lysed; RNA concentration was measured and equal concentration was separated by sucrose gradients centrifugation on 10 to 50% sucrose gradient as described in Section 2.3.12. The polysomes profile was detected using a UV monitor at A_{245}. In HCT-116, HCT-116 p53$^{-/-}$ and K562 the reduction of *RPL27A* resulted in a reduction of the 60S subunit and slight increase in the 40S subunit in comparison with the non-infected cells and the cells infected with empty vector (see Figure 4.17). *RPL27A*-sh4 was only examined in HCT-116 cell line and showed a small reduction in the 60S compared to the control. As expected, the depletion of *RPS14* caused a reduction in the 40S subunit in HCT-116 and HCT-116 p53$^{-/-}$. HEL cells analyses failed, the profiling result of the sucrose fractions from this cell line did not give any analysable data of the cells infected with *RPL27A* shRNA due mainly to low RNA concentration that was used in the fractionation. It is also likely that the high apoptotic level (see Section 4.4.6) also contributed to the failure to obtain a ribosomal profile. The profiling experiment was

performed in duplicate in all other cell lines and results were similar. Data obtained suggested that this ribosomal protein is essential for ribosome synthesis and maturation.

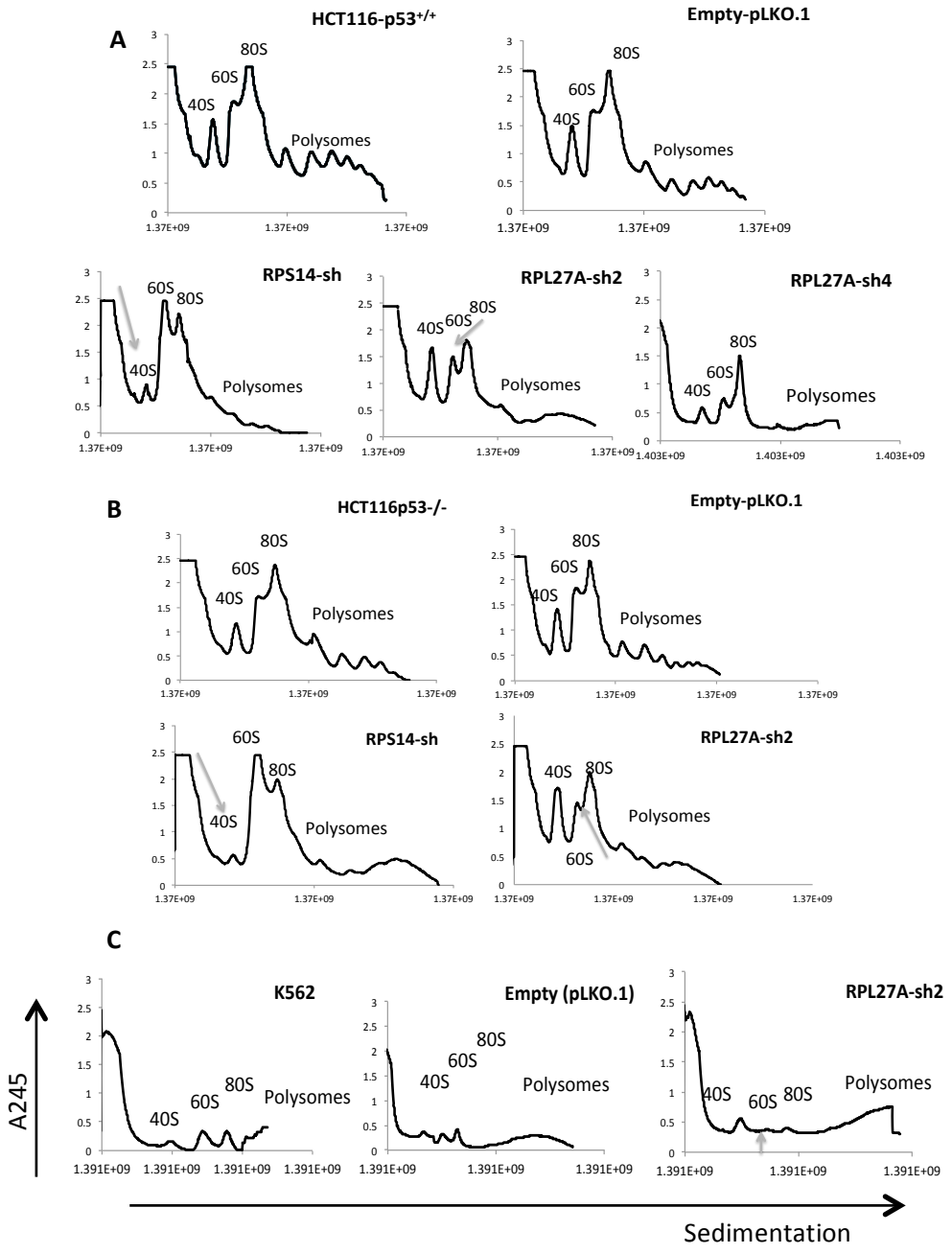

Figure 4.17: Depletion of *RPL27A* causes defects in 60S subunit maturation.

Polysomes profile of cells infected with lentivirus-expressing *RPL27A* shRNA, *RPS14* shRNA and empty vector pLKO.1 on day 6 post-infection. Polysomes profiling was performed by sucrose gradient fractionation on a 10% to 50% sucrose gradient. Polysomes were detected at A_{245} using a UV monitor. Ribosome native subunits 40S, 60S and 80S monosomes are indicated. **A, B)** In HCT-116 and HCT-116 p53-/-, *RPL27A* depletion reduced the 60S subunit, where *RPS14* shRNA reduced the 40S subunit compared to the relative control. **C)** K562 cells infected with *RPL27A* shRNA reduced the 60S subunit. These results are representative of duplicate experiments with each shRNA.

4.4.9 Depletion of *RPL27A*, *RPS14* and *RPL5* disrupts nucleolar signals

In order to examine if the deficiency of *RPL27A* and the other ribosomal proteins were involved in the alteration of nucleolar structure or the synthesis of ribosomes, which normally occurs in the nucleolus, nucleolar staining was performed. The nucleolus is composed of three main components: one of them is a dense fibrillar component, which can be visualized by staining with nucleolar protein, fibrillarin.

In this experiment, HCT-116 and HCT-116 $p53^{-/-}$ infected with empty vector pLKO.1, *RPL27A*-sh2, *RPS14*-shRNA and *RPL5*-shRNA, cells were puromycin selected and on day 6 post- infection, cells were fixed on slides and stained with anti fibrillarin antibody (see Section 2.3.11.5). Depletion of *RPL27A*, *RPS14* and *RPL5* resulted in abnormal staining of fibrillarin in all cell lines (Figure 4.18). Ribosomal protein depleted cells showed dispersion of fibrillarin in the nucleolus whereas cells treated with control empty vector (pLKO.1) did not show this disruption by screening at least three different positions in each slide. These results suggesting the importance of these ribosomal proteins in maintaining the nucleolar integrity and might explain the observed p53-independent effects described in previous sections. This experiment was performed in duplicate in each cell lines and analysed by confocal microscopy in Prof Warren's lab, Cambridge, the analyses was performed by the help of Dr. Shengjiang Tan

A

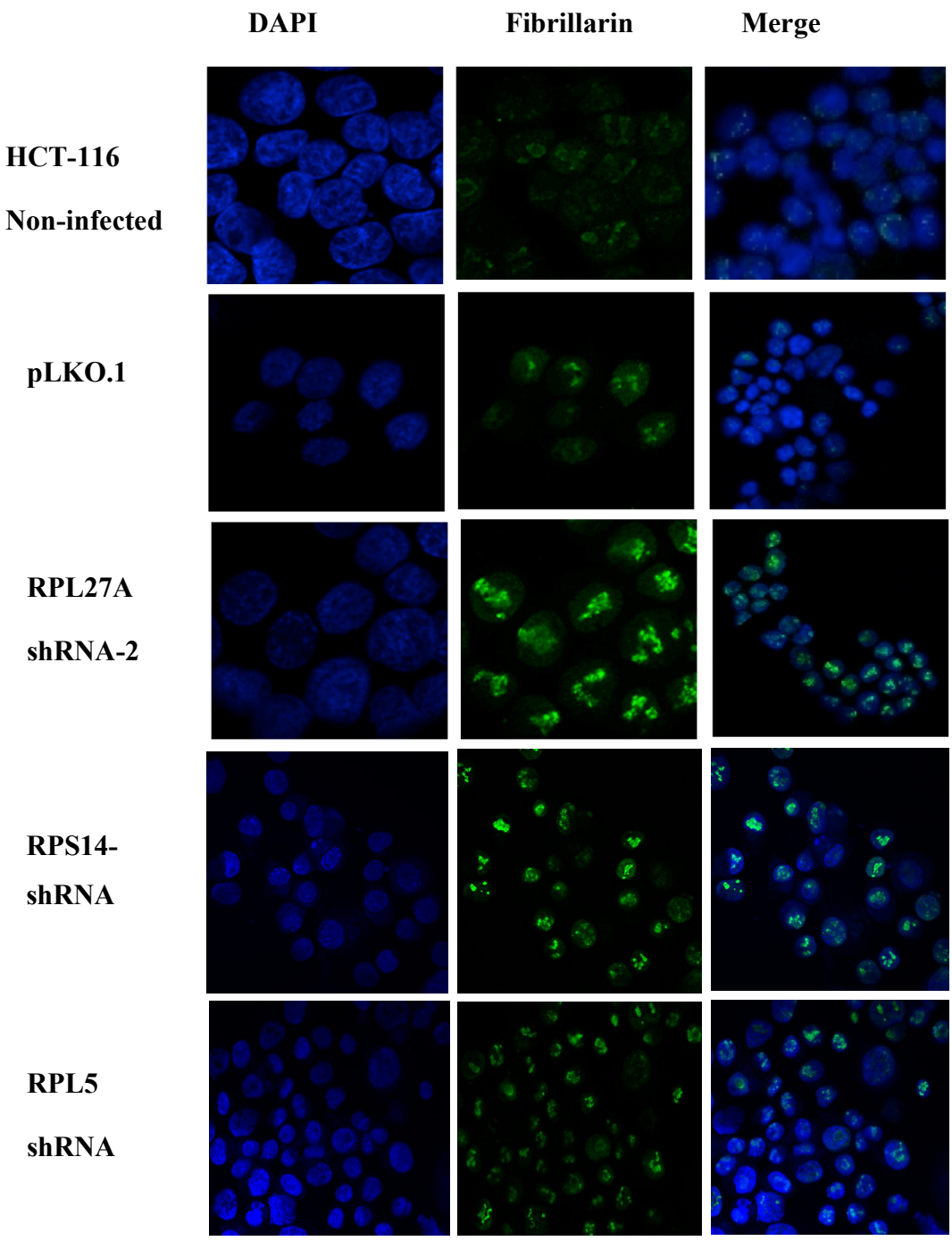
DAPI
Fibrillarin
Merge
HCT-116
Non-infected
pLKO.1
RPL27A
shRNA-2
RPS14-
shRNA
RPL5
shRNA

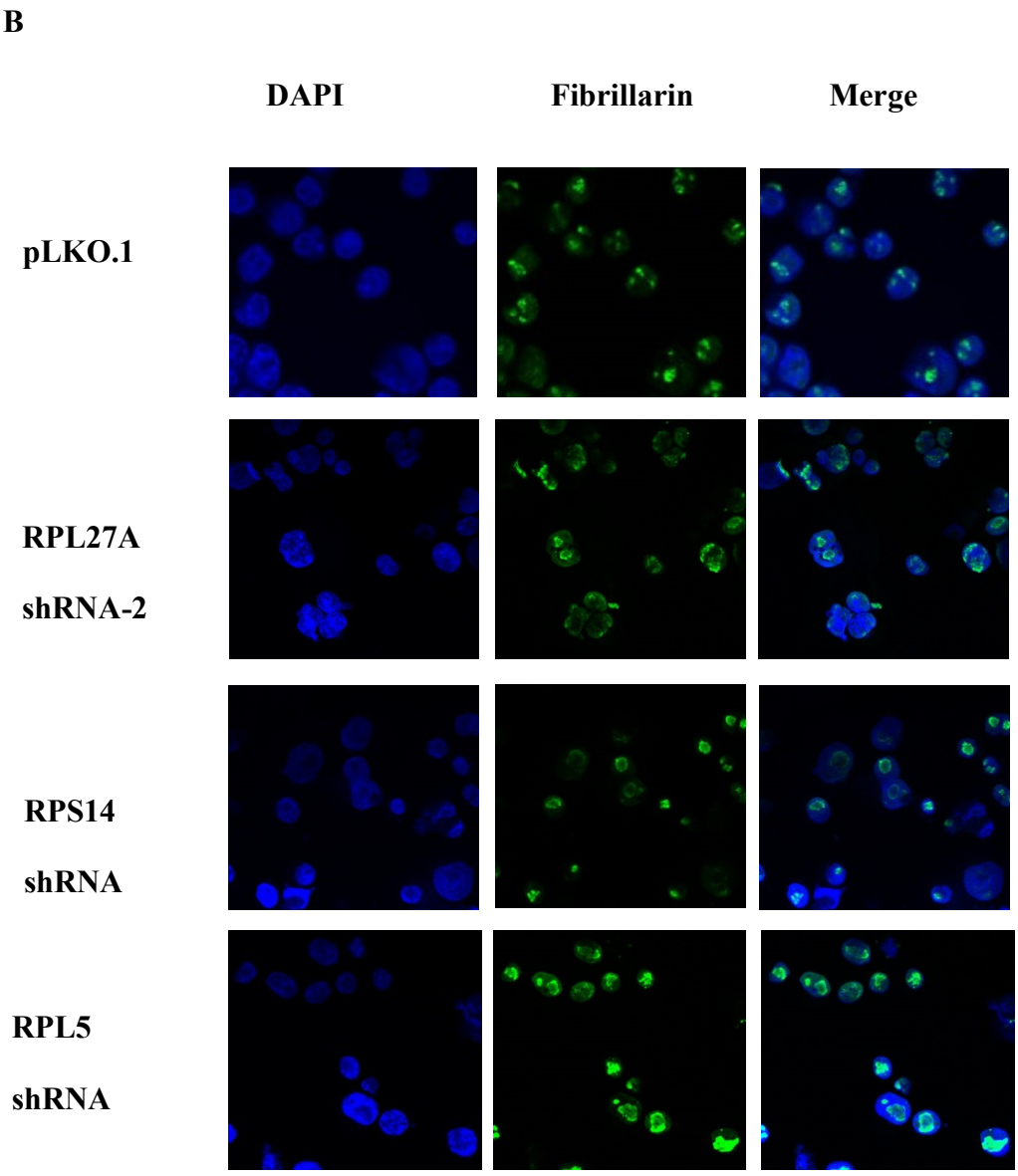

Figure 4.18: *RPL27A*, *RPS14* and *RPL5* are required for nucleolar organization.

A) HCT-116 and **B)** HCT-116 p53 $^{-/-}$ cells, infected with empty vector (the top panel) and the ribosomal protein shRNAs, were fixed on slides and stained with anti fibrillarin antibody (green: nucleolar marker) on day 6 post infection. The nucleus was stained with DAPI (blue). The slides were analysed using 40x objective Zeiss LSM780 confocal microscopy, ZEN 2010 software. The results represent n=2 experiments and showed disruption of nucleolar fibrillarin staining in cells infected with shRNAs against all ribosomal proteins compared to pLKO.1 empty vector in both cell lines.

4.4.10 Depletion of *RPL27A* and *RPS14* causes p53 dependent effect at an early time point

In order to investigate the effect of *RPL27A* depletion at early time points, some of the experiments were repeated on HCT-116 and HCT-116 $p53^{-/-}$ cells 48hrs post infection. HCT-116 and HCT-116 $p53^{-/-}$ cells were infected with *RPL27A* shRNAs, *RPS14* shRNA and *RPL5* shRNA as explained in Section 2.8.3.8. Samples for apoptosis, MTT assay and ribosome profiling were collected as explained earlier.

Apoptosis assays were performed using double staining with Annexin V and 7-AAD on $1x10^5$ cells collected from cells which were infected with *RPL27A* shRNAs, *RPS14* shRNA and *RPL5* shRNA compared to cells infected with control empty vector. *RPL27A*-sh2, *RPS14* shRNA and *RPL5* shRNA infection induced p53 dependent apoptosis, see Figure 4.19.The observed induction of apoptosis was significant based on the *p* value derived by a two tail student *t-test*. There were no significant changes in apoptosis observed in the p53 null cell line.

MTT assay was performed on 2000 cells suspended in 100µl complete culture medium and seeded into 96 well plates. Subsequently, MTT reagent was added to the cells and to the blank wells as explained earlier in Section 4.4.5. After overnight incubation plates were read on a platereader and the obtained data was analysed as explained in Section 4.4.5. The results showed a reduction in cell viability in cells infected with *RPL27A* shRNA and *RPS14* shRNA only in the p53 expressing cell line but *RPL5* depletion did not affect the cell viability in both cell lines as shown in Figure 4.20-A.

Polysomes profiling was performed on the HCT-116 cell line. Cells were infected with empty pLKO.1 and *RPL27A*-sh2 in triplicate and approximately $1x\ 10^6$ cells were collected after cyclohexamide treatment. Ribosome profiling and analysis was performed as explained in Section 4.4.8. The result showed that *RPL27A* depletion reduced the 60S subunit compared to the control empty vector, see Figure 4.20-B. However, the reduction in the 60S subunit was less than what was seen on day 6 suggesting that the reduction in the 60S ribosomal subunit increased with time, implying a p53 independent effect, which increased with time due to defects in ribosome biogenesis.

.

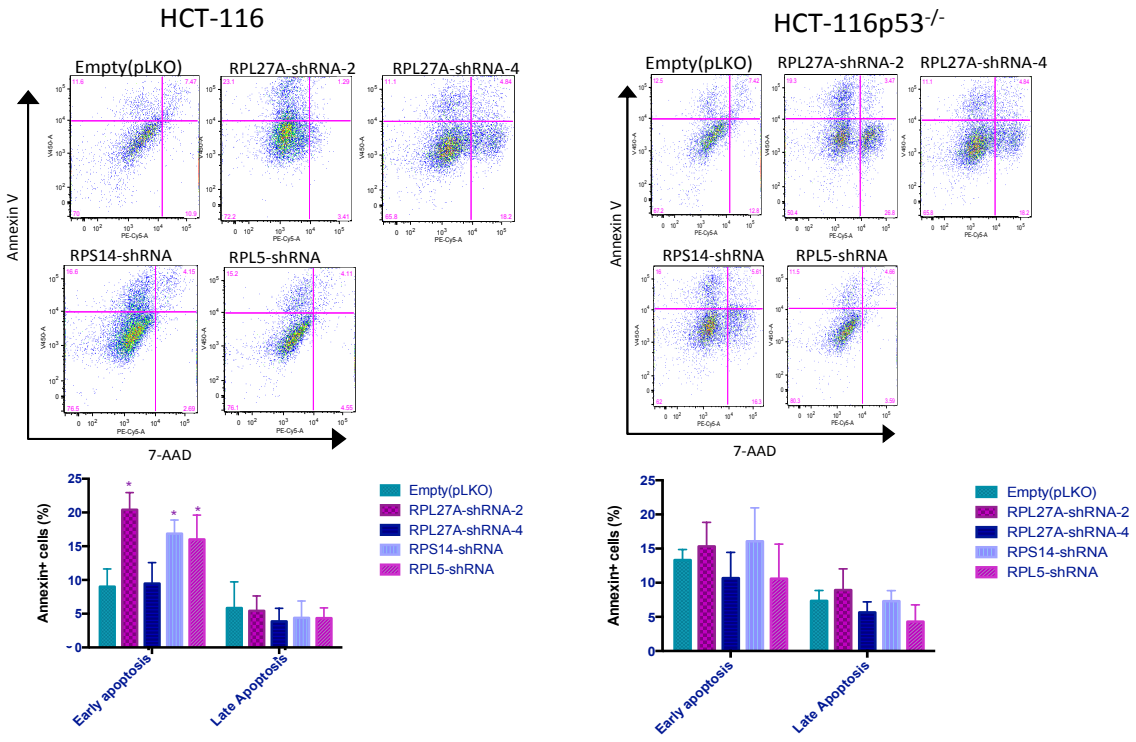

Figure 4.19: *RPL27A* deficiency resulted in apoptotic p53 dependent defect at 48hrs post infection.

HCT-116 and HCT-116 p53$^{-/-}$ cells were infected with control empty vector and shRNA against *RPL27A*, *RPS14* and *RPL5*. Then at 48hrs post infections samples were collected for several assays. Cells were stained with Annexin and 7-AAD and followed by flow cytometer analysis. Cells on the upper left quadrant indicate Annexin positive, early apoptotic cells. The cells in the upper right quadrant indicate Annexin-positive/ 7-AAD-positive, late apoptosis. In comparison with empty vector, *RPL27A* sh-2, *RPS14* shRNA and *RPL5* shRNA significantly induced apoptosis in HCT-116 only. Column diagram represents the mean of apoptotic cells from three independent experiments ±S.D. **P*(<0.05), ***P*(<0.005).

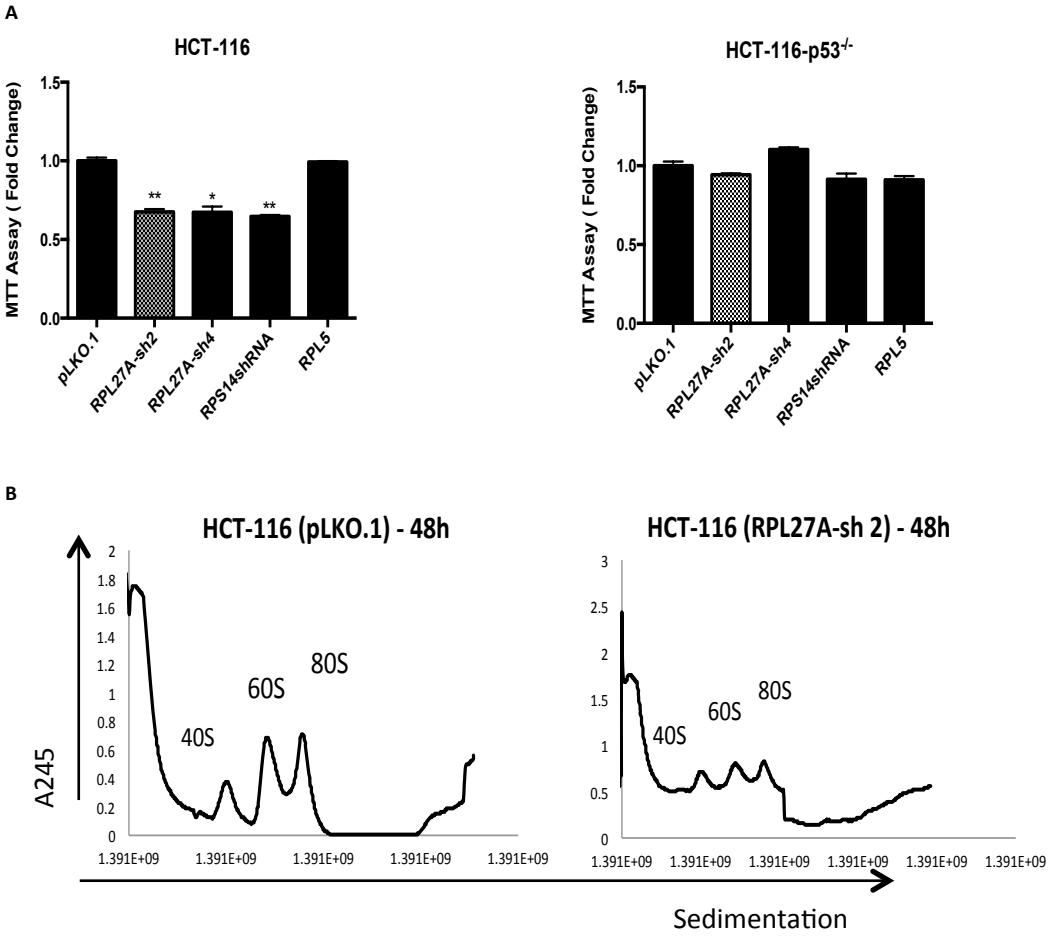

Figure 4.20: *RPL27A* deficiency resulted in p53 dependent defect at 48hrs post infection.

HCT-116 and HCT-116 $p53^{-/-}$ cells were infected with control empty vector and shRNA against *RPL27A*, *RPS14* and *RPL5*. Then at 48hrs post infections samples were collected for several assays. **A)** MTT assay to examine the knockdown effect on cell viability, the result showed significant reduction in cell viability with *RPL27A*-sh2, sh4 and *RPS14* shRNA in HCT-116 only. Results are expressed as fold change mean ±,S.D. relative to the control empty vector and are representative of three independent experiments each performed in triplicate **P*<0.05,**P*<0.005**. B)** Polysomes profiles were performed only in HCT-116 with *RPL27A*-sh2 and control empty vector only. Polysomes separation was performed by sucrose gradient fractionation on a 10% to 50% sucrose gradient. Polysomes were detected at A_{245} using UV monitor. Ribosome native subunit (40S and 60S) and 80S monosomes are indicated. *RPL27A* depletion reduced the 60S subunit compared with relevant control; experiments performed in duplicate.

4.4.11 RPL27A interacts with MDM2 and RPL5 in cells

The fact that several ribosomal proteins cause p53 induction through their interaction with MDM2 suggests that RPL27A might also interact with MDM2. This is strengthened by my observation that *RPL27A* depletion reduced MDM2 levels. To examine the possible interaction between RPL27A and MDM2 co-immunoprecipitation (IP)-immunoblot (IB) assays were performed as explained in 2.3.11.5.

The HCT-116 cell line was cultured and expanded until it almost reached confluence; $5x10^6$ cells were collected for each pull down assay and IgG control, IP assay was performed as explained in Section 2.3.11.5. Cells were lysed and incubated overnight with the appropriate antibodies; the pull down was performed with RPL27A antibody, the relevant IgG rabbit antibody, MDM2 antibody and the mouse IgG control. Also, a small aliquot from cell lysate without antibodies was stored at -20°C and used as a total input sample in western blot analysis. Following the overnight incubation with the antibodies at 4°C, lysed proteins were immobilised on protein A/G beads and incubated for 1hrs at 4°C. Subsequently, several washes were carried out followed by western blot analysis to determine the possible binding between RPL27A and MDM2. Interestingly, the endogenous MDM2 could be immuneprecipitated with RPL27A (Figure 4.21). However, the RPL27A pull down with MDM2 could not be confirmed due to the overlap with light chain, which was predicted to be of the same size as RPL27A (20KDa). Several attempts were made to address this including: changing the composition of IP lysis buffer, lysing the protein without using reducing agent in the lysis buffer, running the IB on a higher acrylamide gel, 20% instead of 14%, which should separate smaller bands better and finally using commercial secondary antibodies against light chain such as easy blot. All of these measures failed in overcoming this problem and no further optimizations were performed.

Although it has been reported that RPL5 binds to MDM2, so I performed western blot analysis for RPL5 and its interaction with MDM2 and RPL27A by probing MDM2 pull down lysate and RPL27A pull down lysate with RPL5 antibody. This was done to investigate whether the association of RPL27A with MDM2 in cells might be indirect via other ribosomal proteins. The result in Figure (4.21) showed that endogenous RPL5 bound to MDM2 as well as RPL27A. Suggesting a possible indirect interaction between RPL27A and MDM2. Further investigations to determine the binding site on MDM2 needs be carried out in future studies.

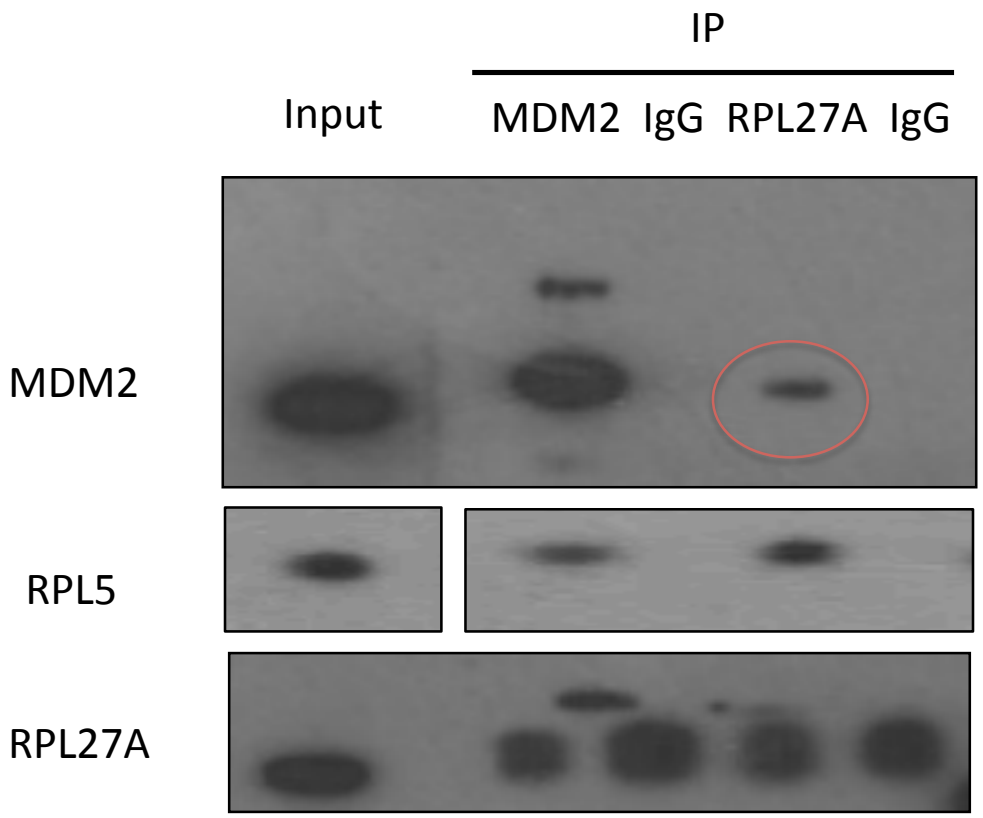

Figure 4.21: RPL27A interacts with MDM2 and RPL5 in cells.

Endogenous RPL27A interacts with endogenous MDM2 and RPL5 in HCT-116 cells. Cell lysate ($5x10^6$ cells) were prepared and IP was performed with anti-RPL27A or rabbit IgG and anti-MDM2 or mouse IgG followed by IB with anti-MDM2, anti-RPL27A and anti-RPL5. Experiments were performed at least two times. The result showed that MDM2 and RPL5 proteins are co-precipitated with RPL27A pull down in comparison with the input samples.

4.4.12 *RPL27A* overexpression has no effect on cell survival

It has been previously shown that the ribosomal proteins that interact with MDM2 inhibit MDM2 –E3 liagase activity and stabilize p53. To test this, I cloned *RPL27A* into FLAG expressing vector as explained in 2.3.3

The plasmid p3xFLAG-myc-CMV empty vector and p3xFLAG-*RPL27A* were introduced into HCT-116 cells using the lipofectamine transfection method as explained in Section 2.3.7.1. Transfections were performed in 24 well plate and 48 hrs post transfection cells were transferred to 175 cm^2 flask; cells were selected with G418 and samples were collected on day 14 post-selection. Samples for RNA, western blot and cell cycle analysis were collected. mRNA level of *RPL27A* was investigated as explained earlier and the result was normalized with *GAPDH* and compared with the empty vector (p3xFLAG-myc-CMV). The relative *RPL27A* expression was calculated using ΔΔCT and the result in Figure 4.22-A, showed an approximately 2 folds increase in cells transfected with *RPL27A* constructs compared to the empty vector. In order to investigate the overexpression effect on *p53* and *MDM2*, the mRNA expression levels for both of them was determined. *RPL27A* overexpression had no effect on *p53* and *MDM2* expression was only slightly increased in accordance with *RPL27A* overexpression. Protein samples were analysed by western blot as explained earlier. RPL27A antibody was used in addition to loading control antibody, which was γ tubulin. The result showed overexpression of RPL27A as compared to the control, Figure, 4.22-B.

For cell cycle analysis 2x 10^5 cells were fixed in ethanol and stained with PI (DNA content) and analysed by flow cytometer. The results showed normal cell cycle profile in cells transfected with RPL27A constructs as compared to empty vector, see Figure 4.22-C

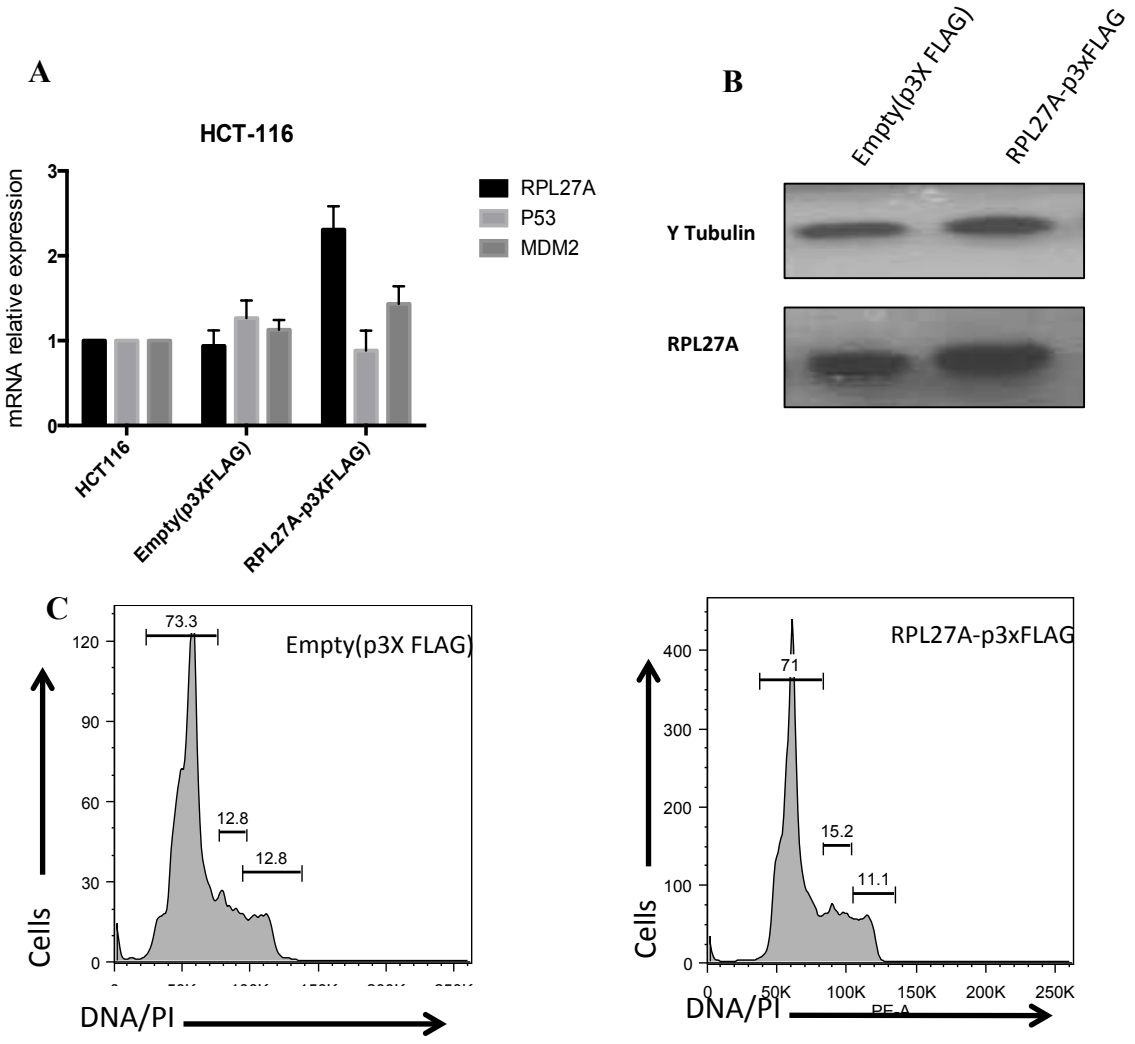

Figure 4.22: Effect of *RPL27A* overexpression

HCT-116 cells were mock transfected, and transfected with empty vector p3X FLAG and p3xFLAG *RPL27A* constructs. Cells were selected with G418 and after 14 days under selection cells were collected to examine the *RPL27A* overexpression level and its effect on p53 and cell cycle. **A)** mRNA relative expression of *RPL27A*, *p53* and *MDM2* normalised to *GAPDH* in cells transfected with *RPL27A* compared with cells transfected with empty vector. Bars represent three independent experiments mean± S.D. **B**) Western blot analyses of protein samples collected from cells transduced with RPL27A and empty vector. Samples were probed with RPL27A antibody and tubulin was used as loading control. **C)** Cell cycle analysis of cells transfected with empty (p3x FLAG) and FLAG-RPL27A. Cells were fixed in ethanol and DNA content was stained with PI and analysed by flow cytometrey. There were no significant changes on the cell cycle phases from three independent experiments.

4.5 Discussion

Impaired ribosome biogenesis caused by ribosomal protein mutations and haploinsufficiency can cause nuclear stress. This phenomenon leads to the development of a clinical entitities collectively known as "ribosomepathies" which refer to the ribosomal defect that is associated with several congenital diseases and bone marrow failure syndromes, such as Diamond Blackfan Anaemia (DBA), Shwachman-Diamond syndrome (SDS), Dyskeratosis Congentia (DS) and Cartilage-Hair Hypoplasia(CHH) in addition to acquired MDS sub type 5q- syndrome (Liu *et al.* 2006, Narla *et al.* 2010).

It is recognised that ribosomal stress is leads to p53 accumulation, although the mechanisms that underlie this phenomenon are not fully understood. Marechal and co-workers were the first to show a link between ribosomal stress and p53 in 1994. They identified the complex interaction between RPL5, p53 and MDM2 (Marechal *et al.* 1994). Other studies followed and identified other ribosomal proteins also interact with MDM2 and increase the expression level of p53. Reduction of *RPS6* (Panic *et al.* 2006), *RPL22* (Anderson *et al.* 2007), *RPL24* (Barkic *et al.* 2009), *RPS19* (Danilova *et al.* 2008), *RPS14* (Ebert *et al.* 2008) and *RPL23* (Jin *et al.* 2004) all have been shown to increase the p53 levels while the reduction of other ribosomal proteins including *RPL11* (Zhang *et al.* 2003), *RPL5* (Dai *et al.* 2004) decrease the p53 level. By contrast the overexpression of *RPL5*(Dai *et al.* 2004), *RPL26* (Takagi *et al.* 2005) and *RPL11* (Lohrum *et al.* 2003, Zhang *et al.* 2003, Bhat *et al.* 2004) and other ribosomal proteins, induced p53. Uniquely, however, *RPL23* and *RPS14* reduction and overexpression increase p53 expression (Jin *et al.* 2004, Zhou *et al.* 2013).

Various studies on ribosomal protein depletion, including *RPL27A* have been done in mice and showed different phenotypes, as summarized in Table 4.1. The *RPL27A* study on mice is the only available study of this ribosomal protein; all other information about this ribosomal protein comes from expression array data and profiling results of different diseases (Terzian *et al.* 2011). Terzian *et al,* discovered the effect of reduced expression of *RPL27A* in sooty foot ataxia (SFA) mice on the p53 pathway. They isolated a *SFA* mutation and, by using mitotic mapping, they identified 13 genes within that mutation. The scan for the mutations of *SFA* heterozygous mice identified a point mutation within the *RPL27A* gene: an A>G at position 15 in the final splice acceptor of intron 4. Terzian and co-workers identified a phenotype similar to the high *p53* mouse model and those with reduced *MDM2*

and *MDM4*.This phenotype includes the four major p53-dependent phenotypes: cerebellar ataxia, pancytopenia and epidermal hyperpigmentation and radio sensitivity. The reduction of *RPL27A* increase p53 levels and affected survival, and decreased number of haematopoietic stem cells (HSC) in the bone marrow in the severely affected mice. Also, downregulation of *c-Kit* and increased apoptosis was observed mainly in the mice with reduced HSC leading to postnatal lethality, which was attributed to a p53-dependent effect. Terzian *et al*, indicated the importance of *RPL27A* in maintaining p53 levels and suggested that the severity of depleted *RPL27A* depends on the expression levels of *RPL27A* and the affected tissue type, as well as the development stage.

Therefore, in the current study, the effect of *RPL27A* depletion on ribosome biogenesis, cell proliferation and survival in comparison with other ribosomal proteins was investigated. The conducted experiments in this chapter were performed on different cancer cell lines that included cells expressing *p53* and cells null for *p53*. Using lentiviral strategies, the achieved knockdown level was more than 80% with one shRNA (shRNA-2) and approximately 40-50% with another shRNA (shRNA-4).

In relation to *p53*, it has been shown that deficiency of *RPS14* and other ribosomal proteins as mentioned earlier lead to activation of p53 *in vivo* and *in vitro*. That activation was accompanied with *p53*-dependent apoptotic cell death and cell -cycle arrest, which are mediated through induction of *p53* targets such as *p21* and *Bax*. Thus, *RPS14* knockdown was performed and used as positive control. *RPL5,* which has been known with inducing *p53* by its upregulation, was also knocked down. The knockdown level for *RPS14* and *RPPL5* was more than 80%. Therefore, the knockdown levels of these ribosomal proteins were comparable with *RPL27A*-sh2.

RPL27A depletion was carried out in different cell lines to investigate the effect on the p53 pathway, as mentioned earlier, and the reduction of *RPL27A* was carried out using the two shRNAs. The expression levels of p53 were measured at mRNA and protein level and the result showed an induction of p53 at variable levels in both transcriptional and protein levels. As expected *RPS14* depletion also led to the increased levels of p53. To validate whether p53 is active or not, the expression levels of some of the known p53 target genes were examined including *p21* and *Bax*. In the $p53^{+/+}$ cell lines the expression levels of these genes were increased significantly in comparison with the control empty vector in cells deficient for *RPL27A*. This increase in the expression of p53 target genes was also

associated with *RPS14* depletion, which was in agreement with other studies (Dutt *et al.* 2011). However, in the null p53 cell lines, the expression level of *p21* and *Bax* did not change. This implies that RPL27A is similar to other ribosomal proteins, functioning through a p53-dependent mechanism.

However, the induction of *p53* at the mRNA level was not detectable in the HEL cell line that expresses p53; though the *p53* targets *p21 and Bax* were increased, which indicates p53-dependent induction. The undetectable induction of p53 at mRNA level could be due to the global translation inhibition caused by *RPL27A* depletion. A similar finding was reported when *RPS19* and *RPL5* were knocked down in CD34+ cells (Dutt *et al.* 2011). In the study by Dutt *et al*, p53 induction was only observed at the protein level and the failure to detect changes at the p53 mRNA level was thought to be due to general translation inhibition. Similar finding was also reported by Mu-Shui and Hua Lu who found that p53 induction as a result of *RPL5* overexpression was only detected at protein level and not at the mRNA level but they were able to detect increases in *p21* at mRNA level (Dai *et al.* 2004).

The expression level of MDM2 was also investigated to study the effect of ribosomal protein depletion on p53 to determine whether these effects are through MDM2 or through independent mechanism. Interestingly, MDM2 expression was reduced in all cell lines suggesting that *RPL27A* inhibit MDM2-mediated p53 degradation resulting in increased levels of p53. MDM2 is a key regulator of p53 and plays an important role in cell survival (Manfredi 2010).

In order to investigate the knockdown effect on the cell survival mechanism, cell proliferation, apoptosis and cell cycle were investigated. Silencing of *RPL27A, RPS14* and *RPL5* reduced the proliferation of HEL and K562 cells. The reduction of proliferation in K562 was surprising, as K562 does not express p53 and the effect was similar to that seen in the HEL cell line resulting in complete cell death by day 10. For HCT-116 cells, as explained in section 4.2.4, the proliferation monitoring based on cell count was not reliable. Therefore an MTT assay was performed which showed a significant reduction in cell metabolic activity on day 6, detectable in both $p53^{+/+}$ and $p53^{-/-}$ cells, but the reduction was less in $p53^{-/-}$ cells. Therefore, to verify the p53-independent effect, another cell line U937 (null p53) was obtained and results of *RPL27A* depletion in these cells proliferation showed

a moderate reduction in proliferation suggesting a p53 independent mechanisms that could result from defects in ribosome biogenesis.

To investigate whether the reduction in cell proliferation is due to apoptosis, Annexin V and 7-AAD double-staining was performed. *RPL27A* (sh2 and sh4), *RPS14* and *RPL5* reduction was associated with increased apoptosis in both $p53^{+/+}$ and $p53^{-/-}$ cells. These results are similar to what was observed in the proliferation assay, the increase in apoptosis was highest in the HEL and K562 cell lines. However, a significant increase in apoptosis was still seen in HCT-$116^{-/-}$ and U937 cell lines, but it was less than in HEL and K562. Also, the cell cycle analysis results confirmed the findings in the apoptosis assay namely accumulation of cells in the sub-G1 phase and a considerable cell death. However, G2/M arrest was observed in U937 and HCT-116 $p53^{-/-}$ at day 6, which is suggested to be caused by p53 independent mechanisms.

It was surprising to find that, upon reduction of *RPL27A*, *RPS14* and *RPL5* in both $p53^{+/+}$ and $p53^{-/-}$ cells, there was a significant induction of apoptosis in the null p53 cells lines in addition to the reduction in cell proliferation. This suggests the existence of p53-independent mechanisms that affect the biological process in the long run. The independent effect by *RPL27A* was also seen *in vivo* by Terzian and co-workers study. In the SFA an association was found between *RPL27A* reduction and tumour transformation and prevention independent of p53. They tested the effect of tumour formation and overall survival in mice with p53+/- and mice with p53+/-:SFA/+ with reduced *RPL27A*. The depleted *RPL27A* mice had a higher risk of metastasis compared with p53+/-mice. This metastatic effect implies the p53-independent effect of *RPL27A*. The fact that the same investigation was performed in another study using *RPL24* knockout mice with a p53+/- background and in this study no differences were noticed either in tumour development or metastasis emphasizing the specificity of this effect to *RPL27A*, which cannot be generalized to other ribosomal proteins. The observed independent damage emphasizes the importance of this ribosomal protein in mutant p53 cancer. In contrast, the depletion of *RPL5* does not lead to induction of p53 in the literatures, but it has been reported that reduction of *RPL5* decreased the 60S ribosomal subunit with a concomitant increase in 40S. This had an inhibitory effect on ribosome biogenesis and global protein translation, which caused a delay in proliferation independent of p53 (Teng *et al.* 2013). This observation could explain the observed defect on proliferation and increased apoptosis

independent of p53, as observed by day 6. Further supportive evidence of the effect of *RPL5* deficiency on apoptosis induction is consistent with what was seen in other studies of *RPL5* and *RPL11* depletion in $CD34^{+}$-derived erythroid cells. Normally to induce erythroid differentiation the experiments are carried out in long-term culture procedures, therefore after 10 days on culture the depletion of *RPL5* showed significant induction of apoptosis. These findings suggest the importance of a p53- independent mechanism in the onset of tumourgenesis mainly in tumours with non -functional p53.

The observed cell death in myeloid erythro-leukaemia cell lines (HEL-K562) could be attributed to either a cell type -specific effect, which would be an effect against erythroid cells, or it could be a cell line-specific genetic defect (k562 is a BCR-Abl cell line and HEL carries JAK2 mutation).

Given that the effects appear to be erythroid specific, several reports have pointed to the involvement of ribosomal defects in erythroid differentiation such as the effect of *RPS19* and further11 ribosomal proteins mutations, which reduced the genes expression, in the erythroid cells in DBA patients and the association of *RPS14* haploinsufficiency with erythroid depletion in 5q-syndrome (Narla *et al.* 2010, Dutt *et al.* 2011).

Goetz and co-workers reported that the presence of BCR-Abl control the MDM2 level and keep it at high levels. They have shown that BCR-Abl-positive cells, which are normally resistant to apoptosis and cell death caused by pro-apoptotic stimuli such as cytotoxic agents and growth factors deficiency, are not resistant to cell death caused by MDM2 depletion (Goetz *et al.* 2001). This could explain the observed high apoptotic in K562 cell line, which is a BCR-Abl positive cell line, as a result of the decreased expression of *RPL27A*, *RPS14* and *RPL5*, which reduced the expression of MDM2.

The *RPL27A* depletion using shRNA-4, which caused less than 50 % knockdown, has no significant effect on the null p53 cell lines (HCT-116 $p53^{-/-}$) and the observed effect on the p53 cell lines (HCT-116 and HEL) was less than what was seen with shRNA-2. This indicated that although a 50 % reduction led to the induction of p53, but this reduction is insufficient to induce cell death. This is supported by the knockout studies in mice, which showed that ribosomal protein deficiency by heterozygous mutations in mice had no adverse effect on the mice whereas mice homozygous for several mutated ribosomal proteins, including *RPS19* and *RPL27A*, were embryonic lethal as summarised in Table 4.1.

Also, the complete loss of *RPS14* lead to cell death as seen in yeast (Ferreira-Cerca *et al.* 2005).This homozygous deletion of RPS14 is not seen in 5q- patients (Ebert *et al.* 2008). This also could explains the rescued phenotype in mice with heterozygous deletion of *RPL27A* (Terzian *et al.* 2011) *RPS14* (Barlow *et al.* 2010) and *RPS19* (Devlin *et al.* 2010) in these models, a normal cellular phenotype was restored.

To my knowledge, thus far, no studies have shown the importance of *RPL27A* on the ribosome assembly and ribosome biogenesis in humans. Therefore, in this project ribosome profiling was performed on three cell lines (including HCT-116, HCT-116 p53-/- and K562) with reduced *RPL27A*.The knockdown using *RPL27A*-sh2 caused a depletion in the large subunit, accompanied by an increase in the 40S subunit in comparison with the control and the non-infected cells. Also, the knockdown of *RPS14* caused a reduction in the 40S subunit and resulted in accumulation in the 60S subunit, which is in agreement with what was seen in the Ebert et al (Ebert *et al.* 2008). The above results were obtained from samples isolated on day 6 post-infection. To confirm the presence of the effect at an earlier time point, the experiment was repeated in one cell line (HCT-116) 48hrs post –infection. The result showed a reduction of 60S ribosomal subunit, but this was less than what was observed on day 6; this indicated that the ribosomal defect was not a consequent of cell death and apoptosis; it was a specific defect of *RPL27A* deficiency. This finding contradicts what was reported in Terzian *et al* study, that *RPL27A* has no effect on ribosome biogenesis. In the Terzian study, the maximum knockdown level was 40% in cerebellum and approximately 30% and 20% in bone marrow and skin respectively. These low levels of knockdown are the reason they did not observe any defect in ribosome biogenesis; in this study the knockdown with *RPL27A*-sh4, which caused 40-50% knockdown resulted in only a very small reduction of the 60S subunit. These findings taken together and suggests that *RPL27A* impairs ribosome assembly only when the depletion exceeds 50%.

The knockdown of *RPL27A* caused a reduction in the large subunit, which in turn caused a reduction in other proteins that are part of the large subunit assembly such as *RPL5*, which is probably a response to the global translation inhibition. This is in agreement with what was observed with knockdown of *RPS19,* which caused a dramatic reduction in the ribosomal proteins that are part of the same subunit (Badhai *et al.* 2009). The regulation of other ribosomal proteins important for p53-MDM2 pathway might be involved indirectly with the induction of p53 and impaired ribosome biogenesis.

Activation of p53 as a result of ribosomal dysfunction has been attributed to two pathways, either *via* increased expression of *RPL11* or nucleolar stress, which affects the nucleolar structure. The current study showed that the reduction in *RPL27A, RPS14* and *RPL5* caused a disruption of the nucleolar marker, fibrillarin, in HCT-116 and HCT-116 $p53^{-/-}$ on day 6 post infection. This indicates that these ribosomal proteins could activate p53 through nucleolar stress suggesting their importance for ribosome biogenesis. The current study contradicts another study that investigated the effect of *RPS14* deficiency on the nucleoli (Dutt *et al.* 2011). Dutt *et al*, showed that both *RPS14* and *RPS19* knockdown did not affect the nucleolar integrity by staining with the nucleophosmin (B23). Dutt et al, discussed the similarity of their finding with another study on RPS6; the effect of *RPS6* depletion on p53 induction is caused by an increase in the expression levels of *RPL11*. This occurred without affecting the nucleolar integrity, which was observed by staining with another nucleolar protein marker, nucleolin (Fumagalli *et al.* 2009). Increases in RPL11 translation elevated the binding of RPL11 to MDM2 and therefore increased the expression of p53 (Lohrum *et al.* 2003). This contradiction with the data presented here can be explained in several ways. First, the nucleolar staining was performed with different nucleolar markers, i.e. fibrillarin in the current study and two different markers in the other studies. Second, the duration of the experiments was different between the studies mentioned and as shown in this thesis timing plays a crucial role to observe the effect of ribosomal protein knockdown on ribosome biogenesis. The experiments performed in the other studies were terminated within 48 -72hrs post- depletion, while in the current study it was measured on day 6 post-infection. In this study some experiments were carried out 48hrs post transduction and it was very clear that the effect on the ribosome profiling was moderate and the reduction of the 60S subunit was much less than what was seen by day 6. Therefore the majority of the damaging effects seen at a late stage are mainly due to the disruption of ribosome biogenesis. These findings show the importance of these ribosomal proteins on the ribosome machinery and ribosomal structure.

Regulation of MDM2 activity is a complex process due to the abundance of interacting ribosomal proteins that can modulate MDM2 function following ribosomal or nucleolar stress (Deisenroth *et al.* 2010). Co-immunoprecipitation of RPL27A identified the possible interaction with MDM2 in HCT-116 cells. The pull-down experiment showed that RPL27A interacts with MDM2 and RPL5. The function of this interaction might be the prevention

of p53 ubiquitination and degradation by MDM2. However, to further investigate whether the RPL27A interaction with MDM2 was mediated through other ribosomal proteins, further experiments should be carried out to identify binding sites of ribosomal proteins on MDM2.

Finally, overexpression of *RPL27A* was carried out and showed no effect on the p53 pathway and showed normal cell proliferation and a normal cell cycle profile. However, the effect of *RPL27A* overexpression on the p53 pathway and cell survival cannot be conclusive, because the increase in the expression level was only 2-folds. Therefore, the effect of *RPL27A* overexpression levels has to be ascertained by increasing the expression level, in order to assess the relation between *RPL27A* overexpression and other cellular mechanisms. However, the achieved upregulation, which has no effect on cell surveillance mechanism, and is supported by the observations from other studies, which showed increases in the expression level of *RPL27A* in different tumours and human cancer cell lines (Ross *et al.* 2000).

The results described in this chapter shed light on the mechanism of cell death following depletion of *RPL27A* and the subsequent defect in ribosome biogenesis due to a reduction of the 60S ribosomal subunit. It became clear that *RPL27A* depletion leads to a severe cellular insult, and there is a possibility that *RPL27A* deficiency leads to an activation of several cell death pathways, including the p53 pathway and global translation inhibition.

The results seen in the erythroid cell lines seem to indicate that *RPL27A* plays a role in erythroid cell survival. To confirm this and to identify whether RPL27A is another ribosomal protein that controls erythropoiesis similar to RPS14, RPS19 and RPL5, the aim of the following chapter was to perform *RPL27A* knockdown on CD34+ cells - derived erythroid cells and to examine the knockdown effect on erythroid differentiation and cell survival.

Chapter 5: *RPL27A* knockdown in normal haematopoietic progenitor CD34+ cells

5.1 Introduction

The deletions or mutations of genes, which are able to encode ribosomal proteins, have been identified in haematological diseases, particularly 5q- MDS and inherited hypoproliferative anaemia DBA. This has led to a new terminology "ribosomopathies", which is used to refer to disorders caused by impaired ribosome biogenesis and function (Narla *et al.* 2010). DBA is the first known disease to be caused by mutations in ribosomal protein genes, and it leads to impairment of erythropoiesis and the development of a disease specific phenotype (Draptchinskaia *et al.* 1999). DBA is a congenital bone marrow failure syndrome, characterised by red blood cell aplasia; a model disease for erythroid differentiation. Half of DBA patients have heterozygous mutations in multiple ribosomal protein genes, leading to defects in ribosome function (Boria *et al.* 2010). The *RPS19* mutation was the first discovered, and the most frequent mutation in DBA patients, as it represents around 25% (Draptchinskaia *et al.* 1999, Choesmel *et al.* 2007). Later, several other ribosomal protein gene mutations were identified in DBA patients including *RPS24* (Choesmel *et al.* 2008), *RPS17* (Cmejla *et al.* 2007) and *RPL35a* (Farrar *et al.* 2008). This is in addition to mutations in *RPL5* and *RPL11* (Gazda *et al.* 2008), which have been identified in 11.4% of DBA patients. A large-scale study of DBA patients identified mutations in other ribosomal protein genes such as *RPS27A*, *RPS7*, *RPS15* and *RPL36* (Gazda *et al.* 2008).

Mutations in other genes which are required for ribosome synthesis have been implicated in different congenital bone marrow failure syndromes such as SDS, DC and CHH (Liu *et al.* 2006).

In addition to congenital disease, ribosomal proteins have also been implicated in acquired disorders such as 5q– syndrome, which is a subtype of MDS, as described in Chapter 1. 5q– syndrome is characterised by a defect in erythropoiesis, which leads to macrocytic anaemia, patients usually have a normal or elevated platelet count. The potential importance of ribosomal protein genes in 5q- MDS is derived from the findings of Ebert and colleagues (Ebert *et al.* 2008). The haploinsufficiency of *RPS14,* localised to 5q segment, in normal haematopoietic progenitor cells leads to the characteristic disease phenotype. A decrease in the expression of *RPS14* has been identified in patients with 5q- syndrome (Ebert *et al.* 2008, Pellagatti *et al.* 2008). *RPS14* deficiency results in impairment of the pre-RNA processing of 18S RNA, and causes a reduction of the 40S subunit. This is similar to what

was observed with *RPS19* deficient cells in DBA patients, which links the 5q- syndrome pathophysiology to defects in ribosomal proteins function, in a similar way to congenital bone marrow failure syndromes (Choesmel *et al.* 2007, Ebert *et al.* 2008).

The association between ribosomal protein mutations and the development of specific defects, throughout the haematological systems, can be attributed to various mechanisms. The main mechanism is attributed to the activation of the p53 pathway, which is described in the Chapter 4 (Figure 4.2). The disruption of ribosome biogenesis leads to the release of free ribosomal proteins, which interact with MDM2 and prevent the degradation of p53. The accumulation of p53 leads to apoptosis and cell cycle arrest, and inhibits cell proliferation, leading to anaemia (McGowan *et al.* 2008, Fumagalli *et al.* 2009).

The other suggested mechanism is inherently linked to the active proliferative machinery seen in erythroid cells. Erythroid cell maturation and differentiation, which is also known as erythropoiesis, is a dynamic process regulated by different proteins, with the power to cause the developmental changes required by specific lineages. These changes affect the development of progenitor erythroid cells into mature erythrocyte (Weissman 2000, Flygare *et al.* 2007). Erythroid progenitor cells are notable for their high proliferation rate, which double every 12 to 24 hours, and require elevated ribosomal activity and ribosome biogenesis (Lajtha *et al.* 1961, Narla *et al.* 2010). The insufficiency of ribosomal protein causes ribosomal stress, which affects globin synthesis and leads to the release of excess free haem, resulting in apoptosis of erythroid cells and leading to anaemia (Quigley *et al.* 2005, Keel *et al.* 2008, Narla *et al.* 2010).

The identification of the genes involved in erythroid differentiation provides an insight into understanding the biology of erythrocyte and erythroid disease. Therefore, the aim of this chapter is to study the effects of *RPL27A* deficiency on normal haematopoietic progenitor cells, and particularly on erythropoiesis. According to the findings from the previous chapter, about the effects of *RPL27A* knockdown on ribosome biogenesis, cell proliferation and apoptosis, it was of interest to investigate the extra ribosomal function of this ribosomal protein gene on erythropoiesis mainly through *p53* activation and to demonstrate if there are any functional similarities with other ribosomal protein genes or any possible links with bone marrow failure syndrome.

5.2 Aim

- Investigate *RPL27A* Knockdown in normal haematopoietic progenitor cells using lentiviral shRNA.
- Investigate the consequent effects of *RPL27A* deficiency on the p53 pathway.
- Examine the knockdown effect of haematopoietic subpopulations mainly on erythroid differentiation.

5.3 Experimental Design

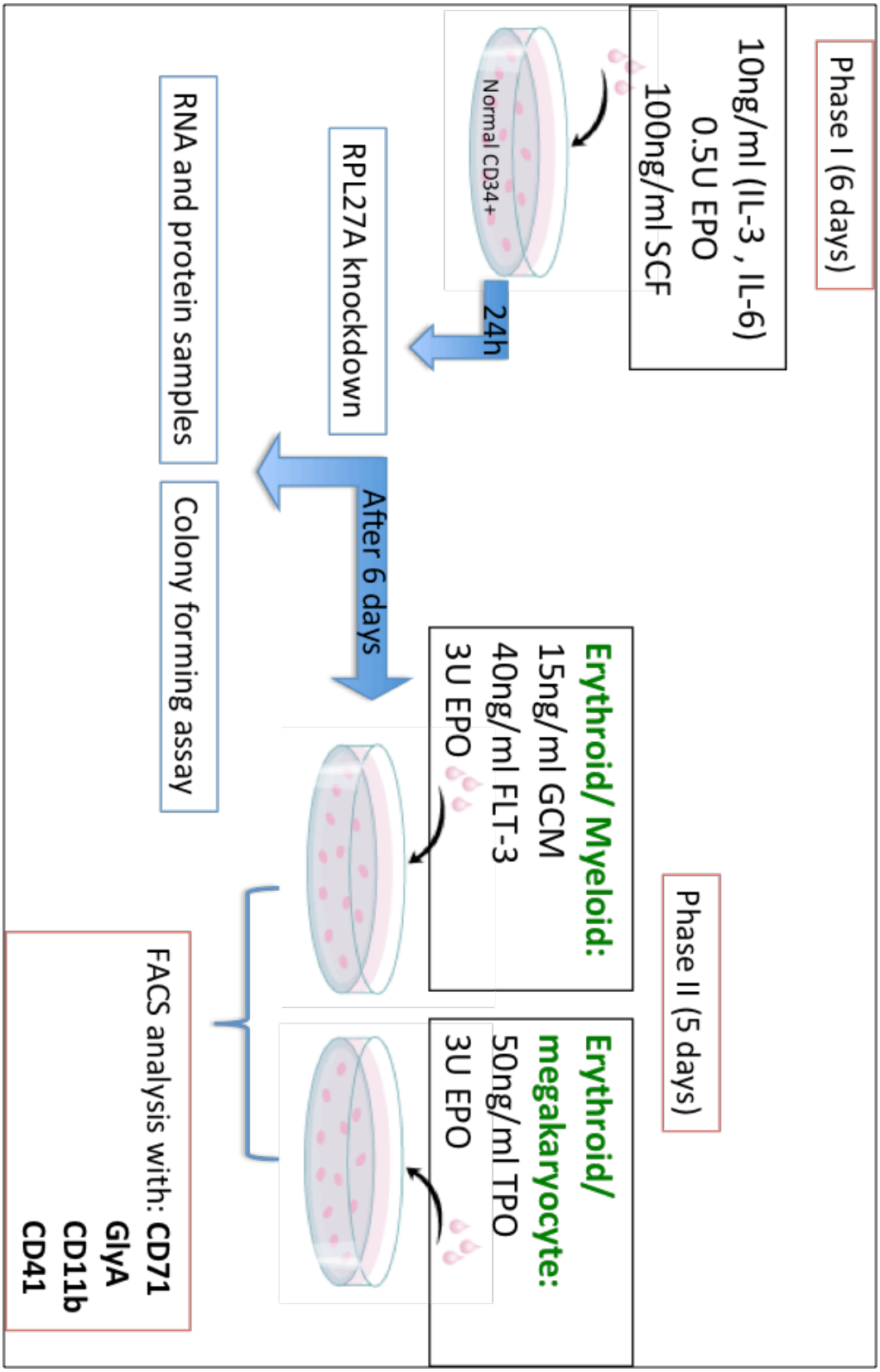

5.4 Result

5.4 1 *RPL27A* knockdown in BM CD34+ inhibits cellular proliferation

The knockdown experiment was first performed on CD34+ cells from viably frozen BM cells, which were obtained from Lonza. The cells (1×10^6 cells) were defrosted at room temperature and cultured to induce erythroid differentiation in a two-phase liquid culture systems, as explained in Section 2.3.6.6. In Phase I, cells were cultured in Serum-Free Expansion Medium supplemented with penicillin/streptomycin, glutamine, 100 ng/ml SCF, 10 ng/ml IL-3, 10 ng/ml IL-6 and 0.5 IU/ml Epo. After 6–7 days, the cells were induced to differentiate into two lineages; erythroid-myeloid and erythroid-megakaryocyte. Therefore, the same culture medium used in Phase I was used with the addition of 3 IU Epo, 40 ng/ml FLT3 and 15 ng/ml G-CSF to induce the cells to differentiate along the erythroid and myeloid lineages. On the other hand, to induce megakaryocyte differentiation, Phase I culture medium was used and was supplemented with 3 IU Epo and 50 ng/ml TPO.

During Phase I, which is the expansion phase, the recovered $CD34^+$ cells were cultured in 1 ml medium in a 24-well plate. After one day in the culture, the cells were counted and divided into three wells (with $3–4 \times 10^5$ cells/ml/ well). One of the wells was left as mock (non-infected cells), and the other two wells were infected with retroviral plasmid. One was infected with 10 µl of the 100× concentrated lentiviral empty pLKO.1 and the other one infected with 10 µl of the 100× concentrated lentiviral expressing *RPL27A* shRNA-2 as explained in Section 2.3.6.6. After 24 hrs, cells were selected using puromycin. The cell count was monitored every 2 days using trypan blue staining, and due to increases in the cell count, cells were transferred to a 6-well plate on day 3 (post infection), with cell density preserved at 1×10^6/ ml. On day 6 (post infection), cells were transferred to Phase II in the culture system. The cells in each well were divided into two culture conditions using different cytokine cocktails, as explained earlier, and the two different linages were induced. This experiment was repeated several times, until the final optimisation condition was achieved. This led to the loss of several BM samples. As such, the following result is a preliminary result generated from only one BM CD34+ sample. The knockdown level was examined on day 6 (post infection), by qRT-PCR and western blot analysis. The levels of *RPL27A* mRNA and protein were decreased by 40% and 80%, respectively, as shown in Figure 5.1 A and C. Also, p53 expression levels were examined and showed an induction

of p53 at both the transcriptional and post-transcription levels, (Figure 5.1 A). The activation of p53 was confirmed with the upregulation of p53 targets *p21* and *Bax* by qRT-PCR (Figure 5.1 B). The knockdown effect on cell proliferation was assessed based on the cell count, every 48hrs. The reduction of *RPL27A* expression led to a reduction in the cell count by day 4, and this reduction continued with time. Accordingly, *RPL27A* deficiency blocked cell proliferation and led to cellular death within 10 days, compared to the control empty pLKO.1 and the mock (Figure 5.1 D). The cells were cultured until day 10 (which is day 4-5 of Phase II), when cell death dramatically increased. At this point, the cells were harvested and FACS analysis was performed on protein surface markers of different lineages, in order to investigate the knockdown effect on erythroid, myeloid, and megakaryocytic lineages. However, on day 10 there were very few live cells in *RPL27A* sh-2, excepting cells, which were harvested for FACS analysis (approximately $< 5 \times 10^4$ cells). The FACS result was not very clear, due to the small cell number and small number of recorded events. Whilst there was a clear reduction in erythroid cells, relative to the myeloid and megakaryocytic lineages, this data had to be further validated (Figure 5.2).

Therefore, these experiments were repeated on CD34+ cells, isolated from PBMCs. The reason for changing from the marrow to the blood was primarily due to the practical difficulties and cost implications surrounding the acquirement of normal bone marrow mononuclear CD34+ cells.

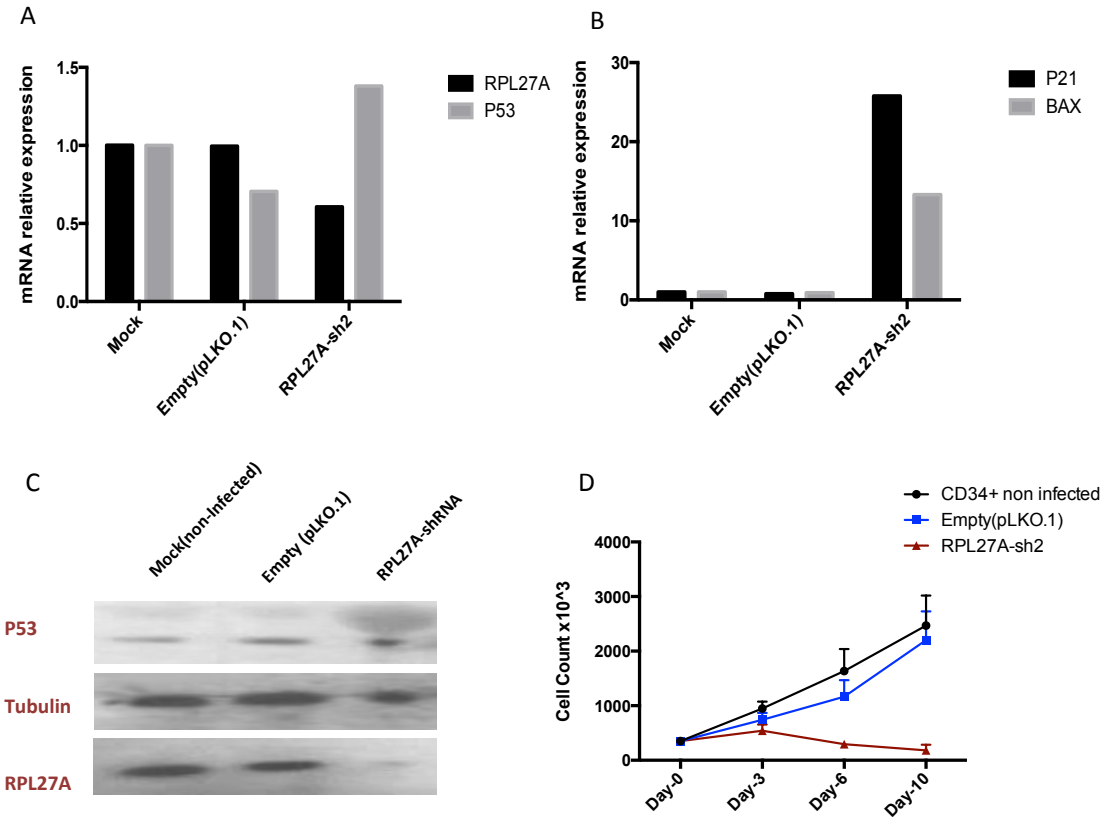

Figure 5.1: *RPL27A* knockdown in normal BM CD34+ leads to p53 activation.

A) RNA samples collected on day 6 (post-infection) and the mRNA expression of *RPL27A* and *P53,* relative to *GAPDH,* was measured by quantitative real time PCR and showed an induction of *p53,* associated with the reduction of *RPL27A*. **B)** The mRNA expression of p53 target genes *p21* and *Bax,* relative to *GAPDH,* was measured by quantitative real time PCR, and showed increased expression of *p21* and *Bax* in cells with depleted *RPL27A*. All qRT-PCR results were compared to cells infected with empty vector. **C)** Protein extracts were collected on day 6 from non-infected cells and cells infected with empty vector and shRNAs, against *RPL27A,* and analysed on 4–12% polyacrylamide gels probed with antibodies, in order to detect RPL27A and p53. Equal protein loading per well was determined by Y tubulin loading control. The reduction of RPL27A was very high and resulted in p53 induction. **D)** Cells were counted every 48 h, and the results showed a reduction in cell numbers by day 4, reaching complete cell death by day 10 in cells infected with *RPL27A*-sh2, compared with control, empty vector and non-infected cells. The presented data is preliminary, and the results obtained from one experiment.

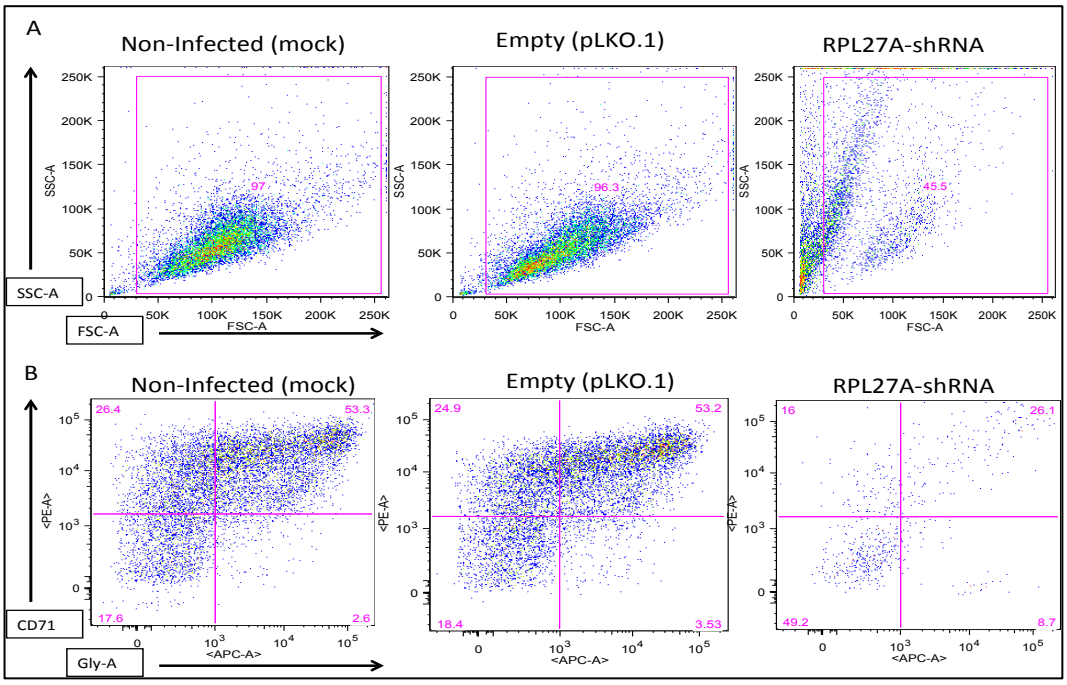
A
Non-Infected (mock)
Empty (pLKO.1)
RPL27A-shRNA
SSC-A
FSC-A
97
96.3
45.5
B
Non-Infected (mock)
Empty (pLKO.1)
RPL27A-shRNA
CD71
Gly-A
26.4
53.3
17.6
2.6
24.9
53.2
18.4
3.53
16
26.1
49.2
8.7

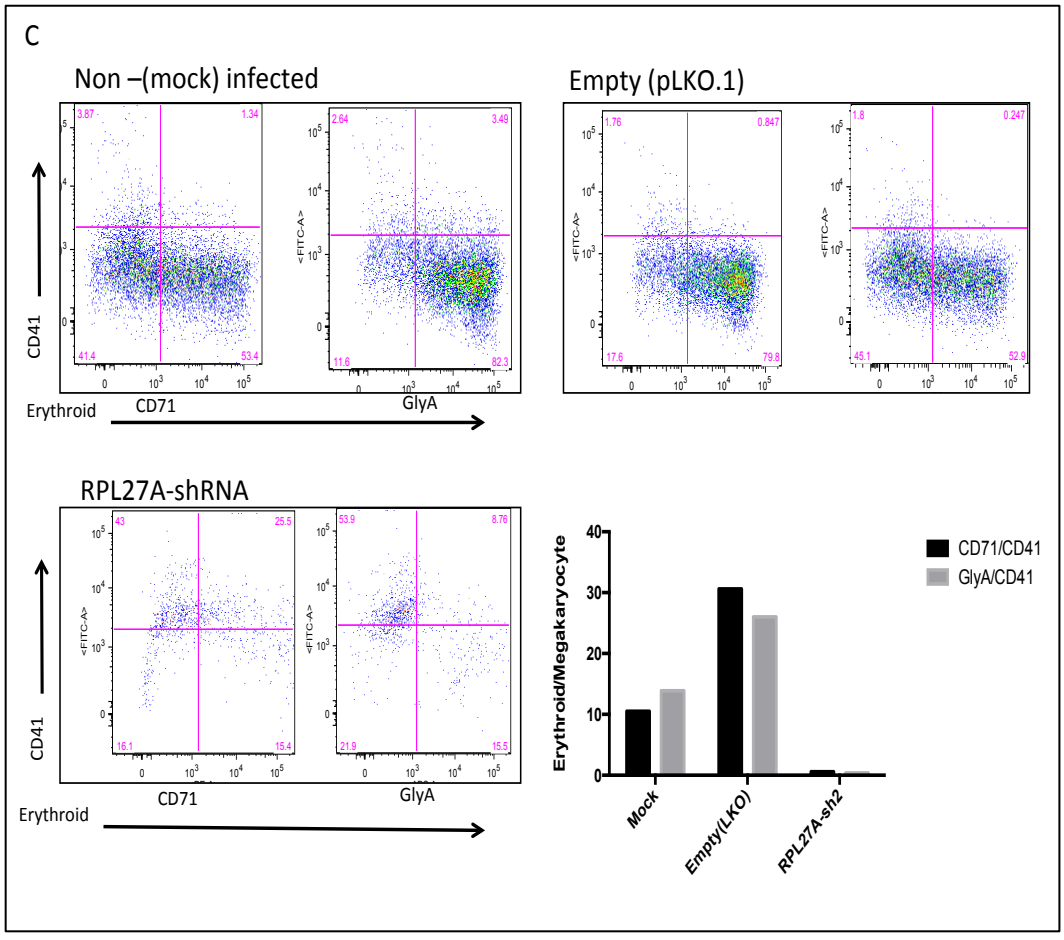
C
Non –(mock) infected
Empty (pLKO.1)
RPL27A-shRNA
CD41
CD71
GlyA
Erythroid
Erythroid/Megakaryocyte
CD71/CD41
GlyA/CD41
Mock
Empty(LKO)
RPL27A-sh2

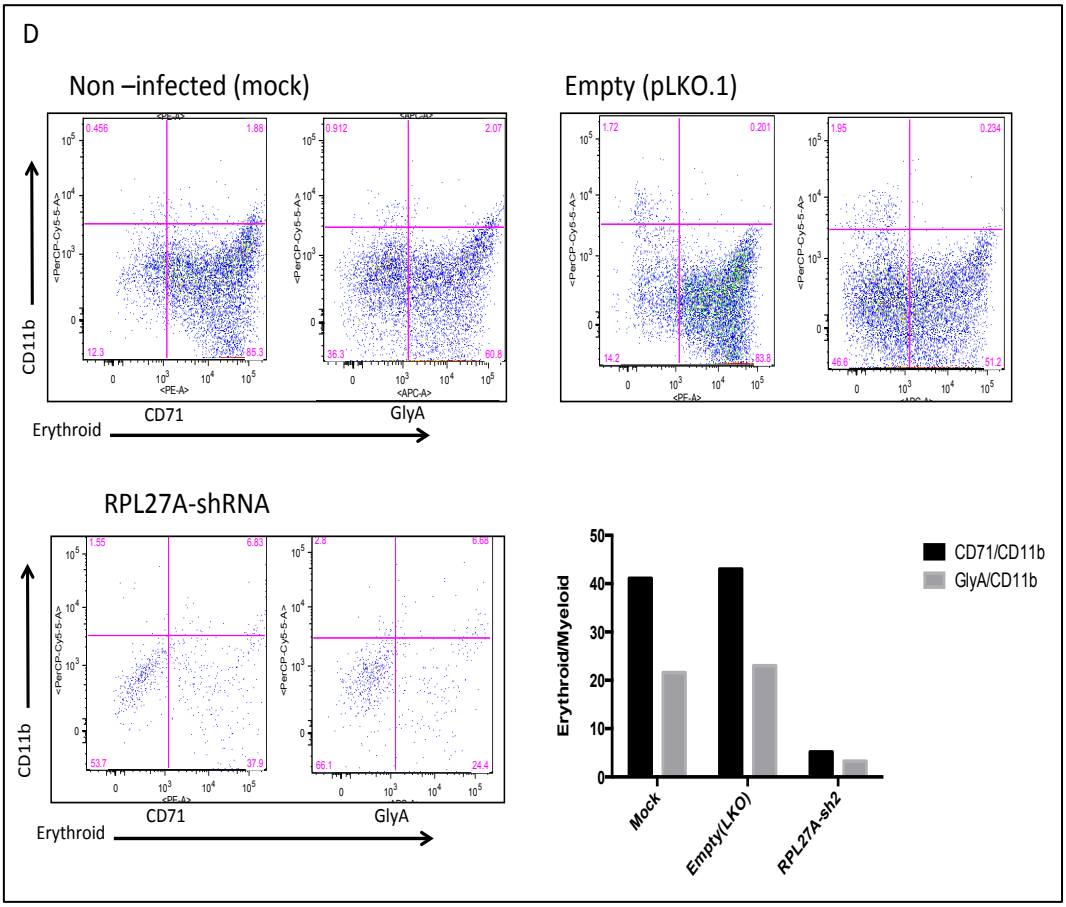

Figure 5.2: *RPL27A* knockdown in normal BM CD34+ blocks HSC proliferation and differentiation.

Cells were harvested on day 10–11, after retroviral infection for flow cytometry. Approximately 0.5–1 × 10^5 cells were labelled with a mixture of conjugated antibodies, including live/dead staining with (780), immature erythroid (CD71), mature erythroid (GlyA), myeloid (CD11b) and megakaryocyte (CD41). **A)** Identical gating was applied in all examined cells, and showed that cells expressing *RPL27A* shRNA were less viable. **B)** Comparing immature and mature erythroid did not show a clear effect on terminal erythroid differentiation, as assessed by flow cytometry using antibodies against CD71 and GlyA. **C)** *RPL27A* knockdown blocks erythroid, relative to megakaryocyte differentiation, compared to a control empty vector and non-infected cells. The ratio of cells from erythroid and megakaryocytic lineages was assessed by flow cytometry, using immature and mature erythroid antibodies (CD71 (right-bottom) GlyA (left-bottom)) against megakaryocyte (CD41 antibodies). **D)** *RPL27A* knockdown reduces erythroid, relative to myeloid differentiation, and the ratio was assessed using immature and mature erythroid antibodies (CD71 (right-bottom) GlyA (left-bottom)) against myeloid antibody (CD11b). In all panels, the effect was compared to the control empty vector and the non-infected cells.

5.4.2 *RPL27A* knockdown in CD34+ cells isolated from PBMCs reduces cell proliferation and induces p53

Peripheral blood CD34+ cells have been used in other studies, in order to examine the consequent effect of ribosomal protein gene knockdown on haematopoietic subpopulations (Ohene-Abuakwa *et al.* 2005, Dutt *et al.* 2011). Therefore, the experiment performed on the bone marrow CD34+ was repeated on CD34+ cells isolated from four blood samples. CD34+ cells were isolated from PBMCs, using leukocyte cones, as described in Section 2.3.6.5. Mononuclear cells were collected after histopaque separation from the interface layer, then CD34+ cells were isolated using the MACS-LS separation columns and the CD34+ microbead kit. The isolated CD34+ cells were counted (the cell count was in the range of 1 to 1.5 × 10^6 cells) and cultured, in the same way as described in the previous section. The cells were counted and divided as 2.5–3 × 10^5 cells/ml for each experiment, which were mock (non-infected cells) and cells infected with either empty vector pLKO.1 or targeted shRNAs against *RPL27A* and *RPS14* shRNA. After 24 h, the infected cells were selected with puromycin, and cells were transferred to larger wells due to the rapid increase in cell density. Similar to what was observed in BM CD34+ cells, the growth rate of cells expressing the shRNAs targeting *RPL27A* was reduced, relative to empty vector control, by day 4. This is based on cell counts, and the same observation was noted in *RPS14* shRNA. Therefore, cells were harvested on day 6, and cells from each experiment were divided for several more experiments including qRT-PCR, protein analysis, Phase II culture and colony forming assay. The knockdown efficiency of *RPL27A* and *RPS14* was determined by qRT-PCR and western blot. RNA was purified from cells preserved in Trizol, and cDNA was produced using Superscript II reverse transcriptase; qRT-PCR was carried out as described in Section 2.3.10.3. *RPL27A* mRNA levels were normalised with *GAPDH,* and relative expression in cells expressing *RPL27A*-shRNA was calculated relative to the expression level in the control empty vector. The qRT-PCR results showed approximately 70% reduction in the expression level of *RPL27A* and *RPS14* in cells infected with *RPL27A shRNA* and *RPS14* shRNA, respectively relative to the control empty vector (Figure 5.3-A). Furthermore, the reduction of *RPL27A* and *RPS14* caused a significant reduction in *RPL5* expression (P= 0.0055 and P=0.0120, respectively), whereas *RPL27A* reduction did not significantly affect the *RPS14* expression, or vice versa. *RPL27A* expression was further validated by western blot analysis, which showed a clear reduction in the protein

expression, as shown in Figure 5.3 C. The expression level of p53 was determined by qRT-PCR and western blot analysis. The mRNA expression of *p53* was surprisingly decreased in both *RPL27A* and *RPS14* depleted cells, whilst the protein expression showed increases in p53 protein expression (Figure 5.3 B and C). This was further confirmed with the detection of significant increases in the expression level of p53 targets. The mRNA relative expression of *p21,* in both *RPL27A* and *RPS14* deficient cells compared to the empty vector, was significantly increased with P=0.00062 and P =0.01732, respectively. *Bax* expression was also significantly increased in both *RPL27A* and *RPS14* deficient cells, compared to the empty vector (P =0.00156 and P =0.00610, respectively) (Figure 5.3-B). To investigate the effects on cell cycle, cell cycle marker RB was used (pRB antibody was kindly provided by Prof. Shaun Thomas). The western blot analysis, using phosphorylated RB, showed hypophosphorylation in the cells infected with *RPL27A* shRNA, as well as *RPS14* shRNA. This indicates an arrest within the cell cycle (Figure 5.3-C). The reason for not investigating the cell cycle profile, and only screening the cell cycle marker, was the limitation in cell number. The cells, which were infected with targeted shRNA, were apoptotic and all the live cells were used for FACS analyses.

In order to investigate the knockdown effect on cell proliferation, cell counting was carried out every 48 h. It showed a dramatic reduction in cell count, which increased in both *RPL27A* shRNA and *RPS14* shRNA expressing cells, compared to the control and non-infected cells, as shown in Figure 5.3-D.

On day 10/11 in culture, very few viable cells from the knocked down cells were left. Therefore, the effect of *RPL27A* knockdown on erythroid, myeloid and megakaryocytic linages was only assessed by flow cytometry, using specific cell surface markers. Cells were stained, as explained in Section 2.3.6.6. Erythroid differentiation was assessed by measuring the expression of erythroid- specific surface proteins CD71 and GlyA. Myeloid cells were assessed using CD11b, and the megakaryocytes cells were determined by CD41. The analysis was performed using Flowjo, and single cell gating was first performed. Then, live/dead discrimination was conducted, according to the live/dead staining within 780 markers. This staining showed a dramatic reduction in the percentage of cells in the live-gated populations of cells expressing *RPL27A* shRNA(17.6%) and *RPS14* shRNA(9.09%), compared to control (79.2%) and non-infected cells (80.9%), see Figure 5.4-A. The analysis of erythroid cells within the live population showed a massive reduction in the

production of both immature and mature erythroid cells in both *RPL27A* and *RPS14* deficient cells ($CD71^+/GlyA^+$: ±5.8% and ± 3.3%, respectively), compared to the relevant control ($CD71^+/GlyA^+$: ±74.9% in empty vector infected cells and ±64.8% in mock non infected cells), Figure5.4-B. The staining, relative to myeloid and megakaryocyte lineages, was not conclusive due to insufficient induction of both lineages. To assess whether or not the cell death was a result of apoptosis, annexin V staining was performed on day 6 (post infection), and cells were stained with CD71 to determine the apoptosis effect relative to erythroid cells. *RPL27A* shRNA and *RPS14* shRNA significantly induced apoptosis ($P<0.001$), relative to erythroid cells differentiation, as shown in Figure 5.4-C.

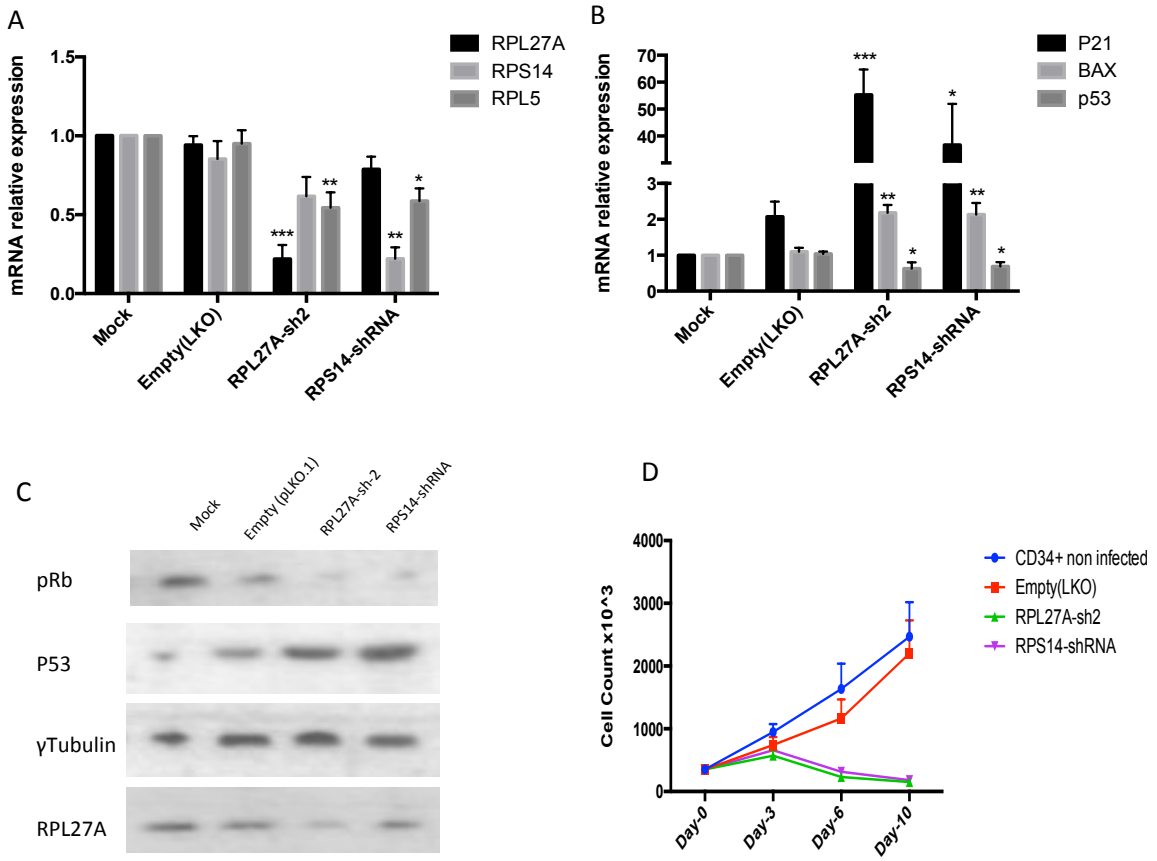

Figure 5.3: *RPL27A* knockdown in CD34+ form PBMC'S

A) RNA samples collected on day 6 (post infection) and the mRNA expression of *RPL27A, RPS14* and *RPL5,* relative to *GAPDH,* was measured by quantitative real time PCR. It showed a significant reduction of *RPL27A* and *RPL5,* in cells expressing *RPL27A-shRNA* and *RPS14, and* and *RPL5* reduction in cells expressing *RPS14 shRNA* **B)** The mRNA expression of *p53 and its* target genes *p21* and *Bax,* relative to *GAPDH,* was measured by quantitative real time PCR, and showed a reduction in *p53* expression, with increased expression of *p21* and *Bax* in cells with depleted *RPL27A* and *RPS14.* All qRT-PCR results were compared to cells infected with empty vector. **C)** Protein extracts were collected on day 6 from non-infected cells and cells infected with empty vector and shRNAs, against *RPL27A* and *RPS14*. They were analysed on 4–12% polyacrylamide gels, and probed with antibodies to detect RPL27A, p53 and pRb. Equal protein loading per well was determined by Y tubulin loading control. The depletion of *RPL27A* and *RPS14* resulted in p53 induction and hypophosphorylation of pRB. **D)** Cells were counted every 48 h and the result showed a reduction in cell number by day 4, reaching massive cell death by day 10 in cells infected with *RPL27A*-sh2 and *RPS14*-shRNA, compared with control, empty vector and non-infected cells. The presented data represents 4 independent experiments. Error bars represent the mean ± S.D.

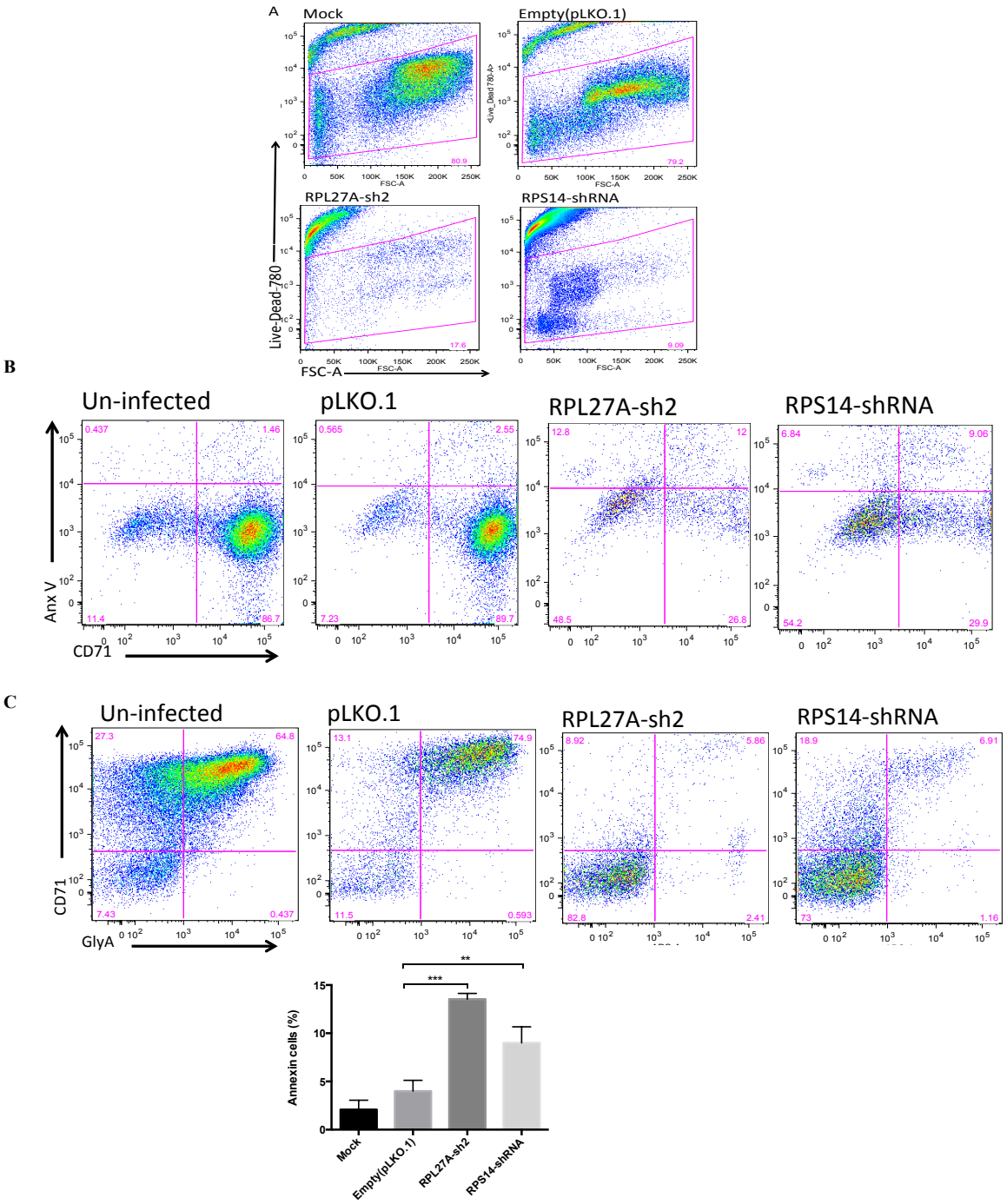

Figure 5.4: *RPL27A* knockdown in normal CD34+ from PBMCs blocks HSC proliferation and differentiation.

Cells were harvested on day 10–11 after infection, for flow cytometry analysis. **A-B)** Cells were labelled with a mixture of conjugated antibodies including live/dead staining (780), immature erythroid (CD71) and mature erythroid (GlyA). Cells expressing *RPL27A-shRNA* and *RPS14* shRNA showed a significant reduction in erythroid cells. **C)** Staining with Annexin V and CD71 showed a significant increase in apoptosis in erythroid positive cells, and in cells with depleted *RPL27A* and *RPS14*. Data represents 4 independent experiments, bars represent the mean ±SEM.

5.4.3 Methylcellulose colony assay

At day 6, after retroviral infection, and day 5 from puromycin selection, cultured cells were plated in methylcellulose medium containing Epo, and supplemented with penicillin /streptomycin in a 6-well plate. The plated cell suspension, which was at the end of pre-EPO culture, was made from 2000 cells (mock and control cells) suspended in 3 ml of methylcellulose medium per well, and 5000 cells (*RPL27A* and *RPS14* shRNA infected cells) suspended in 3 ml of methylcellulose medium per well. One well was filled with water, in order to preserve humidity and avoid the medium drying out. Also, the plate was placed in a glass container, filled with water, and incubated in a humidified incubator with 5% CO_2 at 37°C. Colony formation was determined after 14–16 days of culture. Evaluation of the colony was performed under the supervision of Dr. Nigel Westwood. Expression of *RPL27A* shRNA and *RPS14* shRNA severely decreased the formation of all haematopoietic colonies (Figure 5.5). The decrease in erythroid colonies (BFU-E) was more dramatic, with statistically significant *p* value less than 0.005 for *RPL27A* and *RPS14* deficient cells, compared to the control and non-infected cells (n=4). The suppression of the other haematopoietic colonies (CFU-GM) was also significant, with statistically significant p value less than 0.005 in *RPL27A* and *RPS14* shRNA expressing cells. The reduction of erythroid colony formation in *RPL27A* shRNA expressing cells was more than the decrease in the other colonies, with statistically significant p of less than 0.05. A similar observation was made with similar significance for *RPS14* shRNA expressing cells. The *p* values were determined by a two-tailed Student's *t* test.

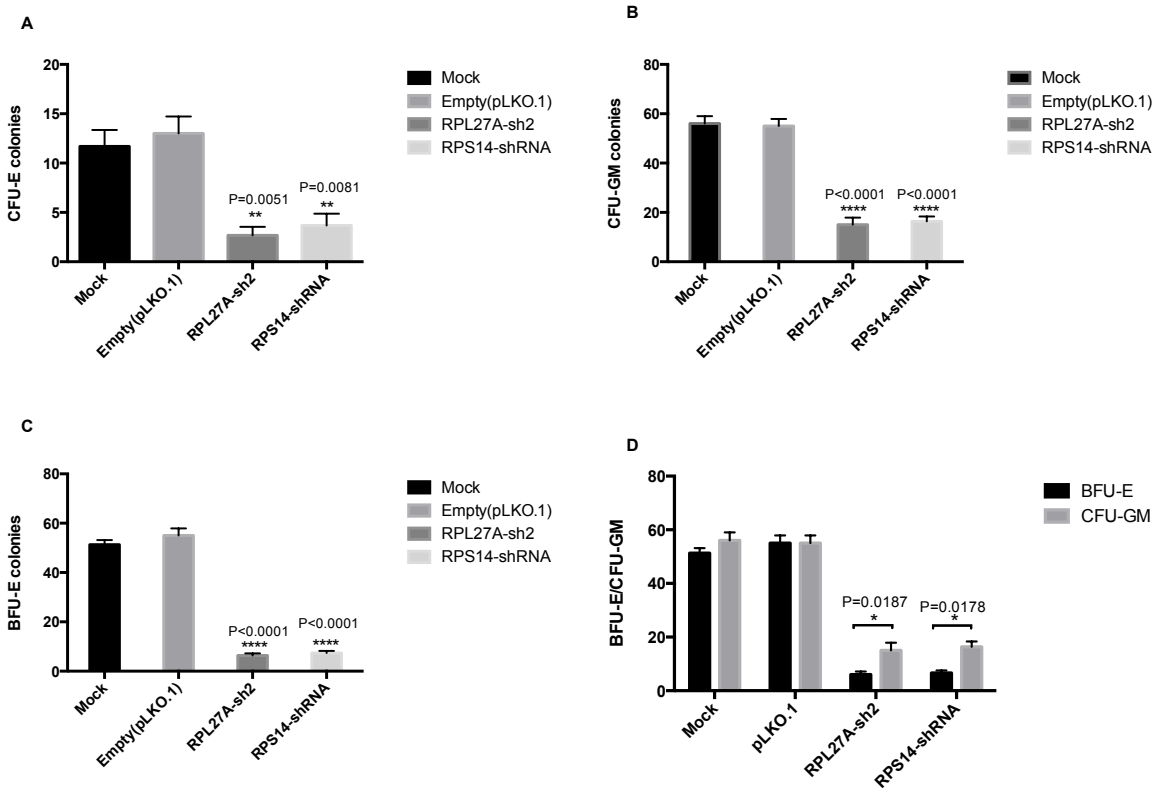

Figure 5.5: Colony forming ability of cells with depleted *RPL27A* and *RPS14*.

A-D) Frequencies of progenitor cells in methylcellulose assay from cells infected with control, *RPL27A*-shRNA and *RPS14* shRNA showed significant reduction of erythroid and granulocyte/macrophage colonies in *RPL27A* and *RPS14* deficient cells. CFU-E: colony forming unit -erythroid, BFU-E: burst forming unit CFU-GM: Colony forming unit-granulocyte/macrophage colonies. Data represents 4 independent experiments, bars represent the mean ±SEM.

5.5 Discussion

Decreases in various types of ribosomal proteins have been implicated in the reduction of mature ribosomes, which inhibits the translation of proteins essential to cellular processes like erythropoiesis. This effect could be a result of the extra ribosomal function of certain ribosomal proteins, which activate the p53 pathway and lead to the development of anaemia (reviewed in (Narla *et al.* 2010). As demonstrated in the previous chapter, *RPL27A* knockdown in human cell lines is associated with p53 activation, and induces the downstream effect of *p53* activation. Thus, chapter I investigated whether *RPL27A* knockdown in normal CD34+ cells has a similar effect on p53, and if that effect consequently blocks erythroid proliferation and differentiation, in a similar way to other ribosomal protein genes.

The knockdown of *RPL27A* in normal CD34+ resulted in a marked reduction of RPL27A expression, at both the transcriptional and post-transcriptional levels, in both BM and PB mononuclear CD34+ cells. The knockdown experiment, which was performed on the BM CD34+, was a preliminary experiment, which showed an induction of p53 and p53 targets, but was only on one sample. The challenges involved in obtaining more BM CD34+ samples led to the repetition of the same set of experiments on circulating CD34+ from peripheral blood. The knockdown experiment was repeated and validated on normal CD34+, isolated from four different leukocyte cones.

The reduction of *RPL27A* using retrovirally-expressed shRNA in cultured CD34+ cells recapitulated the findings observed in human cell lines.

The knockdown of *RPL27A* was approximately more than 70%, according to the qRT-PCR and western blot analysis. Due to the high expansion rate in CD34+ from blood, it was possible to perform *RPS14* knockdown and use it as a positive control. The knockdown of *RPS14* was also more than 70%, according to the qRT-PCR. *RPL27A* and *RPS14* depletion increased p53 expression at the post-transcriptional level only. The lack of *p53* induction at mRNA level could be the consequence of global inhibition of translation, due to impaired ribosome biogenesis. According to the results from the previous chapter, reduction of *RPL27A* by more than 50% leads to a decrease in the 60S subunit, which causes the disruption of ribosome biogenesis and affects protein translation. Even though the knockdown experiment on CD34+ from BM was only conducted on one sample, it showed

upregulation of *p53*. Of note is the fact that a lack of *p53* induction, at the mRNA level, has been observed in another study (Dutt *et al.* 2011).

The knockdown effect on the p53 pathway was confirmed by significant increases in *p21* and *Bax* expression. Furthermore, the reduction of *RPL27A* had a dramatic effect on cell viability and proliferation, which can also be attributed to either ribosomal stress, or to p53 activation induced by perturbed ribosome biogenesis. These observations were also seen with *RPS14* knockdown, and were in agreement with other studies, which link ribosomal haploinsufficiency to p53 activation (Ebert *et al.* 2008, Pellagatti *et al.* 2010). However, a p53 independent effect was reported in recent studies on mouse embryonic stem cells and zebra fish embryos, with depleted ribosomal proteins, which have developed anaemia regardless of p53 status. This supports the p53 independent mechanism associated with anaemia in DBA and 5q- syndrome (Teng *et al.* 2013, Narla *et al.* 2014, Singh *et al.* 2014).

Due to the high knockdown level, the number of *RPL27A* and *RPS14* deficient cells was markedly decreased, making further screening difficult. Therefore, cell cycle marker Retinoblastoma protein RB was examined by western blot to show the knockdown effect on the cell cycle, based on the phosphorylation status of RB. The knockdown showed a significant reduction in the phosphorylated RB (hypophosphorylation), which indicates that arrest in the cell cycle is due to *RPL27A* reduction. This is consistent with the haematopoietic phenotype of DBA and 5q-MDS.

Furthermore, *RPL27A* depletion is associated with a significant reduction in *RPL5*, which belongs to the same ribosomal subunit. This emphasises the correlation between ribosomal insufficiency and reduced cellularity. The role of inhibition of cellular proliferation, due to *RPL5* reduction, is discussed in chapter 4. The effect on proliferation could be a direct impact of *RPL27A* depletion, or indirectly, *via RPL5* reduction. Of note, RPL27A showed possible interaction with RPL5 *via* co-immunoprecipitation (Section 4.4.1), which could explain the effects of *RPL27A* depletion on *RPL5* expression. This observation is in agreement with the effects of *RPS14* reduction on *RPL5,* as observed in this project and in other studies, which have shown that *RPS14* knockdown reduces the expression of other ribosomal proteins, in addition to its direct effect on genes involved in translation (Pellagatti *et al.* 2008).

After 10 days under erythroid differentiation conditions, the knockdown of *RPL27A* impaired the proliferation of HSCs. The effect on erythroid lineage was more dramatic, compared to myeloid/megakaryocytic lineages. Both *RPL27A* and *RPS14* shRNA decreased erythroid differentiation, relative to myeloid and megakaryocytic differentiation. The reduction of erythroid differentiation was primarily caused by the reduction of erythroid proliferation, which was assessed by counting the cells during the culture. This is similar to defects caused by the knockdown of other ribosomal protein genes, in normal haematopoietic progenitor cells and in zebra fish models.

The reduction of *RPL27A and RPS14* did not show any increase in the ratio of immature to mature erythroid cells, which contradicts the results observed in *RPS14,* in Ebert's study. This can be explained by the dramatic increase in cell death, which mainly affects erythroid cells. Only a small percentage of the FACS analysed cells were erythroid positive cells.

Interestingly, in a study conducted by da Cunha *et a*l, on the gene expression analysis of genes involved in erythroid differentiation, researchers reported upregulation of *RPL27A* during erythroid differentiation (da Cunha *et al.* 2010). They performed large-scale gene expression, using SAGE, on blood from normal donors, which was cultured in medium supplemented with EPO. The analysed samples collected at three time points, 0 hrs, 192 hrs and 336 hrs, showed an upregulation of *RPL27A* which reached a maximum at 192 h, then the expression reduced at 336 hrs. Thus, *RPL27A* is important for early erythroid differentiation, and a deficiency blocks erythroid differentiation. In accordance with this finding is another study by Ebert, which shows that the expression levels of *RPS19* during erythroid differentiation *in vitro*, and their expression data, demonstrates a similar effect on *RPL27A* expression (Ebert *et al.* 2005). *RPS19* and *RPL27A* expression were high in primitive cells, and decreased gradually with cell maturation to erythrocyte. Thus, the proliferative defect caused by *RPL27A* insufficiency may occur in the primitive hematopoietic progenitors, similar to *RPS19* when deficiency decreases the proliferation rate in progenitor cells.

Also, the colony assay confirmed that *RPL27A* deficiency blocks erythroid and other haematopoietic colony formations, and is in agreement with the observation of RPL27A knockdown in sooty foot ataxia mouse. *In vivo*, homozygous mutations were embryonically lethal, and as explained in the previous chapter, heterozygous mutation in sooty foot ataxia mouse led to a reduction in the level of *RPL27A* (on average, between 20–30%), and

affected the HSC proliferation, but in a less aggressive way than the effects observed in this study.

The severity of *RPL27A* deficiency on cell survival is mainly due to the knockdown level. The shRNA used in this study decreased *RPL27A* expression to a very low level, and this primarily affected ribosomal maturation and led to disruption of ribosome biogenesis. This finding is in agreement with another (Flygare *et al.* 2005). It showed that the effect of *RPS19* knockdown in cultured human CD34+ on erythropoiesis and myelopoiesis is selectively related to the knockdown level. Additionally, in the current study, different *RPL27A* shRNA (*RPL27A* sh4) was used to reduce expression levels to 20-30%. Unfortunately, all of the performed experiments failed to induce significant changes in the expression level of *RPL27A*. Also, differences in the knockdown effect between studies could be attributed to multiple variables other than the level of ribosomal protein insufficiency; for example, species effect and *in vivo* haematopoietic requirements, and culture conditions within *in vitro* experiments.

RPL27A loss is similar to other ribosomal proteins in its effect on p53. As such, it can be postulated that a similar effect would be observed in other BM diseases. In this respect, the reduction of *RPL27A* may contribute to identifying new target genes involved in defects in erythropoiesis.

Taken together with the previous studies, our work suggests the importance of alterations in ribosomal protein gene levels on the haematopoietic system. As *RPS14* is implicated in the 5q- phenotype, miRNAs are also critical mediators of certain clinical features of 5q- disease, such as the involvement of *miR-145* and *miR-146a* in 5q- syndrome. Thus, to get an insight into the relative contribution of *miR-595* and *RPL27A* in MDS, with chromosome 7 abnormalities or other MDS subtypes, the expression levels of *miR-595* and its target *RPL27A* were examined in MDS with monosomy 7, and compared with other MDS subtypes, as explained in the following chapter.

Chapter 6: *RPL27A* and *miR-595* expression in MDS patients

6.1 Introduction

Whilst the molecular pathogenesis of MDS is slowly being unravelled, its disease heterogeneity makes it challenging to identify all of the key molecular lesions. However, the clinical and biological features, including cytogenetic and molecular abnormalities, have guided researchers in defining disease stages, prognosis, and risk to AML progression (Greenberg 2006). The miRNA and gene expression profiles in AML/MDS have helped to segregate patients into risk categories, which provide important diagnostic and prognostic information for disease classifications.

It is plausible that miRNAs play a critical role in the pathogenesis of a heterogeneous disease like MDS. As described in Chapter 1, there are several studies, which offer insights into the importance of miRNAs in the pathogenesis of MDS, such as miR-145 and miR-146a and its association with the development of 5q- phenotype (Starczynowski *et al.* 2010a). Monosomy 7 or 7q deletion is the second most frequent chromosomal abnormality in MDS, and identifies a subgroup of patients with a poor prognosis (Yunis *et al.* 1986). The commonly deleted regions in MDS on chromosome 7 are 7q36 and 7q22. No recurrent mutations or haploinsufficiency of genes localised to the deleted regions of chromosome 7 have been consistently linked with the disease phenotype. Thus, it is important to examine the expression of miR-595, localised to 7q36.3 in MDS patients with monosomy 7, and compare it with MDS patients with a normal karyotype.

A lack of recurrent somatic mutations in 40 genes localised to the deleted region of 5q led investigators to pursue the role of alternate mechanisms for disease phenotype, and eventually led to the concept of haploinsufficiency; *i.e.* the effect of gene dosage (Ebert *et al.* 2008). The strong link between ribosomal haploinsufficiency and 5q- syndrome, coupled with our data linking miR-595 (localised to 7q36) and its target *RPL27A* (11p.15), led us to examine the expression of *RPL27A* on MDS patients, particularly MDS patients with -7/7q-.

.

6.2 Aim

- Investigate the expression level of *miR-595* in MDS patients with -7/7q- and compare with normal control and other MDS subtypes including MDS with normal karyotype and MDS with 5q-.
- Examine the expression level of *RPL27A* and other ribosomal protein genes (*RPS14* and *RPL5*) in MDS patients with -7/7q- and compare with normal control and other MDS subtypes including MDS with normal karyotype and MDS with 5q-.

6.3 Experimental design

6.3.1 Patients

The study comprised 31 BM (CD34+) samples from patients with MDS. Bone marrow CD34+ trizol stock was obtained from the King's College London Haemato-Oncology Tissue Bank, which is a Human Tissue Authority licenced research biobank (licence number 12223). The samples were collected, stored and used in accordance with donor consent given under the auspices of ethics approval, provided by the UK National Research Ethics Service (NRES) (approval reference 08/H0906/94).

The clinical and cytogenetic details are summarised in Table 6.1. Four normal CD34+ cells from viably frozen BM cells, were obtained from Lonza.

6.3.2 Quantitative RT-PCR

Total RNA was extracted using an RNeasy Mini kit, according to manufacturer protocols. To quantify miRNA expression, TaqMan MicroRNA Expression Assay was performed, as described in Section 2.3.10, and data was normalised to the endogenous control RNU6B, and relative expression was calculated according to the ΔΔCT method. *RPL27A* was amplified form patients cDNA, and the expression was determined according to the qRT-PCR protocol described in Section 2.3.10, and data normalised to *GAPDH,* and relative expression was calculated according to the ΔΔCT method. Statistical analysis was performed using GraphPad Prism 6 (GraphPad Software, SanDiego, CA, USA, http://www.graphPad.com).

Table 6.1: Patients characteristics

UPN	Karyotype	FAB	WHO	IPSS
1	45,XX,-7 [30]	RAEBt	AML	HR
2	45,XY,-7 [3]46,XY [5]	RAEB	RAEB-2	HR
3	45,-7	RAEB	RAEB-1	I-2
4	45,XX,-7[5],46 XX[15]	RAEB	RAEB-2	HR
5	45,XY,-7[9]/ 46,XY [1]	RA	RCMD	VH
6	45,XY,inv(3)(q21q26),-7 [9]/46,XY [1]	RAEB	RAEB-2	HR
7	46,XY,-7,+mar [4]/45,XY-7 [3]/46,XY [8]	RAEB	RAEB-1	HR
8	45,XY,-7 [17]/46,XY [3]	RA	RCMD	HR
9	46,XY,+Y,-7 [6]/46.XY [3]	RAEBt	AML	HR
10	45,XY,-7 [3]/46,XY [7]	RAEB	RAEB-2	VH
11	45,XY,-7[7]/46,XY[3]	sAML	sAML	H
12	LOH 7Q34-Q36.3	RAEB	RAEB-1	VH
13	COMPLEX	CMML	CMML	H
14	COMPLEX	RAEB	RAEB	H
15	COMPLEX	RA	RA	L
16	COMPLEX	AML	tAML	VH
17	COMPLEX	RAEB	RAEB-1	VH
18	COMPLEX	RAEBt	AML	VH
19	COMPLEX (7q22)	RA	RCMD	VH
20	46,XX,del(5)(q13q31) [9]/46,XX [11]	RA	5q	L
21	46,XX,del(5)(q22q35) [13]/46,XX[2]	RA	5q	L
22	46,XX,del(5)(q31q31) [15]	RA	5q	L
23	46,XX,del(5)(q11q31) [9]	RA	5q	VL
24	46,XY,del(5)(q13q33) [11]/46,XY [19]	RA	5q	L
25	46,XY,del(5)(q13q31) [30]	RAEB	RAEB-2	VH
26	46,XX,del(5)(q13q31) [20]	RA	5q	L
27	Nk	RAEB	RAEB-1	L
28	Nk	RA	RA	L
29	Nk	RAEB	RAEB-1	I
30	Nk	RARS	RCMD	L
31	Nk	RA	5q	L
*NK: normal karyotype				

6.4 Result

6.4.1 *miR-595* expression in patients with MDS

miR-595 expression was measured in CD34+ cells isolated from BM cells from 31 MDS patients and 4 normal controls. Reverse transcriptase reaction was carried out as explained in Section 2.3.10.1 using specific reverse transcriptase primers for *miR-595* and two endogenous controls (*RNU48* and *RNU6B*). Subsequently, qRT-PCR was performed in triplicate and carried out according to the protocol described in Section 2.3.10.2. Data was normalised with *RNUB6* and relative expression was calculated, relative to the normal control using ΔΔCT methods. Out of the 31 patients and 4 controls, *miR-595* was detected in 27 patients and 3 controls, and 4 patients and 1 control were excluded. From the 27 patients, 11 were with mono 7/7q-, 5 with del 5q, 6 with complex karyotype, and 5 with normal karyotype.

miR-595 was significantly downregulated in MDS with mono7/7q- MDS, compared with MDS with normal karyotype (P=0.0179). Furthermore, *miR-595* was also significantly downregulated in MDS with complex karyotype, compared with normal karyotype MDS (P=0.0205). Due to the small number of control samples, it was not possible to identify any distinct expression between MDS and a normal control. Also, there were no significant changes between 5q- and any other groups, as demonstrated in Figure 6.1-A. Data was analysed using nonparametric Kruskal-Wallis one-way analysis methods.

Furthermore, in order to identify a potential association between *miR-595,* and the clinical and biological characteristics of the disease, *miR-595* expression level was compared between high-risk (HR) MDS and low-risk (LR) MDS, according to IPSS scoring. The expression pattern of miR-595 was determined in 18 patients with HR-MDS compared to 9 patients with LR MDS. *miR-595* was overexpressed in 7 out of 9 patients with LR compared with 18 HR MDS. The differences in the expression were statistically significant (P=0.0009), as shown in Figure 6.1-B. Data was analysed using nonparametric Mann-Whitney tests.

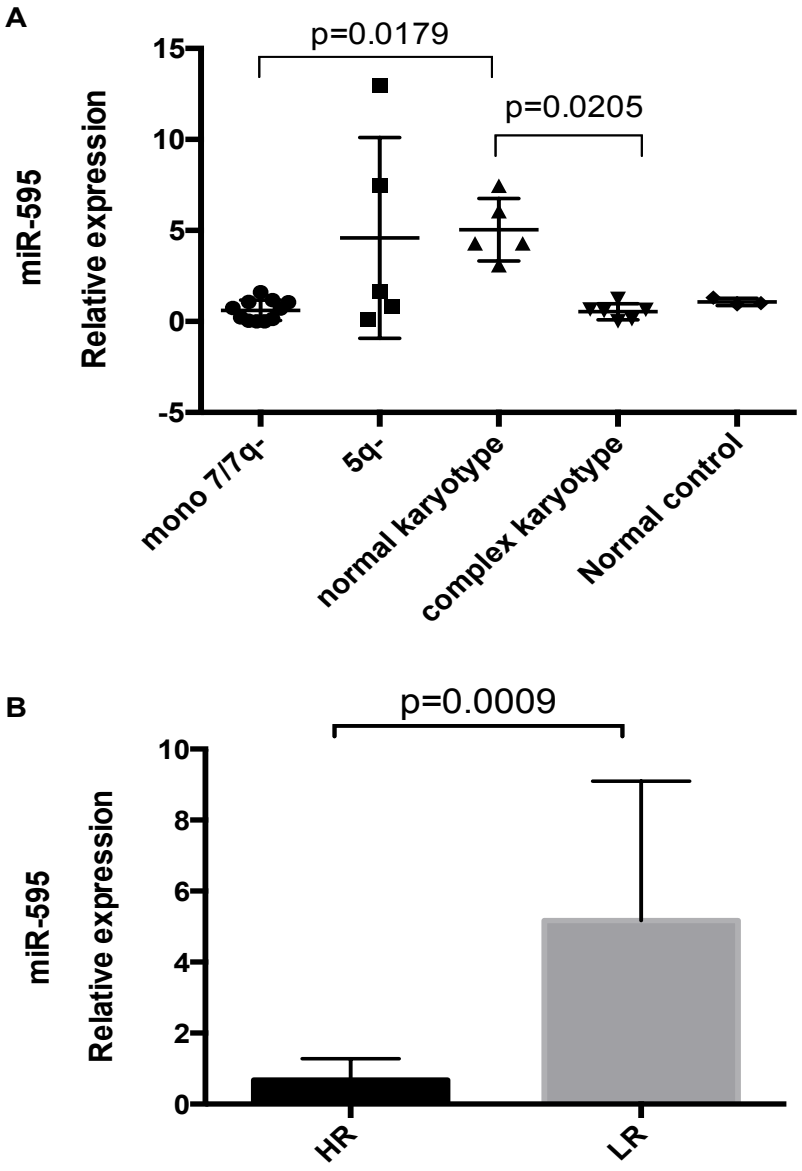

Figure 6.1:*miR-595* expressions in MDS patients.

miR-595 expression was analysed in BM CD34+ samples from 27 MDS patients. **A)** MDS patients were categorised according to their chromosomal abnormalities. From the 27 patients, 11 were with mono 7/7q-, 5 with del 5q, 6 with complex karyotype, and 5 with normal karyotype; significant differences in *miR-595* expression were determined between MDS with mono7/7q- and MDS with normal karyotype. Significant differences were also determined between MDS with complex karyotype and MDS with normal karyotype. **B)** The same samples were re-analysed according to their IPSS scoring (HR=18, LR=9), and *miR-595* was significantly upregulated in LR MDS, compared with HR MDS. *RNU6B* was used to normalise all samples, and relative expression was calculated using ΔΔCT method. Bars represent mean ±S.D.

6.4.2 *RPL27A* expression in patients with MDS

The relative expression of *RPL27A,* and other ribosomal proteins genes *RPS14* and *RPL5,* were determined in CD34+ BM samples, from 31 MDS patients and 4 controls. From the 31 patients, 11 were with mono 7/7q-, 7 with del 5q, 8 with complex karyotype, and 5 with normal karyotype. The transcription level of *RPL27A* and the other genes were determined by qRT-PCR, as explained in Section 2.3.10.4. Data was normalised with *GAPDH,* and the relative expression calculated using ΔΔCT methods. *RPL27A* was significantly upregulated in patients with mon7/7q-, compared with 5q- patients (*P*=0.0042). There were no significant changes with the other MDS groups, as well as no significant difference predicted between MDS patients and a normal control, as shown in Figure 6.2 A. Similarly, *RPS14* and *RPL5* were significantly upregulated in mono7/7q-, compared with 5q- MDS (*P*= 0.0012 and *P*= 0.0027, respectively). Also, significant downregulation of *RPS14* was detected in 5q- patient, compared with 3 normal controls. One was failed (*P*= 0.0108), and *RPL5* was significantly downregulated in MDS with 5q-, compared with MDS with a normal control (*P*= 0.0405), as shown in Figure 6.2.B and C. Data was analysed using nonparametric Kruskal-Wallis one-way analysis. RPL5 analysis in 4 normal controls failed in two instances, and therefore normal controls were excluded from the analysis.

Interestingly, attempts to determine the expression of *RPL27A* in MDS, according to IPSS scoring, have shown a relatively high expression of *RPL27A* in (19) HR MDS versus (12) LR-MDS (*P*= 0.027), as demonstrated in Figure 6.2 D. This data also demonstrates an increased *RPS14* expression in HR- MDS patients, compared with LR-MDS (*P*= 0.027). No significant change was detected in *RPL5* expression between HR and LR- MDS, as shown in Figure 6.2 E and F. Data was analysed using nonparametric Mann-Whitney tests.

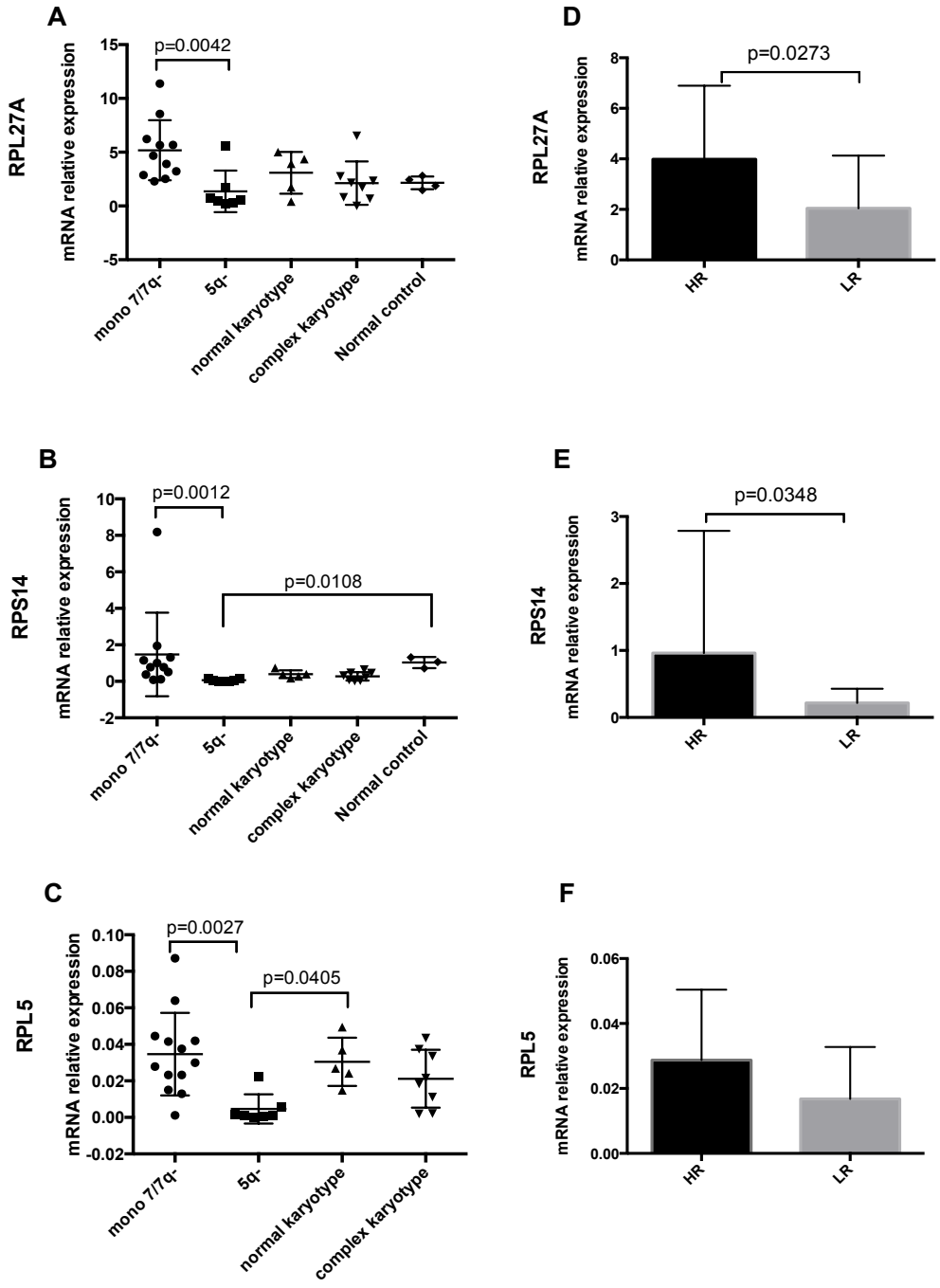

Figure 6.2: *RPL27A, RPS14 and RPL5* expression in MDS patients.

RPL27A, *RPS14* and *RPL5* expressions were determined in BM CD34+ samples from 31 MDS patients. A, B, C) MDS patients were categorised according to their chromosomal abnormalities. From the 31 patients, 11 were with mono 7/7q-, 7 with del 5q, 8 with complex karyotype, and 5 with normal karyotype, in addition to four normal control. Significant differences in the expression of RPL27A, RPS14 and RPL5 were determined between MDS with mono7/7q- and MDS with 5q-. Significant difference was also determined in RPS14 expression between MDS with 5q- and normal control. D, E, F) Samples were re-analysed, according to their IPSS scores (HR=19, LR=12), and RPL27A and RPS14 were significantly upregulated in HR MDS, compared with LR MDS. GAPDH was used to normalise all samples, and relative expression was calculated using ΔΔCT method. Bars represent mean ±S.D.

6.5 Discussion

There are various studies on gene expression and miRNA expression in the profiles of in MDS patients, which have increased our knowledge of MDS (Hofmann *et al.* 2002, Chen *et al.* 2004, Pellagatti *et al.* 2006, Sridhar *et al.* 2009, Vasikova *et al.* 2010, Dostalova Merkerova *et al.* 2011). In this PhD project, we focused on analysing the expression patterns of *miR-595* and *RPL27A,* because we anticipated that this analysis might provide new information relating to disease pathogenesis and development.

miR-595 expression level was examined in CD34+ cells obtained from 27 patients with MDS and 3 controls. Patients were classified according to their chromosomal abnormalities. As expected, *miR-595* was significantly downregulated in MDS with -7/7q-, compared with patients with normal karyotype. Interestingly, *miR-595* was also significantly downregulated in MDS with complex karyotype versus MDS with normal karyotype. This observation was further confirmed by the detection of significant downregulation of *miR-595* in HR-MDS, compared with LR-MDS. This significant contribution of *miR-595* in distinguishing between MDS patients is reported for the first time in this study. Comparison relative to normal control was not significant and is mainly due to the small number of control samples. Of not is the downregulation of *miR-595* in patients with complex karyotype without abnormalities in chromosome 7, particularly at q36.3 position. This could be attributed to the existence of other factors which control the expression of this miRNA, at this stage of the disease. For instance, *miR-595* downregulation can be attributed to epigenetic silencing of the gene which encodes this miRNA. Menigatti *et al.*'s study on early stage colorectal tumoriginesis, identified 56 miRNAs, including *miR-595,* that were re-expressed in normal colorectal mucosa and HT29 colorectal cancer cells after treatment with the DNA demethylating agent, 5-aza-2-deoxcytidine, and trichostain the histone deacytylase inhibitor (Menigatti *et al.* 2013). Thus, epigenetic regulation of this miRNA is possible primarily in association with mutations in epigenetic modifiers that are commonly seen in MDS such as *EZH2, TET2, IDH1,2*, *DNMT3A, MLL* and *ASXL1;* reviewed in (Shih *et al.* 2012). Interestingly, Mendler *et al.* identified an upregulation of *miR-595* in AML patients with normal cytogenetic karyotype and with mutation in *RUNX1,* and it might explain the exceptional upregulation of *miR-595* in some cases with monosomy 7 or complex karyotype, which might have

mutations that control the expression of this miRNA (Mendler *et al.* 2012). Thus, miR-595 may hold valuable implications for leukomogenesis, which is still shrouded by uncertainty.

On the other hand, the expression levels of *RPL27A*, *RPS14* and *RPL5* were measured in 31 MDS patients, classified according to their cytogenetic abnormalities. *RPL27A* was upregulated in MDS with -7/7q-, compared with 5q- MDS. Similarly *RPS14* and *RPL5* were significantly upregulated in MDS with chromosome 7 abnormalities, compared with 5q- MDS. Overexpression in *RPL27A* and *RPS14* was also determined in HR-MDS, compared with LR-MDS, but no significant difference was observed in *RPL5* expression between the two groups. The non-significant difference in *RPL27A* expression between MDS and the normal control could be attributed to the small number of control samples. However, *RPS14* was significantly low in 5q- MDS, compared with the normal control, and this is consistent with previous studies (Ebert *et al.* 2008, Pellagatti *et al.* 2008). Pellagatti et al. demonstrated that the expression profile of ribosomal and translation related gene in CD34+ of MDS patients identified 90% of the differentially expressed ribosomal proteins to be lower expressed in 5q- syndrome (Pellagatti *et al.* 2008).

In my study, 'low risk' MDS patients showed decreased expression of all investigated ribosomal proteins. This group of patients includes patients with del (5q) and with normal karyotype, and this observation is consistent with other studies, which show downregulation of ribosomal protein genes, including *RPL27A* in patients with 5q- and detection of upregulation in tMDS (Sridhar *et al.* 2009).

As shown in chapters 4 and 5, the downregulation of *RPL27A* is associated with *p53* induction and negatively regulated haematopoiesis, particularly erythroid proliferation and differentiation. Thus, the putative role of *RPL27A* is supported by the downregulation of *RPL27A* in LR MDS patients, including patients with 5q-, and this suggests the involvement of *RPL27A* downregulation in LR MDS.

The upregulation of *RPL27A* in patients with -7/7q- and HR-MDS is in agreement with other studies, which correlate the overexpression of ribosomal protein with disease aggressiveness and progression. Mendiburu *et al.* study was the first study to determine gene expression using serials of gene expression (SAGE) in MDS, particularly in patients with RAEB. They showed that 40% of the most expressed genes in RAEB belong to ribosomal genes, including *RPL27A*. The *RPL27A* was from the highest expressed gene in

RAEB, in addition to other ribosomal protein genes, including *RPS19* (Mendiburu *et al.* 2008). This implies possible functional similarities between *RPL27A* and *RPS19*, which are discussed in chapter 5, in terms of their expression in erythroid cells. This observation highlights the importance of *RPL27A* in RAEB, and its frequent association with -7/7q- abnormalities. Furthermore, Dorsam *et al.* showed that *HOXA9* regulates *RPL27A* expression, transient overexpression of *HOXA9* in haematopoietic stem cell resulted in upregulation of several genes including *RPL27A* (Dorsam *et al.* 2004). *HOXA9* overexpression recognised as a poor prognostic marker in MDS and AML patients and was detected in MDS patients with -7/7q- (Chen *et al.* 2004). This observation suggests that *RPL27A* overexpression could be similarly considered as a poor prognostic marker in MDS.

Thus, monosomy 7 or deletion 7q results in the downregulation of *miR-595,* and the upregulation of its target *RPL27A*. Despite the small sample size, and the relative heterogeneity of different disease stages, this data provides insights into a new miRNA, and its implication for disease mechanism *via* its regulation of the target protein, which was identified by a novel functional assay. These findings, if verified on larger cohort, could have a valuable impact on disease prognosis.

Chapter 7: General Discussion

7.1 Discussion

The importance of miRNAs and their implication in hematological disorders including MDS has been addressed by previous studies as described in the introduction.

The microRNAs recognised in 5q- syndrome, such as miR-145 and miR-146a have been associated with the development of the disease. However, in monosomy 7 there were no reported studies that have examined the role of miRNA expression in this MDS subtype. There are a small number of studies that focused on the deregulation of a few miRNAs located on chromosome 7 in relation to other subtypes of MDS, which was discussed in the Introduction Chapter. Therefore, the aim of my PhD was to examine one of the miRNAs on the q terminus of chromosome 7, which is miR-595, and apply an in-house developed functional assay to identify targets for this miRNA. The other aim of this project was to identify the biological function of the identified targets and their implication in the disease pathogenesis.

The available miRNA target prediction methods predict hundreds of target genes for a given miRNA of which a large percentage are false-positives. MicroRNAs can either degrade their mRNA target or cause inhibition of translation therefore target prediction based on expression profiling which will miss targets that are regulated by translational inhibition. Furthermore, these expression studies cannot discriminate cause from consequence. Therefore, a novel 'in-house' functional assay for microRNA target identification was used. This assay has the potential for rapid and specific detection of several targets in a single assay and will identify targets that are either regulated by mRNA degradation or translational inhibition.

The functional assay is based on introducing a cDNA library representing approximately 17,000 genes downstream of a TKzeo selectable marker providing both resistance to zeocin and sensitivity to GCV. The plasmid library was transduced into the MCF7 cell line, which does not express the mir-595 and was selected with zeocin resulting in cells that contain at least one member of the library. The cells resistant to zeocin were expanded and subsequently transfected with plasmid expressing *miR-595,* which also conferred puromycin resistance. For target identification, the transfected cells were selected with GCV which selects for cells in which mir-595 has downregulated a target gene from the library which also results in downregulation of Tkzeo. Resistant colonies were isolated and

DNA was extracted and the library genes were amplified by PCR. The amplified DNAs were analysed on agarose gel and bands of different sizes were isolated and sequenced. The sequencing result of 12 different bands identified 2 transcripts, *RPL27A, HSPA14, GRM5* and *SEC36*. I focused on ascertaining the function of *RPL27A* due to the association between previously identified ribosomal protein gene (RPS14) involved in the pathogenesis of 5q-, a subtype of MDS. Target validation confirmed that *RPL27A* is a target for miR-595; subsequently I tested the biological function of *RPL27A* using retroviral shRNA to knockdown *RPL27A*.

A previous report that studied *RPL27A* knockdown showed p53 accumulation in Sooty foot ataxia mice and these findings where confirmed in this PhD in a number of human cell lines. I measured the effect of *RPL27A* knockdown on day 6 post-infection and the knockdown resulted in downregulation of RPL27A at both transcriptional and translational levels by more than 70% for shRNA2 and a 40–50% reduction was achieved with shRNA-4. The knockdown of *RPL27A* increased the expression of p53 in different human cell lines and led to the induction of the p53 targets *p21* and *Bax*. As a control, *RPS14* knockdown was performed and a similar result was obtained. Another control was also examined which was *RPL5*, the knockdown of which did not cause any significant changes in the p53 expression.

In addition to p53 activation, induction of apoptosis and inhibition of cell proliferation was observed in all cell lines infected with *RPL27A* and *RPS14* shRNA.

The knockdown reduces cell proliferation and induces apoptosis which leads to >75% cell death within 6 days in a p53-dependent manner. However, the knockdown effect in p53 (null) cell lines also led to apoptosis but this was less marked in comparison to $p53^{+/+}$ cell lines. These results suggest that the observed induction of apoptosis in p53 null cells is due to mechanisms independent of p53 or is the result of a general defect in ribosome biogenesis due to *RPL27A* knockdown. To further investigate this possibility ribosome profiling was performed on cells infected with *RPL27A* and *RPS14* shRNA lentiviral vectors and compared to cells infected with control lentiviral vectors. Ribosome profiling experiments were performed in the MRC laboratory, University of Cambridge. Interestingly, the reduction of *RPL27A* reduced the large (60S) ribosomal subunit in HCT-116 cell lines (WT cells and null p53 cells). As expected, *RPS14* depletion was associated with reduction of the 40S subunit. To further validate the effect of *RPL27A* depletion on

ribosome biogenesis, nucleolar staining was performed using anti-fibrillarin antibody. The results showed a disruption in nucleolar staining and diffused fibrillarin in *RPL27A* shRNA expressing cells. These results showed the importance of *RPL27A* in the regulation of ribosome biogenesis and the subsequent effect on cellular proliferation and survival. Similar results were obtained in *RPS14* and *RPL5* depleted cells.

All the above described experiments were performed on day 6 post-infection and to verify the p53 dependent induction of apoptosis, some experiments were repeated at 48-hrs post-infection. The apoptosis and cell viability assays confirmed the p53-dependent effect because significant changes were only observed in cell lines that express p53 (HCT-116 and HEL). At the same time point (48-hr), ribosome profiling was performed and showed a reduction in the 60S subunit in cells with reduced *RPL27A* but the reduction in the 60S subunit was considerably less than what was observed on day 6.

To investigate whether *RPL27A* reduction activated p53 *via* its interaction with MDM2, a Co-IP- assay was performed which confirmed the interaction between RPL27A-MDM2 by the detection of MDM2 after pull-down with RPL27A antibody. However, detection of RPL27A in MDM2 pull down experiments was not conclusive due to the overlap with the light chain, which has a similar molecular weight as RPL27A. Furthermore, RPL27A pull down experiments showed that it also interacts with RPL5.

Further functional studies were performed on the cell lines to identify the effect of *RPL27A* overexpression on cellular processes. The ectopic expression of *RPL27A* did not show any effect on the cell cycle or the p53 pathway. This is in accordance with previous studies that showed the association of *RPL27A* overexpression with tumor aggressiveness, however, the levels of overexpression achieved in my experiments was only 2 fold and therefore it is not possible to draw firm conclusions as yet.

Haploinsufficiency of ribosomal protein genes has been linked to the development of a haematological phenotype mainly through their effect on erythropoiesis. Therefore I carried out experiments to examine whether there is any association between *RPL27A* deficiency and erythropoiesis.

RPL27A knockdown on normal hematopoietic progenitor cells (CD34+) showed a marked reduction in the erythroid lineage and moderate reduction in other lineages. This was associated with p53 activation as measured by *p21* and *Bax* up-regulation and a reduction in

cell proliferation. These results were similar to the effects seen with *RPS14* knockdown which was investigated similarly at the same time and emphasizes the important role of *RPL27A* in the haematopoiesis

To identify the association of *miR-595* and *RPL27A* with MDS pathogenesis, their expression levels were measured in BM CD34+ from MDS patients with-7/7q- and other MDS subtypes. The results showed that *miR-595* was downregulated in -7/7q- MDS and MDS with complex karyotype as compared to MDS with normal karyotype. On the other hand, the expression level of *RPL27A* was downregulated in MDS with normal karyotype. In marked contrast as expected the *RPL27A* expression was upregulated in MDS with -7/7q-. The data was reanalysed according to the IPSS score and the results confirmed the downregulation of *miR-595* in HR-MDS versus LR-MDS and up-regulation of *RPL27A* in HR-MDS versus LR-MDS. These findings may be of importance when considering ribosomal protein deficiency as a possible prognostic tool in low risk MDS.

Despite the heterogeneity of the disease, the biological and clinical insights into ribosomal insufficiency and microRNA deregulation will manifest certain prognostic and diagnostic biomarkers that will help better understand the molecular pathogenesis of MDS and will guide the improvements in the therapy of these disease.

7.2 Possible Future Experiments

The results of this study raise interesting questions, which can be addressed in future studies.

- To investigate the contribution of other miRNAs located on chromosome 7 especially 7q.
- To identify the mechanistic involvement of RPL27A on the MDM2-p53 loop. Determine whether RPL27A interacts directly with MDM2 or via other auxiliary proteins.
- To assess whether *RPS14* overexpression rescues the 5q- phenotype and can the overexpression of *RPL27A* in LR MDS achieve the same? .
- The results presented in Chapter 6 showed an interesting association of *miR-595* and *RPL27A* expression with MDS with different chromosomal subtypes of MDS.

However, the data was based on a small sample size and needs confirmation in a larger cohort of patient samples.

- The regulation of *miR-595* seems to depend on the epigenetic status as seen in other diseases. Therefore, it is necessary to examine the methylation status in del7q with intact q36.3, where *miR-595* is localised. This could identify important epigenetic mechanism in HR-MDS patients with or without abnormalities of chromosome 7 .

References

Alexiou, P., M. Maragkakis, G. L. Papadopoulos, M. Reczko and A. G. Hatzigeorgiou (2009). "Lost in translation: an assessment and perspective for computational microRNA target identification." Bioinformatics **25**(23): 3049-3055.

Almeida, M. I., R. M. Reis and G. A. Calin (2011). "MicroRNA history: discovery, recent applications, and next frontiers." Mutation research **717**(1-2): 1-8.

Ambros, V. (2004). "The functions of animal microRNAs." Nature **431**(7006): 350-355.

Anderson, S. J., J. P. Lauritsen, M. G. Hartman, A. M. Foushee, J. M. Lefebvre, S. A. Shinton, . . . D. L. Wiest (2007). "Ablation of ribosomal protein L22 selectively impairs alphabeta T cell development by activation of a p53-dependent checkpoint." Immunity **26**(6): 759-772.

Badhai, J., A. S. Frojmark, H. R. Razzaghian, E. Davey, J. Schuster and N. Dahl (2009). "Posttranscriptional down-regulation of small ribosomal subunit proteins correlates with reduction of 18S rRNA in RPS19 deficiency." FEBS letters **583**(12): 2049-2053.

Baek, D., J. Villen, C. Shin, F. D. Camargo, S. P. Gygi and D. P. Bartel (2008). "The impact of microRNAs on protein output." Nature **455**(7209): 64-71.

Baltimore, D., M. P. Boldin, R. M. O'Connell, D. S. Rao and K. D. Taganov (2008). "MicroRNAs: new regulators of immune cell development and function." Nature immunology **9**(8): 839-845.

Barkic, M., S. Crnomarkovic, K. Grabusic, I. Bogetic, L. Panic, S. Tamarut, . . . S. Volarevic (2009). "The p53 tumor suppressor causes congenital malformations in Rpl24-deficient mice and promotes their survival." Mol Cell Biol **29**(10): 2489-2504.

Barlow, J. L., L. F. Drynan, D. R. Hewett, L. R. Holmes, S. Lorenzo-Abalde, A. L. Lane, . . . A. N. McKenzie (2010). "A p53-dependent mechanism underlies macrocytic anemia in a mouse model of human 5q- syndrome." Nat Med **16**(1): 59-66.

Bartel, D. P. (2004a). "MicroRNAs: genomics, biogenesis, mechanism, and function." Cell **116**(2): 281-297.

Bartel, D. P. (2009). "MicroRNAs: target recognition and regulatory functions." Cell **136**(2): 215-233.

Bartel, D. P. and C. Z. Chen (2004b). "Micromanagers of gene expression: the potentially widespread influence of metazoan microRNAs." Nat Rev Genet **5**(5): 396-400.

Bazzoni, F., M. Rossato, M. Fabbri, D. Gaudiosi, M. Mirolo, L. Mori, . . . M. Locati (2009). "Induction and regulatory function of miR-9 in human monocytes and neutrophils exposed to proinflammatory signals." Proc Natl Acad Sci U S A **106**(13): 5282-5287.

Bei, L., Y. Lu and E. A. Eklund (2005). "HOXA9 activates transcription of the gene encoding gp91Phox during myeloid differentiation." J Biol Chem **280**(13): 12359-12370.

Beitzinger, M., L. Peters, J. Y. Zhu, E. Kremmer and G. Meister (2007). "Identification of human microRNA targets from isolated argonaute protein complexes." RNA biology **4**(2): 76-84.

Bejar, R. (2014). "Clinical and genetic predictors of prognosis in myelodysplastic syndromes." Haematologica **99**(6): 956-964.

Bejar, R., K. Stevenson, O. Abdel-Wahab, N. Galili, B. Nilsson, G. Garcia-Manero, . . . B. L. Ebert (2011). "Clinical effect of point mutations in myelodysplastic syndromes." N Engl J Med **364**(26): 2496-2506.

Bennett, J. M., R. D. Brunning and J. W. Vardiman (2002). "Myelodysplastic syndromes: from French-American-British to World Health Organization: a commentary." Blood **99**(8): 3074-3075.

Bennett, J. M., R. Komrokji and P. Kouides (2004). The myelodysplastic syndromes. Clinical oncology. M. D. Abeloff, J. O. Armitage and J. E. Niederhuber. Philadelphia, Churchill Livingstone**:** xxiv, 3205 p.

Bentwich, I., A. Avniel, Y. Karov, R. Aharonov, S. Gilad, O. Barad, . . . Z. Bentwich (2005). "Identification of hundreds of conserved and nonconserved human microRNAs." Nature genetics **37**(7): 766-770.

Bhat, K. P., K. Itahana, A. Jin and Y. Zhang (2004). "Essential role of ribosomal protein L11 in mediating growth inhibition-induced p53 activation." EMBO J **23**(12): 2402-2412.

Borgstrom, G. H., L. Teerenhovi, P. Vuopio, A. de La Chapelle, H. Van den Berghe, L. Brandt, . . . A. A. Sandberg (1980). "Clinical implications of monosomy 7 in acute nonlymphocytic leukaemia." Cancer genetics and cytogenetics **2**: 115-126.

Boria, I., E. Garelli, H. T. Gazda, A. Aspesi, P. Quarello, E. Pavesi, . . . I. Dianzani (2010). "The ribosomal basis of Diamond-Blackfan Anemia: mutation and database update." Hum Mutat **31**(12): 1269-1279.

Boultwood, J., A. Pellagatti, H. Cattan, C. H. Lawrie, A. Giagounidis, L. Malcovati, . . . J. S. Wainscoat (2007). "Gene expression profiling of CD34+ cells in patients with the 5q- syndrome." Br J Haematol **139**(4): 578-589.

Bousquet, M., C. Quelen, R. Rosati, V. Mansat-De Mas, R. La Starza, C. Bastard, . . . P. Brousset (2008). "Myeloid cell differentiation arrest by miR-125b-1 in myelodysplastic syndrome and acute myeloid leukemia with the t(2;11)(p21;q23) translocation." The Journal of experimental medicine **205**(11): 2499-2506.

Brennecke, J., A. Stark, R. B. Russell and S. M. Cohen (2005). "Principles of microRNA-target recognition." PLoS Biol **3**(3): e85.

Brodersen, P. and O. Voinnet (2009). "Revisiting the principles of microRNA target recognition and mode of action." Nature reviews. Molecular cell biology **10**(2): 141-148.

Bruchova, H., M. Merkerova and J. T. Prchal (2008). "Aberrant expression of microRNA in polycythemia vera." Haematologica **93**(7): 1009-1016.

Budkevich, T. V., A. V. El'skaya and K. H. Nierhaus (2008). "Features of 80S mammalian ribosome and its subunits." Nucleic Acids Res **36**(14): 4736-4744.

Caldarola, S., M. C. De Stefano, F. Amaldi and F. Loreni (2009). "Synthesis and function of ribosomal proteins--fading models and new perspectives." FEBS J **276**(12): 3199-3210.

Calin, G. A., C. D. Dumitru, M. Shimizu, R. Bichi, S. Zupo, E. Noch, . . . C. M. Croce (2002). "Frequent deletions and down-regulation of micro- RNA genes miR15 and miR16 at 13q14 in chronic lymphocytic leukemia." Proc Natl Acad Sci U S A **99**(24): 15524-15529.

Calin, G. A., M. Ferracin, A. Cimmino, G. Di Leva, M. Shimizu, S. E. Wojcik, . . . C. M. Croce (2005). "A MicroRNA signature associated with prognosis and progression in chronic lymphocytic leukemia." N Engl J Med **353**(17): 1793-1801.

Calin, G. A., C. Sevignani, C. D. Dumitru, T. Hyslop, E. Noch, S. Yendamuri, . . . C. M. Croce (2004). "Human microRNA genes are frequently located at fragile sites and genomic regions involved in cancers." Proc Natl Acad Sci U S A **101**(9): 2999-3004.

Chamuleau, M. E., T. M. Westers, L. van Dreunen, J. Groenland, A. Zevenbergen, C. M. Eeltink, . . . A. A. van de Loosdrecht (2009). "Immune mediated autologous cytotoxicity against hematopoietic precursor cells in patients with myelodysplastic syndrome." Haematologica **94**(4): 496-506.

Chen, C. Z., L. Li, H. F. Lodish and D. P. Bartel (2004). "MicroRNAs modulate hematopoietic lineage differentiation." Science **303**(5654): 83-86.

Chen, C. Z. and H. F. Lodish (2005). "MicroRNAs as regulators of mammalian hematopoiesis." Seminars in immunology **17**(2): 155-165.

Chen, D., Z. Zhang, M. Li, W. Wang, Y. Li, E. R. Rayburn, . . . R. Zhang (2007). "Ribosomal protein S7 as a novel modulator of p53-MDM2 interaction: binding to MDM2, stabilization of p53 protein, and activation of p53 function." Oncogene **26**(35): 5029-5037.

Chen, G., W. Zeng, A. Miyazato, E. Billings, J. P. Maciejewski, S. Kajigaya, . . . N. S. Young (2004). "Distinctive gene expression profiles of CD34 cells from patients with myelodysplastic syndrome characterized by specific chromosomal abnormalities." Blood **104**(13): 4210-4218.

Cheng, A. M., M. W. Byrom, J. Shelton and L. P. Ford (2005). "Antisense inhibition of human miRNAs and indications for an involvement of miRNA in cell growth and apoptosis." Nucleic Acids Res **33**(4): 1290-1297.

Chiang, H. R., L. W. Schoenfeld, J. G. Ruby, V. C. Auyeung, N. Spies, D. Baek, . . . D. P. Bartel (2010). "Mammalian microRNAs: experimental evaluation of novel and previously annotated genes." Genes Dev **24**(10): 992-1009.

Chigrinova, E., M. Mian, Y. Shen, T. C. Greiner, W. C. Chan, J. M. Vose, . . . F. Bertoni (2011). "Integrated profiling of diffuse large B-cell lymphoma with 7q gain." Br J Haematol **153**(4): 499-503.

Choesmel, V., D. Bacqueville, J. Rouquette, J. Noaillac-Depeyre, S. Fribourg, A. Cretien, . . . P. E. Gleizes (2007). "Impaired ribosome biogenesis in Diamond-Blackfan anemia." Blood **109**(3): 1275-1283.

Choesmel, V., S. Fribourg, A. H. Aguissa-Toure, N. Pinaud, P. Legrand, H. T. Gazda and P. E. Gleizes (2008). "Mutation of ribosomal protein RPS24 in Diamond-Blackfan anemia results in a ribosome biogenesis disorder." Human molecular genetics **17**(9): 1253-1263.

Choong, M. L., H. H. Yang and I. McNiece (2007). "MicroRNA expression profiling during human cord blood-derived CD34 cell erythropoiesis." Exp Hematol **35**(4): 551-564.

Choong, M. L., H. H. Yang and I. McNiece (2007). "MicroRNA expression profiling during human cord blood-derived CD34 cell erythropoiesis." Exp Hematol **35**(4): 551-564.

Cimmino, A., G. A. Calin, M. Fabbri, M. V. Iorio, M. Ferracin, M. Shimizu, . . . C. M. Croce (2005). "miR-15 and miR-16 induce apoptosis by targeting BCL2." Proc Natl Acad Sci U S A **102**(39): 13944-13949.

Cmejla, R., J. Cmejlova, H. Handrkova, J. Petrak and D. Pospisilova (2007). "Ribosomal protein S17 gene (RPS17) is mutated in Diamond-Blackfan anemia." Hum Mutat **28**(12): 1178-1182.

Cordoba, I., J. R. Gonzalez-Porras, B. Nomdedeu, E. Luno, R. de Paz, E. Such, . . . C. del Canizo (2012). "Better prognosis for patients with del(7q) than for patients with monosomy 7 in myelodysplastic syndrome." Cancer **118**(1): 127-133.

Corral, L. G., P. A. Haslett, G. W. Muller, R. Chen, L. M. Wong, C. J. Ocampo, . . . G. Kaplan (1999). "Differential cytokine modulation and T cell activation by two distinct classes of thalidomide analogues that are potent inhibitors of TNF-alpha." Journal of immunology **163**(1): 380-386.

da Cunha, A. F., A. F. Brugnerotto, A. S. Duarte, C. Lanaro, G. G. Costa, S. T. Saad and F. F. Costa (2010). "Global gene expression reveals a set of new genes involved in the modification of cells during erythroid differentiation." Cell Prolif **43**(3): 297-309.

Dai, M. S. and H. Lu (2004). "Inhibition of MDM2-mediated p53 ubiquitination and degradation by ribosomal protein L5." J Biol Chem **279**(43): 44475-44482.

Dai, M. S., S. X. Zeng, Y. Jin, X. X. Sun, L. David and H. Lu (2004). "Ribosomal protein L23 activates p53 by inhibiting MDM2 function in response to ribosomal perturbation but not to translation inhibition." Mol Cell Biol **24**(17): 7654-7668.

Danilova, N., K. M. Sakamoto and S. Lin (2008). "Ribosomal protein S19 deficiency in zebrafish leads to developmental abnormalities and defective erythropoiesis through activation of p53 protein family." Blood **112**(13): 5228-5237.

Debernardi, S., S. Skoulakis, G. Molloy, T. Chaplin, A. Dixon-McIver and B. D. Young (2007). "MicroRNA miR-181a correlates with morphological sub-class of acute myeloid leukaemia and the expression of its target genes in global genome-wide analysis." Leukemia **21**(5): 912-916.

Deisenroth, C. and Y. Zhang (2010). "Ribosome biogenesis surveillance: probing the ribosomal protein-Mdm2-p53 pathway." Oncogene **29**(30): 4253-4260.

Devlin, E. E., L. Dacosta, N. Mohandas, G. Elliott and D. M. Bodine (2010). "A transgenic mouse model demonstrates a dominant negative effect of a point mutation in the RPS19 gene associated with Diamond-Blackfan anemia." Blood **116**(15): 2826-2835.

Di Lisio, L., G. Gomez-Lopez, M. Sanchez-Beato, C. Gomez-Abad, M. E. Rodriguez, R. Villuendas, . . . N. Martinez (2010). "Mantle cell lymphoma: transcriptional regulation by microRNAs." Leukemia **24**(7): 1335-1342.

Didiano, D. and O. Hobert (2006). "Perfect seed pairing is not a generally reliable predictor for miRNA-target interactions." Nat Struct Mol Biol **13**(9): 849-851.

Dohner, K., J. Brown, U. Hehmann, C. Hetzel, J. Stewart, G. Lowther, . . . H. Dohner (1998). "Molecular cytogenetic characterization of a critical region in bands 7q35-q36 commonly deleted in malignant myeloid disorders." Blood **92**(11): 4031-4035.

Donald, S. P., X. Y. Sun, C. A. Hu, J. Yu, J. M. Mei, D. Valle and J. M. Phang (2001). "Proline oxidase, encoded by p53-induced gene-6, catalyzes the generation of proline-dependent reactive oxygen species." Cancer research **61**(5): 1810-1815.

Dorsam, S. T., C. M. Ferrell, G. P. Dorsam, M. K. Derynck, U. Vijapurkar, D. Khodabakhsh, . . . H. J. Lawrence (2004). "The transcriptome of the leukemogenic homeoprotein HOXA9 in human hematopoietic cells." Blood **103**(5): 1676-1684.

Dostalova Merkerova, M., Z. Krejcik, H. Votavova, M. Belickova, A. Vasikova and J. Cermak (2011). "Distinctive microRNA expression profiles in CD34+ bone marrow cells from patients with myelodysplastic syndrome." Eur J Hum Genet **19**(3): 313-319.

Draptchinskaia, N., P. Gustavsson, B. Andersson, M. Pettersson, T. N. Willig, I. Dianzani, . . . N. Dahl (1999). "The gene encoding ribosomal protein S19 is mutated in Diamond-Blackfan anaemia." Nature genetics **21**(2): 169-175.

Du, T. and P. D. Zamore (2005). "microPrimer: the biogenesis and function of microRNA." Development **132**(21): 4645-4652.

Dunbar, A. J., L. P. Gondek, C. L. O'Keefe, H. Makishima, M. S. Rataul, H. Szpurka, . . . J. P. Maciejewski (2008). "250K single nucleotide polymorphism array karyotyping identifies acquired uniparental disomy and homozygous mutations, including novel missense substitutions of c-Cbl, in myeloid malignancies." Cancer Res **68**(24): 10349-10357.

Dutt, S., A. Narla, K. Lin, A. Mullally, N. Abayasekara, C. Megerdichian, . . . B. L. Ebert (2011). "Haploinsufficiency for ribosomal protein genes causes selective activation of p53 in human erythroid progenitor cells." Blood **117**(9): 2567-2576.

Dzionara, M., E. Kaltschmidt and H. G. Wittmann (1970). "Ribosomal proteins. 8. Molecular weights of isolated ribosomal proteins of Escherichia coli." Proc Natl Acad Sci U S A **67**(4): 1909-1913.

Earle, V. L., F. Ross, A. Fisher, P. Strike, S. Berrington, L. Chiecchio, . . . F. Grand (2007). "Haemopoietic growth factors significantly improve the mitotic index and chromosome quality in cytogenetic cultures of myeloid neoplasia." Genes, chromosomes & cancer **46**(7): 670-674.

Easow, G., A. A. Teleman and S. M. Cohen (2007). "Isolation of microRNA targets by miRNP immunopurification." RNA **13**(8): 1198-1204.

Ebert, B. L., M. M. Lee, J. L. Pretz, A. Subramanian, R. Mak, T. R. Golub and C. A. Sieff (2005). "An RNA interference model of RPS19 deficiency in Diamond-Blackfan anemia recapitulates defective hematopoiesis and rescue by dexamethasone: identification of dexamethasone-responsive genes by microarray." Blood **105**(12): 4620-4626.

Ebert, B. L., J. Pretz, J. Bosco, C. Y. Chang, P. Tamayo, N. Galili, . . . T. R. Golub (2008). "Identification of RPS14 as a 5q- syndrome gene by RNA interference screen." Nature **451**(7176): 335-339.

Ebert, M. S., J. R. Neilson and P. A. Sharp (2007). "MicroRNA sponges: competitive inhibitors of small RNAs in mammalian cells." Nature methods **4**(9): 721-726.

Elmen, J., M. Lindow, S. Schutz, M. Lawrence, A. Petri, S. Obad, . . . S. Kauppinen (2008). "LNA-mediated microRNA silencing in non-human primates." Nature **452**(7189): 896-899.

Elmen, J., M. Lindow, A. Silahtaroglu, M. Bak, M. Christensen, A. Lind-Thomsen, . . . S. Kauppinen (2008). "Antagonism of microRNA-122 in mice by systemically administered LNA-antimiR leads to up-regulation of a large set of predicted target mRNAs in the liver." Nucleic acids research **36**(4): 1153-1162.

Erdogan, B., C. Facey, J. Qualtieri, J. Tedesco, E. Rinker, R. B. Isett, . . . A. S. Kim (2011). "Diagnostic microRNAs in myelodysplastic syndrome." Exp Hematol **39**(9): 915-926 e912.

Ernst, T., A. J. Chase, J. Score, C. E. Hidalgo-Curtis, C. Bryant, A. V. Jones, . . . N. C. Cross (2010). "Inactivating mutations of the histone methyltransferase gene EZH2 in myeloid disorders." Nature genetics **42**(8): 722-726.

Ernst, T., A. J. Chase, J. Score, C. E. Hidalgo-Curtis, C. Bryant, A. V. Jones, . . . N. C. Cross (2010). "Inactivating mutations of the histone methyltransferase gene EZH2 in myeloid disorders." Nature genetics **42**(8): 722-726.

Eulalio, A., E. Huntzinger and E. Izaurralde (2008). "Getting to the root of miRNA-mediated gene silencing." Cell **132**(1): 9-14.

Farrar, J. E., M. Nater, E. Caywood, M. A. McDevitt, J. Kowalski, C. M. Takemoto, . . . R. J. Arceci (2008). "Abnormalities of the large ribosomal subunit protein, Rpl35a, in Diamond-Blackfan anemia." Blood **112**(5): 1582-1592.

Felli, N., L. Fontana, E. Pelosi, R. Botta, D. Bonci, F. Facchiano, . . . C. Peschle (2005). "MicroRNAs 221 and 222 inhibit normal erythropoiesis and erythroleukemic cell growth via kit receptor down-modulation." Proc Natl Acad Sci U S A **102**(50): 18081-18086.

Ferreira-Cerca, S., G. Poll, P. E. Gleizes, H. Tschochner and P. Milkereit (2005). "Roles of eukaryotic ribosomal proteins in maturation and transport of pre-18S rRNA and ribosome function." Molecular cell **20**(2): 263-275.

Ferreira-Cerca, S., G. Poll, H. Kuhn, A. Neueder, S. Jakob, H. Tschochner and P. Milkereit (2007). "Analysis of the in vivo assembly pathway of eukaryotic 40S ribosomal proteins." Molecular cell **28**(3): 446-457.

Fitzgibbon, J., L. L. Smith, M. Raghavan, M. L. Smith, S. Debernardi, S. Skoulakis, . . . B. D. Young (2005). "Association between acquired uniparental disomy and homozygous gene mutation in acute myeloid leukemias." Cancer Res **65**(20): 9152-9154.

Flygare, J. and S. Karlsson (2007). "Diamond-Blackfan anemia: erythropoiesis lost in translation." Blood **109**(8): 3152-3154.

Flygare, J., T. Kiefer, K. Miyake, T. Utsugisawa, I. Hamaguchi, L. Da Costa, . . . S. Karlsson (2005). "Deficiency of ribosomal protein S19 in CD34+ cells generated by siRNA blocks erythroid development and mimics defects seen in Diamond-Blackfan anemia." Blood **105**(12): 4627-4634.

Fumagalli, S., A. Di Cara, A. Neb-Gulati, F. Natt, S. Schwemberger, J. Hall, . . . G. Thomas (2009). "Absence of nucleolar disruption after impairment of 40S ribosome biogenesis reveals an rpL11-translation-dependent mechanism of p53 induction." Nature cell biology **11**(4): 501-508.

Gaken, J., A. M. Mohamedali, J. Jiang, F. Malik, D. Stangl, A. E. Smith, . . . G. J. Mufti (2012). "A functional assay for microRNA target identification and validation." Nucleic Acids Res.

Garzon, R., G. A. Calin and C. M. Croce (2009). "MicroRNAs in Cancer." Annu Rev Med **60**: 167-179.

Garzon, R., S. Liu, M. Fabbri, Z. Liu, C. E. Heaphy, E. Callegari, . . . G. Marcucci (2009). "MicroRNA-29b induces global DNA hypomethylation and tumor suppressor gene reexpression in acute myeloid leukemia by targeting directly DNMT3A and 3B and indirectly DNMT1." Blood **113**(25): 6411-6418.

Garzon, R., F. Pichiorri, T. Palumbo, R. Iuliano, A. Cimmino, R. Aqeilan, . . . C. M. Croce (2006). "MicroRNA fingerprints during human megakaryocytopoiesis." Proc Natl Acad Sci U S A **103**(13): 5078-5083.

Garzon, R., S. Volinia, C. G. Liu, C. Fernandez-Cymering, T. Palumbo, F. Pichiorri, . . . C. M. Croce (2008). "MicroRNA signatures associated with cytogenetics and prognosis in acute myeloid leukemia." Blood **111**(6): 3183-3189.

Gazda, H. T., M. R. Sheen, A. Vlachos, V. Choesmel, M. F. O'Donohue, H. Schneider, . . . A. H. Beggs (2008). "Ribosomal protein L5 and L11 mutations are associated with cleft palate and abnormal thumbs in Diamond-Blackfan anemia patients." Am J Hum Genet **83**(6): 769-780.

Ghisi, M., A. Corradin, K. Basso, C. Frasson, V. Serafin, S. Mukherjee, . . . P. Zanovello (2011). "Modulation of microRNA expression in human T-cell development: targeting of NOTCH3 by miR-150." Blood **117**(26): 7053-7062.

Giagounidis, A. A., U. Germing and C. Aul (2006). "Biological and prognostic significance of chromosome 5q deletions in myeloid malignancies." Clin Cancer Res **12**(1): 5-10.

Goetz, A. W., H. van der Kuip, R. Maya, M. Oren and W. E. Aulitzky (2001). "Requirement for Mdm2 in the survival effects of Bcr-Abl and interleukin 3 in hematopoietic cells." Cancer Res **61**(20): 7635-7641.

Gondek, L. P., R. Tiu, C. L. O'Keefe, M. A. Sekeres, K. S. Theil and J. P. Maciejewski (2008). "Chromosomal lesions and uniparental disomy detected by SNP arrays in MDS, MDS/MPD, and MDS-derived AML." Blood **111**(3): 1534-1542.

Greenberg, P., C. Cox, M. M. LeBeau, P. Fenaux, P. Morel, G. Sanz, . . . J. Bennett (1997). "International scoring system for evaluating prognosis in myelodysplastic syndromes." Blood **89**(6): 2079-2088.

Greenberg, P. L. (2006). Myelodysplastic syndromes : clinical and biological advances. Cambridge, UK ; New York, Cambridge University Press.

Guglielmelli, P., L. Tozzi, A. Pancrazzi, C. Bogani, E. Antonioli, V. Ponziani, . . . A. M. Vannucchi (2007). "MicroRNA expression profile in granulocytes from primary myelofibrosis patients." Exp Hematol **35**(11): 1708-1718.

Haase, D., U. Germing, J. Schanz, M. Pfeilstocker, T. Nosslinger, B. Hildebrandt, . . . C. Steidl (2006). "New and comprehensive cytogenetic prognostication and categotization in MDS." Blood **108**: 252 (Abstract).

Haase, D., U. Germing, J. Schanz, M. Pfeilstocker, T. Nosslinger, B. Hildebrandt, . . . C. Steidl (2007). "New insights into the prognostic impact of the karyotype in MDS and correlation with subtypes: evidence from a core dataset of 2124 patients." Blood **110**(13): 4385-4395.

Hafner, M., M. Landthaler, L. Burger, M. Khorshid, J. Hausser, P. Berninger, . . . T. Tuschl (2010). "Transcriptome-wide identification of RNA-binding protein and microRNA target sites by PAR-CLIP." Cell **141**(1): 129-141.

Heinrichs, S., R. V. Kulkarni, C. E. Bueso-Ramos, R. L. Levine, M. L. Loh, C. Li, . . . A. T. Look (2009). "Accurate detection of uniparental disomy and microdeletions by SNP array analysis in myelodysplastic syndromes with normal cytogenetics." Leukemia **23**(9): 1605-1613.

Hendrickson, D. G., D. J. Hogan, D. Herschlag, J. E. Ferrell and P. O. Brown (2008). "Systematic identification of mRNAs recruited to argonaute 2 by specific microRNAs and corresponding changes in transcript abundance." PloS one **3**(5): e2126.

Hofmann, W. K., S. de Vos, M. Komor, D. Hoelzer, W. Wachsman and H. P. Koeffler (2002). "Characterization of gene expression of CD34+ cells from normal and myelodysplastic bone marrow." Blood **100**(10): 3553-3560.

Horiike, S., M. Taniwaki, S. Misawa and T. Abe (1988). "Chromosome abnormalities and karyotypic evolution in 83 patients with myelodysplastic syndrome and predictive value for prognosis." Cancer **62**(6): 1129-1138.

Hou, J., P. Wang, L. Lin, X. Liu, F. Ma, H. An, . . . X. Cao (2009). "MicroRNA-146a feedback inhibits RIG-I-dependent Type I IFN production in macrophages by targeting TRAF6, IRAK1, and IRAK2." Journal of immunology **183**(3): 2150-2158.

Hurlstone, A. F., G. Reid, J. R. Reeves, J. Fraser, G. Strathdee, M. Rahilly, . . . D. M. Black (1999). "Analysis of the CAVEOLIN-1 gene at human chromosome 7q31.1 in primary tumours and tumour-derived cell lines." Oncogene **18**(10): 1881-1890.

Hussein, K., K. Theophile, G. Busche, B. Schlegelberger, G. Gohring, H. Kreipe and O. Bock (2010a). "Aberrant microRNA expression pattern in myelodysplastic bone marrow cells." Leuk Res **34**(9): 1169-1174.

Hussein, K., K. Theophile, G. Busche, B. Schlegelberger, G. Gohring, H. Kreipe and O. Bock (2010b). "Significant inverse correlation of microRNA-150/MYB and microRNA-222/p27 in myelodysplastic syndrome." Leuk Res **34**(3): 328-334.

Iorio, M. V., M. Ferracin, C. G. Liu, A. Veronese, R. Spizzo, S. Sabbioni, . . . C. M. Croce (2005). "MicroRNA gene expression deregulation in human breast cancer." Cancer Res **65**(16): 7065-7070.

Isken, F., B. Steffen, S. Merk, M. Dugas, B. Markus, N. Tidow, . . . C. Muller-Tidow (2008). "Identification of acute myeloid leukaemia associated microRNA expression patterns." Br J Haematol **140**(2): 153-161.

Jadersten, M. and E. Hellstrom-Lindberg (2009). "Myelodysplastic syndromes: biology and treatment." J Intern Med **265**(3): 307-328.

Jankowska, A. M., H. Szpurka, R. V. Tiu, H. Makishima, M. Afable, J. Huh, . . . J. P. Maciejewski (2009). "Loss of heterozygosity 4q24 and TET2 mutations associated with myelodysplastic/myeloproliferative neoplasms." Blood **113**(25): 6403-6410.

Jerez, A., Y. Sugimoto, H. Makishima, A. Verma, A. M. Jankowska, B. Przychodzen, . . . J. P. Maciejewski (2012). "Loss of heterozygosity in 7q myeloid disorders: clinical associations and genomic pathogenesis." Blood **119**(25): 6109-6117.

Jin, A., K. Itahana, K. O'Keefe and Y. Zhang (2004). "Inhibition of HDM2 and activation of p53 by ribosomal protein L23." Mol Cell Biol **24**(17): 7669-7680.

Johansson, B., F. Mertens and F. Mitelman (1993). "Cytogenetic deletion maps of hematologic neoplasms: circumstantial evidence for tumor suppressor loci." Genes, chromosomes & cancer **8**(4): 205-218.

John, B., A. J. Enright, A. Aravin, T. Tuschl, C. Sander and D. S. Marks (2004). "Human MicroRNA targets." PLoS Biol **2**(11): e363.

Kaltschmidt, E., M. Dzionara and H. G. Wittmann (1970). "Ribosomal proteins. XV. Amino acid compositions of isolated ribosomal proteins from 30S and 50S subunits of Escherichia coli." Molecular & general genetics : MGG **109**(4): 292-297.

Kardos, G., I. Baumann, S. J. Passmore, F. Locatelli, H. Hasle, K. R. Schultz, . . . C. M. Niemeyer (2003). "Refractory anemia in childhood: a retrospective analysis of 67 patients with particular reference to monosomy 7." Blood **102**(6): 1997-2003.

Karp, X. and V. Ambros (2005). "Developmental biology. Encountering microRNAs in cell fate signaling." Science **310**(5752): 1288-1289.

Kawai, T. and S. Akira (2010). "The role of pattern-recognition receptors in innate immunity: update on Toll-like receptors." Nature immunology **11**(5): 373-384.

Keel, S. B., R. T. Doty, Z. Yang, J. G. Quigley, J. Chen, S. Knoblaugh, . . . J. L. Abkowitz (2008). "A heme export protein is required for red blood cell differentiation and iron homeostasis." Science **319**(5864): 825-828.

Kere, J. (1989c). "Chromosome 7 long arm deletion breakpoints in preleukemia: mapping by pulsed field gel electrophoresis." Nucleic Acids Res **17**(4): 1511-1520.

Kere, J., H. Donis-Keller, T. Ruutu and A. de la Chapelle (1989a). "Chromosome 7 long-arm deletions in myeloid disorders: terminal DNA sequences are commonly conserved and breakpoints vary." Cytogenetics and cell genetics **50**(4): 226-229.

Kere, J., T. Ruutu, K. A. Davies, I. B. Roninson, P. C. Watkins, R. Winqvist and A. de la Chapelle (1989b). "Chromosome 7 long arm deletion in myeloid disorders: a narrow breakpoint region in 7q22 defined by molecular mapping." Blood **73**(1): 230-234.

Kere, J., T. Ruutu, R. Lahtinen and A. de la Chapelle (1987). "Molecular characterization of chromosome 7 long arm deletions in myeloid disorders." Blood **70**(5): 1349-1353.

Kishimoto, T. (2005). "Interleukin-6: from basic science to medicine--40 years in immunology." Annual review of immunology **23**: 1-21.

Kitagawa, M., S. Yoshida, T. Kuwata, T. Tanizawa and R. Kamiyama (1994). "p53 expression in myeloid cells of myelodysplastic syndromes. Association with evolution of overt leukemia." The American journal of pathology **145**(2): 338-344.

Kong, Y. W., I. G. Cannell, C. H. de Moor, K. Hill, P. G. Garside, T. L. Hamilton, . . . M. Bushell (2008). "The mechanism of micro-RNA-mediated translation repression is determined by the promoter of the target gene." Proceedings of the National Academy of Sciences of the United States of America **105**(26): 8866-8871.

Koopman, G., C. P. Reutelingsperger, G. A. Kuijten, R. M. Keehnen, S. T. Pals and M. H. van Oers (1994). "Annexin V for flow cytometric detection of phosphatidylserine expression on B cells undergoing apoptosis." Blood **84**(5): 1415-1420.

Koralov, S. B., S. A. Muljo, G. R. Galler, A. Krek, T. Chakraborty, C. Kanellopoulou, . . . K. Rajewsky (2008). "Dicer ablation affects antibody diversity and cell survival in the B lymphocyte lineage." Cell **132**(5): 860-874.

Kruse, J. P. and W. Gu (2009). "Modes of p53 regulation." Cell **137**(4): 609-622.

Krutzfeldt, J., N. Rajewsky, R. Braich, K. G. Rajeev, T. Tuschl, M. Manoharan and M. Stoffel (2005). "Silencing of microRNAs in vivo with 'antagomirs'." Nature **438**(7068): 685-689.

Kuhn, D. E., M. M. Martin, D. S. Feldman, A. V. Terry, Jr., G. J. Nuovo and T. S. Elton (2008). "Experimental validation of miRNA targets." Methods **44**(1): 47-54.

Kumar, M. S., A. Narla, A. Nonami, A. Mullally, N. Dimitrova, B. Ball, . . . B. L. Ebert (2011). "Coordinate loss of a microRNA and protein-coding gene cooperate in the pathogenesis of 5q- syndrome." Blood **118**(17): 4666-4673.

Lajtha, L. G. and R. Oliver (1961). "A kinetic model of the erythron." Proc R Soc Med **54**: 369-371.

Lal, A., F. Navarro, C. A. Maher, L. E. Maliszewski, N. Yan, E. O'Day, . . . J. Lieberman (2009). "miR-24 Inhibits cell proliferation by targeting E2F2, MYC, and other cell-cycle genes via binding to "seedless" 3'UTR microRNA recognition elements." Molecular cell **35**(5): 610-625.

Law, J. C., M. K. Ritke, J. C. Yalowich, G. H. Leder and R. E. Ferrell (1993). "Mutational inactivation of the p53 gene in the human erythroid leukemic K562 cell line." Leuk Res **17**(12): 1045-1050.

Lecompte, O., R. Ripp, J. C. Thierry, D. Moras and O. Poch (2002). "Comparative analysis of ribosomal proteins in complete genomes: an example of reductive evolution at the domain scale." Nucleic Acids Res **30**(24): 5382-5390.

Lee, R. C., R. L. Feinbaum and V. Ambros (1993). "The C. elegans heterochronic gene lin-4 encodes small RNAs with antisense complementarity to lin-14." Cell **75**(5): 843-854.

Lee, Y., K. Jeon, J. T. Lee, S. Kim and V. N. Kim (2002). "MicroRNA maturation: stepwise processing and subcellular localization." EMBO J **21**(17): 4663-4670.

Lempiainen, H. and D. Shore (2009). "Growth control and ribosome biogenesis." Current opinion in cell biology **21**(6): 855-863.

Lewis, B. P., C. B. Burge and D. P. Bartel (2005). "Conserved seed pairing, often flanked by adenosines, indicates that thousands of human genes are microRNA targets." Cell **120**(1): 15-20.

Lewis, B. P., I. H. Shih, M. W. Jones-Rhoades, D. P. Bartel and C. B. Burge (2003). "Prediction of mammalian microRNA targets." Cell **115**(7): 787-798.

Lewis, S., G. Abrahamson, J. Boultwood, C. Fidler, A. Potter and J. S. Wainscoat (1996). "Molecular characterization of the 7q deletion in myeloid disorders." Br J Haematol **93**(1): 75-80.

Li, C., S. W. Kim, D. Rai, A. R. Bolla, S. Adhvaryu, M. C. Kinney, . . . R. C. Aguiar (2009). "Copy number abnormalities, MYC activity, and the genetic fingerprint of normal B cells mechanistically define the microRNA profile of diffuse large B-cell lymphoma." Blood **113**(26): 6681-6690.

Liang, H., J. Fairman, D. F. Claxton, P. C. Nowell, E. D. Green and L. Nagarajan (1998). "Molecular anatomy of chromosome 7q deletions in myeloid neoplasms: evidence for multiple critical loci." Proc Natl Acad Sci U S A **95**(7): 3781-3785.

Lim, L. P., M. E. Glasner, S. Yekta, C. B. Burge and D. P. Bartel (2003). "Vertebrate microRNA genes." Science **299**(5612): 1540.

Lim, L. P., N. C. Lau, P. Garrett-Engele, A. Grimson, J. M. Schelter, J. Castle, . . . J. M. Johnson (2005). "Microarray analysis shows that some microRNAs downregulate large numbers of target mRNAs." Nature **433**(7027): 769-773.

Lindstrom, M. S. (2009). "Emerging functions of ribosomal proteins in gene-specific transcription and translation." Biochem Biophys Res Commun **379**(2): 167-170.

Liu, G., A. Friggeri, Y. Yang, Y. J. Park, Y. Tsuruta and E. Abraham (2009). "miR-147, a microRNA that is induced upon Toll-like receptor stimulation, regulates murine macrophage inflammatory responses." Proc Natl Acad Sci U S A **106**(37): 15819-15824.

Liu, J. M. and S. R. Ellis (2006). "Ribosomes and marrow failure: coincidental association or molecular paradigm?" Blood **107**(12): 4583-4588.

Liu, W., O. Zabirnyk, H. Wang, Y. H. Shiao, M. L. Nickerson, S. Khalil, . . . J. M. Phang (2010). "miR-23b targets proline oxidase, a novel tumor suppressor protein in renal cancer." Oncogene **29**(35): 4914-4924.

Liu, Y., G. L. Borchert, S. P. Donald, B. A. Diwan, M. Anver and J. M. Phang (2009). "Proline oxidase functions as a mitochondrial tumor suppressor in human cancers." Cancer research **69**(16): 6414-6422.

Lodish, H. F., B. Zhou, G. Liu and C. Z. Chen (2008). "Micromanagement of the immune system by microRNAs." Nature reviews. Immunology **8**(2): 120-130.

Lohrum, M. A., R. L. Ludwig, M. H. Kubbutat, M. Hanlon and K. H. Vousden (2003). "Regulation of HDM2 activity by the ribosomal protein L11." Cancer cell **3**(6): 577-587.

Lori Nestler, E. E., Jennifer McLaughlin, Donald Munroe, and K. W. Teresa Tan, and Brad Stiles (2004). "TrypLE™ Express: A Temperature Stable

Replacement for Animal Trypsin in

Cell Dissociation Applications." QUEST **1**(1): 6.

Lu, L. F., M. P. Boldin, A. Chaudhry, L. L. Lin, K. D. Taganov, T. Hanada, . . . A. Y. Rudensky (2010). "Function of miR-146a in controlling Treg cell-mediated regulation of Th1 responses." Cell **142**(6): 914-929.

Lujambio, A. and S. W. Lowe (2012). "The microcosmos of cancer." Nature **482**(7385): 347-355.

Luna-Fineman, S., K. M. Shannon and B. J. Lange (1995). "Childhood monosomy 7: epidemiology, biology, and mechanistic implications." Blood **85**(8): 1985-1999.

Lytle, J. R., T. A. Yario and J. A. Steitz (2007). "Target mRNAs are repressed as efficiently by microRNA-binding sites in the 5' UTR as in the 3' UTR." Proceedings of the National Academy of Sciences of the United States of America **104**(23): 9667-9672.

Makishima, H., A. M. Jankowska, R. V. Tiu, H. Szpurka, Y. Sugimoto, Z. Hu, . . . J. P. Maciejewski (2010). "Novel homo- and hemizygous mutations in EZH2 in myeloid malignancies." Leukemia **24**(10): 1799-1804.

Makishima, H., V. Visconte, H. Sakaguchi, A. M. Jankowska, S. Abu Kar, A. Jerez, . . . J. P. Maciejewski (2012). "Mutations in the spliceosome machinery, a novel and ubiquitous pathway in leukemogenesis." Blood **119**(14): 3203-3210.

Manfredi, J. J. (2010). "The Mdm2-p53 relationship evolves: Mdm2 swings both ways as an oncogene and a tumor suppressor." Genes & development **24**(15): 1580-1589.

Marechal, V., B. Elenbaas, J. Piette, J. C. Nicolas and A. J. Levine (1994). "The ribosomal L5 protein is associated with mdm-2 and mdm-2-p53 complexes." Mol Cell Biol **14**(11): 7414-7420.

Mateo, M., M. Mollejo, R. Villuendas, P. Algara, M. Sanchez-Beato, P. Martinez and M. A. Piris (1999). "7q31-32 allelic loss is a frequent finding in splenic marginal zone lymphoma." The American journal of pathology **154**(5): 1583-1589.

McGowan, K. A., J. Z. Li, C. Y. Park, V. Beaudry, H. K. Tabor, A. J. Sabnis, . . . G. S. Barsh (2008). "Ribosomal mutations cause p53-mediated dark skin and pleiotropic effects." Nature genetics **40**(8): 963-970.

McGowan, K. A., W. W. Pang, R. Bhardwaj, M. G. Perez, J. V. Pluvinage, B. E. Glader, . . . G. S. Barsh (2011). "Reduced ribosomal protein gene dosage and p53 activation in low-risk myelodysplastic syndrome." Blood **118**(13): 3622-3633.

Medzhitov, R., P. Preston-Hurlburt and C. A. Janeway, Jr. (1997). "A human homologue of the Drosophila Toll protein signals activation of adaptive immunity." Nature **388**(6640): 394-397.

Mendell, J. T. and E. N. Olson (2012). "MicroRNAs in stress signaling and human disease." Cell **148**(6): 1172-1187.

Mendiburu, C. F., W. A. Silva, Jr., O. Ricci, Jr., C. R. Bonini-Domingos and A. C. Fett-Conte (2008). "Global gene expression profile in myelodysplastic syndromes using SAGE." Genetics and molecular research : GMR **7**(4): 1245-1250.

Mendiburu, C. F., W. A. Silva, Jr., O. Ricci, Jr., C. R. Bonini-Domingos and A. C. Fett-Conte (2008). "Global gene expression profile in myelodysplastic syndromes using SAGE." Genetics and molecular research : GMR **7**(4): 1245-1250.

Mendler, J. H., K. Maharry, M. D. Radmacher, K. Mrozek, H. Becker, K. H. Metzeler, . . . C. D. Bloomfield (2012). "RUNX1 mutations are associated with poor outcome in younger and older patients with cytogenetically normal acute myeloid leukemia and with distinct gene and MicroRNA expression signatures." J Clin Oncol **30**(25): 3109-3118.

Menigatti, M., T. Staiano, C. N. Manser, P. Bauerfeind, A. Komljenovic, M. Robinson, . . . G. Marra (2013). "Epigenetic silencing of monoallelically methylated miRNA loci in precancerous colorectal lesions." Oncogenesis **2**: e56.

Metzler, M., M. Wilda, K. Busch, S. Viehmann and A. Borkhardt (2004). "High expression of precursor microRNA-155/BIC RNA in children with Burkitt lymphoma." Genes, chromosomes & cancer **39**(2): 167-169.

Mi, S., Z. Li, P. Chen, C. He, D. Cao, A. Elkahloun, . . . J. Chen (2010). "Aberrant overexpression and function of the miR-17-92 cluster in MLL-rearranged acute leukemia." Proc Natl Acad Sci U S A **107**(8): 3710-3715.

Mi, S., J. Lu, M. Sun, Z. Li, H. Zhang, M. B. Neilly, . . . J. Chen (2007). "MicroRNA expression signatures accurately discriminate acute lymphoblastic leukemia from acute myeloid leukemia." Proc Natl Acad Sci U S A **104**(50): 19971-19976.

Michael, M. Z., O. C. SM, N. G. van Holst Pellekaan, G. P. Young and R. J. James (2003). "Reduced accumulation of specific microRNAs in colorectal neoplasia." Molecular cancer research : MCR **1**(12): 882-891.

Mili, S. and J. A. Steitz (2004). "Evidence for reassociation of RNA-binding proteins after cell lysis: implications for the interpretation of immunoprecipitation analyses." RNA **10**(11): 1692-1694.

Mohamedali, A., J. Gaken, N. A. Twine, W. Ingram, N. Westwood, N. C. Lea, . . . G. J. Mufti (2007). "Prevalence and prognostic significance of allelic imbalance by single-nucleotide polymorphism analysis in low-risk myelodysplastic syndromes." Blood **110**(9): 3365-3373.

Montanaro, L., D. Trere and M. Derenzini (2008). "Nucleolus, ribosomes, and cancer." The American journal of pathology **173**(2): 301-310.

Morgenstern, J. P. and H. Land (1990). "Advanced mammalian gene transfer: high titre retroviral vectors with multiple drug selection markers and a complementary helper-free packaging cell line." Nucleic Acids Res **18**(12): 3587-3596.

Moss, E. G., R. C. Lee and V. Ambros (1997). "The cold shock domain protein LIN-28 controls developmental timing in C. elegans and is regulated by the lin-4 RNA." Cell **88**(5): 637-646.

Mufti, G. J. (2004). "Pathobiology, classification, and diagnosis of myelodysplastic syndrome." Best practice & research. Clinical haematology **17**(4): 543-557.

Mufti, G. J., J. M. Bennett, J. Goasguen, B. J. Bain, I. Baumann, R. Brunning, . . . A. Yoshimi (2008). "Diagnosis and classification of myelodysplastic syndrome: International

Working Group on Morphology of myelodysplastic syndrome (IWGM-MDS) consensus proposals for the definition and enumeration of myeloblasts and ring sideroblasts." Haematologica **93**(11): 1712-1717.

Muljo, S. A., K. M. Ansel, C. Kanellopoulou, D. M. Livingston, A. Rao and K. Rajewsky (2005). "Aberrant T cell differentiation in the absence of Dicer." The Journal of experimental medicine **202**(2): 261-269.

Myatt, S. S., J. Wang, L. J. Monteiro, M. Christian, K. K. Ho, L. Fusi, . . . E. W. Lam (2010). "Definition of microRNAs that repress expression of the tumor suppressor gene FOXO1 in endometrial cancer." Cancer Res **70**(1): 367-377.

Najfeld, V. (2003). "Diagnostic application of FISH to hematological malignancies." Cancer investigation **21**(5): 807-814.

Narla, A. and B. L. Ebert (2010). "Ribosomopathies: human disorders of ribosome dysfunction." Blood **115**(16): 3196-3205.

Narla, A., E. M. Payne, N. Abayasekara, S. N. Hurst, D. M. Raiser, A. T. Look, . . . A. Khanna-Gupta (2014). "L-Leucine improves the anaemia in models of Diamond Blackfan anaemia and the 5q- syndrome in a TP53-independent way." Br J Haematol.

Nikoloski, G., S. M. Langemeijer, R. P. Kuiper, R. Knops, M. Massop, E. R. Tonnissen, . . . J. H. Jansen (2010). "Somatic mutations of the histone methyltransferase gene EZH2 in myelodysplastic syndromes." Nature genetics **42**(8): 665-667.

O'Connell, R. M., D. S. Rao, A. A. Chaudhuri and D. Baltimore (2010). "Physiological and pathological roles for microRNAs in the immune system." Nature reviews. Immunology **10**(2): 111-122.

O'Connell, R. M., D. S. Rao, A. A. Chaudhuri, M. P. Boldin, K. D. Taganov, J. Nicoll, . . . D. Baltimore (2008). "Sustained expression of microRNA-155 in hematopoietic stem cells causes a myeloproliferative disorder." The Journal of experimental medicine **205**(3): 585-594.

O'Connell, R. M., K. D. Taganov, M. P. Boldin, G. Cheng and D. Baltimore (2007). "MicroRNA-155 is induced during the macrophage inflammatory response." Proc Natl Acad Sci U S A **104**(5): 1604-1609.

O'Connell, R. M., J. L. Zhao and D. S. Rao (2011). "MicroRNA function in myeloid biology." Blood **118**(11): 2960-2969.

O'Neill, L. A., F. J. Sheedy and C. E. McCoy (2011). "MicroRNAs: the fine-tuners of Toll-like receptor signalling." Nature reviews. Immunology **11**(3): 163-175.

Ofir-Rosenfeld, Y., K. Boggs, D. Michael, M. B. Kastan and M. Oren (2008). "Mdm2 regulates p53 mRNA translation through inhibitory interactions with ribosomal protein L26." Molecular cell **32**(2): 180-189.

Ohene-Abuakwa, Y., K. A. Orfali, C. Marius and S. E. Ball (2005). "Two-phase culture in Diamond Blackfan anemia: localization of erythroid defect." Blood **105**(2): 838-846.

Oliva, E. N., M. Cuzzola, F. Nobile, F. Ronco, M. G. D'Errigo, C. Lagana, . . . R. Latagliata (2010). "Changes in RPS14 expression levels during lenalidomide treatment in Low- and Intermediate-1-risk myelodysplastic syndromes with chromosome 5q deletion." Eur J Haematol **85**(3): 231-235.

Olnes, M. J. and E. M. Sloand (2011). "Targeting immune dysregulation in myelodysplastic syndromes." JAMA : the journal of the American Medical Association **305**(8): 814-819.

Orom, U. A., F. C. Nielsen and A. H. Lund (2008). "MicroRNA-10a binds the 5'UTR of ribosomal protein mRNAs and enhances their translation." Molecular cell **30**(4): 460-471.

Panic, L., S. Tamarut, M. Sticker-Jantscheff, M. Barkic, D. Solter, M. Uzelac, . . . S. Volarevic (2006). "Ribosomal protein S6 gene haploinsufficiency is associated with activation of a p53-dependent checkpoint during gastrulation." Mol Cell Biol **26**(23): 8880-8891.

Panja, S., P. Aich, B. Jana and T. Basu (2008). "How does plasmid DNA penetrate cell membranes in artificial transformation process of Escherichia coli?" Molecular membrane biology **25**(5): 411-422.

Panse, V. G. and A. W. Johnson (2010). "Maturation of eukaryotic ribosomes: acquisition of functionality." Trends in biochemical sciences **35**(5): 260-266.

Papaemmanuil, E., M. Cazzola, J. Boultwood, L. Malcovati, P. Vyas, D. Bowen, . . . C. Chronic Myeloid Disorders Working Group of the International Cancer Genome (2011). "Somatic SF3B1 mutation in myelodysplasia with ring sideroblasts." N Engl J Med **365**(15): 1384-1395.

Parker, J. S., S. M. Roe and D. Barford (2004). "Crystal structure of a PIWI protein suggests mechanisms for siRNA recognition and slicer activity." EMBO J **23**(24): 4727-4737.

Pedersen-Bjergaard, J., P. Philip, S. O. Larsen, G. Jensen and K. Byrsting (1990). "Chromosome aberrations and prognostic factors in therapy-related myelodysplasia and acute nonlymphocytic leukemia." Blood **76**(6): 1083-1091.

Pellagatti, A., M. Cazzola, A. A. Giagounidis, L. Malcovati, M. G. Porta, S. Killick, . . . J. Boultwood (2006). "Gene expression profiles of CD34+ cells in myelodysplastic

syndromes: involvement of interferon-stimulated genes and correlation to FAB subtype and karyotype." Blood **108**(1): 337-345.

Pellagatti, A., E. Hellstrom-Lindberg, A. Giagounidis, J. Perry, L. Malcovati, M. G. Della Porta, . . . J. Boultwood (2008). "Haploinsufficiency of RPS14 in 5q- syndrome is associated with deregulation of ribosomal- and translation-related genes." Br J Haematol **142**(1): 57-64.

Pellagatti, A., T. Marafioti, J. C. Paterson, J. L. Barlow, L. F. Drynan, A. Giagounidis, . . . J. Boultwood (2010). "Induction of p53 and up-regulation of the p53 pathway in the human 5q- syndrome." Blood **115**(13): 2721-2723.

Pons, A., B. Nomdedeu, A. Navarro, A. Gaya, B. Gel, T. Diaz, . . . M. Monzo (2009). "Hematopoiesis-related microRNA expression in myelodysplastic syndromes." Leuk Lymphoma **50**(11): 1854-1859.

Quigley, J. G., H. Gazda, Z. Yang, S. Ball, C. A. Sieff and J. L. Abkowitz (2005). "Investigation of a putative role for FLVCR, a cytoplasmic heme exporter, in Diamond-Blackfan anemia." Blood cells, molecules & diseases **35**(2): 189-192.

Raghavan, M., D. M. Lillington, S. Skoulakis, S. Debernardi, T. Chaplin, N. J. Foot, . . . B. D. Young (2005). "Genome-wide single nucleotide polymorphism analysis reveals frequent partial uniparental disomy due to somatic recombination in acute myeloid leukemias." Cancer Res **65**(2): 375-378.

Rhoades, M. W., B. J. Reinhart, L. P. Lim, C. B. Burge, B. Bartel and D. P. Bartel (2002). "Prediction of plant microRNA targets." Cell **110**(4): 513-520.

Rhyasen, G. W. and D. T. Starczynowski (2012). "Deregulation of microRNAs in myelodysplastic syndrome." Leukemia **26**(1): 13-22.

Rigolin, G. M., R. Bigoni, R. Milani, F. Cavazzini, M. G. Roberti, A. Bardi, . . . G. Castoldi (2001). "Clinical importance of interphase cytogenetics detecting occult chromosome lesions in myelodysplastic syndromes with normal karyotype." Leukemia **15**(12): 1841-1847.

Rodnina, M. V. and W. Wintermeyer (2009). "Recent mechanistic insights into eukaryotic ribosomes." Current opinion in cell biology **21**(3): 435-443.

Rodriguez, A., S. Griffiths-Jones, J. L. Ashurst and A. Bradley (2004). "Identification of mammalian microRNA host genes and transcription units." Genome research **14**(10A): 1902-1910.

Ross, D. T., U. Scherf, M. B. Eisen, C. M. Perou, C. Rees, P. Spellman, . . . P. O. Brown (2000). "Systematic variation in gene expression patterns in human cancer cell lines." Nature genetics **24**(3): 227-235.

Rudra, D. and J. R. Warner (2004). "What better measure than ribosome synthesis?" Genes & development **18**(20): 2431-2436.

Ruiz-Ballesteros, E., M. Mollejo, M. Mateo, P. Algara, P. Martinez and M. A. Piris (2007). "MicroRNA losses in the frequently deleted region of 7q in SMZL." Leukemia **21**(12): 2547-2549.

Schiffer, C. A., E. J. Lee, T. Tomiyasu, P. H. Wiernik and J. R. Testa (1989). "Prognostic impact of cytogenetic abnormalities in patients with de novo acute nonlymphocytic leukemia." Blood **73**(1): 263-270.

Schwarz, D. S., G. Hutvagner, T. Du, Z. Xu, N. Aronin and P. D. Zamore (2003). "Asymmetry in the assembly of the RNAi enzyme complex." Cell **115**(2): 199-208.

Sheedy, F. J., E. Palsson-McDermott, E. J. Hennessy, C. Martin, J. J. O'Leary, Q. Ruan, . . . L. A. O'Neill (2010). "Negative regulation of TLR4 via targeting of the proinflammatory tumor suppressor PDCD4 by the microRNA miR-21." Nature immunology **11**(2): 141-147.

Shih, A. H., O. Abdel-Wahab, J. P. Patel and R. L. Levine (2012). "The role of mutations in epigenetic regulators in myeloid malignancies." Nature reviews. Cancer **12**(9): 599-612.

Simon, J. A. and C. A. Lange (2008). "Roles of the EZH2 histone methyltransferase in cancer epigenetics." Mutation research **647**(1-2): 21-29.

Singh, S. A., T. A. Goldberg, A. L. Henson, S. Husain-Krautter, A. Nihrane, L. Blanc, . . . J. M. Liu (2014). "p53-Independent cell cycle and erythroid differentiation defects in murine embryonic stem cells haploinsufficient for Diamond Blackfan anemia-proteins: RPS19 versus RPL5." PloS one **9**(2): e89098.

Sokol, L., G. Caceres, S. Volinia, H. Alder, G. J. Nuovo, C. G. Liu, . . . A. F. List (2011). "Identification of a risk dependent microRNA expression signature in myelodysplastic syndromes." Br J Haematol **153**(1): 24-32.

Sole, F., E. Luno, C. Sanzo, B. Espinet, G. F. Sanz, J. Cervera, . . . L. Florensa (2005). "Identification of novel cytogenetic markers with prognostic significance in a series of 968 patients with primary myelodysplastic syndromes." Haematologica **90**(9): 1168-1178.

Song, J. J., J. Liu, N. H. Tolia, J. Schneiderman, S. K. Smith, R. A. Martienssen, . . . L. Joshua-Tor (2003). "The crystal structure of the Argonaute2 PAZ domain reveals an RNA binding motif in RNAi effector complexes." Nat Struct Biol **10**(12): 1026-1032.

Song, J. J., S. K. Smith, G. J. Hannon and L. Joshua-Tor (2004). "Crystal structure of Argonaute and its implications for RISC slicer activity." Science **305**(5689): 1434-1437.

Sridhar, K., D. T. Ross, R. Tibshirani, A. J. Butte and P. L. Greenberg (2009). "Relationship of differential gene expression profiles in CD34+ myelodysplastic syndrome marrow cells to disease subtype and progression." Blood **114**(23): 4847-4858.

Starczynowski, D. T. and A. Karsan (2010). "Innate immune signaling in the myelodysplastic syndromes." Hematology/oncology clinics of North America **24**(2): 343-359.

Starczynowski, D. T., F. Kuchenbauer, B. Argiropoulos, S. Sung, R. Morin, A. Muranyi, . . . A. Karsan (2010a). "Identification of miR-145 and miR-146a as mediators of the 5q-syndrome phenotype." Nat Med **16**(1): 49-58.

Starczynowski, D. T., F. Kuchenbauer, J. Wegrzyn, A. Rouhi, O. Petriv, C. L. Hansen, . . . A. Karsan (2010d). "MicroRNA-146a disrupts hematopoietic differentiation and survival." Exp Hematol **39**(2): 167-178 e164.

Starczynowski, D. T., S. Vercauteren, A. Telenius, S. Sung, K. Tohyama, A. Brooks-Wilson, . . . A. Karsan (2008). "High-resolution whole genome tiling path array CGH analysis of CD34+ cells from patients with low-risk myelodysplastic syndromes reveals cryptic copy number alterations and predicts overall and leukemia-free survival." Blood **112**(8): 3412-3424.

Steensma, D. P. and A. Tefferi (2003). "The myelodysplastic syndrome(s): a perspective and review highlighting current controversies." Leuk Res **27**(2): 95-120.

Steitz, T. A. and P. B. Moore (2003). "RNA, the first macromolecular catalyst: the ribosome is a ribozyme." Trends in biochemical sciences **28**(8): 411-418.

Stelzl, U. and K. H. Nierhaus (2001). "A short fragment of 23S rRNA containing the binding sites for two ribosomal proteins, L24 and L4, is a key element for rRNA folding during early assembly." RNA **7**(4): 598-609.

Strom, A. R. and L. P. Visentin (1973). "Acidic ribosomal proteins from the extreme halophile, Halobacterium cutirubrum. The simultaneous separation, identification and molecular weight determination." FEBS letters **37**(2): 274-280.

Sugimoto, K., H. Toyoshima, R. Sakai, K. Miyagawa, K. Hagiwara, F. Ishikawa, . . . H. Hirai (1992). "Frequent mutations in the p53 gene in human myeloid leukemia cell lines." Blood **79**(9): 2378-2383.

Szpurka, H., L. P. Gondek, S. R. Mohan, E. D. Hsi, K. S. Theil and J. P. Maciejewski (2009). "UPD1p indicates the presence of MPL W515L mutation in RARS-T, a mechanism analogous to UPD9p and JAK2 V617F mutation." Leukemia **23**(3): 610-614.

Taganov, K. D., M. P. Boldin, K. J. Chang and D. Baltimore (2006). "NF-kappaB-dependent induction of microRNA miR-146, an inhibitor targeted to signaling proteins of innate immune responses." Proc Natl Acad Sci U S A **103**(33): 12481-12486.

Takada, S., Y. Yamashita, E. Berezikov, H. Hatanaka, S. I. Fujiwara, K. Kurashina, . . . H. Mano (2008). "MicroRNA expression profiles of human leukemias." Leukemia **22**(6): 1274-1278.

Takagi, M., M. J. Absalon, K. G. McLure and M. B. Kastan (2005). "Regulation of p53 translation and induction after DNA damage by ribosomal protein L26 and nucleolin." Cell **123**(1): 49-63.

Teng, T., C. A. Mercer, P. Hexley, G. Thomas and S. Fumagalli (2013). "Loss of tumor suppressor RPL5/RPL11 does not induce cell cycle arrest but impedes proliferation due to reduced ribosome content and translation capacity." Mol Cell Biol **33**(23): 4660-4671.

Terzian, T. and N. Box (2013). "Genetics of ribosomal proteins: "curiouser and curiouser"." PLoS genetics **9**(1): e1003300.

Terzian, T., M. Dumble, F. Arbab, C. Thaller, L. A. Donehower, G. Lozano, . . . N. F. Box (2011). "Rpl27a mutation in the sooty foot ataxia mouse phenocopies high p53 mouse models." The Journal of pathology **224**(4): 540-552.

Thomas, M., J. Lieberman and A. Lal (2010). "Desperately seeking microRNA targets." Nat Struct Mol Biol **17**(10): 1169-1174.

Thomson, D. W., C. P. Bracken and G. J. Goodall (2011). "Experimental strategies for microRNA target identification." Nucleic acids research **39**(16): 6845-6853.

Thomson, J. M., J. Parker, C. M. Perou and S. M. Hammond (2004). "A custom microarray platform for analysis of microRNA gene expression." Nat Methods **1**(1): 47-53.

Tosi, S., S. W. Scherer, G. Giudici, B. Czepulkowski, A. Biondi and L. Kearney (1999). "Delineation of multiple deleted regions in 7q in myeloid disorders." Genes, chromosomes & cancer **25**(4): 384-392.

Toyama, K., K. Ohyashiki, Y. Yoshida, T. Abe, S. Asano, H. Hirai, . . . et al. (1993a). "Clinical and cytogenetic findings of myelodysplastic syndromes showing hypocellular bone marrow or minimal dysplasia, in comparison with typical myelodysplastic syndromes." International journal of hematology **58**(1-2): 53-61.

Toyama, K., K. Ohyashiki, Y. Yoshida, T. Abe, S. Asano, H. Hirai, . . . et al. (1993b). "Clinical implications of chromosomal abnormalities in 401 patients with myelodysplastic syndromes: a multicentric study in Japan." Leukemia **7**(4): 499-508.

Tsurugi, K., E. Collatz, K. Todokoro and I. G. Wool (1977). "Isolation of eukaryotic ribosomal proteins. Purification and characterization of 60 S ribosomal subunit proteins L3, L6, L7', L8, L10, L15, L17, L18, L19, L23', L25, L27', L28, L29, L31, L32, L34, L35, L36, L36', and L37'." J Biol Chem **252**(11): 3961-3969.

Tuschl, T. (2002). "Expanding small RNA interference." Nature biotechnology **20**(5): 446-448.

Van Etten, R. A. and K. M. Shannon (2004). "Focus on myeloproliferative diseases and myelodysplastic syndromes." Cancer cell **6**(6): 547-552.

Vasikova, A., M. Belickova, E. Budinska and J. Cermak (2010). "A distinct expression of various gene subsets in CD34+ cells from patients with early and advanced myelodysplastic syndrome." Leuk Res **34**(12): 1566-1572.

Venturini, L., K. Battmer, M. Castoldi, B. Schultheis, A. Hochhaus, M. U. Muckenthaler, . . . M. Scherr (2007). "Expression of the miR-17-92 polycistron in chronic myeloid leukemia (CML) CD34+ cells." Blood **109**(10): 4399-4405.

Votavova, H., M. Grmanova, M. Dostalova Merkerova, M. Belickova, A. Vasikova, R. Neuwirtova and J. Cermak (2011). "Differential expression of microRNAs in CD34+ cells of 5q- syndrome." J Hematol Oncol **4**: 1.

Walker, B. A., P. E. Leone, M. W. Jenner, C. Li, D. Gonzalez, D. C. Johnson, . . . G. J. Morgan (2006). "Integration of global SNP-based mapping and expression arrays reveals key regions, mechanisms, and genes important in the pathogenesis of multiple myeloma." Blood **108**(5): 1733-1743.

Waller, J. P. and J. I. Harris (1961). "Studies on the composition of the protein from Escherichia coli ribosomes." Proc Natl Acad Sci U S A **47**: 18-23.

Wang, L., C. Fidler, N. Nadig, A. Giagounidis, M. G. Della Porta, L. Malcovati, . . . J. S. Wainscoat (2008). "Genome-wide analysis of copy number changes and loss of heterozygosity in myelodysplastic syndrome with del(5q) using high-density single nucleotide polymorphism arrays." Haematologica **93**(7): 994-1000.

Warner, J. R. (1999). "The economics of ribosome biosynthesis in yeast." Trends in biochemical sciences **24**(11): 437-440.

Weissman, I. L. (2000). "Stem cells: units of development, units of regeneration, and units in evolution." Cell **100**(1): 157-168.

Wiesen, J. L. and T. B. Tomasi (2009). "Dicer is regulated by cellular stresses and interferons." Molecular immunology **46**(6): 1222-1228.

Witkos, T. M., E. Koscianska and W. J. Krzyzosiak (2011). "Practical Aspects of microRNA Target Prediction." Current molecular medicine **11**(2): 93-109.

Wool, I. G. (1996). "Extraribosomal functions of ribosomal proteins." Trends in biochemical sciences **21**(5): 164-165.

Xue, S. and M. Barna (2012). "Specialized ribosomes: a new frontier in gene regulation and organismal biology." Nature reviews. Molecular cell biology **13**(6): 355-369.

Yadavilli, S., L. D. Mayo, M. Higgins, S. Lain, V. Hegde and W. A. Deutsch (2009). "Ribosomal protein S3: A multi-functional protein that interacts with both p53 and MDM2 through its KH domain." DNA repair **8**(10): 1215-1224.

Yan, K. S., S. Yan, A. Farooq, A. Han, L. Zeng and M. M. Zhou (2003). "Structure and conserved RNA binding of the PAZ domain." Nature **426**(6965): 468-474.

Yang, B. F., Y. J. Lu and Z. G. Wang (2009). "MicroRNAs and apoptosis: implications in the molecular therapy of human disease." Clin Exp Pharmacol Physiol **36**(10): 951-960.

Yang, W., T. P. Chendrimada, Q. Wang, M. Higuchi, P. H. Seeburg, R. Shiekhattar and K. Nishikura (2006). "Modulation of microRNA processing and expression through RNA editing by ADAR deaminases." Nat Struct Mol Biol **13**(1): 13-21.

Yi, R., Y. Qin, I. G. Macara and B. R. Cullen (2003). "Exportin-5 mediates the nuclear export of pre-microRNAs and short hairpin RNAs." Genes & development **17**(24): 3011-3016.

Yoshida, K., M. Sanada, Y. Shiraishi, D. Nowak, Y. Nagata, R. Yamamoto, . . . S. Ogawa (2011). "Frequent pathway mutations of splicing machinery in myelodysplasia." Nature **478**(7367): 64-69.

Yunis, J. J., R. E. Rydell, M. M. Oken, M. A. Arnesen, M. G. Mayer and M. Lobell (1986). "Refined chromosome analysis as an independent prognostic indicator in de novo myelodysplastic syndromes." Blood **67**(6): 1721-1730.

Zenklusen, J. C. and C. J. Conti (1996). "Cytogenetic, molecular and functional evidence for novel tumor suppressor genes on the long arm of human chromosome 7." Mol Carcinog **15**(3): 167-175.

Zhang, B., X. Pan, G. P. Cobb and T. A. Anderson (2007). "microRNAs as oncogenes and tumor suppressors." Dev Biol **302**(1): 1-12.

Zhang, Y. and H. Lu (2009). "Signaling to p53: ribosomal proteins find their way." Cancer cell **16**(5): 369-377.

Zhang, Y., G. W. Wolf, K. Bhat, A. Jin, T. Allio, W. A. Burkhart and Y. Xiong (2003). "Ribosomal protein L11 negatively regulates oncoprotein MDM2 and mediates a p53-dependent ribosomal-stress checkpoint pathway." Mol Cell Biol **23**(23): 8902-8912.

Zhao, W., Y. Du, W. T. Ho, X. Fu and Z. J. Zhao (2012). "JAK2V617F and p53 mutations coexist in erythroleukemia and megakaryoblastic leukemic cell lines." Experimental hematology & oncology **1**(1): 15.

Zhou, X., Q. Hao, J. Liao, Q. Zhang and H. Lu (2013). "Ribosomal protein S14 unties the MDM2-p53 loop upon ribosomal stress." Oncogene **32**(3): 388-396.

Appendix

A1.1 miR-595 Primer Sequence

CCCAGTATCTCCAGGGATTTGAGAATCAGTTCATTCTGCAAGTAACAAAACTAG
GGAAGGAAGTGGTTTTCAAGCTCCCGTGGTTGTTGGAGGTGAGCTAATTCTTTG
CGAGTTATTAATTGCTGGTCTCTTGGAATGGCTTGGGAGCACAAAGTGACAGG
AACCCAAGTCATTTCTGTTCTGTTTGCTTGTGTTTGTTTTGCTTTAAGTTAATCCT
TTGGTGGTTCTGGGGATGAGGCCTTGTCCCTGGCTTGGTAGAGAGAGGCCAGTC
AGGAGGGAGCAGGTGTGGTGGAGCCTGGCCGTCCCTGAGCCATCAAGATGGTC
TGCGCGTCAGAGTGCAGCACGGGCCACATTCTCTCTGCCATGTGCAGAGGGCT
CCTGCACGGAAGCCTGCACGCATTTAACACCAGCACGCTCAATGTAGTCTTGTA
AGGAACAGGTTGAAGTGTGCCGTGGTGTGTCTGGAGGAAGCGCCTGTTGCTGG
TTTTTGTTGTTTTGTTATGTATTTTTTGCCATGTTCCATGCTGTTCCTCTAATCAC
ATCATGTCCCGGGTTTTTGAAGTTTAGTGACGTTTTTGGTCTTTTCTTACTTTTTA
CCCATGTTTTTTCCTCTTTGTAGGATCAAAGTCACATACAATAGCAACTTTATTA
TAACGCACGGTCCACCACGCTCCAACTTCCAGTGTGGAGGCATCGGTGGGGGT
TTGCTGAAAGTCTGAGCAAATCTCATGGCTGTCTCTGCTGTCTCCGTGATGACT
CTGTGGGGCACGTGACTGGAATGCTCTGATGCCTGTTTGACATCTGGGGCTTCT
CAGAAGCCACAGGAGCCACGCTGGGGGCTGACAGTTTCCTCTCCCAATGTCGC
TT

Mature sequence

Pre-miRNAsequence

A1.2 Sequencing result of miRNA-595 amplified from MCF7cells

A1.2.1 Mir-595 with forward primer

```
>lcl|18163

Length=605

 Score =  911 bits (493),  Expect = 0.0

 Identities = 510/518 (99%), Gaps = 2/518 (0%)

 Strand=Plus/Minus

Query  968   GCACGCTCAATGTAGTCTTGTAAGGAACAGGTTGAAGTGTGCCGTGGTGTGTCTGGAGGA  1027
              ||||||||||||||||||||||||||||||||||||||||||||||||||||||||||||
Sbjct  605   GCACGCTCAATGTAGTCTTGTAAGGAACAGGTTGAAGTGTGCCGTGGTGTGTCTGGAGGA  546

Query  1028  AGCGCCTGTTGCTGGtttttgttgttttgttatgtatttttgCCATGTTCCATGCTGTT  1087
              ||| ||||||||||||||||||||||||||||||||||||||||||||||||||||||||
Sbjct  545   AGCACCTGTTGCTGGTTTTTGTTGTTTTGTTATGTATTTTTTGCCATGTTCCATGCTGTT  486

Query  1088  CCTCTAATCACATCATGTCCCGGgtttttgaagtttagtgac--gtttttggtcttttct  1145
              |||||||||||||||||| ||||||||||||||||||||   ||||||||||||||||
Sbjct  485   CCTCTAATCACATCATGTCCTGGGTTTTTGAAGTTTAGTGACTTTTTTTTGGTCTTTTCT  426

Query  1146  actttttacccatgttttttcctctttGTAGGATCAAAGTCACATACAATAGCAACTTT  1205
              |||||||||||||||| ||||||||||||||||||||||||||||||||||||||||||
Sbjct  425   TACTTTTTACCCATGTTCTTTCCTCTTTGTAGGATCAAAGTCACATACAATAGCAACTTT  366

Query  1206  ATTATAACGCACGGTCCACCACGCTCCAACTTCCAGTGTGGAGGCATCGGTGGGGGTTTG  1265
              |||||||||||||||||||||||||||||||||||| ||||||||||||||||||||||
Sbjct  365   ATTATAACGCACGGTCCACCACGCTCCAACTTCCAGTGTGGGGGCATCGGTGGGGGTTTG  306

Query  1266  CTGAAAGTCTGAGCAAATCTCATGGCTGTCTCTGCTGTCTCCGTGATGACTCTGTGGGGC  1325
              ||||||| ||||||||||||||||||||||||||||||||||||||||||||||||||||
Sbjct  305   CTGAAAGCCTGAGCAAATCTCATGGCTGTCTCTGCTGTCTCCGTGATGACTCTGTGGGGC  246

Query  1326  ACGTGACTGGAATGCTCTGATGCCTGTTTGACATCTGGGGCTTCTCAGAAGCCACAGGAG  1385
              ||||||||||||||||||||||||||||||||||||||||||||||||||||||||||||
Sbjct  245   ACGTGACTGGAATGCTCTGATGCCTGTTTGACATCTGGGGCTTCTCAGAAGCCACAGGAG  186

Query  1386  CCACGCTGGGGGCTGACAGTTTCCTCTCCCAATGTCGCTTTTGGGCATCTAAGAGCCTGG  1445
              ||||||||||||||||||||||||||||||||||||||||||||||||||||||||||||
Sbjct  185   CCACGCTGGGGGCTGACAGTTTCCTCTCCCAATGTCGCTTTTGGGCATCTAAGAGCCTGG  126
```

```
Query  1446  TCATAGAGACGTGACGTGGCTTGAGAATGGACAGAGGC  1483
             |||||||||||||||||||||||||||||||||||||
Sbjct  125   TCATAGAGACGTGACGTGGCTTGAGAATGGACAGAGGC  88
```

A1.2.2 Mir-595 with the reverse primer

```
>lcl|21203
Length=627
 Score =  915 bits (495),  Expect = 0.0
 Identities = 510/517 (99%), Gaps = 2/517 (0%)
 Strand=Plus/Minus
Query  969   CACGCTCAATGTAGTCTTGTAAGGAACAGGTTGAAGTGTGCCGTGGTGTGTCTGGAGGAA  1028
             ||||||||||||||||||||||||||||||||||||||||||||||||||||||||||||
Sbjct  627   CACGCTCAATGTAGTCTTGTAAGGAACAGGTTGAAGTGTGCCGTGGTGTGTCTGGAGGAA  568
Query  1029  GCGCCTGTTGCTGgtttttgttgttttgttatgtatttttttgCCATGTTCCATGCTGTTC  1088
             || ||||||||||||||||||||||||||||||||||||||||||||||||||||||||||
Sbjct  567   GCACCTGTTGCTGGTTTTTGTTGTTTTGTTATGTATTTTTTGCCATGTTCCATGCTGTTC  508
Query  1089  CTCTAATCACATCATGTCCCGGgtttttgaagtttagtgac--gtttttggtcttttctt  1146
             |||||||||||||||||| ||||||||||||||||||||   ||||||||||||||||
Sbjct  507   CTCTAATCACATCATGTCCTGGGTTTTTGAAGTTTAGTGACTTTTTTTTTGGTCTTTTCTT  448
Query  1147  acttttacccatgttttttcctctttGTAGGATCAAAGTCACATACAATAGCAACTTTA  1206
             ||||||||||||||||||||||||||||||||||||||||||||||||||||||||||||
Sbjct  447   ACTTTTTACCCATGTTTTTTCCTCTTTGTAGGATCAAAGTCACATACAATAGCAACTTTA  388
Query  1207  TTATAACGCACGGTCCACCACGCTCCAACTTCCAGTGTGGAGGCATCGGTGGGGGTTTGC  1266
             ||||||||||||||||||||||||||||||||||||||||||||||||||||||||||||
Sbjct  387   TTATAACGCACGGTCCACCACGCTCCAACTTCCAGTGTGGAGGCATCGGTGGGGGTTTGC  328
Query  1267  TGAAAGTCTGAGCAAATCTCATGGCTGTCTCTGCTGTCTCCGTGATGACTCTGTGGGGCA  1326
             ||| || ||||||||||||||||||||||||||||||||||||||||||||||||||||||
Sbjct  327   TGAGAGCCTGAGCAAATCTCATGGCTGTCTCTGCTGTCTCCGTGATGACTCTGTGGGGCA  268
Query  1327  CGTGACTGGAATGCTCTGATGCCTGTTTGACATCTGGGGCTTCTCAGAAGCCACAGGAGC  1386
             ||||||||||||||||||||||||||||||||||||||||||||||||||||||||||||
Sbjct  267   CGTGACTGGAATGCTCTGATGCCTGTTTGACATCTGGGGCTTCTCAGAAGCCACAGGAGC  208
Query  1387  CACGCTGGGGGCTGACAGTTTCCTCTCCCAATGTCGCTTTTGGGCATCTAAGAGCCTGGT  1446
```

```
            ||||||||||||||||||||||||||||||||||||||||||||||||||||||||||||||||
Sbjct  207  CACGCTGGGGGCTGACAGTTTCCTCTCCCAATGTCGCTTTTGGGCATCTAAGAGCCTGGT  148

Query  1447 CATAGAGACGTGACGTGGCTTGAGAATGGACAGAGGC  1483

            ||||||||||||||||||||||||||||||||||||
Sbjct  147  CATAGAGACGTGACGTGGCTTGAGAATGGACAGAGGC  111
```

Error in the Pre-miRNA sequence

A1.3 Sequencing result of miRNA-595 amplified from HeLa cells

A1.3.1 Mir-595 with the forward primer

```
>lcl|33681
Length=655
 Score =  950 bits (514),  Expect = 0.0
 Identities = 520/523 (99%), Gaps = 0/523 (0%)
 Strand=Plus/Plus
Query  345  GGGCCACATTCTCTCTGCCATGTGCAGAGGGCTCCTGCACGGAAGCCTGCACGCATTTAA  404
            ||| || ||||||||||||||||||||||||||||||||||||||||||||||||||||||
Sbjct  6    GGGTCAAATTCTCTCTGCCATGTGCAGAGGGCTCCTGCACGGAAGCCTGCACGCATTTAA  65
Query  405  CACCAGCACGCTCAATGTAGTCTTGTAAGGAACAGGTTGAAGTGTGCCGTGGTGTGTCTG  464
            ||||||||||||||||||||||||||||||||||||||||||||||||||||||||||||
Sbjct  66   CACCAGCACGCTCAATGTAGTCTTGTAAGGAACAGGTTGAAGTGTGCCGTGGTGTGTCTG  125
Query  465  GAGGAAGCGCCTGTTGCTGgttttgttgttttgttatgtatttttgCCATGTTCCATG  524
            ||||||||||||||||||||||||||||||||||||||||||||||||||||||||||||
Sbjct  126  GAGGAAGCGCCTGTTGCTGGTTTTTGTTGTTTTGTTATGTATTTTTTGCCATGTTCCATG  185
Query  525  CTGTTCCTCTAATCACATCATGTCCCGGgtttttgaagtttagtgacgttttttggtcttt  584
            ||||||||||||||||||||||||||||||||||||||||||||||||||||||||||||
Sbjct  186  CTGTTCCTCTAATCACATCATGTCCCGGGTTTTTGAAGTTTAGTGACGTTTTTGGTCTTT  245
Query  585  tcttacttttacccatgttttttcctctttGTAGGATCAAAGTCACATACAATAGCAAC  644
            ||||||||||||||||||||||||||||||||||||||||||||||||||||||||||||
Sbjct  246  TCTTACTTTTTACCCATGTTTTTTCCTCTTTGTAGGATCAAAGTCACATACAATAGCAAC  305
Query  645  TTTATTATAACGCACGGTCCACCACGCTCCAACTTCCAGTGTGGAGGCATCGGTGGGGGT  704
            ||||||||||||||||||||||||||||||||||||||||||||||||||||||||||||
Sbjct  306  TTTATTATAACGCACGGTCCACCACGCTCCAACTTCCAGTGTGGAGGCATCGGTGGGGGT  365
Query  705  TTGCTGAAAGTCTGAGCAAATCTCATGGCTGTCTCTGCTGTCTCCGTGATGACTCTGTGG  764
            |||||||||| ||||||||||||||||||||||||||||||||||||||||||||||||||
Sbjct  366  TTGCTGAAAGCCTGAGCAAATCTCATGGCTGTCTCTGCTGTCTCCGTGATGACTCTGTGG  425
Query  765  GGCACGTGACTGGAATGCTCTGATGCCTGTTTGACATCTGGGGCTTCTCAGAAGCCACAG
```

```
824

            ||||||||||||||||||||||||||||||||||||||||||||||||||||||||||||||||
Sbjct  426  GGCACGTGACTGGAATGCTCTGATGCCTGTTTGACATCTGGGGCTTCTCAGAAGCCACAG
485

Query  825  GAGCCACGCTGGGGGCTGACAGTTTCCTCTCCCAATGTCGCTT  867
            |||||||||||||||||||||||||||||||||||||||||||
Sbjct  486  GAGCCACGCTGGGGGCTGACAGTTTCCTCTCCCAATGTCGCTT  528
```

A1.3.2 Mir-595 with the reverse primer

```
>lcl|55633

Length=697

 Score =  924 bits (500),  Expect = 0.0

 Identities = 507/510 (99%), Gaps = 2/510 (0%)

 Strand=Plus/Minus

Query  1    CCCAGTATCTCCAGGGATTTGAGAATCAGTTCATTCTGCAAGTAACAAAACTAGGGAAGG
60

            |||||||||||||||||||||||||||||||||||| ||||||||||||||||||||||
Sbjct  517  CCCAGTATCTCCAGGGATTTGAGAATCAGTTCATTCTACAAGTAACAAAACTAGGGAAGG
458

Query  61   AAGTGGTTTTCAAGCTCCCGTGGTTGTTGGAGGTGAGCTAATTCTTTGCGAGTTATTAAT
120

            ||||||||||||||||||||||||||||||||||||||||||||||||||||||||||||||
Sbjct  457  AAGTGGTTTTCAAGCTCCCGTGGTTGTTGGAGGTGAGCTAATTCTTTGCGAGTTATTAAT
398

Query  121  TGCTGGTCTCTTGGAATGGCTTGGGAGCACAAAGTGACAGGAACCCAAGTCATTTCTGTT
180

            ||||||||||||||||||||||||||||||||||||||||||||||||||||||||||||||
Sbjct  397  TGCTGGTCTCTTGGAATGGCTTGGGAGCACAAAGTGACAGGAACCCAAGTCATTTCTGTT
338

Query  181  CTGTTTGCTTGTGTTTGTTTTGCTTTAAGTTAATCCTTTGGTGGTTCTGGGGATGAGGCC
240

            ||||||||||||||||||||||||||||||||||||||||||||||||||||||||||||||
Sbjct  337  CTGTTTGCTTGTGTTTGTTTTGCTTTAAGTTAATCCTTTGGTGGTTCTGGGGATGAGGCC
278

Query  241  TTGTCCCTGGCTTGGTAGAGAGAGGCCAGTCAGGAGGGAGCAGGTGTGGTGGAGCCTGGC
300

            ||||||||||||||||||||||||||||||||||||||||||||||||||||||||||||||
Sbjct  277  TTGTCCCTGGCTTGGTAGAGAGAGGCCAGTCAGGAGGGAGCAGGTGTGGTGGAGCCTGGC
218

Query  301  CGTCCCTGAGCCATCAAGATGGTCTGCGCGTCAGAGTGCAGCACGGGCCACATTCTCTCT
360

            ||||||||||||||||||||||||||||||||||||||||||||||||||||||||||||||
Sbjct  217  CGTCCCTGAGCCATCAAGATGGTCTGCGCGTCAGAGTGCAGCACGGGCCACATTCTCTCT
```

```
158

Query  361  GCCATGTGCAGAGGGCTCCTGCACGGAAGCCTGCACGCATTTAACACCAGCACGCTCAAT
420

             ||||||||||||||||||||||||||||||||||||||||||||||||||||||||||||

Sbjct  157  GCCATGTGCAGAGGGCTCCTGCACGGAAGCCTGCACGCATTTAACACCAGCACGCTCAAT
98

Query  421  GTAGTCTTGTAAGGAACAGGTTGAAGTGTGCCGTGGTGTGTCTGGAGGAAGCGCCTGTTG
480

             ||||||||||||||||||||||||||||||||||||||||||||||||||||||||||||

Sbjct  97   GTAGTCTTGTAAGGAACAGGTTGAAGTGTGCCGTGGTGTGTCTGGAGGAAGCGCCTGTTG
38

Query  481  CTGgtttttgttgttttgttatgtattttt  510
             ||||||||||| |||| ||||||||||||

Sbjct  37   CTGGTTTTTGT-GTTT-GTTATGTATTTTT  10
```

A1.4 p3'UTRTkzeo sequence with primers alignment

GGATCCCCCGGGCTGCAGGAATTCGATATCAAGCTTATCGCATGGCTTCGTACCCCGGCCATCAACACGCGTCTGCGTTCGACCAGGCTGCGCGTTCTCGCGGCCATA
GCAACCGACGTACGGCGTTGCGCCCTCGCCGGCAGCAAGAAGCCACGGAAGTCCGCCCGGAGCAGAAAATGCCCACGCTACTGCGGGTTTATATAGACGGTCCCCA
CGGGATGGGGAAAACCACCACCACGCAACTGCTGGTGGCCCTGGGTTCGCGCGACGATATCGTCTACGTACCCGAGCCGATGACTTACTGGCGGGTGCTGGGGGCTT
CCGAGACAATCGCGAACATCTACACCACACAACACCGCCTCGACCAGGGTGAGATATCGGCCGGGGACGCGGCGGTGGTAATGACAAGCGCCCAGATAACAATGGG
CATGCCTTATGCCGTGACCGACGCCGTTCTGGCTCCTCATATCGGGGGGGAGGCTGGGAGCTCACATGCCCCGCCCCCGGCCCTCACCCTCATCTTCGACCGCCATCC
CATCGCCGCCCTCCTGTGCTACCCGGCCGCGCGGTACCTTATGGGCAGCATGACCCCCCAGGCCGTGCTGGCGTTCGTGGCCCTCATCCCGCCGACCTTGCCCGGCAC
CAACATCGTGCTTGGGGCCCTTCCGGAGGACAGACACATCGACCGCCTGGCCAAACGCCAGCGCCCCGGCGAGCGGCTGGACCTGGCTATGCTGGCTGCGATTCGCC
GCGTTTACGGGCTACTTGCCAATACGGTGCGGTATCTGCAGTGCGGCGGGTCGTGGCGGGAGGACTGGGGACAGCTTTCGGGGACGGCCGTGCCGCCCCAGGGTGCC
GAGCCCCAGAGCAACGCGGGCCCACGACCCCATATCGGGGACACGTTATTTACCCTGTTTCGGGCCCCCGAGTTGCTGGCCCCCAACGGCGACCTGTATAACGTGTTT
GCCTGGGCCTTGGACGTCTTGGCCAAACGCCTCCGTTCCATGCACGTCTTTATCCTGGATTACGACCAATCGCCCGCCGGCTGCCGGGACGCCCTGCTGCAACTTACC
TCCGGGATGGTCCAGACCCACGTCACCACCCCCGGCTCCATACCGACGATATGCGACCTGGCGCGCACGTTTGCCCGAGAGATGATCAGCGGAGCTAATGGCGTCAT
GGCCAAGTTGACCAGTGCCGTTCCGGTGCTCACCGCGCGCGACGTCGCCGGAGCGGTCGAGTTCTGGACCGACCGGCTCGGGTTCTCCCGGGACTTCGTGGAGGACG
ACTTCGCCGGTGTGGTCCGGGACGACGTGACCCTGTTCATCAGCGCGGTCCAGGACCAGGTGGTGCCGGACAACACCCTGGCCTGGGTGTGGGTGCGCGGCCTGGAC
GAGCTGTACGCCGAGTGGTCGGAGGTCGTGTCCACGAACTTCCGGGACGCCTCCGGGCCGGCCATGACCGAGATCGGCGAGCAGCCGTGGGGGCGGGAGTTCGCCC
TGCGCGACCCGGCCGGCAACTGCGTGCACTTCGTGGCCGAGGAGCAGGACTGACCGACGCCGACCAACACCGCCGGTCCGACGCGGCCCGACGGGTCCGAGGGGGG
TCGACCTCGAATCCTTAGGCCATTAAGGCCGGCCGCCTCGGCCCACTTCGTGGGGTACCGAGCTCGAATTCACTGGCCGTCGTTTTACAACGTCGTGACTGGGAAAAC
CCTGGCGTTACCCAACTTAATCGCCTTGCAGCACATCCCCCTTTCGCCAGCTGGCGTAATAGCGAAGAGGCCCGCACCGATCGCCCTTCCCAACAGTTGCGGCCGAGG
AGCAGGACTGACACGTGCTACGAGATTTCGATTCCACCGCCGCCTTCTATGAAAGGTTGGGCTTCGGAATCGTTTTCCGGGACGCCGGCTGGATGATCCTCCAGCGCG
GGGATCTCATGCTGGAGTTCTTCGCCCACCCCAACTTGTTTATTGCAGCTTATAATGGTTACAAATAAAGCAATAGCATCACAAATTTCACAAATAAAGCATTTTTTTC
ACTGCATTCTAGTTGTGGTTTGTCCAAACTCATCAATGTATCTTATCATGTCTGTATACCGTCGACCTCTAGCTAGAGCTTGGCGTAATCATGGTCATAGCTGTTTCCTG
TGTGAAATTGTTATCCGCTCACAATTCCACACAACATACGAGCCGGAAGCATAAAGTGTAAAGCCTGGGGTGCCTAATGAGTGAGCTAACTCACATTAATTGCGTTG
CGCTCACTGCCCGCTTTCCAGTCGGGAAACCTGTCGTGCCAGCTGCATTAATGAATCGGCCAACGCGCGGGGAGAGGCGGTTTGCGTATTGGGCGCTCTTCCGCTTCC
TCGCTCACTGACTCGCTGCGCTCGGTCGTTCGGCTGCGGCGAGCGGTATCAGCTCACTCAAAGGCGGTAATACGGTTATCCACAGAATCAGGGGATAACGCAGGAAA
GAACATGTGAGCAAAAGGCCAGCAAAAGGCCAGGAACCGTAAAAAGGCCGCGTTGCTGGCGTTTTTCCATAGGCTCCGCCCCCCTGACGAGCATCACAAAAATCGA
CGCTCAAGTCAGAGGTGGCGAAACCCGACAGGACTATAAAGATACCAGGCGTTTCCCCCTGGAAGCTCCCTCGTGCGCTCTCCTGTTCCGACCCTGCCGCTTACCGGA
TACCTGTCCGCCTTTCTCCCTTCGGGAAGCGTGGCGCTTTCTCAATGCTCACGCTGTAGGTATCTCAGTTCGGTGTAGGTCGTTCGCTCCAAGCTGGGCTGTGTGCACG
AACCCCCCGTTCAGCCCGACCGCTGCGCCTTATCCGGTAACTATCGTCTTGAGTCCAACCCGGTAAGACACGACTTATCGCCACTGGCAGCAGCCACTGGTAACAGGA
TTAGCAGAGCGAGGTATGTAGGCGGTGCTACAGAGTTCTTGAAGTGGTGGCCTAACTACGGCTACACTAGAAGGACAGTATTTGGTATCTGCGCTCTGCTGAAGCCA
GTTACCTTCGGAAAAAGAGTTGGTAGCTCTTGATCCGGCAAACAAACCACCGCTGGTAGCGGTGGTTTTTTTGTTTGCAAGCAGCAGATTACGCGCAGAAAAAAAGG
ATCTCAAGAAGATCCTTTGATCTTTTCTACGGGGTCTGACGCTCAGTGGAACGAAAACTCACGTTAAGGGATTTTGGTCATGAGATTATCAAAAAGGATCTTCACCTA
GATCCTTTTAAATTAAAAATGAAGTTTTAAATCAATCTAAAGTATATATGAGTAAACTTGGTCTGACAGTTACCAATGCTTAATCAGTGAGGCACCTATCTCAGCGAT
CTGTCTATTTCGTTCATCCATAGTTGCCTGACTCCCCGTCGTGTAGATAACTACGATACGGGAGGGCTTACCATCTGGCCCCAGTGCTGCAATGATACCGCGAGACCC
ACGCTCACCGGCTCCAGATTTATCAGCAATAAACCAGCCAGCCGGAAGGGCCGAGCGCAGAAGTGGTCCTGCAACTTTATCCGCCTCCATCCAGTCTATTAATTGTTG
CCGGGAAGCTAGAGTAAGTAGTTCGCCAGTTAATAGTTTGCGCAACGTTGTTGCCATTGCTACAGGCATCGTGGTGTCACGCTCGTCGTTTGGTATGGCTTCATTCAG
CTCCGGTTCCCAACGATCAAGGCGAGTTACATGATCCCCCATGTTGTGCAAAAAAGCGGTTAGCTCCTTCGGTCCTCCGATCGTTGTCAGAAGTAAGTTGGCCGCAGT
GTTATCACTCATGGTTATGGCAGCACTGCATAATTCTCTTACTGTCATGCCATCCGTAAGATGCTTTTCTGTGACTGGTGAGTACTCAACCAAGTCATTCTGAGAATAG
TGTATGCGGCGACCGAGTTGCTCTTGCCCGGCGTCAATACGGGATAATACCGCGCCACATAGCAGAACTTTAAAAGTGCTCATCATTGGAAAACGTTCTTCGGGGCG
AAAACTCTCAAGGATCTTACCGCTGTTGAGATCCAGTTCGATGTAACCCACTCGTGCACCCAACTGATCTTCAGCATCTTTTACTTTCACCAGCGTTTCTGGGTGAGCA
AAAACAGGAAGGCAAAATGCCGCAAAAAAGGGAATAAGGGCGACACGGAAATGTTGAATACTCATACTCTTCCTTTTTCAATATTATTGAAGCATTTATCAGGGTTA
TTGTCTCATGAGCGGATACATATTTGAATGTATTTAGAAAAATAAACAAATAGGGGTTCCGCGCACATTTCCCCGAAAAGTGCCACCTGACGTCGACGGATCGGGAG
ATCTCCCGATCCCCTATGGTCGACTCTCAGTACAATCTGCTCTGATGCCGCATAGTTAAGCCAGTATCTGCTCCCTGCTTGTGTGTTGGAGGTCGCTGAGTAGTGCGCG
AGCAAAATTTAAGCTACAACAAGGCAAGGCTTGACCGACAATTGCATGAAGAATCTGCTTAGGGTTAGGCGTTTTGCGCTGCTTCGCGATGTACGGGCCAGATATAC
GCGTTGACATTGATTATTGACTAGTTATTAATAGTAATCAATTACGGGGTCATTAGTTCATAGCCCATATATGGAGTTCCGCGTTACATAACTTACGGTAAATGGCCC
GCCTGGCTGACCGCCCAACGACCCCCGCCCATTGACGTCAATAATGACGTATGTTCCCATAGTAACGCCAATAGGGACTTTCCATTGACGTCAATGGGTGGACTATTT
ACGGTAAACTGCCCACTTGGCAGTACATCAAGTGTATCATATGCCAAGTACGCCCCCTATTGACGTCAATGACGGTAAATGGCCCGCCTGGCATTATGCCCAGTACAT
GACCTTATGGGACTTTCCTACTTGGCAGTACATCTACGTATTAGTCATCGCTATTACCATGGTGATGCGGTTTTGGCAGTACATCAATGGGCGTGGATAGCGGTTTGAC
TCACGGGGATTTCCAAGTCTCCACCCCATTGACGTCAATGGGAGTTTGTTTTGGCACCAAAATCAACGGGACTTTCCAAAATGTCGTAACAACTCCGCCCCATTGACG
CAAATGGGCGGTAGGCGTGTACGGTGGGAGGTCTATATAAGCAGAGCTCTCTGGCTAACTAGAGAACCCACTGCTTACTGGCTTATCGAAATTAATACGACTCACTA
TAGGGAGACCCAAGCTGGCTAGT

9Reverse

3Fowrword

11Fowerward

SFI sites